

SHEAR STRENGTH BEHAVIOUR OF SUGARCANE BAGASSE REINFORCED SOILS

By

Vincent Oderah



Supervisor: Dr Denis Kalumba

**A thesis submitted to the University of Cape Town in partial fulfilment of the
requirement for the degree of Master of Science in Engineering**

August 2015

The copyright of this thesis vests in the author. No quotation from it or information derived from it is to be published without full acknowledgement of the source. The thesis is to be used for private study or non-commercial research purposes only.

Published by the University of Cape Town (UCT) in terms of the non-exclusive license granted to UCT by the author.

Plagiarism declaration

1. I know the meaning of plagiarism and declare that all the work in the document, save for that which is properly acknowledged, is my own.
2. I have used Harvard Convention for citation and referencing. Each significant contribution to and quotation in this thesis from work or works of other people has been attributed and has been cited and referenced.
3. I have not allowed and will not allow anyone to copy my work with the intention of passing it as his or her own work.

Signed by candidate

Signature Removed

Vincent Oderah

ODRVIN001

Dedication

To Mom,

Pamela Oderah

For the endless and overwhelming love. I love you Mama Dorothy

Acknowledgements

I would like to thank the almighty God for the immense blessings and protection.

Sincere gratitude goes to my supervisor Dr. Denis Kalumba for the guidance, advice, open door policy and needed criticism all through the period of this research.

A special thank you for the assistance accorded by the UCT laboratory staff especially Nooredein Hassen, Elvino Witbooi, Hector Zwelixelile Mafungwa and Charles May.

Thank you Charles Nicholas, the workshop manager, for fabricating all the necessary equipment, helping with the material requisition and all the witty conversations in between. I came to learn through you the importance of design performance.

I am grateful for TSB Sugar Company for providing the fibre material – mainly to Nico Stolz, TSB energy specialist for his insights that significantly contributed to my thought process.

My deepest gratitude goes out to my geotechnical research group colleagues: Dennis Kiptoo, Johnny Oriokot, Byron Mawer, Samuel Jjukko, Angela Lekea, Sam Wagener, Dercio Chim Jin, Lita Noluthshungu, Paul Wanyama, Sanelisiwe Buthelezi, Vuyiseka Mapangwana, Joan Ong'ondia, and Laxmee Sobhee for providing the most conducive environment to carry out research and the detours that made postgraduate life interesting.

I acknowledge the unconditional and steady financial support from ARISE Consortium. I wish to thank Ms. Norma Derby, Carol Ojwang' and Jody Feldon, the ARISE co-ordinators, for the assistance provided during my two years of post-graduate study at UCT.

I am grateful to Prof Chuma Imonga for her motherly advice. Patrick Reizandt and Cally Dewaal for the enabling academic environment, Godfrey Gakingo for being the best flat mate, Chris Zenim for being my late night study partner. Alfred Mitema for providing the opportunity to speak Luo in foreign lands, Ken Nyaundi for the warm welcome in Cape Town and all the Africa House fraternity to whom am indebted.

Finally, I would like to thank my family and friends especially Justus Olima, Mburu Mwangi, King'ori Maina, Angela Hiuhu and Anne Olang'o for their patience, sacrifices and well wishes throughout my education life, home and away. Profound gratitude to Kayla Hill for the reminder, "keep trying and never settle", and making sure I keep my health on check.

I love you all. God Bless.

Ochieng' Vincent Oderah

Abstract

Sugarcane is considered as the most abundant plant based crop grown in the tropics and part of the temperate climates. Its by-product, sugarcane bagasse, constitutes 30% of the total production. In the past, it was considered as waste material but contemporaries through innovative research projects over the years have found uses for it. Among these projects is soil reinforcement, which provides an alternative application to industrial by-products and natural fibres as a way of reducing their environmental footprints and contributing to sustainable geotechnics. Although bagasse morphological composition contains structural elements ideal for reinforcement and composite materials, it has received little research as a standalone reinforcement material. Because of this, a direct shear test was therefore initiated to establish the usefulness of using sugarcane bagasse as a soil reinforcement material by comparing the extent of shear strength and stiffness response due to its inclusion to unreinforced soil.

Three different types of bagasse, fibre, millrun and pith, were added to unreinforced soil in percentage by weight content of 0.3 – 1.7. The bagasse was added to Klipheuwel sand, Cape Flats sand and Kaolin Clay at both dry and moist conditions. In addition, durability studies involving 12 cycles of wetting and drying, and soaking for a period of 14 days were constituted.

The results showed that inclusion of the fibre and millrun bagasse improved the shear strength of the selected soils up to a maximum content of 1.4 percent for Klipheuwel sand and 1.0 percent for Cape Flats sand. Insignificant improvement in Kaolin clay properties were observed over the percentage by weight content ranges investigated. Furthermore, bagasse reduced the loss in the post-peak shear strengths of soils by making the soils more ductile. The improvement in angle of internal friction was found to be profound in fibre bagasse as compared to millrun and pith by about 30% for Klipheuwel sand. The study also showed that even though the addition of water reduced the peak shear strengths of soils, it did not affect the percentage increase in the angle of internal friction as observed for Klipheuwel sand with a 1.4% fibre content. Similarly, cycles of wetting and drying insignificantly affected the shear strength of reinforced sands apart from smoothening the fibres surfaces. On the contrary, soaking of the fibre-soil composite over 2 days considerably reduced the shear strength and angle of internal friction by 15%. Coating of the fibres, studies thereof and installation of adequate surface and sub-surface soil drainage systems are therefore recommended.

Based on the experimental results, a non-linear regression analysis was performed as a function of the descriptor variables and a FEM slope stability analysis in an embankment fill. From the results, it was clear that sugarcane bagasse could be used as a reinforcing material. This could provide an alternative way of using bagasse in an embankment fill of a low volume road.

Table of contents

Plagiarism declaration.....	i
Dedication.....	ii
Acknowledgements.....	iii
Abstract.....	iv
Table of contents	v
List of figures	x
List of tables.....	xiv
Acronyms and annotations.....	xvi
CHAPTER 1.....	1
1 INTRODUCTION	1
1.1 Background.....	1
1.2 Problem statement.....	2
1.3 Justification	3
1.4 Key questions	4
1.5 Hypothesis	4
1.6 Objectives.....	4
1.7 Research overview	5
CHAPTER 2.....	6
2 THEORY OF SOIL REINFORCEMENT	6
2.1 Introduction	6
2.2 Development of soil reinforcing system.....	6
2.3 Methods of soil reinforcement	7
2.3.1 Based on material.....	7
2.3.1.1 Geosynthetics	8
2.3.1.2 Fibres	9
2.3.1.3 Waste materials	11
2.3.2 Based on method of placement/inclusion.....	12
2.3.2.1 Systematic/planar inclusion	13

2.3.2.2	Random inclusion.....	13
2.4	Randomly distributed fibre reinforced soils.....	14
2.4.1	Relevant definition and concepts	14
2.4.2	Reinforcing mechanism	15
2.5	Predictive models.....	18
2.6	Review of previous research on fibre reinforcement.....	24
2.6.1	Effect of types of soil on fibre reinforcement	24
2.6.1.1	Sandy soils.....	24
2.6.1.2	Cohesive soils	25
2.6.2	Effect of fibre content	26
2.6.3	Effect of water content on reinforced soil	29
2.6.4	Durability and effect of fibre coating	29
2.7	Studies carried out on bagasse fibre	31
2.8	Potential application.....	32
2.9	Summary of the literature reviewed.....	33
CHAPTER 3.....		35
3	REVIEW OF PLANT NATURAL FIBRES	35
3.1	Introduction	35
3.2	Natural fibre characterization	35
3.3	Composition of natural fibres	35
3.3.1	Cellulose	36
3.3.2	Hemicellulose	37
3.3.3	Pectin and waxes.....	38
3.3.4	Lignin	38
3.4	Methods of extracting the natural fibre constituents	40
3.5	Mechanical properties of fibres	40
3.6	Factors affecting mechanical properties of fibres	41
3.7	Bagasse fibre characteristics and uses	43
3.7.1	Process of manufacturing bagasse	43

3.7.1.1	Mill tandem process	44
3.7.1.2	Diffusion	44
3.7.2	Depithing of bagasse	45
3.7.3	Composition of bagasse	45
3.7.4	Properties of bagasse	46
3.7.5	Current uses of bagasse	47
CHAPTER 4:	48
4	RESEARCH MATERIALS AND METHODOLOGY	48
4.1	Introduction	48
4.2	Research materials	48
4.2.1	Soil characterization tests	48
4.2.2	Soil materials	48
4.2.2.1	Klipheuwel Sand	48
4.2.2.2	Cape Flats sand	49
4.2.2.3	Kaolin Clay	50
4.2.3	Fibre material	51
4.2.3.1	Fibre bagasse	52
4.2.3.2	Millrun bagasse	53
4.2.3.3	Pith bagasse	54
4.3	Electron micrographs of the research materials	55
4.4	Test Equipment	57
4.4.1	Direct shear	57
4.4.2	Durability moulds	59
4.4.3	Other apparatus	60
4.5	Methodology	61
4.5.1	Testing regime	61
4.5.2	Sample preparation	68
4.5.2.1	Soil only	69
4.5.2.2	Soil-fibre composite	70

4.5.3	Durability design	72
4.5.4	Assembly of apparatus	73
4.5.5	Experimental procedures	73
4.5.5.1	Wetting/drying and soaking	76
4.5.5.2	Repeatability	76
4.5.6	Quality concerns	76
4.5.7	Data calculation	77
CHAPTER 5.....		79
5	RESULTS, ANALYSIS AND DISCUSSIONS	79
5.1	Introduction	79
5.2	Repeatability results.....	79
5.3	Control test results and discussion.....	80
5.4	Direct shear results on fibre-soil composite.....	82
5.4.1	Shear deformation relationships at dry soil conditions.....	83
5.4.1.1	Klipheuwel sand	83
5.4.1.2	Cape Flats sand	88
5.4.1.3	Kaolin clay.....	92
5.4.2	Shear deformation relationships at moist conditions	93
5.4.2.1	Klipheuwel sand	93
5.4.2.2	Cape Flats sand	97
5.4.2.3	Kaolin clay.....	98
5.4.3	Shear stress-normal stress relationships	99
5.4.3.1	Shear envelope for fibre bagasse	99
5.4.3.2	Shear envelope for millrun bagasse reinforced soils.....	101
5.4.3.3	Shear envelope for pith bagasse reinforced soils	103
5.4.4	Shear stress-normal stress relationship for moist soils.....	105
5.4.4.1	Shear envelope for fibre bagasse moist-reinforced soils.....	105
5.4.4.2	Shear envelope of millrun moist reinforced soils.....	107
5.4.4.3	Shear envelope of pith bagasse moist reinforced soils	108

5.5	Effect of bagasse concentration on angle of internal friction (ϕ) and cohesion (c) of dry soils	110
5.5.1	Fibre bagasse	110
5.5.2	Millrun bagasse.....	111
5.5.3	Pith bagasse	112
5.6	Effect of bagasse concentration on angle of internal friction (ϕ) and cohesion (c) of moist soils	112
5.7	Comparison of results on the various bagasse type	115
5.8	Durability study results and discussions	117
5.8.1	12 cycle wetting and drying.....	117
5.8.2	Soaked composite results	117
5.9	Regression models for granular soils	120
CHAPTER 6.....		125
6	PRACTICAL APPLICATIONS	125
6.1	Introduction	125
6.2	Quality guidelines	125
6.3	Design example	126
6.3.1	Model computations.....	127
6.3.2	Results and discussion	129
CHAPTER 7.....		132
7	CONCLUSIONS AND RECOMMENDATIONS.....	132
7.1	Introduction	132
7.2	Conclusions	132
7.2.1	Specific conclusions.....	132
7.2.2	General conclusions	133
7.3	Recommendations	134
References		135
Appendices.....		141

List of figures

Figure 1.1: Fermenting sugarcane bagasse at 40% moisture content.....	2
Figure 2.1: Pictures of selected natural fibres. From left to right: coir, bamboo, sisal (from www.naturalfibres2009.org)	10
Figure 2.2: EPS and its effect on the angle of internal friction of sand (From figure 2 and 7 of Donald and Kalumba)	11
Figure 2.3: Friction angle and sand mixed with different length of perforated polyethylene bags (Figure 1b and 3c of Kalumba and Chebet).....	12
Figure 2.4: Shear strength of Klipheuwel and mixed with tyre shreds (Figure 1b and 8a of Chebet et.al)	12
Figure 2.5: Method of reinforcement (a) random and (b) systematic/planar.....	13
Figure 2.6: Idealised concept for the mechanism of randomly distributed reinforced soil (a) unreinforced and (b) reinforced	15
Figure 2.7: Model envelope of fibre-reinforced sand (redrawn from Gray & Ohashi, 1983; Li, 2005)	16
Figure 2.8: Shear strength envelope of Onsorio sand under triaxial testing (redrawn from figure 1b Consoli et al., 2007)	17
Figure 2.9: Model strength envelope of fibre-reinforced clay (adapted from Nataraj & McManis, 1997)	17
Figure 2.10: Fibre mechanistic model (a) vertical (b) inclined (Gray & Ohashi, 1983).....	19
Figure 2.11: Deformation pattern of fibre-soil composite (Michalowski, 2003)	20
Figure 2.12: Comparison of prediction and experimental results for coarse sand reinforced with polyamide fibres (redrawn from Michalowski and Čermák, 2003)	22
Figure 2.13: Comparison between predicted and measured friction angles based on energy and discrete models (Sadek et al 2010)	23
Figure 2.14: Experimental comparison of fine and coarse sands with fibre content (Sadek et al., 2010).....	25
Figure 2.15: Stress-strain relationship of unreinforced and reinforced clay (Figure 4 of Nataraj and McManis)	26
Figure 2.16: Effect of fibre content on the stress-strain relationship, showing no change in initial stiffness ((a) Li and Zornberg, 2013 (b) Shao et.al 2014))	27
Figure 2.17: Shear envelope of (a) unreinforced sand (b) reinforced sand with increase in water content (Figure 6 and 7 of Lovisa et.al, 2010).....	29
Figure 2.18: Water take between untreated fibres (UTF) and treated fibres (TF1, 2, Rahman et.al (2007)).....	30

Figure 2.19: Effect of fibre content on tensile strength of untreated bagasse fibre composites (Cao, 2006).....	32
Figure 3.1: Subdivision and origin of natural fibres (adapted from Fuqua et. al, 2012)	36
Figure 3.2: Molecular structure of cellulose (Watford, 2008; Faqua et al., 2013)	37
Figure 3.3: Molecular structure of hemicellulose (Watford, 2008).....	37
Figure 3.4: Molecular structure of selected lignin (Fuqua et. al., 2013).....	38
Figure 3.5: Structure of a single fibre cell (Fuqua et al., 2012)	41
Figure 3.6: Fibre composition responsible for the functional properties (Adapted from Azwa et al. (2013).....	42
Figure 3.7: Idealized Fickian diffusion concept (adapted from Azwa et al. (2013).....	43
Figure 3.8: Showing the Bagasse production process (Adapted from Patarau, 1998)	45
Figure 3.9: Cross-section of cane (extracted from Rein, 1972).....	47
Figure 3.10: Current uses of bagasse (adapted from Loh et al. 2013).....	47
Figure 4.1: (a) Klipheuwel Sand, (b) Cape Flats Sand, (c) Kaolin Clay.....	49
Figure 4.2: Particle grading curves.....	50
Figure 4.3: Bagasse (a) Stockpiled for 2 months (b) Millrun wet and dry just after production	52
Figure 4.4: Fibre bagasse	53
Figure 4.5: Average length of fibre bagasse.....	54
Figure 4.6: (a) Millrun bagasse, (b) pith Bagasse	54
Figure 4.7: Showing Bagasse after screening used in the study	55
Figure 4.8: SEM micrographs of the research materials at a resolution of x10,000	56
Figure 4.9: Direct shear apparatus (a) before shear and (b) after shearing, all dimensions in mm.....	58
Figure 4.10: ShearTrac-III components.....	59
Figure 4.11: Durability mould picture and cross-section, dimensions in mm.....	60
Figure 4.12: Mechanical mixer, 0.45 m in diameter and 0.25 m deep.....	60
Figure 4.13: Hand compactor, all dimensions in mm	61
Figure 4.14: Sample preparation and end results.....	71
Figure 4.15: Moist sample preparation and placement in the split box	72
Figure 4.16: 14 days soaked composite ready for testing.....	73
Figure 4.17: ShearTrac-III software set-up screen shot.....	74
Figure 4.18: Experimental procedure	75
Figure 4.19: Summary of the research methodology	78
Figure 5.1: Quality test results, showing results at 1.0% fibre, 50 kPa normal pressure	79
Figure 5.2: Control test results (a) sands (clay) at dry state.....	81
Figure 5.3: Control test results (a) sands (b) clay at moist condition.....	82

Figure 5.4: Shear deformation of dry Klipheuwel sand with varying fibre content	84
Figure 5.5: Fibre floating at 1.7% fibre content before testing.....	84
Figure 5.6: Shear deformation of millrun reinforced dry Klipheuwel sand at varied content .	86
Figure 5.7: Shear deformation of dry Klipheuwel sand at various pith contents	87
Figure 5.8: Shear deformation of dry Cape Flats sand at various fibre bagasse content	88
Figure 5.9: Shear deformation of dry Cape Flats sand at various millrun content stress.....	90
Figure 5.10: Shear deformation of dry Cape Flats sand at various pith contents	91
Figure 5.11: Shear deformation of dry Kaolin clay at reinforced with 1.0% fibre/millrun/pith	92
Figure 5.12: Shear deformation of moist Klipheuwel sand at various fibre bagasse content	93
Figure 5.13: Shear deformation of moist Klipheuwel sand at various millrun content	95
Figure 5.14: Shear deformation of moist Klipheuwel sand at various pith content	96
Figure 5.15: Shear deformation of moist Cape Flats sand reinforced with 1.0% fibre/millrun/pith	97
Figure 5.16: Shear deformation of moist Kaolin clay reinforced with 1.0% fibre/millrun/pith.	98
Figure 5.17: Shear strength parameters of dry Klipheuwel sand reinforced with fibre bagasse	100
Figure 5.18: Shear strength parameters of dry Cape Flats sand reinforced with fibre	101
Figure 5.19: Shear strength parameters of Klipheuwel sand reinforced with millrun.....	102
Figure 5.20: Shear strength envelope of Cape Flats sand reinforced with millrun	102
Figure 5.21: Shear strength envelope of Klipheuwel sand reinforced with pith	103
Figure 5.22: Shear strength envelope of Cape Flats sand reinforced with pith	104
Figure 5.23: Shear strength envelope of Kaolin clay at dry moisture content reinforced with 1.0% fibre/millrun/pith.....	105
Figure 5.24: Shear strength envelope of moist Klipheuwel sand reinforced with fibre bagasse	105
Figure 5.25: Shear strength envelope of moist Cape Flats sand reinforced with 1.0% fibre/millrun/pith bagasse.	106
Figure 5.26: Shear strength envelope of moist Klipheuwel sand reinforced with millrun....	107
Figure 5.27: Shear strength envelope of moist Klipheuwel sand reinforced with pith bagasse	108
Figure 5.28: Shear strength envelope of moist Kaolin Clay reinforced with 1.0% fibre/millrun/pith bagasse	109
Figure 5.29: Effect of fibre bagasse concentration on (a) angle of internal friction (b) cohesion	111
Figure 5.30: Effect of millrun bagasse concentration on (a) angle of internal friction (b) cohesion	111

Figure 5.31: Effect of pith bagasse concentration on (a) angle of internal friction (b) cohesion	112
Figure 5.32: Effect of fibre concentration on (a) angle of internal friction (b) cohesion of moist soils	113
Figure 5.33: Effect of millrun bagasse concentration on (a) angle of internal friction (b) cohesion of moist typical soils	114
Figure 5.34: Effect of pith bagasse concentration on (a) angle of internal friction (b) cohesion of typical moist soils	114
Figure 5.35: Comparison of the effect of the various types of bagasse on dry (a) Klipheuwel sand (b) Cape Flats sand (c) Kaolin clay.....	116
Figure 5.36: Micrograph of an isolated dry fibre strand (a) before and (b) after 12 cycles of wetting and drying	117
Figure 5.37: Effect of submerging on shear strength parameters on reinforced Klipheuwel sand	119
Figure 5.38: Effect of submerging on shear strength parameters on reinforced Klipheuwel sand	119
Figure 5.39: Exhumed fibres after soaking (a) visual (b) micrograph.....	120
Figure 5.40: Histogram of plots	122
Figure 5.41: Normal P-P Plot of Regression Standardized Residual	122
Figure 5.42: Predicted and measured values of peak shear stress for bagasse fibre reinforced sand.....	123
Figure 5.43: Particle distribution of the sandy soil used in the model validation.....	124
Figure 5.44: Comparison of predicted and experimental values failure envelope using a different sandy soil	124
Figure 6.1: Geometry of the normal and reinforced fill.....	128
Figure 6.2: Model calculation stage inputs	129
Figure 6.3: Probable failure mechanism (a) unreinforced fill (b) reinforced fill	131
Figure 6.4: Failure plane results from Plaxis (a) unreinforced (b) reinforced embankment, and Prokon (c) unreinforced (d) reinforced embankment	131

List of tables

Table 2.1: Summary of some techniques used in the improvement of mechanical and engineering properties of soil	7
Table 2.2: Comparative behaviour of soil reinforcement materials (Mc Gown et al, 1978; Swami, 2010).....	8
Table 2.3: Type and functions of geosynthetics (adapted from Koerner, 2005)	9
Table 2.4: Selected previous studies on natural fibres	28
Table 2.5: Factors affecting soil reinforcement (adapted from Jones, 1996).....	31
Table 3.1: Summary of the typical mechanical properties of selected plant fibres (Fuqua et.al 2012).....	39
Table 3.2: Typical physical composition of bagasse (Rein, 1972)	46
Table 4.1: Soil classification tests conducted	48
Table 4.2: Soil characterization results.....	51
Table 4.3: Chemical properties of Kaolin clay*	51
Table 4.4: Summary of fibre characterization	52
Table 4.5: Definition of terms	62
Table 4.6: Testing regime for reinforced dry Cape Flats sand	62
Table 4.7: Testing regime for reinforced dry Klipheuwel sand	64
Table 4.8: Testing regime for reinforced dry Kaolin Clay	65
Table 4.9: Testing regime for reinforced moist Cape Flats Sand	65
Table 4.10: Testing regime for reinforced moist Klipheuwel Sand	67
Table 4.11: Testing regime for reinforced moist Kaolin Clay.....	67
Table 4.12: Testing regime for durability studies	68
Table 5.1: Repeatability results computations	80
Table 5.2: Summary of peak shear strength for fibre bagasse reinforced Klipheuwel sand .	85
Table 5.3: Summary of peak shear strengths for millrun bagasse reinforced Klipheuwel sand	86
Table 5.4: Summary of peak shear strengths for pith bagasse reinforced Klipheuwel sand	87
Table 5.5: Summary of peak shear strengths for Cape flats/ fibre composite	89
Table 5.6: Summary of peak shear for Cape flats/ millrun composite	90
Table 5.7: Summary of peak shear strength of Cape flats/ millrun composite	91
Table 5.8: Summary of peak shear strengths of Kaolin clay reinforced 1% fibre/millrun/pith bagasse	92
Table 5.9: Summary of peak shear strengths of fibre bagasse reinforced moist Klipheuwel sand.....	94

Table 5.10: Summary of peak shear strengths for millrun bagasse reinforced moist Klipheuwel sand.....	95
Table 5.11: Summary of peak shear for pith bagasse reinforced Klipheuwel sand at OMC .	96
Table 5.12: Summary of peak shear strengths of moist Cape Flats sand reinforced with 1.0% fibre/millrun/pith bagasse	98
Table 5.13: Summary of peak shear strengths for Kaolin reinforced with 1.0% fibre/millrun/pith	99
Table 5.14: Summary of peak strength parameters for fibre reinforced soils	101
Table 5.15: Summary of peak strength parameters for millrun reinforced soils	103
Table 5.16: Summary of peak strength parameters for pithreinforced soils	104
Table 5.17: Summary of peak strength parameters for fibre reinforced moist soils.....	106
Table 5.18: Summary of peak strength parameters for millrun reinforced moist soils	108
Table 5.19: Summary of peak strength parameters for pith reinforced moist soils.....	109
Table 5.20: Peak shear strengths of soaked Klipheuwel sand reinforced with 1% fibre bagasse.	118
Table 5.21: t-test results.....	121
Table 6.1: Plaxis 8.2 input parameters	126
Table 6.2: Properties of the embankment concrete platform	128
Table 6.3: Embankment fill displacement and slope analysis results.....	129

Acronyms and annotations

Symbol	Unit	Description
ϕ	$^{\circ}$	Angle of internal friction
θ	$^{\circ}$	Distortion angle
v	m^3	Composite volume
δ	$^{\circ}$	Fibre skin friction
ξ	-	Empirical coefficient, soil-fibre interaction
τ_{eq}	kPa	Equivalent shear strength
τ_f	$^{\circ}$	Interface friction, fibre/soil
v_f	m^3	Volume of fibre
σ_n	kPa	Normal stress
σ_N	kPa	Normal confining stress
$\sigma_{n,crit}$	kPa	Critical normal stress
Δs	kPa	Change in shear strength
σ_t	kPa	Fibre induced tension
A	m^2	Area of soil
α	kPa	Adhesion
A_f	m^2	Area of fibre
A_r	m^2	Aspect ratio
c	kPa	Cohesion
C	-	Normal pressure
CD	-	Consolidated drained
C_{eq}	kPa	Equivalent cohesion
CFS	-	Cape Flat sand
$c_{i,c}/c_{i,\phi}$	-	Interaction coefficients
CU	-	Consolidated undrained
D	-	Dry state
d_f	m	Diameter of fibre
E_f	GPa	Fibre modulus
EPS	-	Expanded Polyesterene
F	-	Fibre (true)
F1, F2, F3, F4, F5	-	Bagasse volumetric concentrations of 0.3%, 0.7%, 1.0%, 1.4%, 1.7%, respectively
FAO	-	Food agriculture organization
i	$^{\circ}$	Orientation angle

Symbol	Unit	Description
KC	-	Kaolin clay
k_p	--	Coefficient of earth pressure
KS	-	Klipheuwel sand
l_f	<i>m</i>	Length of fibre
LVDT	-	Linear variable displacement transducer
M	$^\circ$	Macroscopic angle
MR	-	Mill-run
MR1,MR2,MR3,MR4, MR5	-	Mill-run concentration of 0.3%, 0.7%, 1.0%, 1.4%, 1.7% respectively
N_f	-	Number of fibres
OMC	-	Optimum moisture content
P	-	Pith
P1, P2, P3,P4,P5	-	Pith concentration of 0.3%, 0.7%, 1.0%, 1.4%, 1.7% respectively
D_r	-	Relative density
RDFS	-	Randomly distributed fibre soils
RS	-	Reinforced soil
SASA	-	South African Sugar Association
SCB	-	Sugarcane bagasse
SEM	-	Scanning Electron microscope
t_f	<i>kPa</i>	Fibre tensile strength
UCS	-	Unconfined compression strength
UCT	-	University of Cape Town
UND	-	United Nations Data
US	-	Unreinforced soil
USCS	-	Unified soil Classification Systems
z	<i>m</i>	Shear thickness zone
α	-	Coefficient of fibre partial contribution

CHAPTER 1

1 INTRODUCTION

1.1 Background

The balance between satisfying human construction needs and minimizing the construction impacts on the environment calls for a more sustainable approach. According to Basu et.al (2013), sustainability in the engineering domain is a multifaceted concept that revolves around striking a balance between environment, economy and equity. Environmental aspects in this balance hold a greater threshold because of the increased depletion of the natural resources and concerns to reduce the carbon footprints. This has compelled engineers to sustainably use the scarce resources, innovate others and re-use some of the waste materials from the industries and construction sites.

One way of achieving this initiative particularly by geotechnical engineers is through soil reinforcement. That is, the inclusion of various innovative materials and or waste materials to improve the engineering properties of soils thereby making the soils suitable for construction in addition to minimizing effects of the waste materials on the general environment. A process described by Vaníček et al. (2013) as highlighting the positive role of geotechnical engineering in environmental protection and sustainable construction – environmental geotechnics.

Generally, soil reinforcement is an established technique that provides the means to the beneficial re-use of selected industrial or domestic wastes, and natural fibres (Gray & Ohashi, 1983; Hejazi et.al 2012). This is done through random inclusion of these materials in soils at specified contents based on studies conducted either in-situ or in the laboratories. As a technique, it has undergone further research to encompass a wide range of materials over the three decades since its inception. An example of such selected alternative reinforcement material is sugarcane bagasse.

This material is an industrial by-product that is taken as a natural fibre consisting of lignin, cellulose and hemicellulose (Watford, 2008), which are structural components typical of a reinforcement material. It is a fibrous residue remaining after extracting all the juice from the sugarcane. Globally, it is the most lignocellulosic fibre produced. Thirty percent of all the sugarcane produced constitutes sugarcane bagasse. By statistics this amounts to 90 million tonnes a year from Africa (FAO, 2013), South Africa being the largest producer in Africa.

Historically, bagasse was considered as a waste material in the sugar milling industries where its disposal became a major problem. Currently however, it is considered as a raw material for

innovative projects such as cogeneration, animal feed, paper, carbonated sludge productions, composite reinforcement and possibly soil reinforcement material.

1.2 Problem statement

Large quantities of sugarcane bagasse are continuously being produced especially in tropical countries and parts of the temperate regions such as South Africa. For instance, South Africa produces about 7.5 million tonnes of sugarcane bagasse annually from 14 sugarcane mills in KwaZulu Natal, Mpumalanga and Eastern Cape provinces (SASA, 2014).

This bulk volume presents disposal and handling problems. Bagasse is a low-density material occupying a larger space thereby requiring spacious storage facilities especially during peak production seasons. If kept at a moisture content of above 20%, bagasse ferments and decays (Osinubi, 2009) whereas if kept dry it becomes susceptible to combustion. In addition, prolonged exposure to dry bagasse may cause a respiratory disease called *bagassiosis* (Laurianne, 2004). Figure 1.1 shows millrun sugarcane bagasse at 40% moisture content.



Figure 1.1: Fermenting sugarcane bagasse at 40% moisture content

In curbing these problems, millers historically resorted to landfilling. Currently, electricity generation by combustion seems to be the most preferred alternative use of the fibres justified by the reduction in carbon footprints and self-reliance on the side of millers. Use of bagasse in this manner though economical, presents generic problems. For example, large volumes of ash get generated which is currently utilised as capping in landfills without considerable research on its effectiveness, long-term performance or effect on the environment. Furthermore, according to Torres et.al (2014) boilers used to burn bagasse operate at a low efficiency of 60 - 70% requiring millers to use coal to boost the efficiency. The pulverised ash

formed as a by-product of the combustion of coal can contaminate the groundwater and air if improperly disposed of in landfills instead of being used as a soil stabilising agent.

On the other hand, strength of soil is an important parameter in the design of geotechnical systems in addition to cost and ease of construction (Jones, 1996). For these reasons, conventional materials like cement, lime and bitumen have been used to improve the engineering properties of soils. These materials are often expensive and sometimes inaccessible to civil projects especially in rural areas. Further research is therefore needed to find more innovative ways of improving the engineering characteristics of soil. Reinforcing soil with bagasse fibre could be one of the innovative ways. Moreover, using bagasse in soil could be a safe way of reducing its environmental footprint.

1.3 Justification

The existing interest to utilize sugarcane bagasse in soil reinforcement comes in the wake of global research initiatives geared towards the use of cheap alternative materials in industry, conservation of energy and the minimization of waste materials to the environment. Sugarcane bagasse's main constituents: lignin, cellulose, hemicellulose, ash and wax make it ideal as a soil reinforcement material (Walford, 2008). This is evident in its successful use as a composite material involving cement, polythene and adobe blocks (Fuqua et al., 2012; Stephens, 1994).

It is also readily available locally in bulk quantities (United Nations Data, 2010). In fact, it could be said that, as long as human beings continue to use sugar, bagasse production could remain constant. This would ensure its long-term use especially as a soil reinforcement material. However, no work has been published on the use of bagasse as a standalone reinforcement material in spite of its abundance.

Although several studies have been carried out on the effects and benefits of natural fibre and waste material in soil reinforcement as summarised by (Hejazi et al., 2012), no known have been done in South African. The main reason for the limited use in this region is the lack of research, instrumented case studies and design specifications. Alternative use for bagasse could therefore invigorate research, minimize the problems caused by bagasse, and possibly improve the shear strength characteristic of some South African soils.

It should be noted that the use of bagasse as a reinforcement material does not dispute the existing uses of bagasse and those yet to be established nor does it replace the existing conventional soil reinforcement techniques. It rather diversifies the alternative uses of bagasse, consequently contributing to fibre reinforcement research.

1.4 Key questions

Several research questions informed the research on sugarcane bagasse reinforced soils. Some of the key questions included:

1. Can sugarcane bagasse fibre be used in improving engineering properties of soils?
2. What is the optimum quantity of bagasse needed for maximum improvement of shear strength parameters of soils?
3. What is the effect of varying the length of bagasse at optimum concentration on shear strength parameters of soils?
4. Does soil moisture content affect the optimum quantity of bagasse needed for maximum shear strength?
5. What is the effect of water (wetting and drying, submerging) on the durability of bagasse-soil composite?
6. What quality control and quality assurance measures are applicable during construction?
7. How does the use of bagasse in soil reinforcement affect the probability of failure?

1.5 Hypothesis

Increasing sugarcane bagasse content, length and reducing rate of its water absorption improves the shear strength parameters of soils, when randomly included in soils. This is due to the soil-fibre matrix formed, which consequently maintains the isotropy of the soil and limits the possible formation of failure shear planes in bagasse-reinforced soils.

1.6 Objectives

The main objective of the study was to investigate the possible use of sugarcane bagasse as a soil reinforcement material when randomly distributed in selected soils.

After considering resources and time available for the project, the specific objectives were as follows:

1. Study the effect of varying the content of bagasse on the shear strength of selected soils at both dry and optimum moisture content.
2. Investigate the effect of 12 cycles of wetting and drying, and progressive soaking for a maximum of 14 days on the bagasse-soil composite.
3. Make a design recommendation on the use of bagasse in embankment fill.

1.7 Research overview

Chapter 1 introduces the underlying issues pertaining to sustainable geotechnics, sugarcane bagasse production and disposal, and the justifications for carrying out this research.

Chapter 2 presents the theories of fibre reinforcement, theoretical definitions and some of the previous work done on sugarcane bagasse.

In Chapter 3, a review of all the plant-based fibres, their composition and mechanical properties that could make them ideal as soil reinforcement materials is discussed. The chapter also gives an overview of South Africa's sugar production and processes involved in the production of bagasse.

Chapter 4 describes in detail the methodology and research materials used in the study including a thorough characterization of the bagasse fibres. In Chapter 5, the results and a discussion thereof of the results are presented together with a predictive model.

Practical applications including the use of the results obtained in a typical embankment fill design are presented in chapter 6. Chapter 7 gives the summary of the results, conclusions and recommendations on future research motivated by this work.

CHAPTER 2

2 THEORY OF SOIL REINFORCEMENT

2.1 Introduction

In this section the soil reinforcement technique and an overview of its historical development is discussed. In addition, the different existing and emerging forms of reinforcing material and methods of reinforcement are reviewed. Particular attention is paid to randomly distributed fibres that allow the re-use of industrial waste material/by-product and natural fibres.

2.2 Development of soil reinforcing system

Soil reinforcement is an ancient technique dating back as far as biblical times. The Mesopotamians and Romans applied the technique in improving the pathways by mixing weak soil with pulverized limestone or calcium. Some of the existing monuments bear the testimony of earth reinforcement technique over time (Jones, 1996). The concept however remained in crude form until in 1970's when a French engineer, Vidal, demonstrated that including flat reinforcing strips horizontally in a frictional soil improved the soil's shear resistance.

Since then reinforced earth retaining walls have been constructed around the world. During this period also, the concept of using fibrous earth material as a mimicry of the past was started. For instance, early construction materials like adobe blocks incorporated fibrous materials to improve their properties despite a lack of understanding of the mechanism. In addition, the construction of the Great Wall of China incorporated mixed clay soil with tamarisk (Swami, 2010).

The mechanism has recently attracted attention in geotechnical engineering projects for the in both research and field environments (Hejazi et al., 2012). This comes as an innovative option to sustainably contribute to the environment and find alternative reinforcement technique. Jones (1996) gives an elaborate history of the development of soil reinforcement and a review of different systems.

2.3 Methods of soil reinforcement

By definition, soil reinforcement is the technique of improving the engineering properties of soil such as, shear strength, compressibility, density and hydraulic conductivity by incorporating stabilising and/or tension or compression resisting materials. It forms part of the several techniques used in ground improvement as summarised in table 2.1.

Table 2.1: Summary of some techniques used in the improvement of mechanical and engineering properties of soil

Technique	Method
Soil stabilization	<ul style="list-style-type: none"> – Mixing by binding agents (lime, cement, bitumen and chemicals) – Compaction – Pre-consolidation
Reinforced earth	<ul style="list-style-type: none"> – Inclusion in the direction of tensile strength – Strips, grids, sheets, fabrics etc.
Soil nailing	<ul style="list-style-type: none"> – Grouted nails – Driven nails
Texsols	<ul style="list-style-type: none"> – Mixing in-situ by continuous threads of textiles
Fibre reinforced soil/ply soil*	<ul style="list-style-type: none"> – Random inclusion of discrete fibres

*Broad study area

The technique can be divided into two: (1) based on reinforcement material, and (2) based on the method of placement or construction.

2.3.1 Based on material

The resisting materials vary greatly according to form; strips, sheets, grids, bars or fibres; by texture, roughness or smoothness, and relative stiffness (Gray & Ohashi, 1983). Mc Gown et al. (1978) classified these reinforcing materials based on the stress-strain characteristics as mainly; ideally like high modulus metal strips and bars or ideally extensible materials like natural and synthetic fibres. The reinforced soil in the former case was termed as reinforced earth while the latter was termed as ply soil by Gray and Ohashi (1983). The comparison of the two is as given in table 2.2.

Table 2.2: Comparative behaviour of soil reinforcement materials (Mc Gown et al, 1978; Swami, 2010)

Type of reinforcement	Stress-strain behaviour of reinforcement	Role and function of reinforcement
Ideally inextensible	Inclusions may have rupture strains less than the maximum tensile strain in the soil without inclusion, under the same operating stress conditions, i.e. Depending upon the ultimate strength of the inclusions in relation to the imposed loads, these inclusions may or may not rupture	Strengthens soil (increase apparent shear resistance) and inhibits both internal and boundary deformations, Catastrophic failure and collapse of soil can occur if reinforcement breaks.
Ideally extensible inclusions	Inclusions may have rupture strain greater than the maximum tensile strains in the soil without inclusions i.e. these inclusions cannot rupture, no matter their ultimate strength or the imposed load.	Some strengthening; more importantly provides greater extensibility (ductility) and smaller loss of post peak strength compared alone or to reinforced soil.

Commonly used reinforcement materials are geosynthetics (made of synthetic fibres), synthetic fibres alone and natural fibres. However, industrial waste materials such as fly ash and tyre shreds have found their use as reinforcement materials.

Sub-sections 2.3.1.1- 2.3.1.3 outline the various reinforcement materials utilized in the study of the application of soil reinforcement, that is, geosynthetics, synthetic fibres, natural fibres and selected industrial wastes.

2.3.1.1 Geosynthetics

Geosynthetics are planar materials made of fabric or polymers included in the soil to perform a number of functions, soil reinforcement being one of them. As summarised by Koerner (2005), table 2.3, geosynthetics can be involved in different applications.

Table 2.3: Type and functions of geosynthetics (adapted from Koerner, 2005)

Type of Geosynthetic	Function
Geotextile	Separation, containment, filtration, reinforcement
Geogrid	Reinforcement
Geocomposite	Filtration, separation, barrier, drainage, reinforcement
Geomembrane	Containment
Geocells	Erosion control, reinforcement
Geopipe	Drainage
Geocontainer	Erosion control
Geosynthetic Clay Liner	Containment
Geofoam	Reinforcement

Various types of geosynthetics exist depending on the function, method of manufacture and the type of polymer used. Locally in South Africa, a number of companies including Fibertex, Kaytech, Maccaferri and Tensar among others manufacture and market geosynthetics.

2.3.1.2 Fibres

Fibres are commonly differentiated as natural fibres (coir, sisal, bamboo, palm, cane etc.) and synthetic fibres (polypropylene, polyethylene, polyester etc.). Synthetic fibres are generally preferred as reinforcing materials because of their durability and tensile strength properties. However, the availability of natural fibres makes them feasible in geotechnical application as a reduction to the cost of ply soil.

According to Li, (2005), the feasibility is due to the advantages of using natural fibres, which includes:

1. Method of placement: Conventional mixing and compaction equipment like rotary mechanical mixers can be used for mixing. Any compaction method is applicable during construction without concern for rupturing the fibres.
2. A homogenous mixture formed between fibre and soils that offers an interlocking matrix for soil strength isotropy.
3. Construction using fibres can take place in any weather condition. However, due to the hydrophilic nature of natural fibres, care should be taken during construction. Natural fibres have a tendency of absorbing moisture compared to synthetic fibre.

An overview of the selected fibres is discussed below while a full discussion is presented in chapter 3.

- **Coir fibre**

Coir fibres are fibres obtained from seeds of coconut trees. It has high lignin content (about 50%) and has been depicted as the least affected by moisture compared to other fibres. For this reason, it has been applied as erosion control and in embankment fills.

Research reviewed justified the use of coir fibre as soil reinforcement by its abundance in tropical and sub-tropical countries. Sivakumar and Vasudevan (2008) reinforced tropical soil with 1 – 2% coir fibre and showed an increase of 3.5 times in stress-strain over unreinforced soil. Findings supported by Maliakal and Thiyyakkandi (2013) who concluded that the improvement in shear strength of clay soil reinforced with coir fibre is significant at a content of 0.5 – 1%.

- **Bamboo fibre**

Bamboo fibre is extracted from the pulp of bamboo. Bamboo is the largest member of the grass family and does not require pesticides to grow. It has found its use as a soil reinforcement material due to its availability and high tensile strength (140 – 800 MPa).

- **Sisal**

Sisal fibres are extracted from sisal leaves that are predominantly grown in East Africa, Indonesia and India. Sisal fibres have a cellulose content of 78% and tensile strength of 700 MPa. Prabakar and Sridhar (2002) carried out a study on soils reinforced with sisal fibres and mentioned that sisal fibres increases the strength parameters by about four times.

- **Cane fibre**

Cane fibres are of the grass family and can be obtained from crushing sugarcane through either chewing or milling. Inclusion of cane fibres is the focus of this research therefore has been discussed in details in Chapter 3. Figure 2.1 gives a pictorial overview of the typical fibres discussed above.



Figure 2.1: Pictures of selected natural fibres. From left to right: coir, bamboo, sisal (from www.naturalfibres2009.org)

2.3.1.3 Waste materials

Several waste materials have found their way in soil reinforcement for environmental purposes constituting sustainable geotechnics (Basu et al. 2013). Materials such as fly ash, discarded tyre shreds, carpet wastes, polyethylene bags and expanded polystyrene (EPS) have been combined with soil to improve their engineering properties and reduce the effect of these materials on the environment. For example, in the geotechnical engineering research group at the University of Cape Town, carpet wastes (Anyiko et al. 2011), tyre shreds (Chebet et al. 2013), plastic shopping bags (Kalumba & Chebet, 2013), and expanded polystyrene waste (Donald & Kalumba, 2014) have been extensively studied and found to improve the strength of selected typical South African soils.

Anyiko et al (2011) showed that inclusion of 0.1 – 0.5 % carpet wastes improved the cohesion of sandy soil by 27% and insignificantly affected its angle of internal friction. Chebet et al. (2013) studied tyre shreds mixed with sand at 10 - 100% concentration of dry weight of soil and concluded that the addition of tyres makes soil ductile and improves shear strength of soil by 30% at an optimum content of 30%. Kalumba and Chebet (2013) on the other hand, added strips (both plain and perforated) of plastic shopping bags and established an improvement in the angle of internal friction at a concentration of 0.3%, 3 mm length and 2 mm perforation diameter. Similarly, Donald and Kalumba (2014) using 2 – 4 mm diameter beads of EPS wastes (polymeric material commonly used for packaging) presented results on Klipheuwel sand shown in figure 2.2.

Figures 2.2 to 2.4 shows the commonly researched waste material and their investigated effect on the shear strength of soils. Generally, based on these results, it is evident that using waste material in soil reinforcement is feasible.

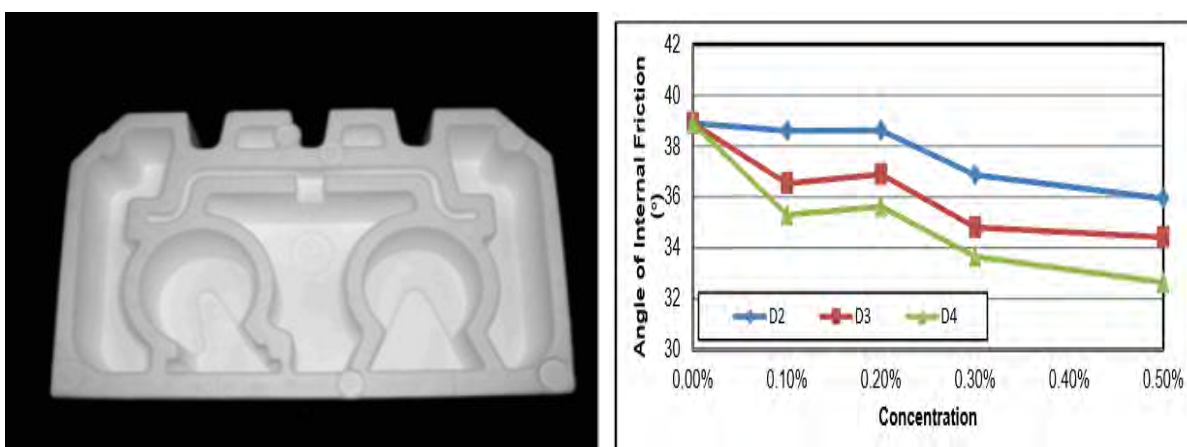


Figure 2.2: EPS and its effect on the angle of internal friction of sand (From figure 2 and 7 of Donald and Kalumba)

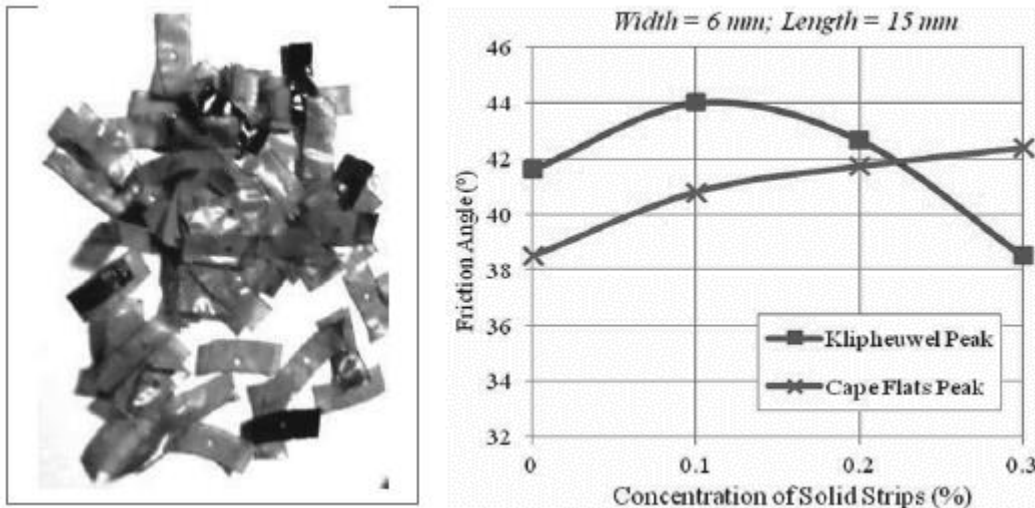


Figure 2.3: Friction angle and sand mixed with different length of perforated polyethylene bags (Figure 1b and 3c of Kalumba and Chebet)

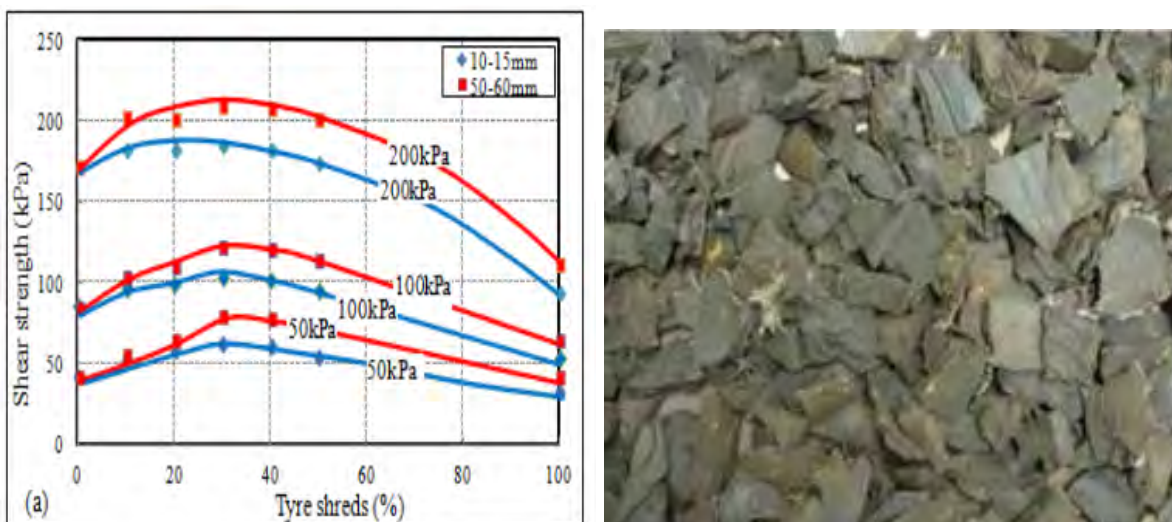


Figure 2.4: Shear strength of Klipheuwel and mixed with tyre shreds (Figure 1b and 8a of Chebet et.al)

2.3.2 Based on method of placement/inclusion

The composite between the fibre and the resisting material can be obtained through two methods, by either incorporating material systematically/planar or randomly mixing the soil with discrete fibres (Shukla et al. 2009).

Alternatively, the methods can be in-situ or constructed (Pedley, 1990). The former category involves placing reinforcing material into virgin soil (soil nailing and dowelling). The latter category includes placing reinforcing material simultaneously with an imported and remoulded soil like geosynthetics and fibres.

Systematic and random inclusion methods are discussed further in the subsequent sections with an emphasis on the random inclusion method.

2.3.2.1 Systematic/planar inclusion

In systematic inclusion, the reinforcement material is placed in layers and the soil is then compacted in the direction parallel to the shear plane, just like steel in concrete. It should be noted that the soil is first compacted to the desired density then the reinforcement material is placed and the sequence repeated until the required lift is achieved. The resulting composite is known as reinforced earth. Figure 2.5 (b) illustrates this phenomenon.

This method allows the incorporation of ideally inextensible and rigid reinforcement materials, with larger surface area such as bars and sheets. The materials are generally included in soil in the direction of tension, because soil is weak in tension. Furthermore, this method enables the use of geosynthetic materials for various application such as retaining structures, sub-grade stabilisation, embankments and footings (Swami, 2010).

Systematic/planar inclusion has its weakness compared to random inclusion. Including material in planar creates planes of weakness. For instance, geosynthetic rupturing has been experienced in tailing dams in the direction parallel to the shear plane (Koerner, 2005).

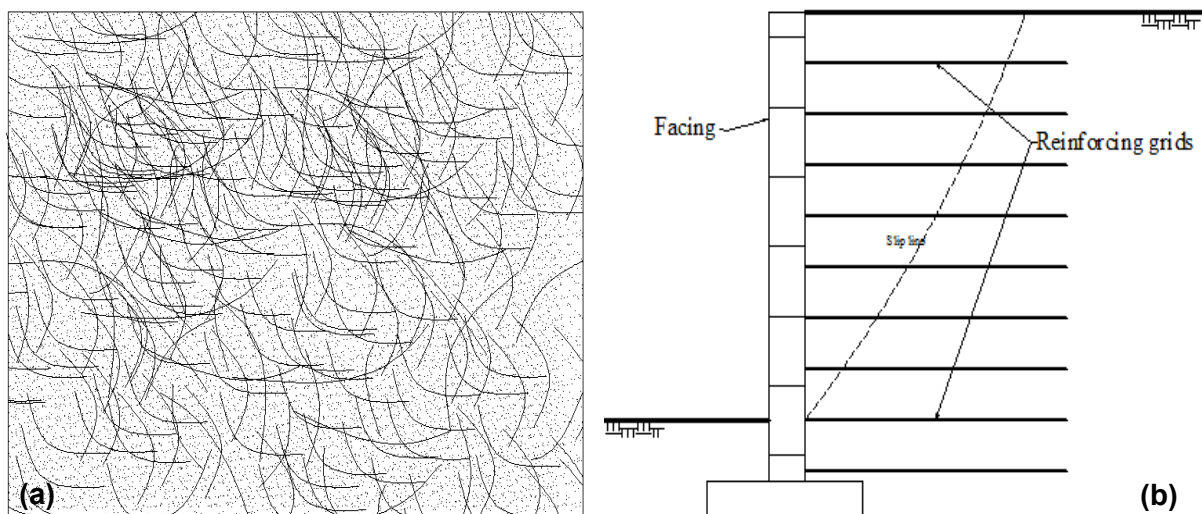


Figure 2.5: Method of reinforcement (a) random and (b) systematic/planar

2.3.2.2 Random inclusion

Random inclusion is a modification of systematic inclusion. In this method, reinforcing materials are mixed with soil in a given proportion and compacted to achieve the desired densities. The concept mimics soil improvement by stabilization. Soil is compacted together with the reinforcing materials.

It differs from the other method of placement in the way the reinforcing materials are oriented. In random inclusion, fibres are mixed randomly in soil, making approximately homogenous

composite as opposed to the other method where materials are laid horizontally at specific intervals. Its drawback would be the probability of obtaining the homogenous mixture, which depends on the method of preparation and quantity of reinforcing materials in the mixture. However, with good quality control and assurance, these disadvantages can be mitigated.

The random inclusion concept is still new in modern geotechnical engineering as more focus is on the use of planar reinforcement (Swami, 2010). Nevertheless, it has some advantages over planar reinforcement. It maintains the soil's strength isotropy and limits the formation of a potential failure planes i.e. in random distribution; fibres make all the possible angles with any arbitrarily chosen fixed axis (Maher & Gray, 1990). It also makes it possible to use discrete materials such as fibres and industrial waste materials (Shukla et.al, 2009). Figure 2.5 (a) illustrates the method.

Random inclusion method is the focus of this research. It has been discussed extensively in section 2.4

2.4 Randomly distributed fibre reinforced soils

2.4.1 Relevant definition and concepts

Studies on randomly distributed reinforced soil are conducted based on fibre and soil parameters in a composite. To obtain the composite and the consequent variables, pertinent mix design is conducted based on the discussed relationships below, adapted from Li (2005) as given in equations 1 – 5.

The volumetric fibre content v_f , defined as:

$$v_f = \frac{v_f}{v} \quad (1)$$

Where v_f is the volume of fibres v and is the combined volume of fibre-soil composite

The fibre content computed as:

$$\rho = \frac{m_f}{m_s} \quad (2)$$

Where m_f the mass of fibres, and m_s is the dry mass of soil. ρ is normally given as a percentage. The fibre-soil composite dry unit weight, γ_d :

$$\gamma_d = \frac{W_s + W_f}{V} \quad (3)$$

Combining the above equations gives the relationship of volumetric and gravimetric fibre content as;

$$\rho_v = \frac{\rho \gamma_d}{(1 + \rho) G_f \gamma_w} \quad (4)$$

Where G_f is the fibres specific gravity and γ_w is the unit weight of water

The fibre monofilament configuration characterized by its length l_f and diameter d_f (aspect ratio), given as:

$$A_r = \frac{l_f}{d_f} \quad (5)$$

This is used interchangeably with the soil mean particle sizes as displayed in section 5.9

2.4.2 Reinforcing mechanism

Interaction mechanism of randomly reinforced soil differs significantly compared to systematically reinforced soil. While systematically reinforced soil is considered as homogenous and anisotropic, randomly fibre reinforced soil composite is taken as homogenous and isotropic. The mechanism can be best explained by simplified situations. Consider an unreinforced specimen, figure 2.6 (a) and a reinforced specimen, figure 2.6 (b) loaded axially. If $\sigma_a > \sigma_b$, then soil deforms as shown in the figures. On the contrary, with the inclusion of the fibres, the isotropy of the soil is maintained, figure 2.6 (b).

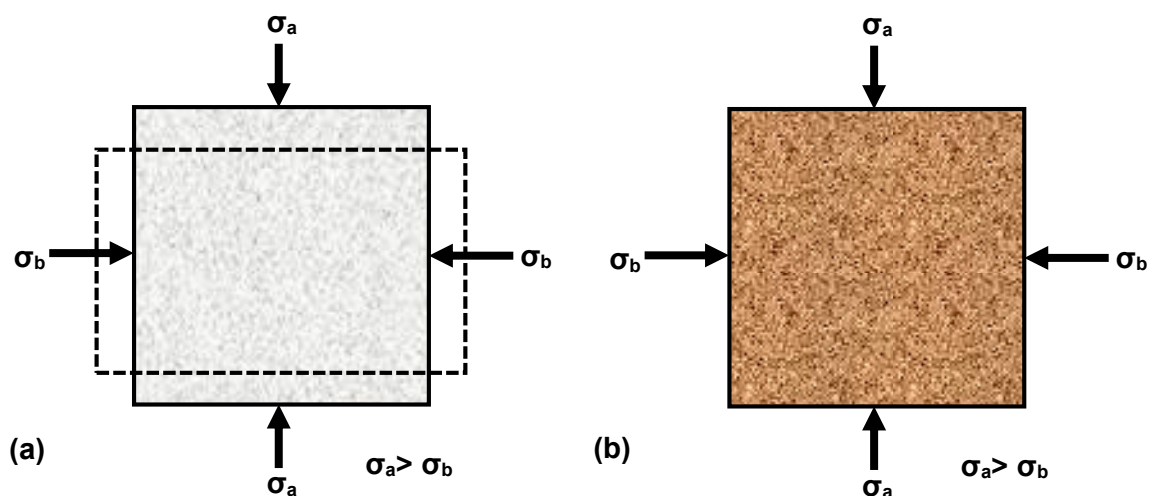


Figure 2.6: Idealised concept for the mechanism of randomly distributed reinforced soil (a) unreinforced and (b) reinforced

Incorporating fibres into soil resists soil's load deformation behaviour by interacting with the soil particles mechanically through surface friction and interlocking. The interlocking bond created mobilizes the tensile strength of the inclusions subsequently accommodating the stress transferred to the soil. This helps reduce the lateral deformation in approximately all directions. Therefore, discrete inclusions (short fibres) work as frictional and tension-resistance elements that constitute the principal pressures in the Mohr-Coulomb envelope.

Li (2005) and Shukla et al. (2009) mentioned an equivalent Mohr-Coulomb failure criterion that could be used to explain the shear mechanism by assuming that the reinforced soil is homogenous and isotropic. Maher and Gray (1990) who conducted a triaxial compression test on sand and presented a failure surface as predicted by the Mohr-Coulomb theory, showed this failure mechanism. The finding suggested a curved-linear or bilinear principal stress envelope, with a threshold confining pressure. Below this pressure, reinforced soils show higher friction angles (slip/pull) and above which, the shear strength envelope of fibre-reinforced soil is parallel to the unreinforced soil envelope as illustrated in the figure 2.7. This mechanism was supported by Consoli et al. (2007) who defined the failure envelope for sand-fibre composite by an approximated bilinear envelope distinctively well defined by a "kink" point. Below this critical point, fibre slip during deformation and beyond this, the yielding and minimal stretching of fibres is depicted. As shown in figure 2.8, the failure mechanism was found to be independent on the stress path in triaxial testing (critical stress).

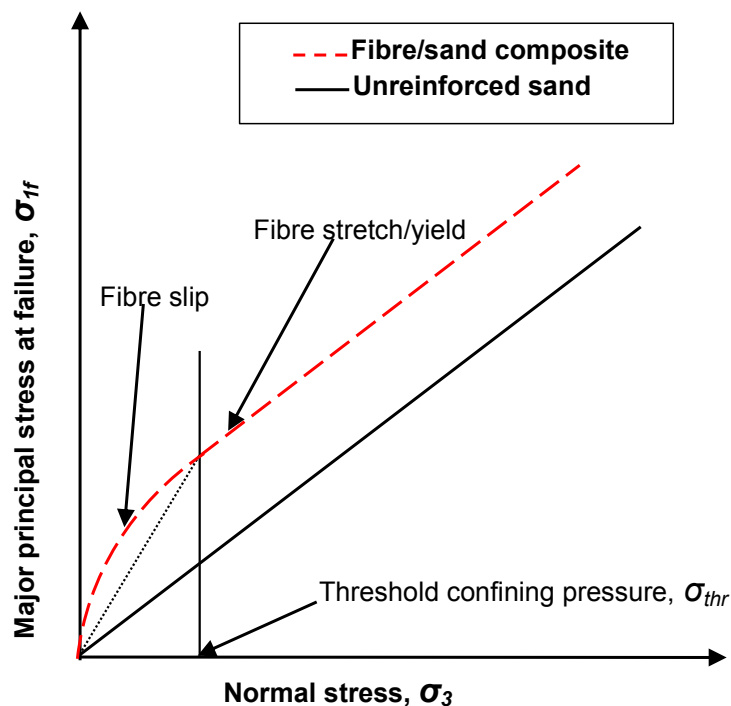


Figure 2.7: Model envelope of fibre-reinforced sand (redrawn from Gray & Ohashi, 1983; Li, 2005)

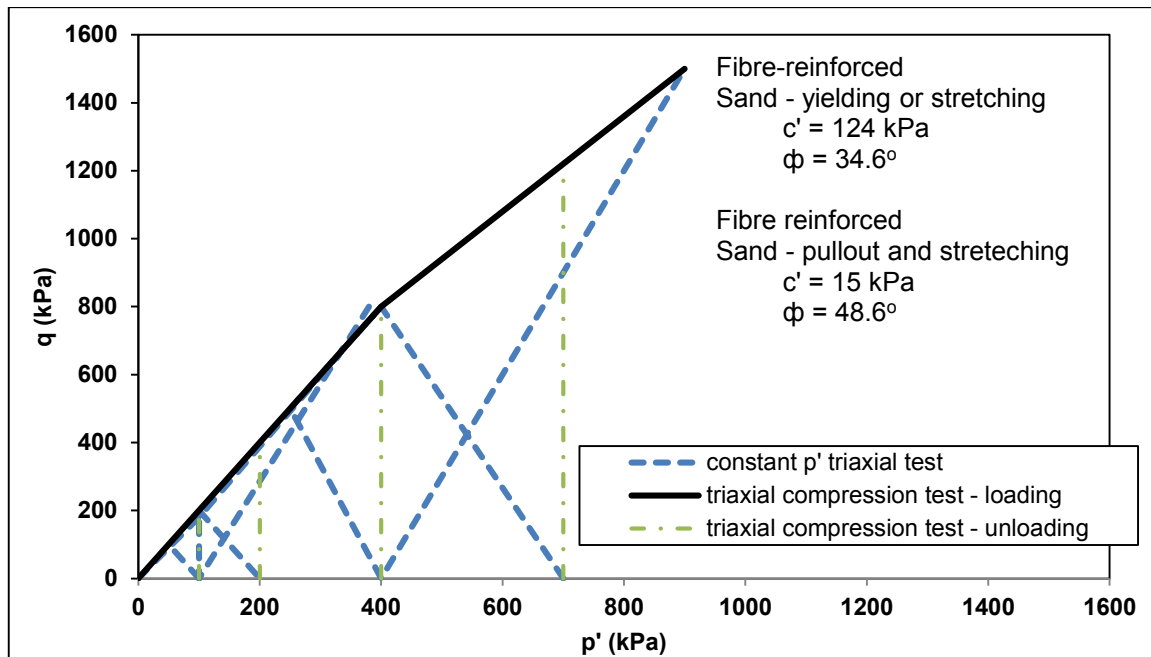


Figure 2.8: Shear strength envelope of Onsorio sand under triaxial testing (redrawn from figure 1b Consoli et al., 2007)

Nataraj and McManis (1997) on the other hand, conducted direct shear test on clay with fibrillated polypropylene and produced a Mohr-Coulomb shear strength envelope as a combination of curve-linear and linear sections as in figure 2.9. The direct shear test results at low normal pressures produced curved graphs and became linear at higher normal pressures.

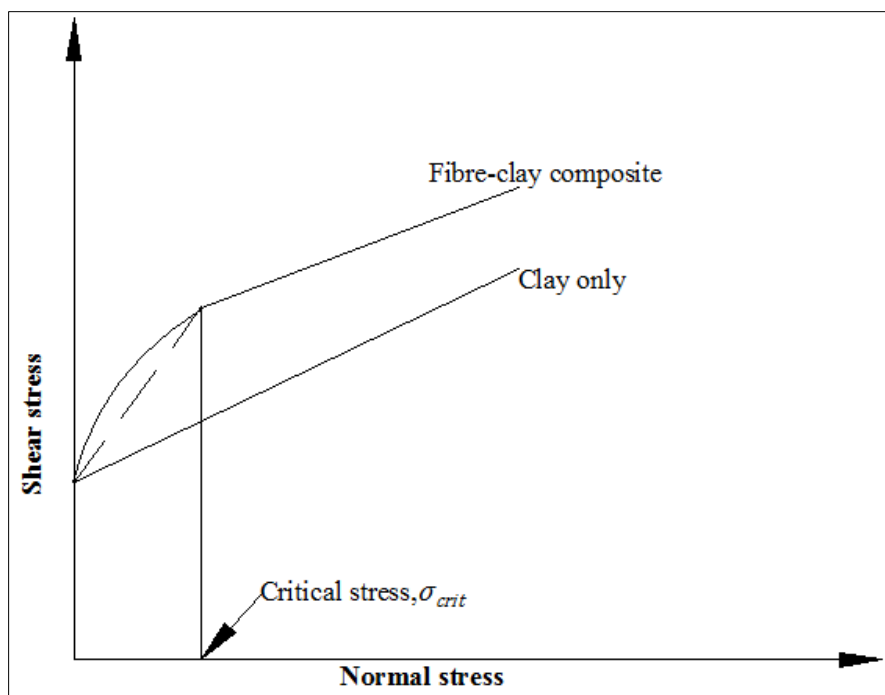


Figure 2.9: Model strength envelope of fibre-reinforced clay (adapted from Nataraj & McManis, 1997)

2.5 Predictive models

In understanding the interaction mechanism and the strength behaviour of randomly distributed fibre reinforced soils, some predictive and constitutive models have been proposed. The proposed predictive models can be summarised as mechanistic (Gray & Ohashi 1983, Maher and Gray 1990, Ranjan et al 1996), statistical (Zonberg 2002), and energy dissipation models (Michalowski and Zhao 1996). These models are formulated to help in predicting the behaviour in fibre reinforced soils without extensive laboratory testing.

Gray and Ohashi (1983) based on a series of direct shear tests conducted on sand, proposed a mechanistic/ force equilibrium model to predict the behaviour of fibre reinforced soils. They made several assumptions such as use of fibres long enough to extend on both sides of the shear plane and thin enough to offer resistance. Also, that the shearing of soils cause fibre distortion and at angle (θ) as shown in figure 2.10.

The fibre-induced tensile stresses developed along the shear plane, σ_t , was therefore determined by considering that the fibre lengths and the confining stresses are large enough to avoid pull out failure and exceeding skin friction respectively.

The induced tension was thus represented in the form of fibre modulus (E_f), interface friction (τ_f), fibre diameter (d_f), and thickness of the shear zone (z), as given in equation 6.

$$\sigma_t = \left(\frac{4E_f \tau_f}{d_f} \right)^{1/2} \{z(\sec\theta - 1)\}^{1/2} \quad (6)$$

This caused an increase in shear strength estimated by the model for fibres perpendicular to shear planes, equation 7.

$$\Delta S = t_f (\sin\theta + \cos\theta \tan\phi) \quad (7)$$

Where t_f is the mobilised tensile strength per unit area given by the ratio of area of fibre, A_f and total area of soil in shear (A), i.e. equation 8.

$$t_f = \left(\frac{A_f}{A} \right) \sigma_t \quad (8)$$

The increase in shear was also estimated for fibres oriented at angle, i to the shear planes as shown in equation 9 and 10.

$$\Delta S = t_f (\sin(90 - \Psi) + \cos(90 - \Psi) \tan \phi) \quad (9)$$

$$\Psi = \tan^{-1} \left[\frac{1}{k + (\tan^{-1} i)^{-1}} \right] \quad (10)$$

Where x is the horizontal shear displacement

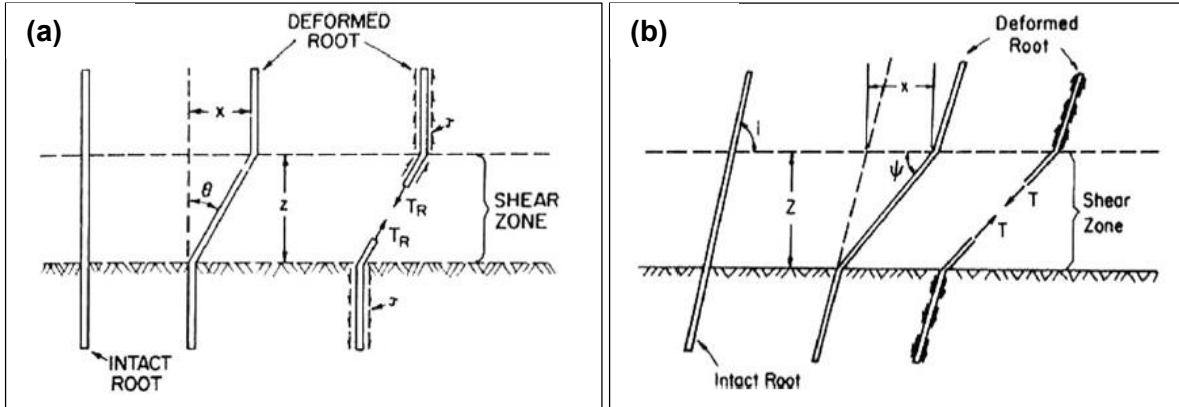


Figure 2.10: Fibre mechanistic model (a) vertical (b) inclined (Gray & Ohashi, 1983)

Maher and Gray (1990) further developed the mechanistic model, equation 6, through incorporating statistical concepts. Statistical concepts such as average embedment length as $\frac{1}{4}$ of the fibre length, fibre orientation as 90° – perpendicular to other plane and number of fibres, N_f estimated from equation 11. Equations 12 – 16 define the mechanistic model.

$$N_f = \frac{2v_f}{\pi d_f^2} \quad (11)$$

Fibre area ratio given by

$$\frac{A_f}{A} = N_f \left(\frac{\pi}{4} d_f^2 \right) \quad (12)$$

Giving an estimated fibre induced tension as:

$$\sigma_t = 2(\sigma_n \tan \delta) \frac{l_f}{d_f} \quad \text{for } \sigma_n < \sigma_{n,crit} \quad (13)$$

$$\sigma_t = 2(\sigma_{n,crit} \tan \delta) \frac{l_f}{d_f} \quad \text{for } \sigma_n \geq \sigma_{n,crit} \quad (14)$$

The change in shear given by Gray and Ohashi (1983) was thus modified to;

$$\Delta S = N_f \left(\frac{\pi}{4} d_f^2 \right) \left[2(\sigma_n \tan \delta) \frac{l_f}{d_f} \right] (\sin \theta + \cos \theta \tan \phi)(\xi) \quad \text{for } \sigma_n < \sigma_{n,crit} \quad (15)$$

$$\Delta S = N_f \left(\frac{\pi}{4} d_f^2 \right) \left[2(\sigma_{n,crit} \tan \delta) \frac{l_f}{d_f} \right] (\sin \theta + \cos \theta \tan \phi)(\xi) \quad \text{for } \sigma_n \geq \sigma_{n,crit} \quad (16)$$

Where δ = fibre skin friction in degrees, ξ = empirical coefficient based on the soil and fibre parameters, σ_n = confining stress acting on fibre, and $\sigma_{n,crit}$ = critical confining pressure corresponding to the threshold shear strength envelope.

Ranjan et al. (1996) having realized the complexity that comes with determining the orientation of the randomly distributed fibres and the thickness of the shear plane proposed by the mechanistic models derived a predictive model using regression analysis. They characterized the fibre-induced tension as a function of fibre content, fibre aspect ratio, fibre-soil interface friction and shear strength of unreinforced soil as given in equation 17.

$$\sigma_t = f(\rho, A_r, f^*, f, \sigma_{n,crit}) \quad \text{With } f^* \text{ given as } \frac{a}{\sigma_N} + \tan \delta \quad \text{and } f \text{ as } \frac{c}{\sigma_N} + \tan \phi \quad (17)$$

c , σ_N and a being cohesion, nominal confining stress (as assumed to be 100 kPa) and adhesion, respectively.

Michalowski and Zhao (1996) improved on the above models by proposing an energy-based model using the assumption that during shear, fibre slippage occurs on both ends of the fibre and the tensile rupture at the middle as shown in figure 2.11.

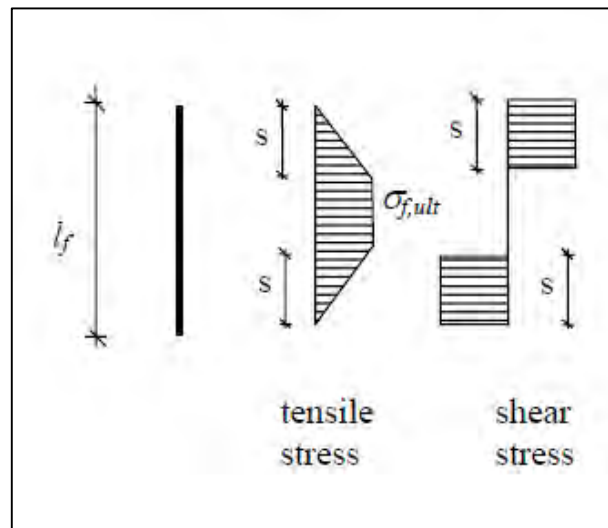


Figure 2.11: Deformation pattern of fibre-soil composite (Michalowski, 2003)

The researchers considered five variables: volumetric fibre content, fibre aspect ratio, fibre yield stress, soil/fibre interface friction and angle of internal friction of the soil. In addition, the plastic deformation phase of the energy dissipation was considered insignificant while the slippage and rupture phase was considered crucial for a single fibre. Slippage and rupture are expressed by equation 18.

$$d = \pi d_f s^2 \sigma_n \tan \delta \langle \varepsilon_\theta \rangle + \frac{1}{4} \pi d_f^2 (l - 2s) \sigma_{f,ult} \langle \varepsilon_\theta \rangle \quad (18)$$

Integrating equation 18 over the volume of reinforcement composite formed, gives the total energy dissipation rate per unit volume of the soil, D in equation 19.

$$D = v_f \sigma_{f,ult} M \left(1 - \frac{\sigma_{f,ult}}{4A_r p \tan \delta} \right) \frac{\varepsilon_1}{3} \quad (19)$$

Where p was given as the average between the confining pressures

Michalowski and Cermak (2003) validated the model proposed by Michalowski and Zhao (1996) through laboratory experiments and introduced a concept of macroscopic angle of internal friction ϕ_r as given in equation 20 – 21.

$$\phi_r = \tan^{-1} \sqrt{\frac{v_f A_r M \tan \phi + 6k_p}{6 - v_f A_r M \tan \phi}} - \frac{\pi}{2} \quad (20)$$

$$\text{Where, } M = k_p \sin \left(\tan^{-1} \sqrt{\frac{k_p}{2}} \right) \text{ and } k_p = \frac{1 - \sin \phi}{1 + \sin \phi} \quad (21)$$

The energy model prediction was approximately consistent with the laboratory results as shown in figure 2.12.

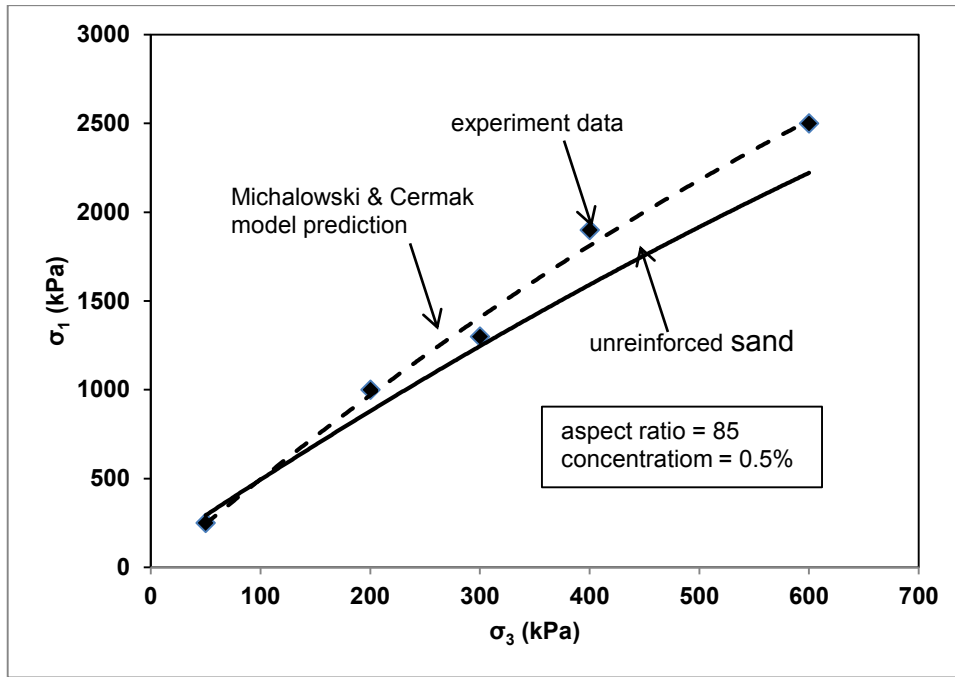


Figure 2.12: Comparison of prediction and experimental results for coarse sand reinforced with polyamide fibres (redrawn from Michalowski and Čermák, 2003)

Zornberg (2002) proposed a discrete model that considered the equivalent shear strength based on individual characterization of soil and fibre specimens. In the discrete model, quantifying the parameters of individual soil and fibre (equation 22) is required as opposed to testing the soil-fibre composites as in the previously discussed models.

$$\tau_{eq} = \tau + \alpha t = c + \sigma_n \tan \phi + \alpha \sigma_t \quad (22)$$

Where α is an empirical coefficient accounting for partial contribution of fibres, assumed as 1 for randomly distributed fibres and σ_t is the fibre induced tension defined as tensile force per unit area. ϕ and c being the shear strength parameters of unreinforced soil.

At low confining pressures, pull out of fibres is more predominant modifying the expression to equations 23 – 25.

$$\tau_{eq,l} = c_{eq,l} + \sigma_n + (\tan \phi)_{eq,l} \quad (23)$$

$$c_{eq,l} = (1 + \alpha v_f A_r c_{i,c}) c \quad (24)$$

$$(\tan \phi)_{eq,l} = (1 + \alpha v_f A_r c_{i,c}) \tan \phi \quad (25)$$

$c_{i,c}$ and $c_{i,\phi}$ being interaction coefficients similar to those obtained from planar reinforcement

defined as $c_{i,c} = \frac{a}{c}$ and $c_{i,\phi} = \frac{\tan \delta}{\tan \phi}$ where a is the adhesion between the soil and fibres and

δ the interface friction. The expression yields a bilinear shear strength envelope similar to the one proposed by Gray and Ohashi (1983) in figure 2.10.

Sadek et al (2010) reviewed the energy and discrete models and listed some of the limitations of the models. The models do not incorporate the grain-size effect, the maximum concentration limit on effectiveness of the reinforced sand, the flexural stiffness of fibres and averages the fibre-soil interface shear stress. The researchers further conducted a direct shear test on coarse and fine sands, and concluded the energy dissipation model as the best predictor of the behaviour of reinforced soil as shown in figure 2.13.

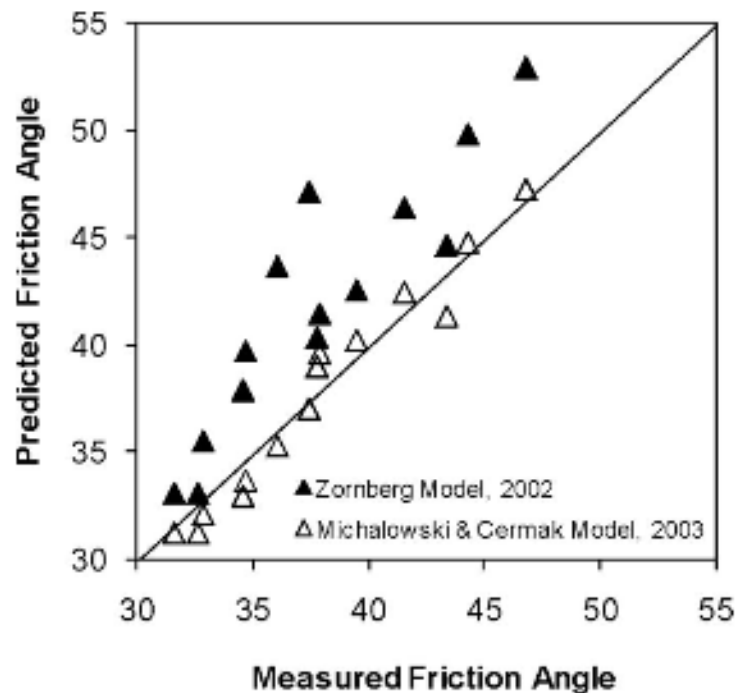


Figure 2.13: Comparison between predicted and measured friction angles based on energy and discrete models (Sadek et al 2010)

Predictive model by Ranjan et.al (1996) formed the basis of the regression analysis discussed in chapter 5 for this study. The model was favoured due to its simplicity in relating the shear strength behaviour reinforced sands with the descriptor variables. However, the model could not be applied entirely since the variables were generated using triaxial test. Furthermore, the model considered length of the fibres, which was very cumbersome to determine for bagasse fibres.

2.6 Review of previous research on fibre reinforcement

Studies on fibre-reinforced soils have been conducted using a number of tests in the laboratory such as triaxial tests (CU and CD), CBR, UC, and direct shear tests. This subsection discusses those variables that affect the behaviour of fibre-reinforced soils and specifically limits it to those variables that have a bearing on this study. That is, fibre content, type of soil and effect of water and the durability issues of fibre-reinforced soils.

2.6.1 Effect of types of soil on fibre reinforcement

2.6.1.1 Sandy soils

The majority of the studies involving fibre reinforcement were conducted using granular soils (e.g. Gray & Ohashi, 1983; Maher & Gray, 1990; Michalowski & Čermák, 2003; Sadek et al., 2010; Gao & Zhao, 2013). Gray and Ohashi (1983) using direct shear tests on reinforced sand concluded that an increase in shear strength is directly proportional to the fibre area ratio and concentration of up to 1.7%, and is greatest at 60° orientation to the shear plane. This increase was approximately the same for loose and dense sand with larger strains required for peak strengths in loose sand. These findings were contrary to those by Anagnostopoulos et al. (2013) that showed no improvement in strength of fibre reinforced dense sand.

Al-Refeai (1991) carried out triaxial tests at different confining stresses on different grades of sandy soils and fibres. The effect of reinforcement was more apparent for fine sub-rounded sand compared to medium-grained sand with sub angular particles. The behaviour of the sand was dependant on the soil-fibre interaction and the extensibility of the fibres. Sadek et al. (2010) also presented similar results by concluding that the reinforcing effect was more profound in fine sands at smaller fibre concentration. However, the trend was reversed in coarse sand at larger fibre concentrations resulting in higher shear strengths, a phenomenon known as fibre-grain scale effect. Michalowski and Cermak (2003) explained this behaviour as the macroscopic influence of the grains in sandy soils.

Sadek et.al (2010) in their study of the effect of sand particle sizes on fibre-reinforced sandy soil showed that the magnitude of peak shear strength depended on the fineness of the sand, fibre content and relative density. Fine sand depicted higher increase in shear strength than coarser sands at lower concentration of 0.5% with a reduction at higher concentration of 1.0%. Tests conducted on Ottawa sand ($D_{50}=0.39$ mm) and BGL sand ($D_{50}=1.45$ mm) indicated a maximum improvement of 17% at 1% fibre content in Ottawa sand (fine) and 22% in BGL sand (coarse) as illustrated in figure 2.14. Anagnostopoulos et al. (2013) confirmed these findings by concluding that fibre reinforcement significantly improved the peak strength of fine

sands by 22.5% compared to 2.4% at 0.5% fibre content for medium dense coarse sand. However, the improvement was insignificant in high dense state sands, 7.8% and 0.1% for fine and coarse sand respectively.

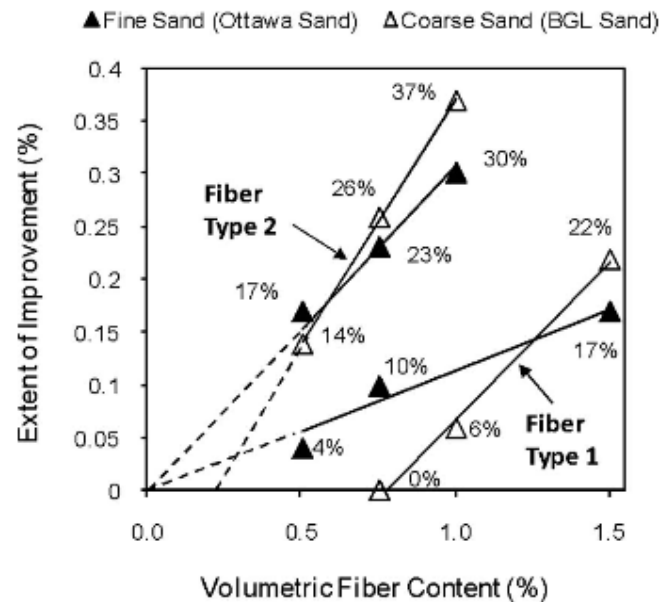


Figure 2.14: Experimental comparison of fine and coarse sands with fibre content (Sadek et al., 2010)

Yetimoglu and Salbas (2003) studied shear strength of fibre-reinforced sands using direct shear tests at 0.1 – 1% fibre content. They found out that fibre reinforcement insignificantly affected the peak shear strength and residual shear strength of the sand and showed a 4.5% reduction in angle of internal friction at 1.0% fibre content. Findings that were contrary to those by Shao et al. (2014), presented an increase in the peak shear strengths from 2.0° - 7.3°. Nevertheless, the researchers alluded to fibre reinforcement reducing soil brittleness, which consequently resulted into a smaller loss in post-peak strength.

2.6.1.2 Cohesive soils

Limited studies have been conducted on fibre-reinforced clay soils due to the difficulty in quantifying the interaction mechanism between fibres and cohesive soils (Li, 2005); interaction mechanisms such as volume change tendency and strain rate of cohesive soils. Still, fibre inclusions improve the strength of cohesive soils mostly studied through UCS, CU and CD tests.

Estabragh et al. (2013) conducted a study on the mechanical behaviour of fibre clay composite using oedometer and triaxial tests. The results indicated a decrease in preconsolidation pressure of up to 44%, 30% increase in compressibility and swelling indices of 0.006 to 0.027 at 30% palm fibre content. The strength and friction angle also increased considerably in terms

of both total and effective stresses to a maximum of about 18 and 33% at the same fibre content.

Mirzababaei et al. (2012) investigation of the unconfined compression of reinforced clay revealed that the effect of carpet waste fibres inclusion into clay soils depended on the clay dry unit weight, moisture content and fibre content. Inclusion of 1 – 5% of carpet waste significantly enhanced the unconfined compression strength (UCS), reduced post peak strength loss by 5%, and changed the failure behaviour from brittle to ductile. In addition, carpet waste reinforcement gradually transformed failure patterns from the apparent classical failure for unreinforced soil specimens to barrel-shaped in reinforced soil.

Figure 2.15 show the direct shear result of clay reinforced with fibres according to the study by Nataraj and McManis (1997) who concluded that 0.3% fibre concentration produces maximum shear strength.

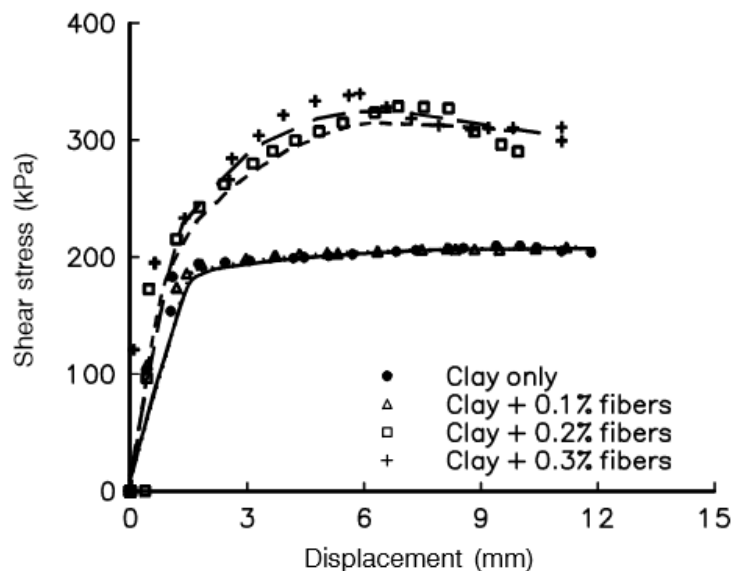


Figure 2.15: Stress-strain relationship of unreinforced and reinforced clay (Figure 4 of Nataraj and McManis)

2.6.2 Effect of fibre content

Most of the previous research majorly focused on quantifying the effect of fibre content (percentage of fibre as dry weight of the soil) on fibre-reinforced soils. As summarised in table 2.4, fibre content studied varied across research based on type of fibres and soil used in the study. A general conclusion is that increasing fibre content improves the shear strength parameters of soils.

As examples, Michalowski and Cermak (2003) established that the increase in fibre concentration up to 2% increases shear strength by about 70% even though this improvement

also depends on aspect ratio, fibre length and the relative size of the grains. Profound improvement was depicted at high concentration and longer fibres greater than the size of the grains.

Additionally, effect of fibre has been studied by increasing the content of fibre systematically until an optimum threshold is achieved. Maximum strength is achieved at optimum fibre concentration and beyond this point; an increase in fibre concentration reduces shear strength. This optimum content also depends on the type of fibre, soil and test regime used and varies across different authors. For instance, Shao et al. (2014) by conducting a direct shear ring test on fibermesh-reinforced soil showed an asymptotic upper limit at 0.9%, beyond which inclusion of fibres decreased shear strength. Many of the other researchers e.g. (Yetimoglu & Salbas 2003; Sadek et al. 2010; Anagnostopoulos et al. 2013) also had a general consensus of the fibre concentration range beyond which segregation occurs as being between 0.1 - 2% of dry weight of soil.

Another predominant outcome on shear strength with fibre content is the similarity of stiffness obtained at low strains regardless of the fibre content. For example, Li and Zornberg (2013) showed that soil-fibre composite compacted at 65% relative density depicted a more ductile behaviour (less loss of post-peak strength) at higher fibre content and similarity between unreinforced and reinforced soil at the initial portion of the stress- strain curves as shown in figure 2.16 (a). Similar results showing no improvement at low strains and great improvement at high strains were obtained by Shao et al. (2014). This phenomenon has been attributed to sliding of fibre at low strains and the pulling/ stretching at high strains, figure 2.16 (b).

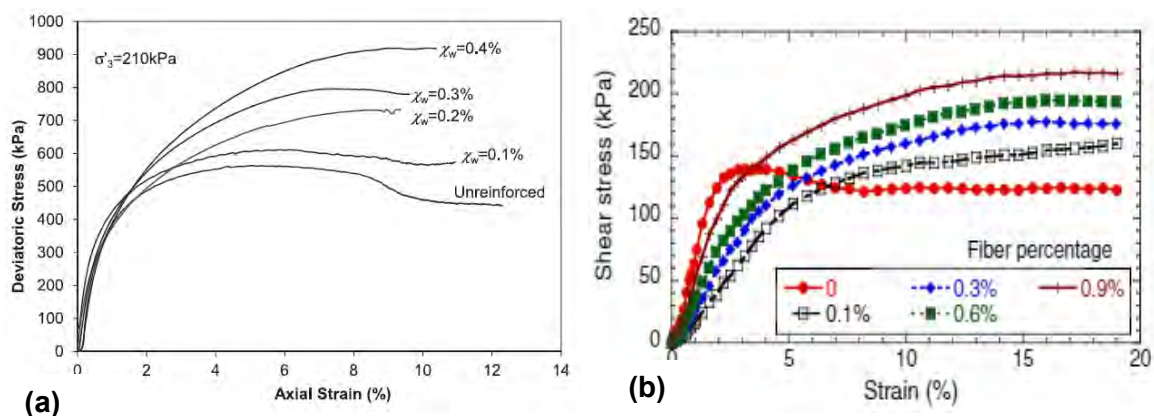


Figure 2.16: Effect of fibre content on the stress-strain relationship, showing no change in initial stiffness ((a) Li and Zornberg, 2013 (b) Shao et.al 2014))

Table 2.4: Selected previous studies on natural fibres

Authors	Fibre type (natural)	Fibre length	Fibre concentration	Soil type	Test type
Prabakar and Sridhar (2002)	Sisal	10 – 25 mm	0.25 – 1%	Clayey	Undrained triaxial 69 – 207 kPa
Yetimoglu & Salbas, (2003)	Polypropylene	20 mm	0.1 – 1 %	Sand	Direct shear 100-300 kPa
Cao (2006)	Bagasse in composite		5 – 20%	Composite	Tensile
Sivakumar & Vasudevan (2008)	Coir	10 & 25 mm	1 – 2%	Tropical	Triaxial 50 – 150 kPa
Marandi (2008)	Palm	20 – 40 mm	0.5 – 2.5%	Silty-sand	UCS, CBR
Osinubi et al. (2009)	Bagasse ash	Ash	8 – 12%	Lateritic	UCS, CBR
Sadek (2010)	Undisclosed	7 & 27 mm	0.5, 1, 1.5, 2%	Sand	Direct shear 100, 200 kPa
Jamellodin et al., (2010)	Oil Palm		0.2 – 1%	Clay	Triaxial 70 – 20 kPa
Amu et al. (2011)	Sugarcane bagasse	Ash	2 – 8 %	Lateritic	UCS, CBR, Triaxial
Maliaka & Thiyyakkandi (2013)	Coir	12, 24, 36 mm	0.5 – 1%	Clay	Triaxial 50 – 200 kPa
Mirzababaei et al., (2012)	Carpet waste	2 – 5 mm	1, 3, 5%	Clay	UCS
Estabragh, et al., (2013)	Palm	4 mm	20 – 30%	Clay	Triaxial 200 – 400 kPa
Sarbaz et al. (2014)	Palm	20 – 40 mm	0.5 – 1%	Sand	CBR

2.6.3 Effect of water content on reinforced soil

There exists a relationship between effective stress and the water content of unreinforced soil. Das (2002) showed that as water content is increased, the shear strength of soil decreases and increases across different water content up to optimum moisture content. In general and according to Holtz and Kovacs (1981), a difference of $1 - 2^\circ$ angle of internal friction exists between dry and wet sand.

Lovisa et al. (2009) in their study on moist reinforced sand showed a reduction in internal friction with increasing moisture content as presented in figure 2.17. This occurrence is attributed to the reduced friction between soil particles because of the additional lubrication. In addition (from figure 2.17), adding water to unreinforced sand introduced an apparent cohesion of 5.3 kPa which the authors attributed to the capillary tension/menisci in pore water which binds particles together. Similarly for the reinforced sand, apparent cohesion independent of the amount of water added was observed, figure 2.17(b).

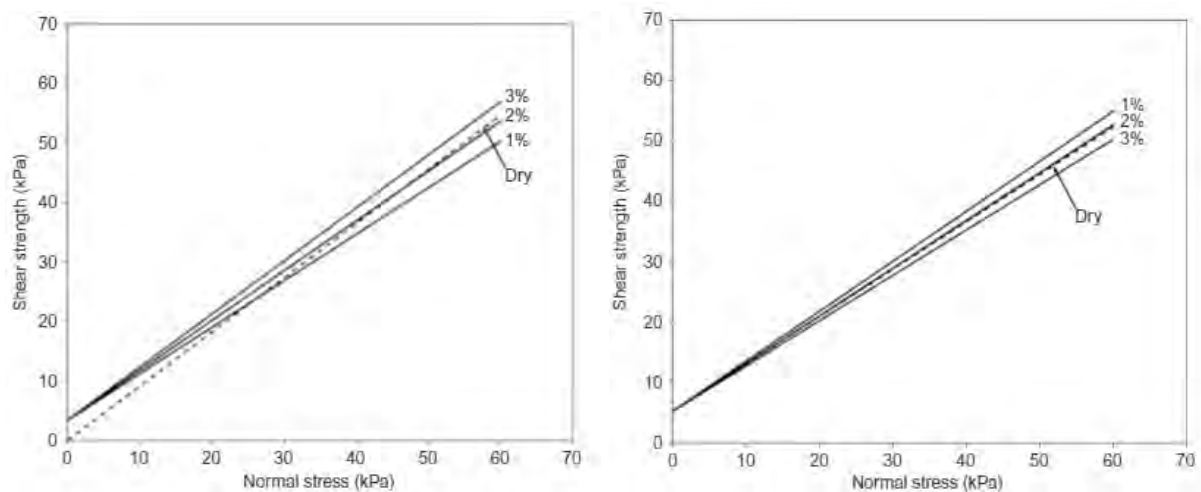


Figure 2.17: Shear envelope of (a) unreinforced sand (b) reinforced sand with increase in water content (Figure 6 and 7 of Lovisa et.al, 2010)

2.6.4 Durability and effect of fibre coating

Natural fibres find their application in geotechnical applications justified by their ready availability, cost and environmental benefits. However, natural fibres have some practical problems of reproducibility and biodegradability due to their susceptibility to alkali attack and decay in the presence of moisture. These drawbacks limit, to some extent, the applicability of these fibres in geotechnical applications. As summarised in table 2.5, durability according to Jones (1996) is one of the factors affecting the use of reinforced soils. This sub-section therefore, discusses some of the research aimed at reducing the water uptake of natural fibres

and making them more durable. The morphology and the effect of water on the morphology of fibres are discussed further in Chapter 3.

Chemical coatings using polymer compounds and alkali treatment have been found beneficial in preventing moisture and alkali attack on fibres. For example, Rahman et.al (2007) indicated that physical and chemical alteration reduces the fibre water intake and increases tensile strength by 20%, figure 2.18. Ahmad et al., (2010) used acrylic butadiene styrene, a polymer of styrene, acrylonitrile and polybutadiene in coating fibres. They showed that coating the fibres with an acrylic material improved the structural characteristics of fibres and increased shear strength of fibre-reinforced soil. Contrary results were obtained by Sarbaz et al. (2014) who established that coating palm fibre with bitumen reduced the CBR strength of soil-fibre composite by 22% after 48 hours of submerging in water. The reduction in CBR was attributed to the reduced sliding mechanism when fibres are coated with bitumen. The study also showed that dry and wet conditions over a period of between 5 – 60 days have no considerable effect on the degradation of natural fibre-soil composite.

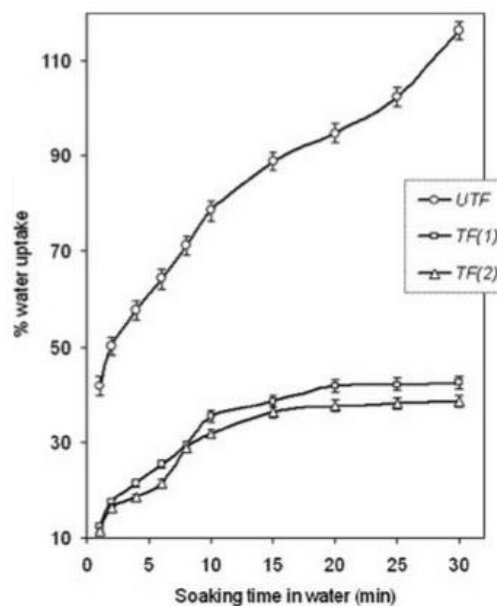


Figure 2.18: Water take between untreated fibres (UTF) and treated fibres (TF1, 2, Rahman et.al (2007))

Pozzolans have also been used in solving the biodegradability of natural fibres. Studies confirmed that some natural fibres behave like pozzolans with a cementation effect that would interlock and hold the soil-fibre composite. For example, rice husk ash (Gram & Nimityongskul, 1987) as cited by Stephens (1994). Stephens (1994) suggested that sugarcane bagasse ash could offer the cementation effect because it has high silica content and thus may display similar pozzolanic properties.

Durability studies form part of this study and have been extensively discussed in Chapter 4 and 5.

Table 2.5: Factors affecting soil reinforcement (adapted from Jones, 1996)

Reinforcement	Reinforcement distribution	Soil properties	Soil state	Construction
Form (fibre grid, anchor, bar, strip)*	Location	Particle size*	Density (void ratio)	Geometry of structure
Dimensions *	Orientation	Grading	Overburden	Compaction
Strength	Spacing	Mineral content	State of stress*	Construction system
Stiffness (bending, longitudinal)	-	Index properties	Degree of saturation	Aesthetics
				Durability*

*Relevant to the study

2.7 Studies carried out on bagasse fibre

Sugarcane bagasse (SCB) has received little attention as a standalone reinforcement material. A major reason according to Hejazi et al. (2012) is that sugarcane bagasse has limited structural properties within the fibre and because of the residual sugars that impede structural strength of bagasse under moist conditions. However, no study has been conducted to support this; in fact, the lack of SCB use can be attributed to the lack of research and design criteria as opposed to structural implications.

Conversely, studies have considered SCB in cement and polymer composites (e.g. Bilba et al, 2003; Cao, 2006; Loh et al., 2013)., Osinubi et al. (2009) in their study concluded that 2% of sugarcane bagasse ash improves the CBR of lateritic soils and could be used in sub base for low load roads. However, this improvement yielded a low CBR value of 16% compared to the required 180%, concluding that SCB ash would not be used as a stand-alone stabilizer, but rather as an admixture. This is due to the loss of strength with the increase in moisture content.

Cao (2006) observed that tensile and flexural strength of soils increased with an increased SCB content up to an optimum fibre content of 65%. He also observed that treating SCB with 1% NaOH improved the optimum tensile strength by 13% as shown in figure 2.19. This stronger fibre-matrix adhesion was attributed to the breaking down of the hemicellulose by the alkali and the increased aspect ratio.

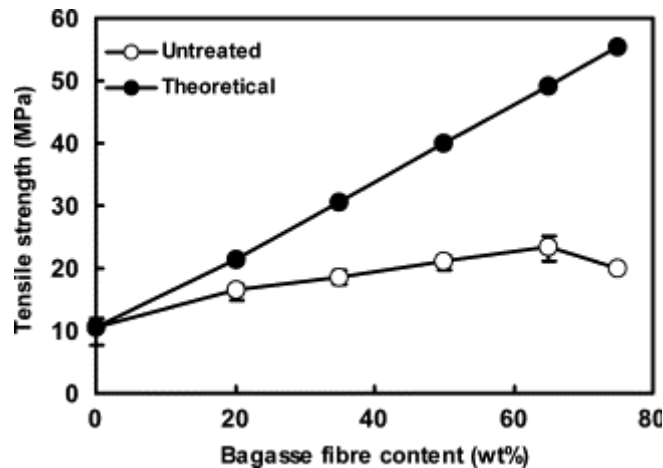


Figure 2.19: Effect of fibre content on tensile strength of untreated bagasse fibre composites (Cao, 2006)

2.8 Potential application

Hejazi et.al (2012) in their fibre application review mentioned several areas where fibre is applied in improving the engineering properties of soils. Some of the research that highlighted the potential application of the fibre-reinforced soil is outlined below.

Fibre-reinforcement has been used in subgrade stabilisation. Tingle et al. (2002) carried a full-scale study on low-volume roads stabilised with fibres. They concluded that sand stabilised with fibres could be an alternative for conventional construction where settlement is not considered, like temporary constructions.

Fibre-reinforcement has also been proposed for stabilisation of expansive soil (Puppala, 2000). Fibre can enhance the unified compression strength of clayey soil, reduce shrinkage and swell pressures. Free swell potential of the soil may also be improved.

Fibre reinforcement was also studied to reduce the desiccation cracks in clayey soils instigated by wet-dry cycles. In this study, reinforcing with fibres created an interlocking bond with soil, which prevented tension crack that would have developed for cohesive soils as investigated by Ziegler et al. (1998).

Most of the potential applications mentioned above considered the use of synthetic fibres as reinforcing materials. Synthetic fibres were preferred due to their hydrophobic properties when subjected to wet conditions. Of all the natural fibre applications reviewed, minimal usage was reported on natural fibres as a standalone reinforcing material. Nevertheless, extensive applications were presented on their use as composite material. For instance, jute fibres were found to be useful in sub-grade stabilisation (Aggarwal & Sharma, 2011). Similarly, Coir and palm fibre showed potential use as a reinforcing material for landfill cover applications.

2.9 Summary of the literature reviewed

Most of the notable previous investigations (as summarised in table 2.4) on fibre-soil composites considered various factors that affect the strength characteristics and other engineering properties of soils and concluded that the effect on strength and stiffness is a function of;

1. Soil types and properties that include shape and particle size gradation of the soil.
2. Fibre characteristics such as fibre type, length, aspect ratio, fibre-soil friction, concentration as a weight fraction, modulus of elasticity and degradability.
3. Test conditions e.g. method of mixing, confining stresses and method of testing.

The literature review examined the work carried out on the investigation of the effect of natural fibre inclusion on the mechanical behaviour of soil-fibre composite. The behaviour was discussed based on the shear strength, type of soil, fibre content and durability (moisture content), which were relevant to the study. It can be concluded that:

- Fibres have been used to reinforce both granular and cohesive soils. The effect on granular soil depends on the grain size, angularity and moisture content with dilation being the main contributor to shear strength. Similarly, the effect on cohesive soils depends on the clay fabric, although with difficulty in quantifying the interaction mechanism.
- Random inclusion of fibres maintains soil strength isotropy and reduces the weakness planes that would exist parallel to the reinforcing material. However, conflicting conclusions were drawn on the isotropic behaviour of soils, especially on sands. While one school of thought reported a bilinear effect, the other presented a unique normal compression line. Bilinear failure mechanism was attributed to the slipping of the fibres, lack of adhesion below critical confining pressure, and soil pull above the critical confining pressure.
- Peak strengths, stiffness, ductility, residual response of soil-fibre composite are affected by the increase in geometric properties of fibres. The magnitude of the influence is also governed by the sample distribution, confining pressures and mode of sample preparation. However, no uniform fibre geometric properties were observed. The range of fibre length and concentration varied from one fibre to the next making comparison very difficult with a lot of variation.
- An optimum fibre concentration exists beyond which any further addition of fibre has no effect on the mechanical behaviour of reinforced soils. At higher fibre concentrations, the segregation of the fibres takes place, uniform mixing is hindered

and the frictional force between the soil and the fibres is reduced. The optimum fibre content varied depending on the type of fibre used in the various studies.

- There are limited applications of the natural fibre reinforcement technique compared to synthetic fibres. Studies attributed this to the problems of reproducibility and biodegradability. However, physical and chemical modification of the fibres were studied and recommended by some of the researchers to solve these problems.
- Most of the previous researchers used either a 60 x 60 mm or a 100 x 100 mm direct shear box. This presented boundary effect and limited the length of the fibres thereby requiring an extensive characterization of the fibre lengths. Moreover, the process of hand mixing the fibres, even though presented homogenous mixtures, would be very difficult to achieve on large-scale projects.

As evident above, extensive research has been conducted on natural fibre reinforcement, using both cohesive and granular soils spanning a wide range of parameters. However, none has considered use of bagasse fibre as a stand-alone soil reinforcement element. Most studies involving the use of sugarcane bagasse have considered it in producing polymeric composite materials (Loh et al., 2013). Owing to the limitations identified in literature, this study improved on the existing literature by showing that sugarcane bagasse fibre could be used as a stand-alone reinforcement material.

Secondly, through this research study, the concerns on the degradability of the natural fibres were tackled. Nevertheless, it was found that the degradability of the fibres is constant after about 2 days of soaking in water and could be solved through coating/treating the fibres with polymers or adequate sub-soil and surface drainage.

Furthermore, the study also showed that the improvement on the strength parameters of fibre-reinforced soil does not depend on the tensile strength of the fibres but on the quantities of fibres, length of fibres and their interactions with soils. Lastly, this study improved on the type of testing method by using a large direct shear of 305 x 305 mm and a rotary mechanical mixer in obtaining the uniform mix between the fibres and the soil.

CHAPTER 3

3 REVIEW OF PLANT NATURAL FIBRES

3.1 Introduction

This chapter presents a review of the general characteristics of natural plant based fibres, their composition and established mechanical properties that would make them unique as a reinforcing material. It also discusses sugarcane bagasse fibre in particular, giving an overview of the South African sugar industry and the process of obtaining bagasse fibre from sugarcane. The chapter concludes with a comparison of the structural component of bagasse fibre with other natural fibres that could make it an ideal material for meeting the study objectives.

3.2 Natural fibre characterization

Natural fibres are mostly plant based with different morphological constitutions depending on the part of plant they are extracted from, either from stem, seed, root or grass. They can also be obtained from animals or minerals. According to John and Thomas (2008), plant fibres include bast, seed, fruit wood, cereal and straw, and grass fibres as presented in figure 3.1.

Apart from the raw material and origin, natural fibres are different from the engineered synthetic fibres in their geometry and chemical structure. The geometry of the natural fibres is made up of bundles of elementary fibres consisting of voids and defects of irregular cross-sections unlike the uniform monofilaments in the synthetic fibres. In addition, the chemical structures of natural fibres have varying surface energy and available bonding sites along their fibre length. This is due to the various natural polymers which creates these bundles of the elementary fibres (Fuqua et al. 2012).

The structural strength of natural fibres as well as their physical and chemical compositions is presented in details in the subsequent sections. It should be noted that these compositions are reviewed in light of their importance in soil reinforcement.

3.3 Composition of natural fibres

Natural fibres structure consists of cellulose, hemicellulose, lignin, pectin, and waxes. These constituents vary depending on the fibre type, prevailing growing conditions, maturity and digestion processes (Fuqua et al. 2012). However, cellulose tends to be more predominant of all the compositions. Therefore, the structure of natural fibres is generally of cellulosic fibrils embedded in lignin matrix.

Generally, cellulose provides the mechanical strength of natural fibres when used in reinforcement (Fuqua et al. 2012; Azwa et al., 2013; John & Thomas, 2008). With an increase

in cellulose, the tensile and flexural strength of fibres increases. Increase in other non-cellulosic components tends to reduce the modulus and strength of fibres.

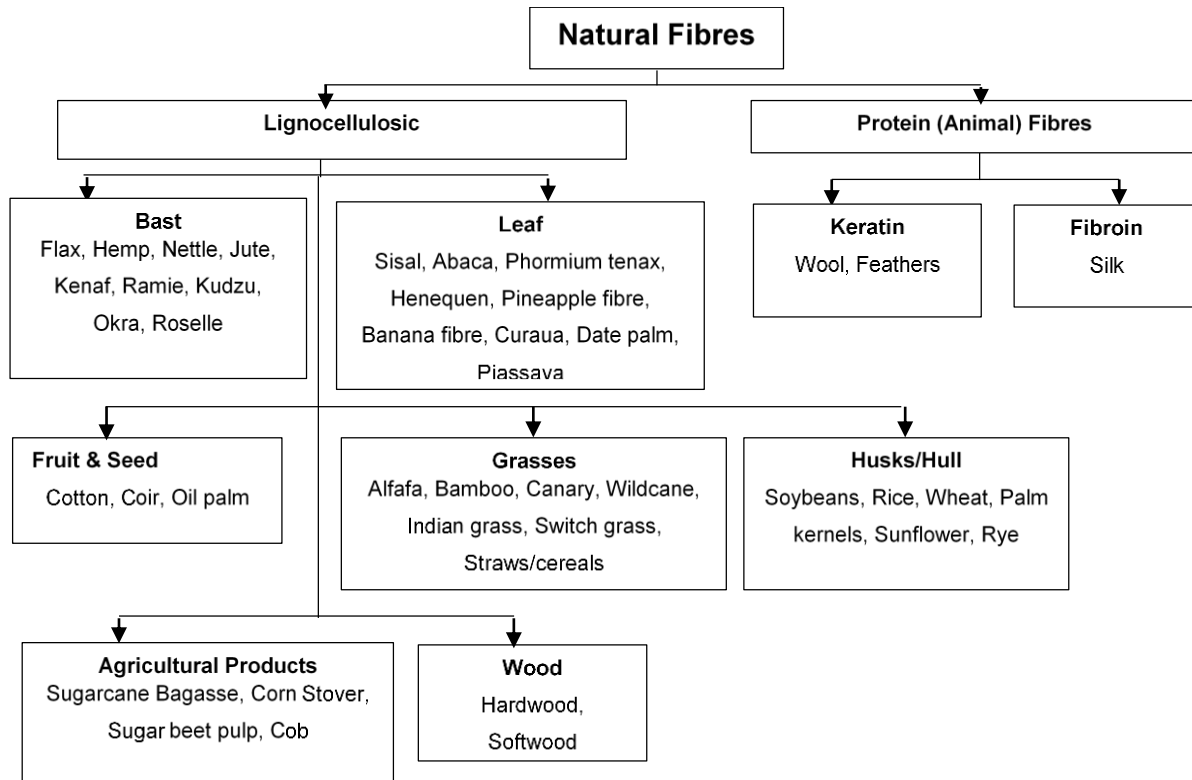


Figure 3.1: Subdivision and origin of natural fibres (adapted from Fuqua et. al, 2012)

3.3.1 Cellulose

Cellulose is a natural polymer consisting of repeating units with each unit containing three hydroxyl groups (d-anhydroglucose, $C_6H_{11}O_5$) joined by β -1, 4-glucosidic linkages as shown in the figure 3.2. It is identified in plants as slender-like crystalline microfibrils along the length of the fibre. The existence of the hydroxyl group gives rise to strong hydrogen bonds and van der Waal forces forming a microcrystalline structure with regions of high and low order i.e. crystalline regions and amorphous regions respectively.

Azwa et al., (2013) found out that the formation of the hydrogen bond gives cellulose a high resistance to hydrolysis, alkali and oxidising agents but cellulose becomes biodegradable in chemical solutions. The crystalline nature gives cellulose a strong tensile strength, which is a crucial characteristic in reinforcement responsible for propagating with a degree of polymerisation (number of glucose units bound together) of around 10,000.

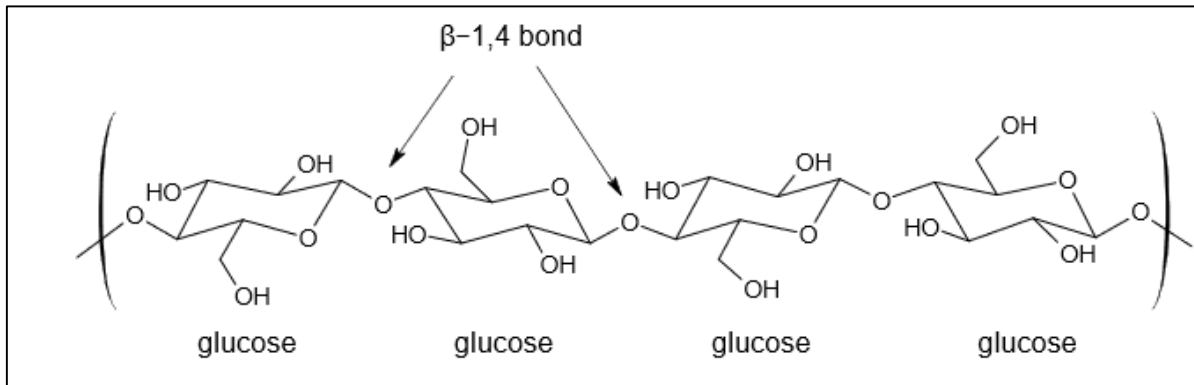


Figure 3.2: Molecular structure of cellulose (Watford, 2008; Faqua et al., 2013)

3.3.2 Hemicellulose

Hemicellulose is a group of polysaccharides; xylose, mannose, glucose, galactose, and arabinose composed of a combination of 5- and 6-carbon ring sugars, as shown in figure 3.3. Bagasse hemicellulose specifically has a number of xylose linked with glucose and arabinose sugar units (Watford, 2008). Hemicellulose is not a form of cellulose and acts as a cementing matrix between cellulose microfibrils and can be identified at the interface of cellulose and lignin. Hemicellulose is highly hydrophilic, soluble in alkaline solution, and easy to hydrolyse in acid. Being a polysaccharide, it contains several different sugar units compared to only 1, 4- β -d-glucopyranose units in cellulose. In addition, it is a purely amorphous branched polymer with decreased strength as opposed to a linear polymer in cellulose. Moreover, the degree of polymerization (DP) of cellulose is 10–100 times higher than that of hemicellulose with a DP range of 50–300.

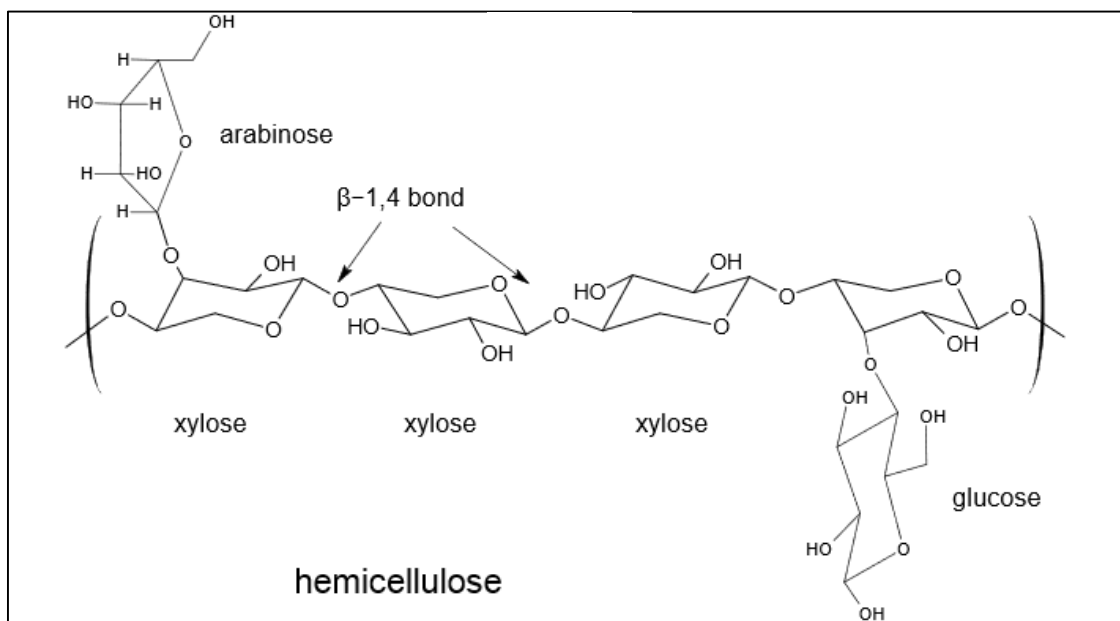


Figure 3.3: Molecular structure of hemicellulose (Watford, 2008)

3.3.3 Pectin and waxes

Pectin is a collective name for heteropolysaccharides, predominantly in bast fibres. Pectin gives plants flexibility and is soluble in water. Waxes consist of different types of alcohols (John & Thomas. 2010). Wax and oil are substances on fibre surface used to protect fibre (Azwa et al., 2013). Table 3.1 provides the chemical compositions of various natural fibres.

3.3.4 Lignin

Lignin, shown in figure 3.4, is a three-dimensional complex hydrocarbon polymer with very high molecular weight. It is very cumbersome to isolate as it is embedded between cellulose and hemicellulose. Lignin gets segregated during extraction; as such, its degree of polymerization is unknown. Lignin gives rigidity to plants (cell stiffening), provides protection against microbial and chemical attack to biomass and assists with the water transportation. It is hydrophobic, resistant to hydrolysis, soluble in hot alkali, susceptible to oxidation and can be condensed by Phenol (Azwa et al. 2013). Typical mechanical properties of selected plant fibre summarised in Table 3.1 indicate lower value for lignin compared to cellulose.

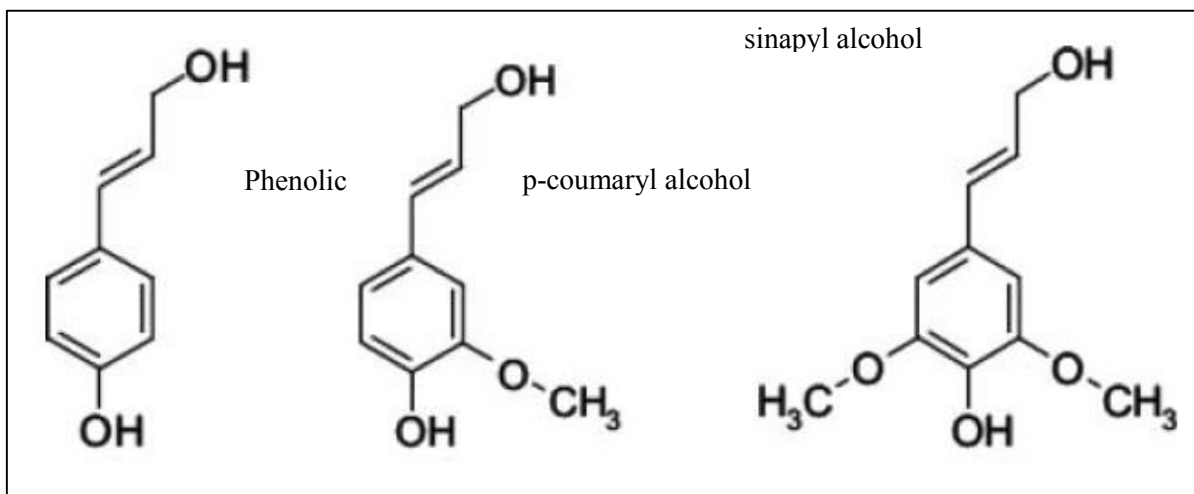


Figure 3.4: Molecular structure of selected lignin (Fuqua et. al., 2013)

Table 3.1: Summary of the typical mechanical properties of selected plant fibres (Fuqua et.al 2012)

Fibre type	Density (g/cm ³)	Length (mm)	Diameter (µm)	Tensile strength (MPa)	Tensile modulus (GPa)	Specific modulus (approx.)	Elongation (%)	Cellulose (wt. %)	Hemi-cellulose (wt. %)	Lignin (wt. %)	Pectin (wt. %)	Waxes (wt. %)	Micro-fibrillar angle (deg)	Moisture content (wt. %)
E-glass	2.5–2.59	–	<17	2000–3500	70–76	29	1.8–4.8	–	–	–	–	–	–	–
Abaca	1.5	–	–	400–980	6.2–20	9	1.0–10	56–63	20–25	7–13	1	3	–	5–10
Alfa	0.89	–	–	35	22	25	5.8	45.4	38.5	14.9	–	2	–	–
Bagasse	1.25	10–300	10–34	222–290	17–27.1	18	1.1	32–55.2	16.8	19–25.3	–	–	–	–
Bamboo	0.6–1.1	1.5–4	25–40	140–800	11–32	25	2.5–3.7	26–65	30	5–31	–	–	–	–
Banana	1.35	300–900	12–30	500	12	9	1.5–9	63–67.6	10–19	5	–	–	–	8.7–12
Coir	1.15–1.46	20–150	10–460	95–230	2.8–6	4	15–51.4	32–43.8	0.15–20	40–45	3–4	–	30–49	8.0
Cotton	1.5–1.6	10–60	10–45	287–800	5.5–12.6	6	3–10	82.7–90	5.7	<2	0–1	0.6	–	7.85–8.5
Curaua	1.4	35	7–10	87–1150	11.8–96	39	1.3–4.9	70.7–73.6	9.9	7.5–11.1	–	–	–	–
Flax	1.4–1.5	5–900	12–600	343–2000	27.6–103	45	1.2–3.3	62–72	18.6–20.6	2–5	2.3	1.5–1.7	5–10	8–12
Hemp	1.4–1.5	5–55	25–500	270–900	23.5–90	40	1–3.5	68–74.4	15–22.4	3.7–10	0.9	0.8	2–6.2	6.2–12
Henequen	1.2	–	–	430–570	10.1–16.3	11	3.7–5.9	60–77.6	4–28	8–13.1	–	0.5	–	–
Isora	1.2–1.3	–	–	500–600	–	–	5–6	74	–	23	–	1.09	–	–
Jute	1.3–1.49	1.5–120	20–200	320–800	8–78	30	1–1.8	59–71.5	13.6–20.4	11.8–13	0.2–0.4	0.5	8.0	12.5–13.7
Kenaf	1.4	–	–	223–930	14.5–53	24	1.5–2.7	31–72	20.3–21.5	8–19	3–5	–	–	–
Nettle	–	–	–	650	38	–	1.7	86	10	–	–	4	–	11–17
Oil palm	0.7–1.55	–	150–500	80–248	0.5–3.2	2	17–25	60–65	–	11–29	–	–	42–46	–
Piassava	1.4	–	–	134–143	1.07–4.59	2	7.8–21.9	28.6	25.8	45	–	–	–	–
PALF	0.8–1.6	900–1500	20–80	180–1627	1.44–82.5	35	1.6–14.5	70–83	–	5–12.7	–	–	14.0	11.8
Ramie	1.0–1.55	900–1200	20–80	400–1000	24.5–128	60	1.2–4.0	68.6–85	13–16.7	0.5–0.7	1.9	0.3	7.5	7.5–17
Sisal	1.33–1.5	900	8–200	363–700	9.0–38	17	2.0–7.0	60–78	10.0–14.2	8.0–14	10.0	2.0	10–22	10–22

3.4 Methods of extracting the natural fibre constituents

The methods and processes of determining the chemical composition of plant fibres are diverse and rigorous and require specialized techniques as stated by Watford (2008). The methods involve use of dilute alkali or acid hydrolysis. The lignocellulosic fibre chemical composition characterization is done through a number of methods such as bacteria and fungi, mechanical and chemical methods. The national renewable energy laboratory (NREL), which is the US department of energy primary laboratory, has developed standard biomass laboratory analytical procedures (LAPs) for characterization of the structural components of lignocellulosic fibres. The procedures have been developed to standardize the results from different research. The procedures are based on the American Society for Testing and Material (ASTM) and Technical Association of the Pulp and Paper Industry (TAPPI) standards. In South Africa, the department of energy (DOE) maintains a database of plant biomass, to monitor feedstock composition.

3.5 Mechanical properties of fibres

Jones (1996) mentioned the importance of knowing the mechanical properties of reinforcement materials such as density, electrical resistivity, ultimate tensile strength, Young's modulus. This is in in with the hypothesis that the performance of reinforced soils is related to the mechanical properties of the reinforcement material. In the same context, the structural components of natural fibres that give rise to the desired mechanical properties of fibres need to be understood as well.

These structural components depend on the internal structure and chemical composition of fibres. As most fibres are identified as a bundle of elementary fibres, the internal structure of the fibre can best be described in a single elementary unit as shown by Fuqua et al., (2012).

Fuqua et al., (2012) in characterizing the morphology of plant-based fibres mentioned that an isolated single fibre structure consists of a complex layer structure made up three secondary walls encased in one primary wall, with a lumen making it a hollow composite as shown in figure 3.5. The primary wall, which is the first layer deposited during plant growth, contains hemicellulose and cellulose. The secondary wall mainly consists of a series of helically wound cellular micro fibrils with a thick middle layer, S2, constituting about 70% of the fibre's Young's modulus (Bledzki & Gassan, 1999). Moreover, the micro fibrils are made up of long chain of cellulose molecules (about 30 to 100), with a diameter of about 10–30 nm, and provide mechanical strength to the fibre.

According to John and Thomas (2008), the overall property of fibres depend on their structure, microfibrillar angle, cell dimensions, defects, and the chemical composition. The microfibrillar angle, which is the angle between the fibre axis and the micro fibrils, varies depending on the type of fibre. This angle determines the stiffness of the fibres and ultimately its shear strength.

Azwa et al. (2013) stated that the ductility of fibres is a function of the micro fibrils orientation to the fibre axis. Parallel microfibrils orientation makes fibres rigid, inflexible and subsequently of a higher tensile strength. In other words as stated by Mohanty et al. (2000), the smaller the microfibrillar angle the better the mechanical properties of the fibre. Lignin and pectin in fibres reduce the mechanical properties and influence the interface interaction in composites due to their waxiness.

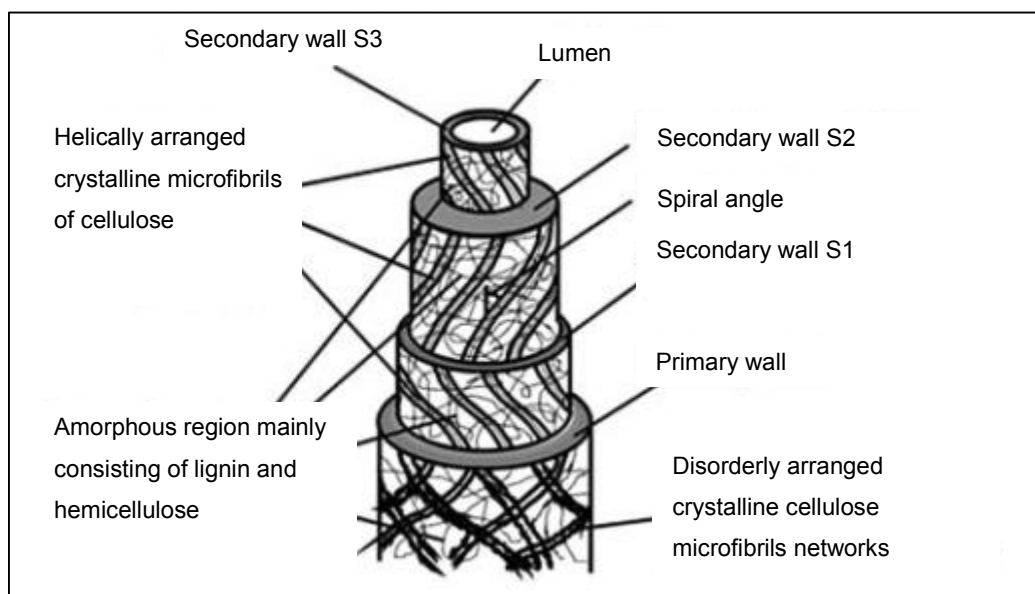


Figure 3.5: Structure of a single fibre cell (Fuqua et al., 2012)

In general, it can be concluded that fibres with a higher cellulose content, a higher degree of polymerisation, longer cell length, and lower microfibrillar angle portray higher tensile strength. However, it is not possible exactly correlating the effect of the internal structural and chemical composition of fibres with the increase in tensile strength due to the complexity of the structure and the drudgery involved in determining the fibre constituents.

3.6 Factors affecting mechanical properties of fibres

From a reinforcement standpoint strength, the crystalline cellulose of the natural fibres is considered as the main factor influencing the performance of the fibre in soil-fibre composites. However, the performance of fibres in outdoor environment is weakened by factors such as moisture, temperature, ultraviolet radiation, and biological activities. These consequently

affect the cellulose content in the plant structure. The morphological compositions affected by the environmental factors are summarised in figure 3.6.

Moisture tends to be the main factor compromising the strength of composite (Li & Zornberg, 2013). The moisture absorption rate is affected by the presence of voids in the fibre. Water, apart from enhancing microbiological attack in the fibres also, reduces the interfacial friction between the fibre and the soil matrix.

The ultraviolet degradation primarily takes place in the lignin cell walls. As lignin degrades, the cell structure becomes richer in cellulose content. Cellulose further degrades. Thermal degradation takes place in the hemicellulose. Lignin forms char that insulates hemicellulose from further degradation.

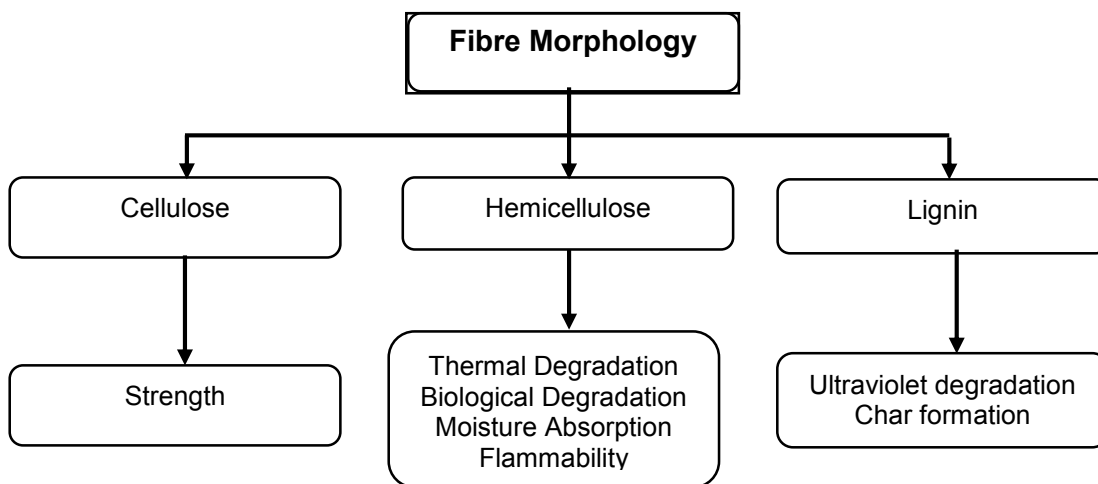


Figure 3.6: Fibre composition responsible for the functional properties (Adapted from Azwa et al. (2013))

As moisture absorption is the in-situ compromising factor, investigating it further is warranted as presented on the absorption mechanism below.

Mechanism of absorption

When plant fibres are exposed to the moist environments (in-situ conditions), the specific enzymes in the hemicellulose cells hydrolyse (biodegrade) the carbohydrate polymers into simple digestible units. This weakens further the lignocellulosic walls and consequently the strength of the fibre. In addition, moisture changes the shape of the cellulose walls, cellulose swells and shrinks after losing moisture. According to Azwa et al. (2013), the water absorption behaviour in natural fibres can best be explained by Fickian diffusion concept. Fickian diffusion concept, simply put, is the spread of water from a region of high to low concentrations due to concentration gradient until equilibrium is achieved, figure 3.7.

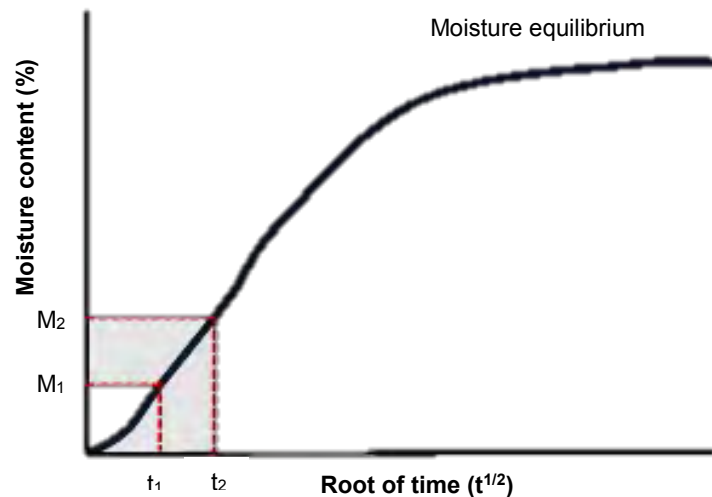


Figure 3.7: Idealized Fickian diffusion concept (adapted from Azwa et al. (2013))

3.7 Bagasse fibre characteristics and uses

Sugarcane consists of 15% dissolved matter, 15% fibre and 70% water when harvested (Nico Stolz, personal communication 2015, February 9). Bagasse is the fibrous waste generated after extracting all the juice from sugarcane. It consists of 70% short fibres and 30% long fibres on a dry mass basis.

During the milling process, out of every 100 tons cane crushed, 30 tonnes comprise bagasse, 12 tons sugar and 4 tonnes molasses suggesting that bagasse constitute 30% of sugarcane produced. However, Rein (1972) mentioned that fibres in South African sugarcane is higher compared to the rest of the world; possibly because South African sugarcane is grown in the temperate climate.

This following sub-section presents an overview of the South African sugar industry and the processes involved in the production of bagasse, characteristic of bagasse and studies done on it. Most of the review is based on the work by Patarau (1989) and Rein (1972).

3.7.1 Process of manufacturing bagasse

Production of bagasse is a subset process of several processes involved in manufacturing sugar. The steps involved are; cane preparation and juice extraction, juice treatment and purification, juice evaporation, sugar boiling/ crystallization, centrifuging and drying (Patarau 1989). However, this section will only focus on the cane preparation and the juice extraction which are the processes involving bagasse as shown in figure 3.8.

Cane preparation involves shredding and cutting the cane stalks through one or two sets of knives and shredders. Normally, mature cane is transported to the millers without the roots, tops and leaves in specially designed vehicles to facilitate offloading. The transported cane is weighed and fed into the cane preparation section where it is cut into smaller pieces using knives and shredders. Juice extraction is then done by either repeated crushing – tandem milling or by washing and squeezing – diffusion.

In South Africa, the diffusion method of extraction is preferred to milling (Nico Stolz, personal communication 2015, February 9). Eighty percent of milling companies use the diffusion method of extraction. The diffusion method is preferred due to its lower capital and operating costs and high sucrose extraction facilitated by adequate shredding and temperature control. However, it has disadvantages in regards to the higher level of sugar retained in bagasse, juice colouration, and longer start-up and shutdown procedures due to the large volume of fibres retained in the diffusers (Rein, 1972).

3.7.1.1 Mill tandem process

In tandem milling (series of 6 mills), extraction is done by squeezing the juice between 3 grooved rollers. The crushed cane is then dewatered to remove all the residual sugars, the end mass being at about 45% moisture content. This process is known as imbibition – which may either be simple imbibition or compound imbibition.

Simple imbibition involves adding water to the bagasse after each mill unit while compound imbibition entails recycling dilute juice (mostly water) obtained from either the last mill unit or the last two mill units, or three mill units that precede the last mill unit. According to Hugot (1986), the quantity of imbibition water affects the moisture content of the final bagasse.

3.7.1.2 Diffusion

In the diffuser system, the shredded mass is conveyed to a juice extractor chamber (diffuser) which is a solid-liquid extractor operating in a counter-current flow with hot water. In this chamber, sugar is extracted using hot water at about 75 – 80°C filtered and processed further. The saturated fibre leaving the diffuser is dewatered in a mill before being used in boilers or in by-product processes. The millrun bagasse is then de-pithed, depending on the milling company, to give a near 100% bagasse fibre sent to boilers for steam production.

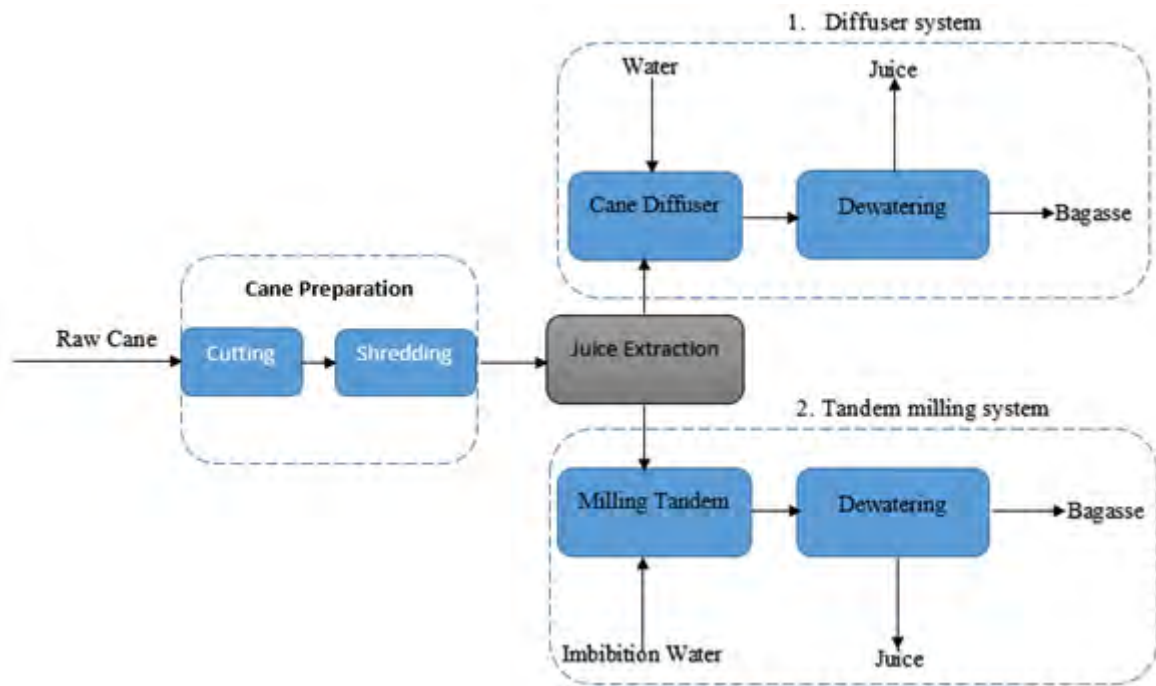


Figure 3.8: Showing the Bagasse production process (Adapted from Patarau, 1998)

3.7.2 Depithing of bagasse

The above two manufacturing processes produce bagasse containing a mixture of pith and fibres – millrun. The fibre and the pith are then separated based on the millers' preference and additional use. This process is known as de-pithing. Bagasse depithing is a tedious task that is based either on separation of the particle sizes or on the buoyancy of the pith particles in air and water (Patarau, 1989). Depithing may be conducted in moist, wet, or dry conditions.

Moist depithing is conducted close to the sugar factory on bagasse emerging from the extraction process at 50% moisture content. Wet depithing may be conducted at the by-product factory. Wet depithing involves suspending bagasse in water at a dry solid content of 5%. Dry depithing is performed either after the bagasse is artificially dried to about 15% humidity or after long periods of storage when bagasse attains a stable humidity level. Dry depithing is generally conducted using rotary drum screen; moist depithing is performed using a mechanical depither, while wet depithing is conducted using a hydropulper.

3.7.3 Composition of bagasse

The mill-run bagasse is composed of three main components;

1. Rind fibres,
2. Fibrous vascular bundles and pith,
3. Parenchyma tissue.

The first two are tough, hard-walled cylindrical cells of the rind and vascular tissue fibres while the third is the soft, thin walled, irregular shaped parenchymatous cells of the inner stalk tissue as shown in figure 3.9. The completely dry fibre-bagasse contains around 65% fibre, 30% pith and around 5% soluble solids. Fibre is the water insoluble component of the bagasse that contains mainly cellulose, lignin, hemicellulose and ash.

The vessels segments are also associated with the vascular bundles, and because of their non-fibrous character, they are generally considered as a pith fraction. Although the fibre and pith have almost similar composition, their structure differs widely. They occur in the ratio by weight of approximately 2.5 according to Patarau, (1989).

The fibres have a high aspect ratio and a relatively high coefficient of expansion and contraction upon wetting and subsequent drying. This translates in close bonding between the fibres and accounts for cohesive strength. The pith cells are irregular in size and shape and are characterised by their absorbent properties. They do not bond together. However, they can absorb water excessively which accounts for their limited use.

3.7.4 Properties of bagasse

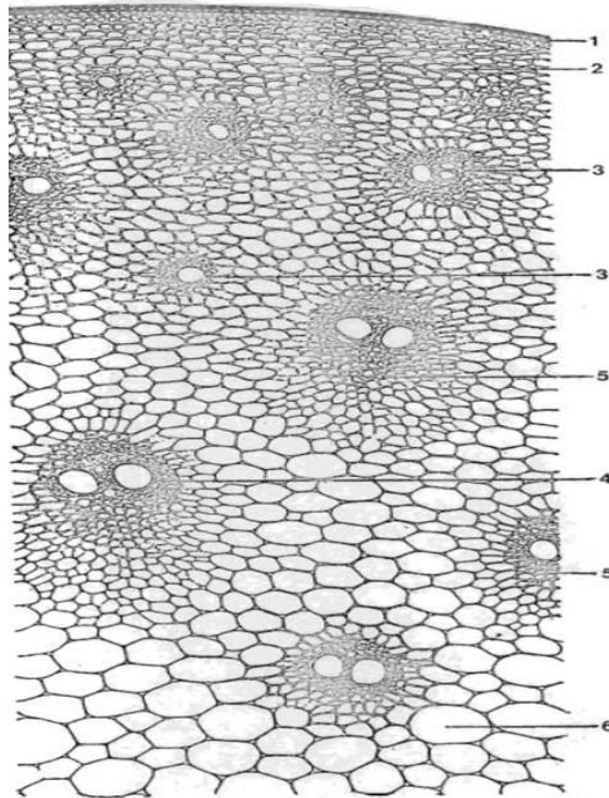
The properties of bagasse depend on the harvesting method, climatic conditions, maturity, method of extraction/efficiency, and sugarcane variety. Maturity is a factor of soil and agronomic techniques while the efficiency of the method of extraction depends on the type of crushing plant. Since sugarcane millers tend to focus more on extracting as much juice from the cane as possible, the above factors cannot be regulated to produce bagasse with ideal mechanical strength for reinforcement owing to the methods used.

Typical physical composition of bagasse can be summarised as in the table below

Table 3.2: Typical physical composition of bagasse (Rein, 1972)

Composition	Percentage by weight (%)
Moisture	49*
Soluble solids	2.3
Fibre	48.7

**the moisture content varies depending on the amount of imbibition water. Typically, it ranges between 40 to 50%*



Cross section through the outer part of an internode of cane stalk. (1) Epidermis (2) Rind (3 &4) vascular bundles (5) sclerenchyma (6) parenchyma

Figure 3.9: Cross-section of cane (extracted from Rein, 1972)

3.7.5 Current uses of bagasse

Figure 3.10 summarises some of the existing uses or applications of sugarcane bagasse. Most of the uses identified vastly consider using bagasse as fuel. According to Mwasiswebe (2005), it is very difficult to quantify the bagasse that could be used in combustion boilers.

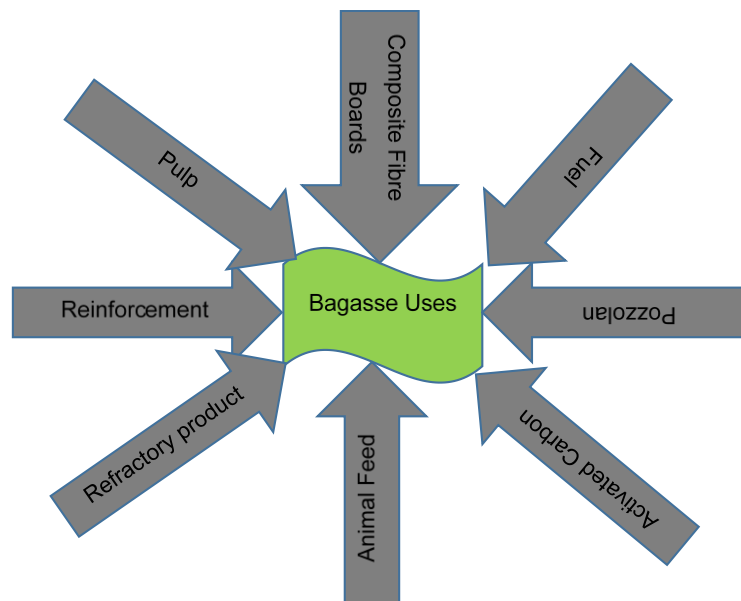


Figure 3.10: Current uses of bagasse (adapted from Loh et al. 2013)

CHAPTER 4:

4 RESEARCH MATERIALS AND METHODOLOGY

4.1 Introduction

This chapter presents a detailed discussion of the various research materials used in the investigation that include sugarcane bagasse, Klipheuwel sand, Cape Flats sand, and Kaolin clay. The second part of this chapter discusses the testing equipment and the experimental procedures followed during the study.

4.2 Research materials

4.2.1 Soil characterization tests

In order to understand the effect of fibre reinforcement on the shear strength of Klipheuwel, Cape Flat sand and Kaolin clay, various soil characterization tests were instituted. These tests, as summarised in the table 4.1 with their corresponding standards, were conducted in the geotechnical laboratory at the University of Cape Town. Details of the results are as presented in the appendix B.

Table 4.1: Soil classification tests conducted

Property	Method	Test Standards
Specific gravity	Small Pyknometer method	ASTM D854-10
In-situ moisture content	Oven drying	ASTM D2216-10
Maximum Dry Density	Standard Proctor Test	ASTM D1557-12
Optimum Moisture Content	Standard Proctor Test	ASTM D1557-12
Particle Grading	Dry sieve Method	ASTM D422-07
Shear Strength	Direct shear method	ASTM D3080-2003
Liquid and plastic limits	Atterberg	ASTM D4318-10e1
Maximum index density	Vibratory table	ASTM D4253 - 14

4.2.2 Soil materials

4.2.2.1 Klipheuwel Sand

The Klipheuwel was sourced from a quarry in Malmesbury, South Africa at an in-situ moisture content of 2.92%. It was classified using the USCS as a well-graded soil with soil particles ranging from 1.118 mm to 0.063 mm. It is a reddish brown soil with a coefficient of uniformity of 1.8 and coefficient of curvature of 0.95 as shown in the grading curve, figure 4.2. From the

scanning electron microscope analysis (see *section 4.3*), the soil can be described as a sandy soil of sub-angular shape.

The standard proctor test provided a maximum dry unit weight of 1833 kg/m^3 at an optimum water content of 10.0%. The angle of internal friction obtained from the direct shear tests was 32.8° with an apparent cohesion of 5.2 kPa at a relative density of 55%. The residual friction angle, obtained under the same test conditions, was 31.5° as presented in table 4.2.

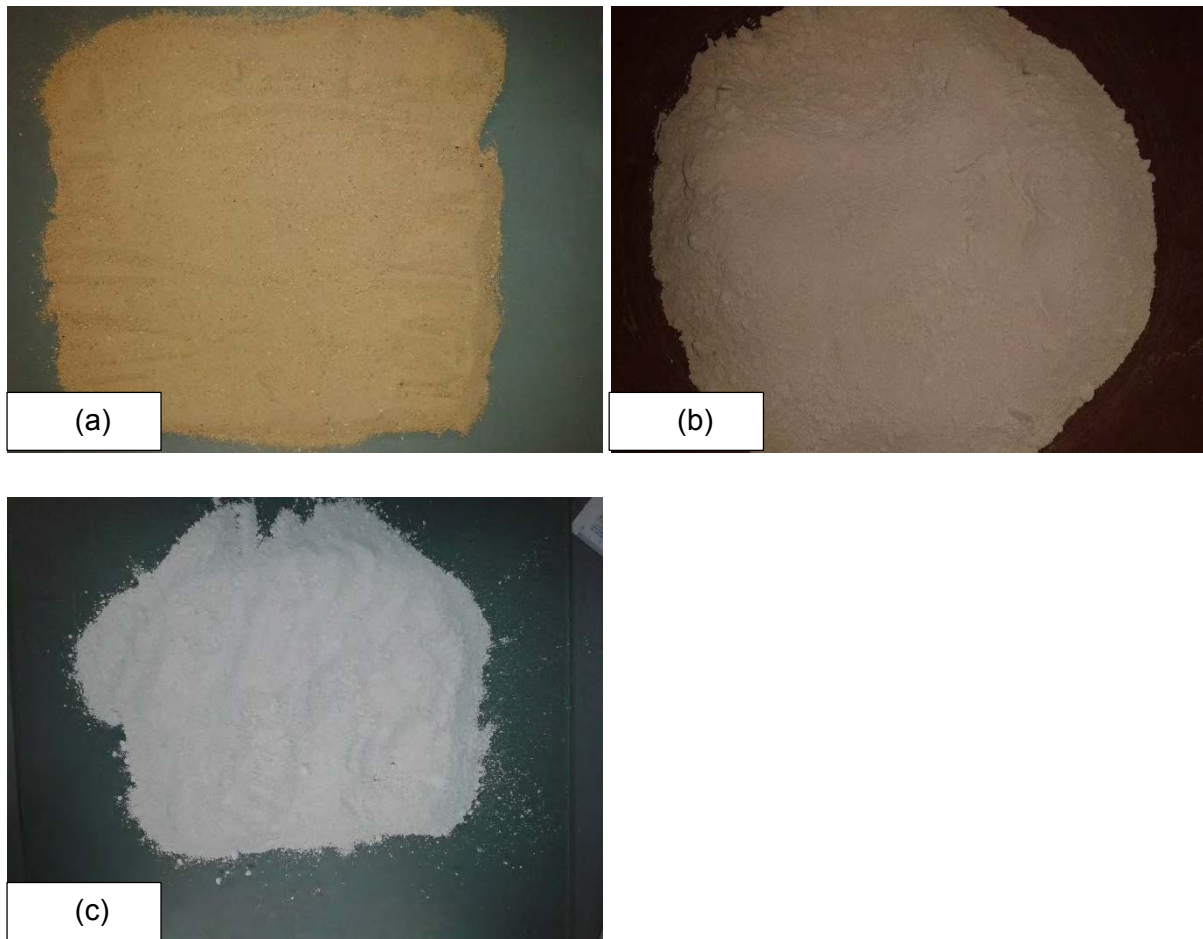


Figure 4.1: (a) *Klipheuwel Sand*, (b) *Cape Flats Sand*, (c) *Kaolin Clay*

4.2.2.2 Cape Flats sand

The sand shown in figures 4.1 (b) and 4.8 was sourced from Philippi Quarry, Cape Town, South Africa. It is a medium dense, light grey quartz sand with sub-rounded grains. The sand was classified using the USCS as poorly graded with little or no fines. The sieve analysis of the soil yielded the particle size-distribution curve shown in figure 4.2 with a varying grain size of between 0.15 mm to 3.00 mm and a coefficient of uniformity and curvature of 2.25 and 1.3, respectively.

4.2.2.3 Kaolin Clay

The Kaolin clay material, also known as China clay, used in this research is a white HB Powder Kaolin supplied by Serina Trading located in Crofters Valley along Sea Cottage Dr, Crofters Valley in Cape Town, South Africa. It has uniform physical and chemical properties and mainly consists of soft, pure, and extremely fine clay materials. It was on this basis that it was selected to aid in the preparation of identical samples for comparison purposes. In addition, it has previously been used by other researchers making it feasible to compare results.

Kaolin was selected to act as a control study for clay-fibre reinforcement principles. As such, only the established optimum fibre content from the experiments conducted on the two sands was used.

The characterization tests conducted gave an optimum moisture content of 23% corresponding to a maximum dry density of 1150kg/m³. All the other mechanical and chemical properties were as given in table 4.2 and 4.3.

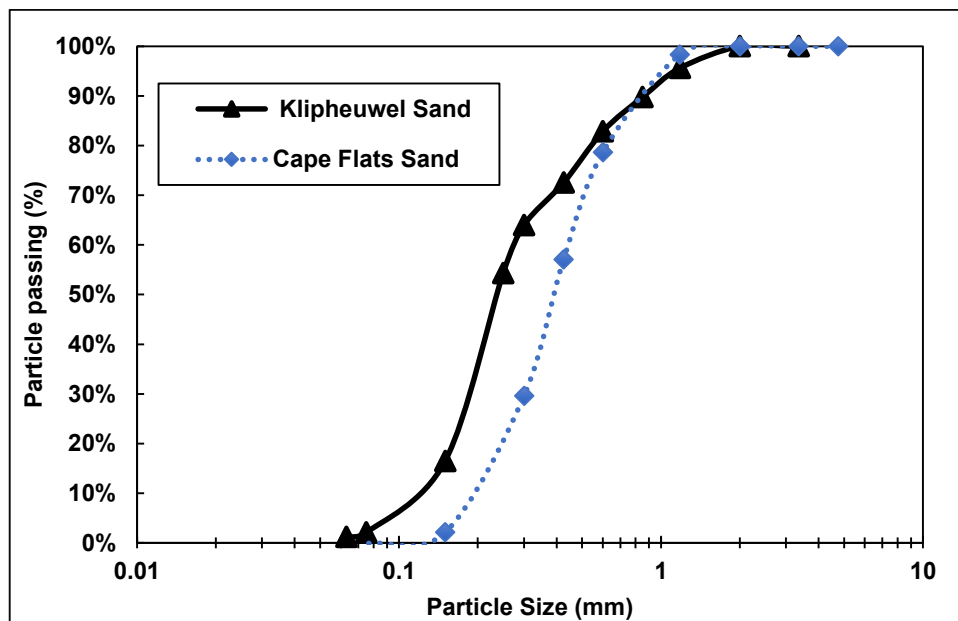


Figure 4.2: Particle grading curves

Table 4.2: Soil characterization results

Property	Unit	Klipheuwel Sand	Cape Flat Sand	Kaolin Clay
Specific Gravity, G_s	-	2.65	2.62	2.60
Natural moisture content	%	2.92	3.15	0.5
Optimum moisture content	%	10	15	23
Maximum dry density	kg/m ³	1833	1742	1550
Average dry density (Loose)	kg/m ³	1606	1542	-
Average dry density (dense)	kg/m ³	1912	1806	-
Particle range	mm	0.063 – 1.18	0.15 – 3.00	-
Mean grain size, D_{50}	mm	0.28	0.40	1.1micron
Coefficient of uniformity, C_u	-	1.8	2.25	-
Coefficient of curvature, C_c	-	0.95	1.3	-
Angle of internal friction, ϕ^*	degrees	32.8	36.6	28.9
Residual shear strength, ϕ_r^*	degrees	31.5	35.8	28.9
Cohesion, c	kN/m ²	5.2	4.3	2.8
Plastic limit	%	-	-	39.7
Liquid limit	%	-	-	28.2
Plasticity index	%	-	-	11.5

*dry state

Table 4.3: Chemical properties of Kaolin clay*

Grade	HB Powder
D_{50} , Microns	1.1
Reflectance (R457)	79
Silicon Dioxide - SiO_2 (%)	49.5
Aluminium (III) Oxide - Al_2O_3 (%)	36.5
Iron (III) Oxide - Fe_2O_3 (%)	0.5
Titanium Oxide - TiO_2 (%)	0.65
Abrasiveness (Einlehner tester)	64 g/m ²
Particle size distribution	87% (< 10 micron); 20% (< 2 micron)
Mean particle size (D_{50})	1.1 micron
Residue (> 45 micron)	1.5%
Reflectance	75% (off-white in colour)
pH value	7 – 8
Mohs hardness	2.0 – 2.5
Oil absorption (linseed oil)	45 mg/100g

*Chemical properties obtained from the manufacturers data sheet

4.2.3 Fibre material

The sugarcane bagasse used in this study was obtained from TSB Sugar Company, Malelane, South Africa. The material was received at a moisture content of about 50% in two batches. The sugarcane bagasse material used in this study is shown in figure 4.3. One batch contained sugarcane bagasse immediately after milling, while the other contained bagasse stockpiled for a period of two months. The essence of using stockpiled fibres was to determine the loss of strength with time on account of the sugarcane having been stored at a higher moisture content.

Both the fresh and stockpiled bagasse was obtained already separated into three different types: fibre, millrun and pith. To improve on the applicability in cases where separation of the fibres could not be done, screening in the laboratory was carried out. The emerging particle size distribution was compared with the particle size distribution of the fibre screened at other sugar factories and presented in sections 4.2.3.1 – 3.

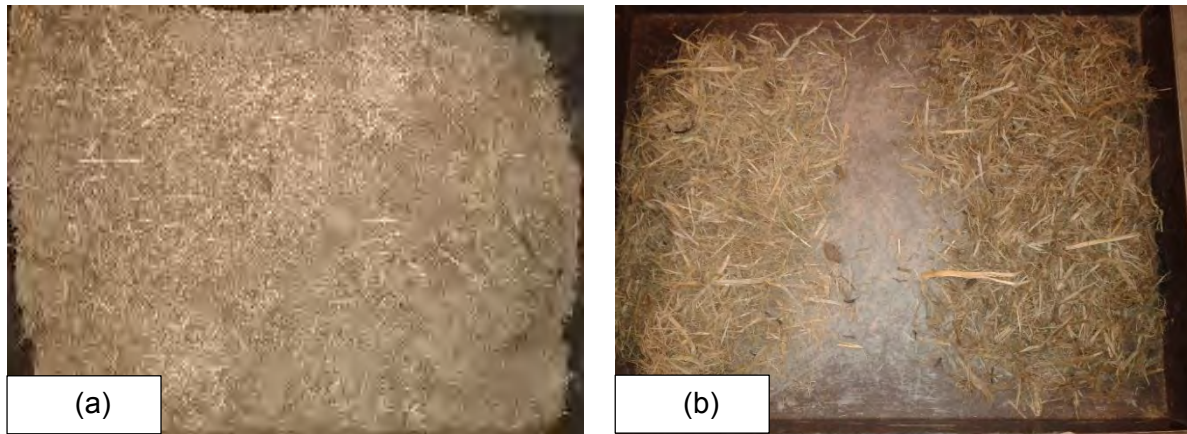


Figure 4.3: Bagasse (a) Stockpiled for 2 months (b) Millrun wet and dry just after production

4.2.3.1 Fibre bagasse

The fibre bagasse shown in figure 4.4 entails de-pithed bagasse with less or no pith. Sugarcane after undergoing sugar juice extraction and obtaining bagasse can be de-pithed by screening out all of the pith material.

These fibres contain mainly the outer rind of sugarcane, which is a hard fibrous material composed mainly of the cellulose and it is what gives strength to bagasse fibre. In characterising fibre bagasse, a Zwick machine was used to determine the tensile strength of a range of fibres and the results are given in table 4.4. Further classification tests were conducted through sieving. The classification tests are discussed in section 4.2.3.2.

Table 4.4: Summary of fibre characterization

Property	Value
Density (g/cm ³)	1.25*
Length (cm)	5–8
Diameter (mm)	2.00 - 6.00
Tensile strength (MPa)	40–80
Tensile modulus (GPa)	17–27.1
Specific modulus (approx.)	18*
Elongation (%)	1.1*
Cellulose (wt. %)	32–55.2*
Hemi-cellulose (wt. %)	16.8*
Lignin (wt. %)	19–25.3*

*adapted from Fuqua et.al (2012)

Sample fibres, similar to those shown in figure 4.4, were randomly chosen and the length measured. From the measurements, it can be inferred that the length of fibre bagasse was in the range of 5 – 8 cm.



Figure 4.4: Fibre bagasse

4.2.3.2 Millrun bagasse

The millrun bagasse represents bagasse at its original form from the juice extraction process just after imbibition. It contains both fibres, pith, and has a considerable amount of residual sugars. From the structural standpoint and because of the residual sugars, its tensile strength was very difficult to estimate. Doing so would require determining the tensile strength of fibres that would have corresponded with those of fibre bagasse.

The obtained millrun fibres from the factory were subjected to screening using a stack of sieves of 6.45 - 2.00 mm aperture size to determine the particle size distribution. It was very cumbersome and tedious screening bagasse fibre because the distribution depended on the particle orientation rather than the diameter. Particles oriented perpendicular to the sieve surface would pass through even though their sizes would not correspond to the sieve aperture size. The same applied to particles oriented in the parallel direction.

In solving this, and to ensure a more representative distribution, the screening was conducted by first using the mechanical shaker for 20 minutes followed by hand shaking. All the bagasse retained on the 6.45 mm and 4.75 mm sieve were combined together and termed coarse/long fibres, those retained on the 3.00 mm and 2.00 mm sieve were termed as fine fibres while all those that passed through the 2.00 mm sieve were termed as pith. Figure 4.7 presents a picture comparison of the bagasse sizes obtained after sieving.



Figure 4.5: Average length of fibre bagasse

Characterizing bagasse through sieving presented approximate fibre sizes comparable to the screened fibre bagasse and pith obtained from the sugar factories. The main objective of doing this was to facilitate the standardisation of fibres in field operations if it so happens that pre-screened fibres is unobtainable.

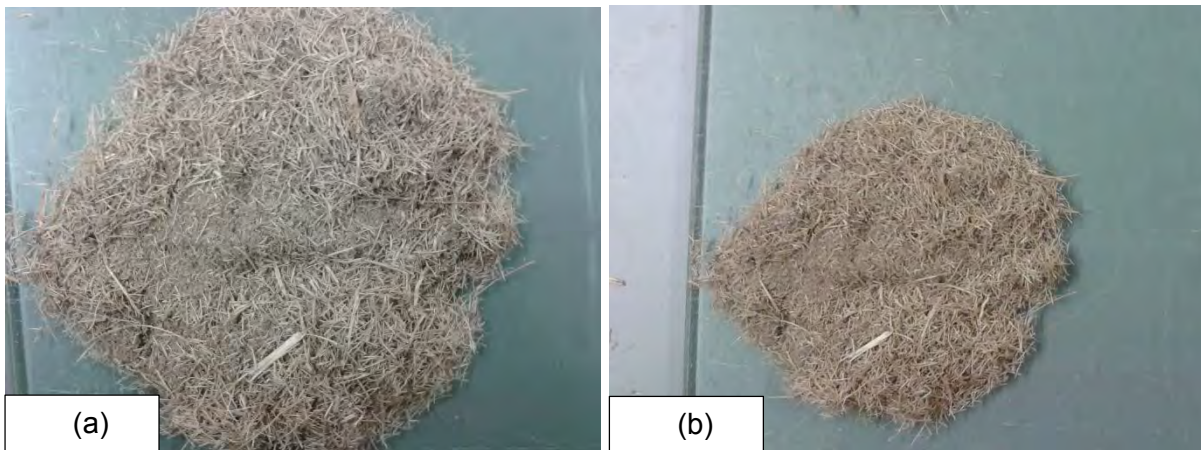


Figure 4.6: (a) Millrun bagasse, (b) pith Bagasse

4.2.3.3 Pith bagasse

All that remains after separation of fibre bagasse from the millrun is termed pith. Pith is the soft middle section of sugarcane plant. It contains a considerable amount of residual sugars, which could be termed as organic matter in soil engineering applications.

In the ensuing sections, the bagasse characterized above will be referred to as fibre, millrun and pith.

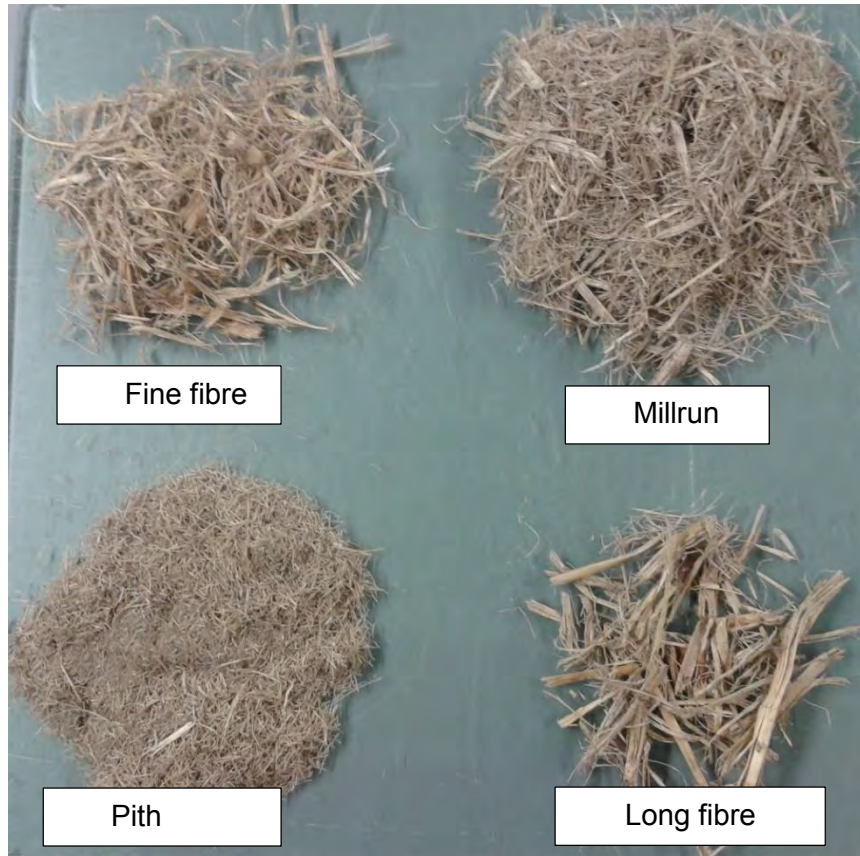


Figure 4.7: Showing Bagasse after screening used in the study

4.3 Electron micrographs of the research materials

According to De wet (2015), the shape of coarse-grained soil is very important in the determination of the shear strength of soils. The obtained shear strength is affected by the shape and size of the individual particle fabric. In line with this, a photo microscopic study of the soil used in this study was taken using a FEI Nova NanoSEM 230 scanning microscope with a resolution of $\times 10,000$ at the UCT imagery department. In addition, bagasse was viewed and the micrographs are shown in figure 4.8.

From the micrographs, it is evident that fibre bagasse before and after storage at a high moisture content differs in the structural morphology. Furthermore, pith bagasse contains flakes of residual sugars that may easily come into solution in the presence of water.

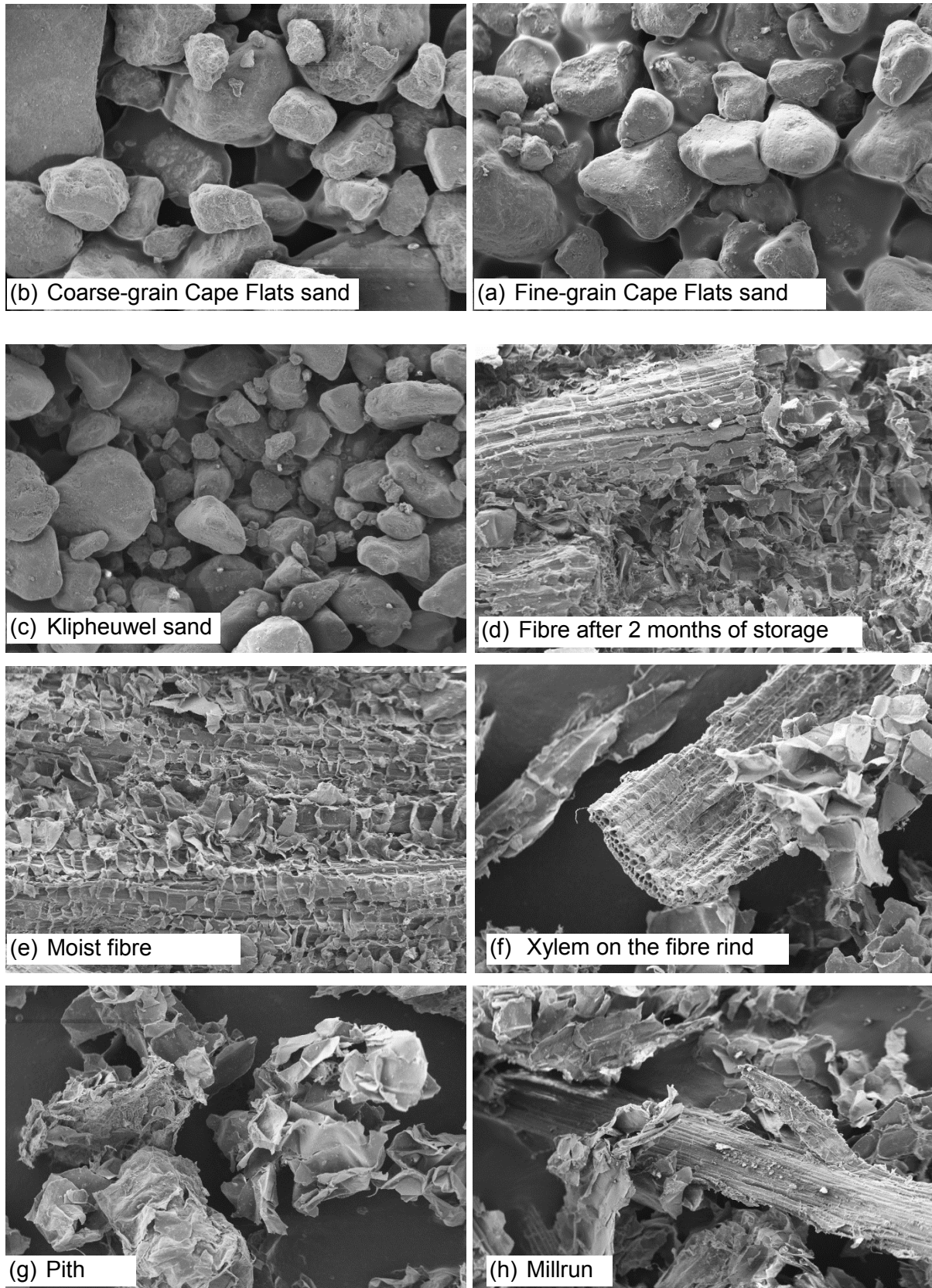


Figure 4.8: SEM micrographs of the research materials at a resolution of x10,000

4.4 Test Equipment

4.4.1 Direct shear

Direct shear test shown in figure 4.9 was adopted over other shear test methods because of its simplicity and applicability over a wide range of materials. It allows a quick comparison on shear strength of different geomaterials. Furthermore, it has been used by most of the previous researchers. The consensus from the researchers is that it overestimates the peak friction angles due to the non-uniform shear zone thickness and the non-uniform distribution of stresses.

Due to the varying length of the bagasse fibres (i.e. 5 – 8 cm), it was envisaged that direct shear would eliminate the boundary conditions. For this reason, and as per the ASTM D3080, which indicates that for reliable direct shear results the maximum length of the fibre should not be greater than a tenth of the box, a 305 mm long by 305 mm wide direct shear box was used for the study. However, this approximately solved the boundary effect since the average fibre length was out of the range. Figure 4.9 shows a cross-section of the direct shear box before and after shearing.

The direct shear box apparatus was fully automated and dubbed “ShearTrac-III” by Geocomp Corporation, the US Company, which manufactures the apparatus. The apparatus consisted of two brass split boxes of dimensions 305 mm long by 305 mm wide and 100 mm deep with vertical and horizontal loading cells fitted with LDVT’s and a display unit as shown in figure 4.10. It was capable of measuring the interface friction between soil-soil, geosynthetic-soil, geosynthetic-geosynthetic and internal friction of a geosynthetic clay liner.

The two split boxes were fitted together by an alignment screw during sample preparation. Of the two boxes, the top was fixed with the bottom free to slide with the aid of linear bearings attached to the brass container during the shear stage. The system also contained vertical and horizontal load cells fitted with LVDT sensors capable of monitoring the vertical and lateral movement pre-set at a 90 mm displacement with a resolution of 0.002 mm. As a safety measure, and to ensure that the displacement units are kept within range, the equipment was fitted with an upper and lower limit switch that triggers depending based on the limit the load cells are set at during testing. The maximum load capacity was 44.5 kN capable of applying a maximum normal pressure of up to 450 kPa. However, to avoid wear and tear a maximum normal pressure of 350 kPa was recommended. The machine was capable of applying a constant strain rate or stress rate of up to 15 mm/minute, with an accurate range of displacement in the range of 0.00003 – 10 mm per minute.

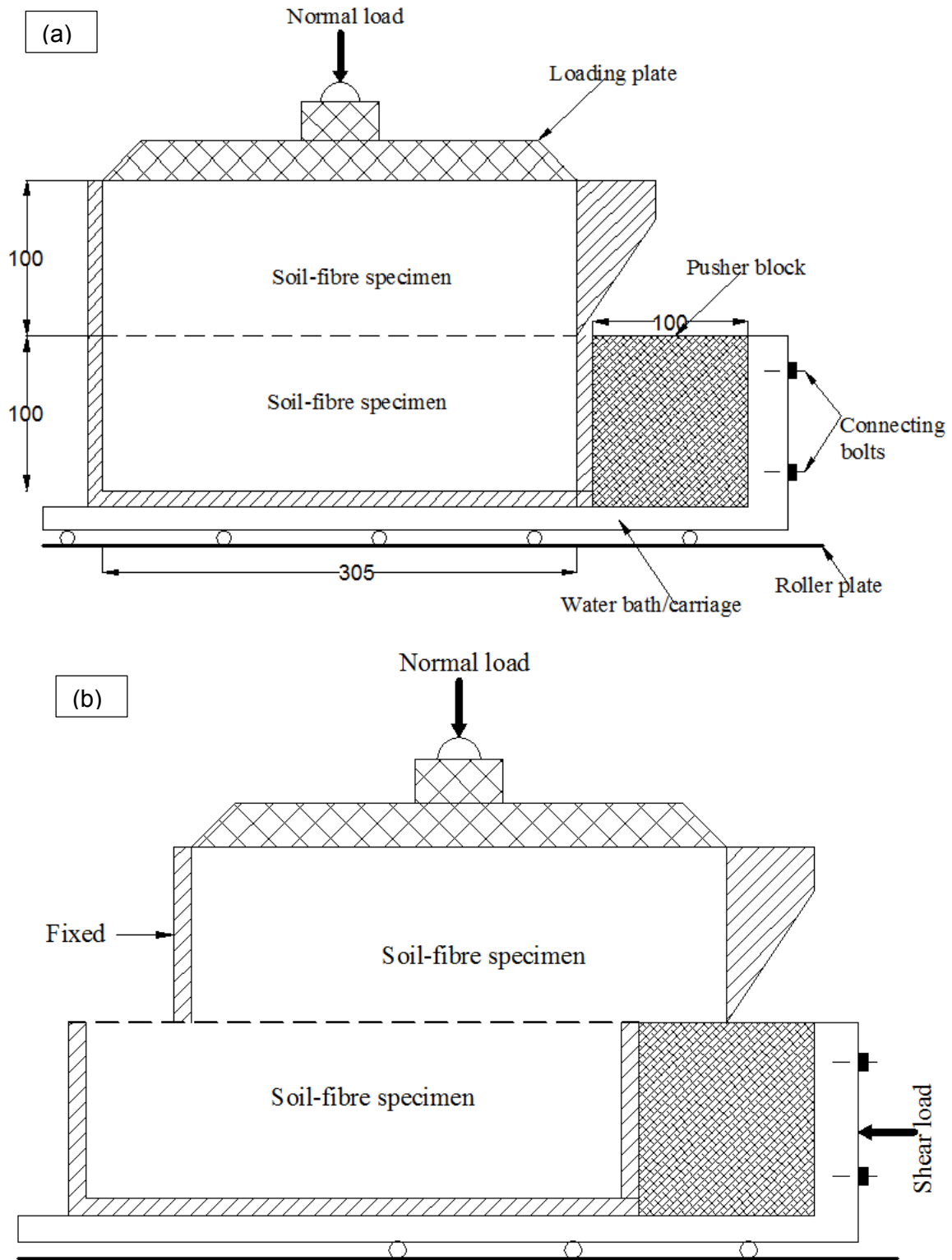


Figure 4.9: Direct shear apparatus (a) before shear and (b) after shearing, all dimensions in mm.

The ShearTrac-III also had a built-in electronic control panel that relayed real time data directly into a computer unit for export to other software packages, like spread sheets for analysis. It had reporting software capable of combining four data sets making it easy to monitor results

obtained from varied normal loads for shear envelope computations. An expanded overview of the machine is shown in the figure 4.10.

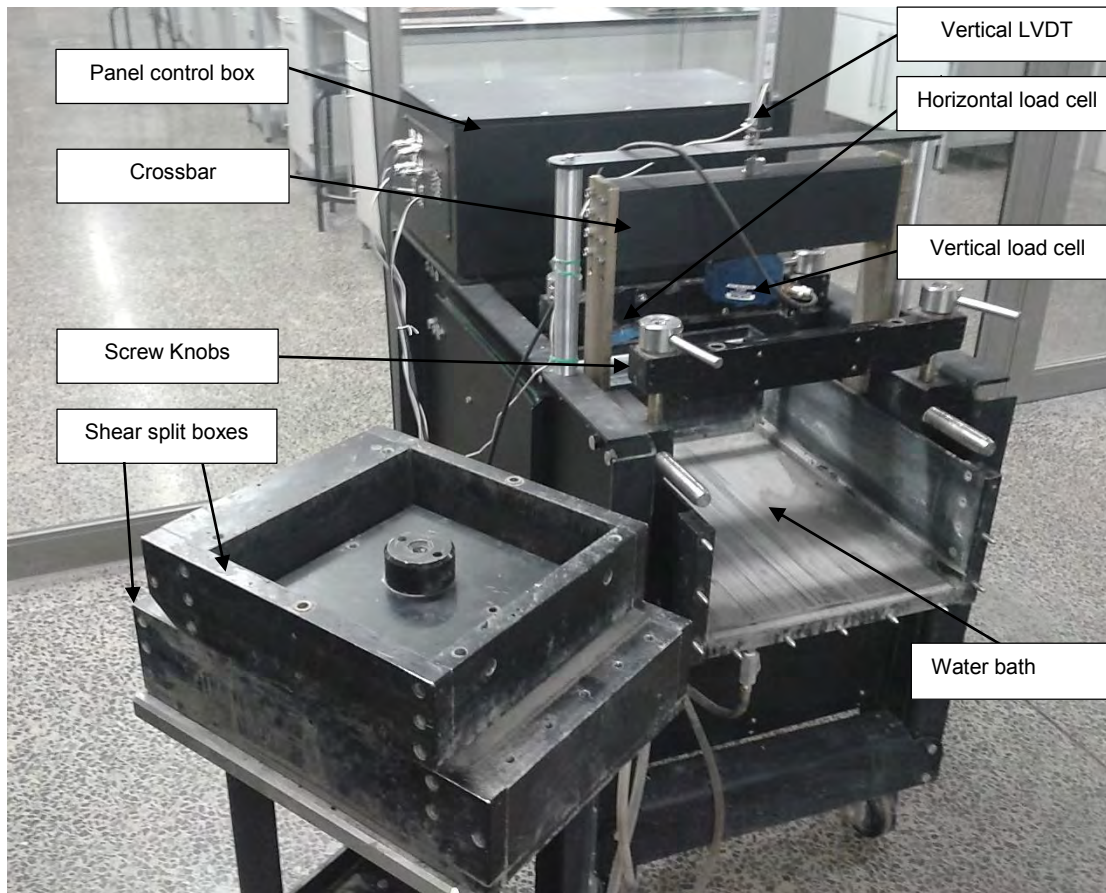


Figure 4.10: ShearTrac-III components

4.4.2 Durability moulds

Part of the research objective was to determine how soaking the soil-bagasse composite would affect its shear strength. To establish this, a durability study mould was designed that enabled the composite to be compacted just as it would be in the construction site. The mould was designed with similar configurations as the ShearTrac-III split boxes, but with reduced dimensions as shown in figure 4.11 to enable de-moulding after soaking. It was made of a 17 mm thick Aluminium plate, fabricated at the UCT civil engineering workshop.

The mould was required to be made of a lightweight and easy to demould material after the completion of the test. It was also required to be thick enough to provide a passage for the alignment screws. It was on this basis that the Aluminium material of was used.

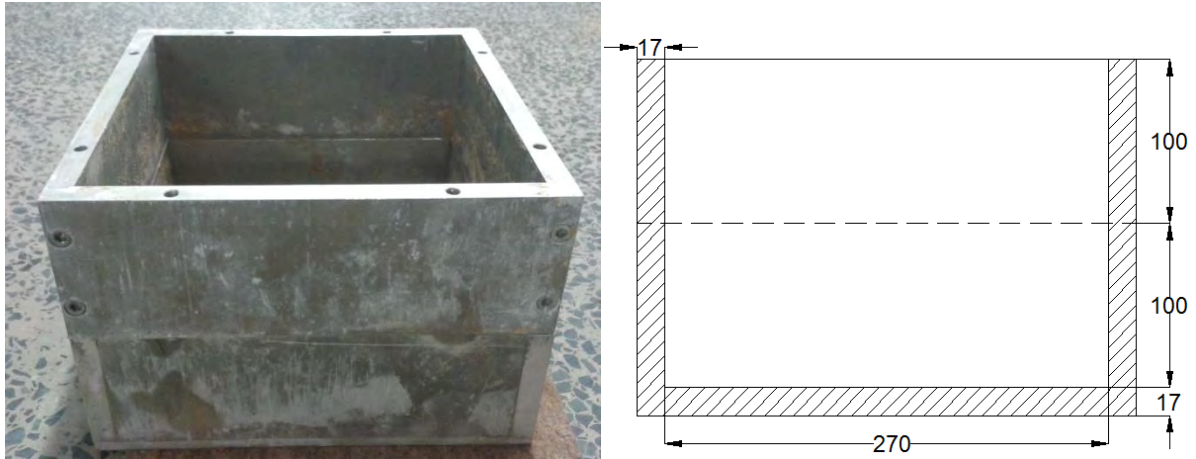


Figure 4.11: Durability mould picture and cross-section, dimensions in mm

4.4.3 Other apparatus

- **Mechanical mixer**

A rotary base pan mechanical mixer was used in obtaining a more homogenous composite of the selected soils and bagasse. The mixer shown in figure 4.12 was a 40 litres pan with a base rotating at 19 RPM, fitted with a motor and two steel paddles for mixing. It ensured the complete mixing of the composite with water to obtain the desired moisture content. It was established that by using a mechanical mixer the fibre segregation slightly reduced as compared to the hand mixing. Additionally, using the mechanical mixer simulated what happens on a construction site, using bagasse for soil reinforcement.



Figure 4.12: Mechanical mixer, 0.45 m in diameter and 0.25 m deep

▪ **Hand compactor**

A 2.5 kg hand compactor with a dropping height of 300 mm (figure 4.13) was used to obtain the desired density during sample preparation. The compactor was fitted on a flat Aluminium base of 303 long and 303 mm wide to ensure a uniform distribution of the load during compaction. The Aluminium base was adopted due to its low weight compared to steel to avoid crushing the sand grains during compaction. Consequently, this avoided unnecessary reduction in volume.

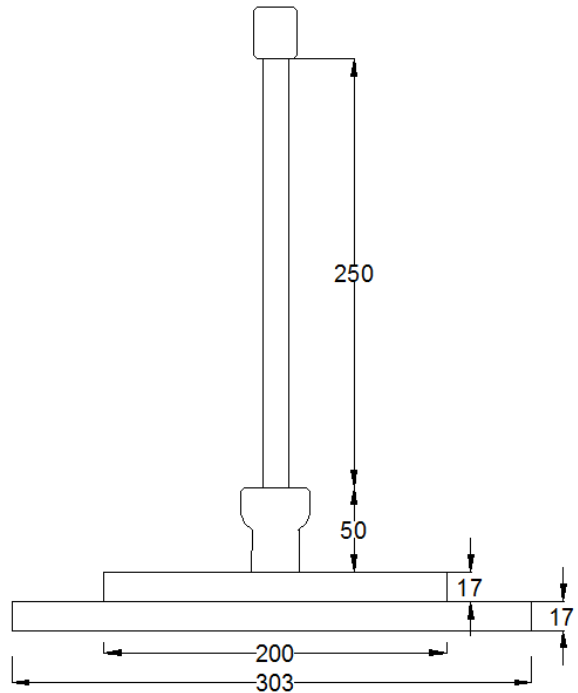


Figure 4.13: Hand compactor, all dimensions in mm

4.5 Methodology

4.5.1 Testing regime

The testing regime was done in two stages. One stage those that dealt with the shear behaviour of the selected soils reinforced with bagasse and the second stage considered the durability of bagasse-soil composite in water.

A total of 183 direct shear tests were carried out on the shear behaviour determination. Out of these, 99 tests were conducted on Klipheuwel sands with 6 being conducted on Klipheuwel sand only. Sixty tests were conducted on Cape flat sand, 3 being control tests while the remaining 24 tests were conducted on Kaolin clay. A large number of tests were conducted on Klipheuwel sand due to its wide range of particle sizes. The tests were conducted for both dry and moist soil conditions.

Durability tests were conducted by mainly considering the effect of water on the degradability of bagasse. The tests were conducted in two sub-groups:

- a) Soaking for three months
- b) 12 cycles of wetting and drying

The durability study was conducted on fibre composites that yielded realistic shear strength results. Table 4.5 describes the symbols used in the test schedules of tables 4.6 – 4.12.

Table 4.5: Definition of terms

Symbol	Description
D	Dry state
OMC	Optimum moisture content
KS	Klipheuwel sand
C	Normal pressure
CFS	Cape Flat sand
KC	Kaolin clay
US	Unreinforced soil
RS	Reinforced soil
F	Fibre (true)
MR	Mill-run
P	Pith
F1, F2, F3, F4, F5	Bagasse mass concentrations of 0.3%, 0.7%, 1.0%, 1.4%, 1.7%, respectively.
MR1, MR2, MR3, MR3, MR4, MR5	Millrun concentration of 0.3%, 0.7%, 1.0%, 1.4%, 1.7% respectively
P1, P2, P3,P4,P5	Pith concentration of 0.3%, 0.7%, 1.0%, 1.4%, 1.7% respectively

Table 4.6: Testing regime for reinforced dry Cape Flats sand

Soil state	Combined group	Test code	Research material	Normal stress (kPa)	Parameters	
Dry	1	US/CFS/C50	0% fibre	50	Control	
		US/CFS/C100		100		
		US/CFS/C200		200		
	2	RS / CFS /F1 / C50	0.3% fibre	50	Fibre	
		RS / CFS /F1 / C100		100		
		RS / CFS /F1 / C200		200		
	3	RS / CFS /F2 / C50	0.7% fibre	50		
		RS / CFS /F2 / C100		100		
		RS / CFS /F2 / C200		200		
	4	RS / CFS /F3 / C50	1.0% fibre	50		
		RS / CFS /F3 / C100		100		
		RS / CFS /F3/ C200		200		
	5		RS / CFS /F4 / C50	1.4% fibre		50

Soil state	Combined group	Test code	Research material	Normal stress (kPa)	Parameters
		RS / CFS /F4 / C100		100	
		RS / CFS /F4/ C200		200	
	6	RS / CFS /F5 / C50	1.7% fibre	50	
		RS / CFS /F5 / C100		100	
		RS / CFS /F5/ C200		200	
	7	RS / CFS /MR1 / C50	0.3% mill-run	50	
		RS / CFS /MR1 / C100		100	
		RS / CFS /MR1 / C200		200	
	8	RS / CFS /MR2 / C50	0.7% mill-run	50	
		RS / CFS /MR2 / C100		100	
		RS / CFS /MR2 / C200		200	
	9	RS / CFS /MR3 / C50	1.0% mill-run	50	
		RS / CFS /MR3 / C100		100	
		RS / CFS /MR3/ C200		200	
	10	RS / CFS /MR4 / C50	1.4% mill-run	50	
		RS / CFS /MR4 / C100		100	
		RS / CFS /MR4/ C200		200	
	11	RS / CFS /MR5 / C50	1.7% mill-run	50	
		RS / CFS /MR5 / C100		100	
		RS / CFS /MR5/ C200		200	
	12	RS / CFS /P1 / C50	0.3% pith	50	
		RS / CFS /P1 / C100		100	
		RS / CFS /P1 / C200		200	
	13	RS / CFS /P2 / C50	0.7% pith	50	
RS / CFS /P2 / C100		100			
RS / CFS /P2 / C200		200			
14	RS / CFS /P3 / C50	1.0% pith	50		
	RS / CFS /P3 / C100		100		
	RS / CFS /P3/ C200		200		
15	RS / CFS /P4 / C50	1.4% pith	50		
	RS / CFS /P4 / C100		100		
	RS / CFS /P4/ C200		200		
16	RS / CFS /P5 / C50	1.7% pith	50		
	RS / CFS /P5 / C100		100		
	RS / CFS /P5/ C200		200		

Table 4.7: Testing regime for reinforced dry Klipheuwel sand

Soil state	Combined group	Test code	Research material	Normal stress (kPa)	Parameters	
Dry	17	US/KS/KS50	0% fibre	50	Control	
		US/KS/KS100		100		
		US/KS/KS200		200		
	18	RS / KS /F1 / KS50	0.3% fibre	50	Fibre	
		RS / CFS /F1 / KS100		100		
		RS / KS /F1 / KS200		200		
	19	RS / KS /F2 / KS50	0.7% fibre	50		
		RS / KS /F2 / KS100		100		
		RS / KS /F2 / KS200		200		
	20	RS / KS /F3 / KS50	1.0% fibre	50		
		RS / KS /F3 / KS100		100		
		RS / KS /F3 / KS200		200		
	21	RS / KS /F4 / KS50	1.4% fibre	50		
		RS / KS /F4 / KS100		100		
		RS / KS /F4 / KS200		200		
	22	RS / KS /F5 / KS50	1.7% fibre	50		
		RS / KS /F5 / KS100		100		
		RS / KS /F5 / KS200		200		
	23	RS / KS /MR1 / KS50	0.3% mill-run	50		Millrun
		RS / KS /MR1 / KS100		100		
		RS / KS /MR1 / KS200		200		
	24	RS / KS /MR2 / KS50	0.7% mill-run	50		
		RS / KS /MR2 / KS100		100		
		RS / KS /MR2 / KS200		200		
	25	RS / KS /MR3 / KS50	1.0% mill-run	50		
		RS / KS /MR3 / KS100		100		
		RS / KS /MR3 / KS200		200		
	26	RS / KS /MR4 / KS50	1.4% mill-run	50		
		RS / KS /MR4 / KS100		100		
		RS / KS /MR4 / KS200		200		
27	RS / KS /MR5 / KS50	1.7% mill-run	50			
	RS / KS /MR5 / KS100		100			
	RS / KS /MR5 / KS200		200			
28	RS / KS /P1 / KS50	0.3% pith	50	Pith		
	RS / KS /P1 / KS100		100			
	RS / KS /P1 / KS200		200			
29	RS / KS /P2 / KS50	0.7% pith	50			
	RS / KS /P2 / KS100		100			
	RS / KS /P2 / KS200		200			
30	RS / KS /P3 / KS50	1.0% pith	50			

Soil state	Combined group	Test code	Research material	Normal stress (kPa)	Parameters
		RS / KS /P3 / KS100		100	
		RS / KS /P3/ KS200		200	
	31	RS / KS /P4 / KS50	1.4% pith	50	
		RS / KS /P4 / KS100		100	
		RS / KS /P4/ KS200		200	
	32	RS / KS /P5 / KS50	1.7% pith	50	
		RS / KS /P5 / KS100		100	
		RS / KS /P5/ KS200		200	

Table 4.8: Testing regime for reinforced dry Kaolin Clay

Soil state	Combined group	Test code	Research material	Normal stress (kPa)	Parameters
Dry	33	US/KC/KC50	0% fibre	50	Control
		US/KC/KC100		100	
		US/KC/KC200		200	
	34	RS / KC /F3 / KC50	1.0% fibre	50	Fibre
		RS / KC /F3 / KC100		100	
		RS / KC /F3/ KC200		200	
	35	RS / KC /MR3 / KC50	1.0% mill-run	50	Millrun
		RS / KC/MR3 / KC100		100	
		RS / KC /MR3/ KC200		200	
	36	RS / KC /P3 / KC50	1.0% pith	50	Pith
		RS / KC/P3 / KC100		100	
		RS / KC /P3/ KC200		200	

The same test regime was followed for testing soil at moist state as given table 4.9 – 4.11.

Table 4.9: Testing regime for reinforced moist Cape Flats Sand

Soil state	Combined group	Test code	Research material	Normal stress (kPa)	Parameters
OMC	37	US/KS/KS50	0% fibre	50	Control
		US/KS/KS100		100	
		US/KS/KS200		200	
	38	RS / KS /F1 / KS50	0.3% fibre	50	Fibre
		RS / CFS /F1 / KS100		100	
		RS / KS /F1 / KS200		200	
39	RS / KS /F2 / KS50	0.7% fibre	50		

Soil state	Combined group	Test code	Research material	Normal stress (kPa)	Parameters
		RS / KS /F2 / KS100		100	
		RS / KS /F2 / KS200		200	
	40	RS / KS /F3 / KS50	1.0% fibre	50	
		RS / KS /F3 / KS100		100	
		RS / KS /F3 / KS200		200	
	41	RS / KS /F4 / KS50	1.4% fibre	50	
		RS / KS /F4 / KS100		100	
		RS / KS /F4 / KS200		200	
	42	RS / KS /F5 / KS50	1.7% fibre	50	
		RS / KS /F5 / KS100		100	
		RS / KS /F5 / KS200		200	
	43	RS / KS /MR1 / KS50	0.3% mill-run	50	
		RS / KS /MR1 / KS100		100	
		RS / KS /MR1 / KS200		200	
	44	RS / KS /MR2 / KS50	0.7% mill-run	50	
		RS / KS /MR2 / KS100		100	
		RS / KS /MR2 / KS200		200	
	45	RS / KS /MR3 / KS50	1.0% mill-run	50	
		RS / KS /MR3 / KS100		100	
		RS / KS /MR3 / KS200		200	
	46	RS / KS /MR4 / KS50	1.4% mill-run	50	
		RS / KS /MR4 / KS100		100	
		RS / KS /MR4 / KS200		200	
	47	RS / KS /MR5 / KS50	1.7% mill-run	50	
		RS / KS /MR5 / KS100		100	
		RS / KS /MR5 / KS200		200	
	48	RS / KS /P1 / KS50	0.3% pith	50	
		RS / KS /P1 / KS100		100	
		RS / KS /P1 / KS200		200	
	49	RS / KS /P2 / KS50	0.7% pith	50	
RS / KS /P2 / KS100		100			
RS / KS /P2 / KS200		200			
50	RS / KS /P3 / KS50	1.0% pith	50		
	RS / KS /P3 / KS100		100		
	RS / KS /P3 / KS200		200		
51	RS / KS /P4 / KS50	1.4% pith	50		
	RS / KS /P4 / KS100		100		
	RS / KS /P4 / KS200		200		
52	RS / KS /P5 / KS50	1.7% pith	50		
	RS / KS /P5 / KS100		100		
	RS / KS /P5 / KS200		200		

Table 4.10: Testing regime for reinforced moist Klipheuwel Sand

Soil state	Combined group	Test code	Research material	Normal stress (kPa)	Parameters
OMC	53	US/CFS/C50	0% fibre	50	Control
		US/CFS/C100		100	
		US/CFS/C200		200	
	54	RS / CFS /F3 / C50	1.0% fibre	50	Fibre
		RS / CFS /F3 / C100		100	
		RS / CFS /F3/ C200		200	
	55	RS / CFS /MR3 /C50	1.0% mill-run	50	Millrun
		RS/CFS/MR3/C100		100	
		RS / CFS /MR3/C200		200	
	56	RS / CFS/P3 / C50	1.0% pith	50	Pith
		RS / CFS/P3 / C100		100	
		RS / CFS /P3/ C200		200	

Table 4.11: Testing regime for reinforced moist Kaolin Clay

Soil state	Combined group	Test code	Research material	Normal stress (kPa)	Parameters
OMC	57	US/KC/KC50	0% fibre	50	Control
		US/KC/KC100		100	
		US/KC/KC200		200	
	58	RS / KC /F3 / KC50	1.0% fibre	50	Fibre
		RS / KC /F3 / KC100		100	
		RS / KC /F3/ KC200		200	
	59	RS / KC /MR3 / KC50	1.0% mill-run	50	Millrun
		RS / KC/MR3 / KC100		100	
		RS / KC /MR3/ KC200		200	
	60	RS / KC /P3 / KC50	1.0% pith	50	Pith
		RS / KC/P3 / KC100		100	
		RS / KC /P3/ KC200		200	

Durability studies test regime

The durability studies were carried out using 1.0% fibre bagasse content as in the test regime below. The study took into consideration the effect of water on the strength of the composite through wetting, drying and soaking. This is because water enhances the rate of organic decomposition and would have a greater effect on the long-term use of soil-bagasse composite.

Table 4.12: Testing regime for durability studies

Combined Group	Test Code	Research Material	Normal Stress (kPa)	Parameters
12 Cycles	RS / KS /F4 / KS50	1.0% fibre	50	Wetting and Drying
	RS / KS /F4 / KS100		100	
	RS / KS /F4/ KS200		200	
6 Hours	RS / KS /F4 / KS50	1.0% fibre	50	Soaking
	RS / KS /F4 / KS100		100	
	RS / KS /F4/ KS200		200	
12 Hours	RS / KS /F4 / KS50	1.0% fibre	50	
	RS / KS /F4 / KS100		100	
	RS / KS /F4/ KS200		200	
24Hours	RS / KS /F4 / KS50	1.0% fibre	50	
	RS / KS /F4 / KS100		100	
	RS / KS /F4/ KS200		200	
48 Hours	RS / KS /F4 / KS50	1.0% fibre	50	
	RS / KS /F4 / KS100		100	
	RS / KS /F4/ KS200		200	
7 Days	RS / KS /F4 / KS50	1.0% fibre	50	
	RS / KS /F4 / KS100		100	
	RS / KS /F4/ KS200		200	
14 Days	RS / KS /F4 / KS50	1.0% fibre	50	
	RS / KS /F4 / KS100		100	
	RS / KS /F4/ KS200		200	

4.5.2 Sample preparation

The shear stress behaviours of both the unreinforced and reinforced soils were determined in accordance with the guidelines given in the ASTM D3080-11 in addition to referencing the operation manual given by Head (1980).

The soil samples used were disturbed and remoulded. As such, the method of under compaction discussed in Ladd (1979) was extensively used in preparing the compacted sample before testing. In order to achieve the 55% relative density of the compacted soil, the method of preparation deviated from the recommendations by Ladd (1979).

All the soil samples and bagasse fibre were first dried to achieve a near dry state condition. Klipheuwel sand was dried for 24 hours in an oven set at 60°C. The 60°C temperature of was chosen to avoid the tendency of Klipheuwel sand particles clumping together and forming clods at temperatures above 60°C. In contrast, Cape Flats sand was oven dried for 24 hours at a temperature of 105°C. The Kaolin Clay, due to its powdery nature and because it was

received in 25 kg bags, was tested without drying. However, the initial moisture content was determined prior to testing.

Since the fibre materials were obtained at a moisture content of about 50%, the materials were dried in the laboratory under room temperature over a period of 7 days. Due to the large quantity of the material required for this project and bearing in mind the bulky nature of bagasse and lack of a storage facility, the drying process was expedited. To achieve this, bagasse was oven dried at a temperature of 35°C. This temperature was high enough to speed up the drying process and low enough to avoid combustion and the destruction of the cellulose matrix in the bagasse.

4.5.2.1 Soil only

A trial compaction procedure based on Ladd's (1979) under compaction method was first constituted in order to achieve a 55% relative density after compaction. This was based on the equation 26 by Das (2002). The compaction was also in accordance with the standard proctor test procedures outlined in the ASTM D698-12, which stipulate, 3 layers of compaction using 25 blows per layer.

$$D_r = \left[\frac{\gamma_d - \gamma_{d(\min)}}{\gamma_{d(\max)} - \gamma_{d(\min)}} \right] \left[\frac{\gamma_{d(\min)}}{\gamma_d} \right] \quad (26)$$

Where $\gamma_{d(\max)}$ and $\gamma_{d(\min)}$, are the maximum and minimum densities calculated from the vibrating table tests as per ASTM D4253 and γ_d , is the in-situ dry density. For this study, the dry density achieved after compaction in the split boxes was used.

Having arrived at the number of blows and layers, 45 kg of Klipheuwel sand was compacted directly in the shear split box by dividing the sample into 3 equal masses of 15 kg per layer. Das (2002) mentioned that, for consistency during compaction, the number of layers, thickness of the layer, moisture content and compaction energy has to be maintained throughout. In other words for the compaction density to be same, the thickness of the compacted layers must be equal.

The soil was compacted and the excess trimmed off, weighed then subtracted from the original masses of 45 kg to attain the volume remaining in the box. 35 kg of soil remained in the box when compacted to a height of 200 mm. To cater for the loading plate and to ensure that the compacted layer did not coincide with the shearing plane, 30 kg of soil was used throughout the soil preparation process.

This 30 kg of Klipheuvel sand was compacted in 3 layers of 10 kg each. Each layer was subjected to 25 blows by dropping a 2.5 kg hand compactor (described in section 4.4.2) raised to a height of 300 mm. The corresponding energy was 32.27 kN-m/m³ calculated by the equation below, which is an ideal energy since some losses occurred during compaction.

$$E = \frac{\left(\begin{array}{c} \text{Number} \\ \text{of blows} \\ \text{per layer} \end{array} \right) \times \left(\begin{array}{c} \text{Number} \\ \text{of} \\ \text{layers} \end{array} \right) \times \left(\begin{array}{c} \text{weight} \\ \text{of} \\ \text{hammer} \end{array} \right) \times \left(\begin{array}{c} \text{Height of} \\ \text{drop of} \\ \text{hammer} \end{array} \right)}{\text{Volume of mould}} \quad (27)$$

The same procedure was repeated for both sands using different volumes. 28 kg and 15 kg of Cape Flats and Kaolin clay were used respectively. The difference in volume was due to the different dry densities and particle distributions depicted by the soil samples. Compacting dry clay soil using the tamping method became very difficult. Instead, Kaolin was loosely prepared before shearing.

Samples were also prepared at moist conditions corresponding to optimum moisture content using the methods previously described. The amount of water added to achieve this was in accordance with ASTM D689. In order to achieve uniformity, a mechanical mixer was used after adding the right amount of water. Mixing was done for a predetermined period of 3 minutes then the material allowed settling whilst covered for a period of one hour between tests.

4.5.2.2 Soil-fibre composite

Mix design

Before compaction of the fibre-soil composite, a mix design was undertaken using equation 2 to obtain percentage concentrations.

For instance, to get 1.0% fibre/pith/millrun content, the computations were as equation 28.

$$\%_{\text{fibre}} = \frac{0.3 \text{ kg}}{(30 - 0.3) \text{ kg}} \times 100 = \frac{0.3}{29.7} = 1.0\% \quad (28)$$

From the above mix design, fibre contents of 0.3%, 0.7%, 1.0%, 1.4% and 1.7% by dry mass of soil were used in this study. It should be noted that higher concentrations could not be achieved due to fibre segregation at a concentration of more than 1.7%. Researchers such as Anagnostopoulos et al. (2013) recommended sprinkling some water while mixing to reduce this segregation. The possibility of having the results compromised meant the

recommendations by Anagnostopoulos et al. (2013) could not be implemented. Figures 4.14 (a) 4.14 (d) show a typical sample preparation, testing and end of shear results (for soil in moist conditions).

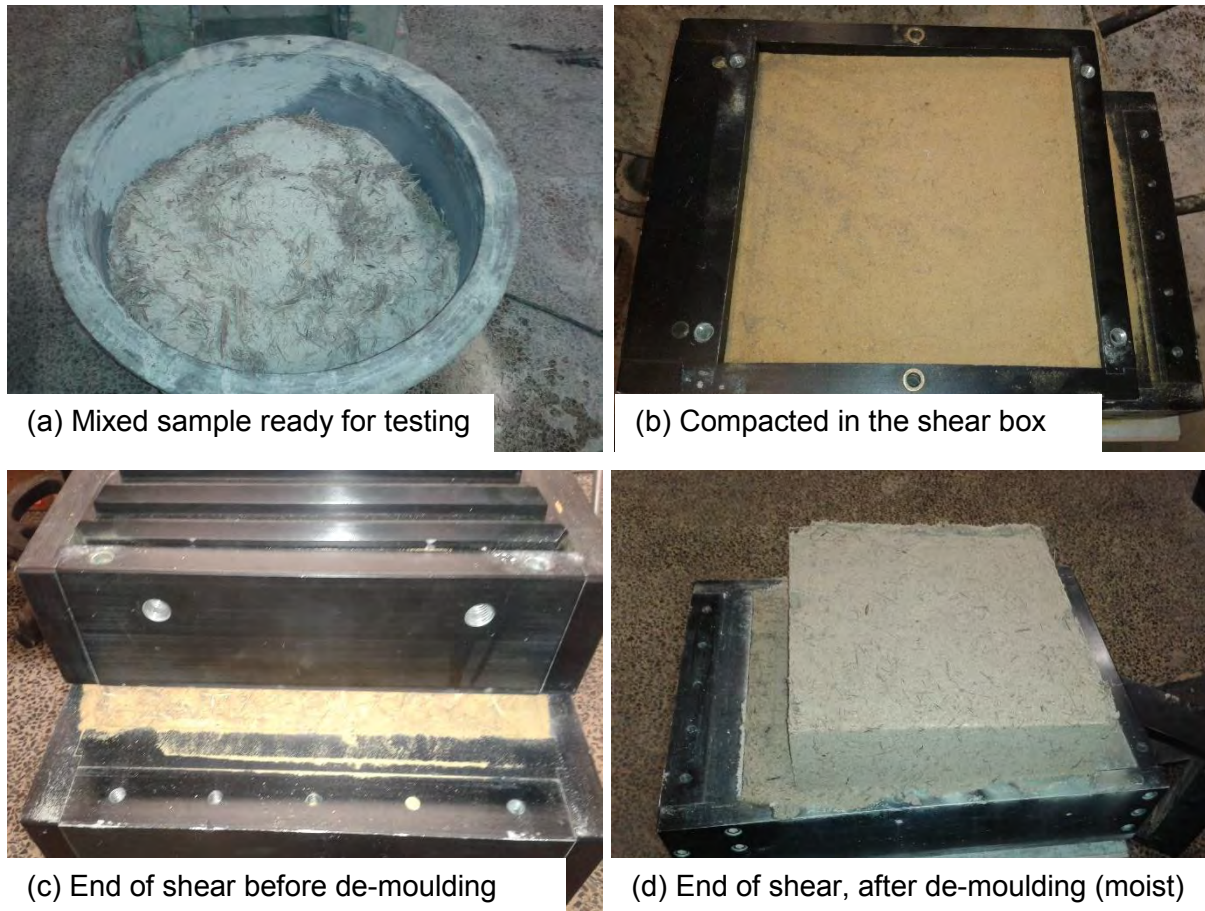


Figure 4.14: Sample preparation and end results

Mixing was done by replacing an equivalent mass of soil with either fibre, pith or millrun bagasse for both soils. For instance, to obtain 1.0%, 300 g of soil was replaced with 300 g of bagasse. Both soil and bagasse was then mixed in the mechanical mixer for a period of 3 minutes. A uniform mix was achieved compared to that obtained when mixing by hand as in the case of previous work reviewed in literature. Mixing for more than 3 minutes would have caused even further segregation.

The uniform composite obtained was carefully placed and compacted in the split box in 3 layers. Care was taken not to segregate the fibres further, although controlling this was sometimes not possible, especially for higher concentrations.

In addition, fibres slightly reduced the density of the compacted soil. Fibres occupy space due to their bulky low-density nature. This hinders the soil from getting compacted and consequently reduces the density of the compacted soil. This reduction was minimal although

Anagnostopoulos et al. (2013) reported to the contrary and recommended using void ratios as opposed to volume in the mix design. Technically, achieving the recommended void ratios would be difficult in the field applications and would be impractical.

As in the case of soil only mix preparation, the samples were also prepared at moist conditions corresponding to the optimum moisture content of the soils. The difference came in how the required water was added. Since bagasse fibre is hydrophilic, water was added to the already mixed soil-bagasse. A further mixing was then conducted. This ensured that both the soil and fibres absorbed the added water uniformly. It was interesting that segregation was incredibly reduced with the addition of water. Furthermore, due to the high water absorption capacity of the fibres, the attained dry densities were slightly reduced compared to soil only mix design. This was expected considering that the standard proctor test was done on soil only and not on the composite. Figure 4.15 shows the composite of moist Cape Flats sand with fibre bagasse ready for testing and placed in the split box respectively – note the absence of fibre segregation.



Figure 4.15: Moist sample preparation and placement in the split box

4.5.3 Durability design

The same procedure was followed as outlined in section 4.5.2.2. For the wetting and drying, the composite was wetted for 24 hours then dried in an oven set at 35°C for another 24 hours. This was repeated 12 times before conducting shear tests. The design simulated the effect of wetting and drying conditions experienced in-situ due to the drawdowns in the ground-water levels. The temperature of 35°C ensured complete drying of the composite with no damage to the fibres.

For the soaking tests, the bagasse soil mixture was compacted dry in the uniquely designed durability moulds then kept under water for a duration of between 6 hours and 14 days as

given in the testing regime. After the set period, the durability moulds were then inserted on the shear split boxes and secured in place ready for shear as shown in figure 4.16.



Figure 4.16: 14 days soaked composite ready for testing

4.5.4 Assembly of apparatus

The soil only mix for control tests and soil-bagasse composite was done under a dust extractor located in the structural engineering general laboratory at UCT, then wheeled to the geotechnical laboratory for testing. Care was taken while wheeling to avoid further re-compaction of the mix due to vibration. At any rate, the compacted mix could not be affected by the vibrations.

The split box fixed in place with the alignment screws was then pushed in to the ShearTrac-III base container with rollers that allowed lateral movement. The crossbar was then lowered and fixed using the control panels on the side of the ShearTrac-III machine or through the PC and the various bolts, respectively. The vertical lowering and the horizontal movement were done until the crossbar coincided with the steel ball placed on the loading plate. All the connections were double-checked before testing using the flow chart shown in figure 4.18.

4.5.5 Experimental procedures

After doing a double check for the apparatus setup, the testing commenced with the 50 kPa load for both the unreinforced control test and the reinforced samples. As the ShearTrac-III machine was fully automated, the necessary input parameters such as consolidation time, water content, shear rate and load, and the frequency of reading were fed into the system via

a PC as shown in screen shot figure 4.17. Only the vertical load was changed for the subsequent tests.

The screenshot shows the SHEAR software interface with a menu bar (File, View, Run, Calibrate, Control, Report, Options, Help) and a main window divided into three sections: Test Parameters, Consolidation Table, and Shear Table. The Test Parameters section includes fields for Project Number, Project Name, Location, Date of Test, Tester, Checker, Description, and Remarks. The Consolidation Table section includes fields for Boring Number, Test Number, Sample Number, Depth, Elevation, and Sample Type. The Shear Table section includes a Read Table field.

Figure 4.17: ShearTrac-III software set-up screen shot

A shearing rate of 1.0 mm/min was used for all the sandy soil tested and a rate of 0.5 mm/min for the clay. These shearing rates were as recommended by Sadek et.al (2010). The high shearing rate for sandy soil was used since no excess pore water pressure was expected, in contrast to the Kaolin clay. A maximum displacement was set at 60 mm corresponding to 20% of the split box dimension. In addition, the consolidation period was set for a minimum of 5 minutes for sand and 10 minutes for clay. The choice was made because sandy soils consolidate faster than clay soils.

The sample was first consolidated until the pre-set consolidation period was attained. This was done by first calibrating both the vertical, horizontal load cells and the displacement LVDT's. The calibration involved zeroing the reading on these sensors by matching up their count numbers. Achieving perfect zero readings was not possible due to the sensitive nature of the sensors.

After consolidation, the shearing phase was initiated by first removing the alignment screws and leaving a gap between the upper and lower box to avoid metal-metal friction. This was done with the aid of the four knobs fixed on the upper box and in accordance with ASTM D3080. It should be noted that ASTM D3080 does not give any guidelines on how to ensure an optimal gap is left between the two split boxes. It only states that the gap should be large

enough to avoid friction and small enough to ensure compacted soil interaction during shear. As such, the four knobs were turned in one revolution to provide this gap. The horizontal load cell was re-zeroed before shearing at a constant rate. This was achieved by sliding the lower box against the upper box while capturing the real time data on the PC.

At the end of the test, both the horizontal and vertical load cells were zeroed to avoid wear and tear and the fixing screws removed. The vertical crossbar was then raised and the sample extracted from the ShearTrac-III lower base. Sample fibres were then exhumed and visually viewed for deformations before discarding the sample. The procedure was repeated for all the 183 tests conducted. A summary of the procedure is given in the flow chart shown in figure 4.18.

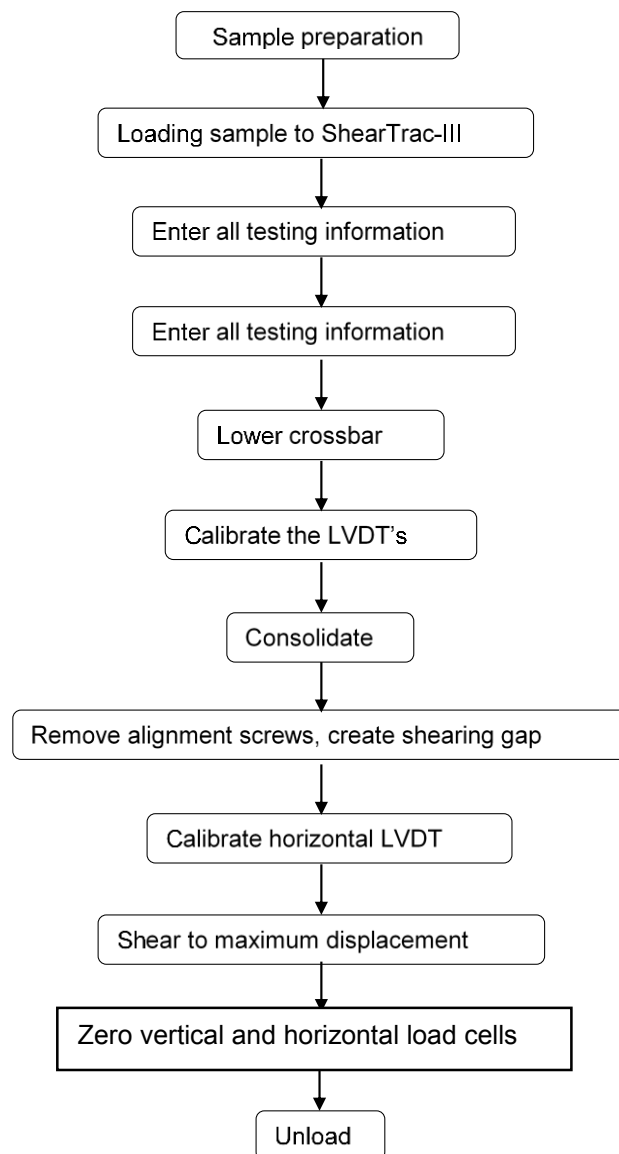


Figure 4.18: Experimental procedure

4.5.5.1 Wetting/drying and soaking

The same procedure was followed as described above, with exceptions on how the sample was prepared and loaded. Since a smaller mould size was used for the soaked samples, a different loading plate was incorporated. The area in contact with the loading cell was also adjusted accordingly to reflect the reduction in the split box size.

4.5.5.2 Repeatability

To verify the repeatability of results from the experimental procedure, tests done on sand only were repeated 3 times. These tests were conducted on Klipheuwel sand using 0.7% fibre content at 50 kPa normal load. The same experimental procedures as described above were followed. All the tests were conducted in a dry state and the results obtained are presented in Chapter 5.

4.5.6 Quality concerns

Several factors were considered to ensure the quality of the results obtained as elaborated below.

- Mixing the bagasse with the selected soils long enough to ensure a homogenous random mixing. The addition of water was controlled to ensure balanced water absorption between the fibres and the soil. A little evaporation was noticed, although minimal, since the mixture was left standing for a shorter period of one hour between tests.
- Sample preparation was done on the same day of testing. In other words, the preparation and testing was simultaneous to reduce the variability of the results obtained.
- For the optimum moisture content tests, representative moisture content determination was undertaken before and after the tests. This was to ensure that the predetermined moistures were achieved.
- No sample was re-used in the testing procedure. In addition, all the equipment was calibrated.

4.5.7 Data calculation

Data processing was in the form of normal/shear stress and vertical/horizontal displacements with time, until maximum displacement was achieved.

Normal stress, σ_n , is given as the vertical pressure applied to the sample through the vertical loading plate. It is a ratio of the force divided by the sample contact area as given in equation 29.

$$\sigma_n = \frac{N}{A} (kN / m^2) \quad (29)$$

Where,

N is the normal load in kN,

A is the sample contact area in m^2 calculated from the dimension of the split box.

Shear stress, τ , in direct shear box tests is the measured resisting force developed in the soil-fibre composite as the lower box slides at a constant rate under the top box . It is computed based on equation 30.

$$\tau = \frac{F}{A} (kN / m^2) \quad (30)$$

Where;

F is the shearing load generated by the horizontal loading cell which causes the lower split box to move relative to the upper box, measured in kN and,

A, is the shear contact area which varies as the lower box moves, compensated through instantaneous reduction in the area in m^2 .

The horizontal and vertical displacements plus all the normal and shear stresses obtained were stored in real time in the set file on the PC. All the large data sets generated were then exported to the spreadsheet and analysed accordingly. The results were as discussed in Chapter 5.

Figure 4.19 gives a summary of the methodology followed to achieve the objective of this study.

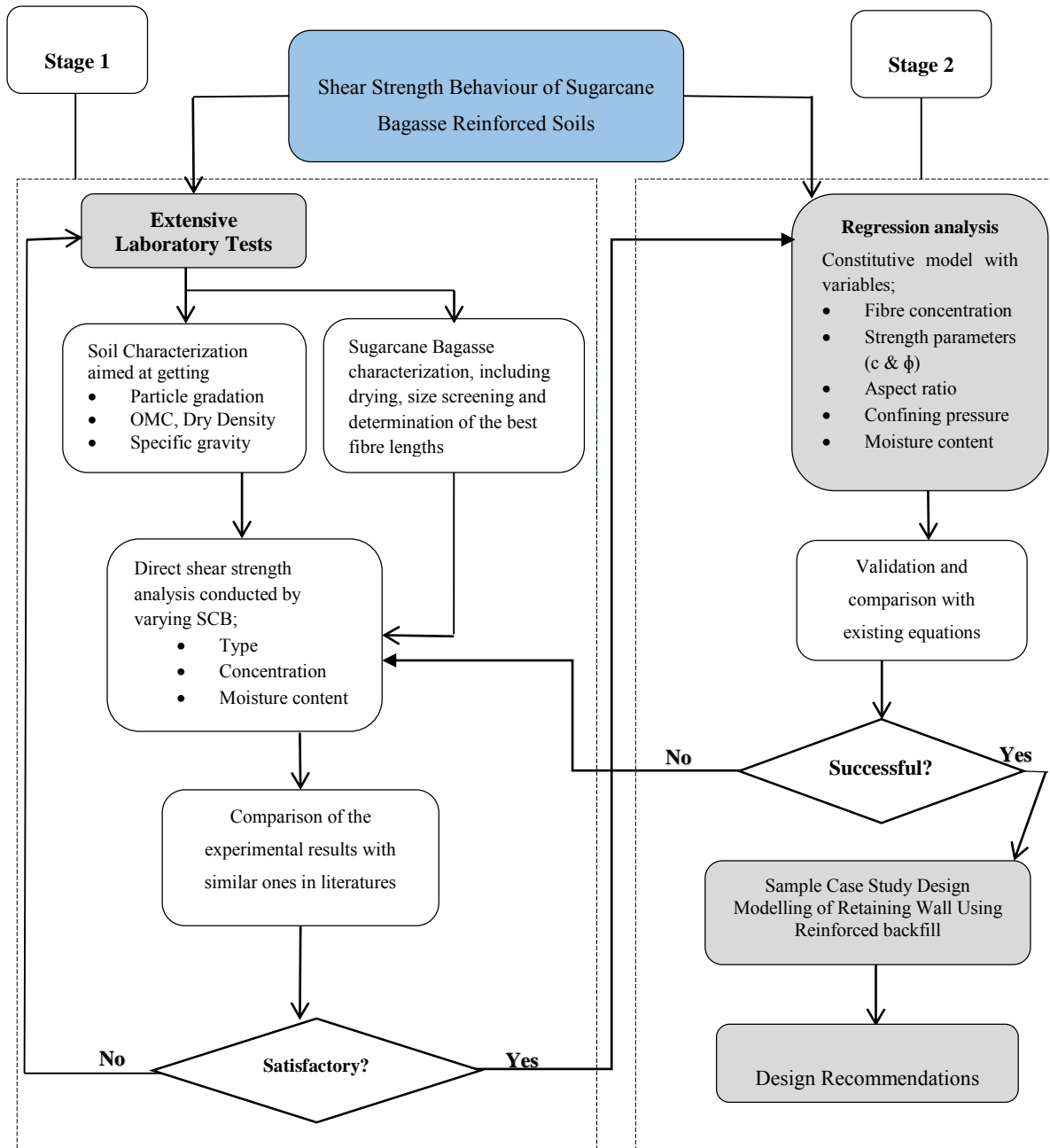


Figure 4.19: Summary of the research methodology

CHAPTER 5

5 RESULTS, ANALYSIS AND DISCUSSIONS

5.1 Introduction

This chapter presents all the direct shear test results conducted on Klipheuwel sand, Cape Flats sand and Kaolin clay reinforced with varying concentrations and types of sugarcane bagasse. An attempt is made at explaining the results obtained and comparing the effect of the bagasse types on the shear strength parameters of the selected soils.

The chapter also details the durability study results obtained through wetting and drying, and soaking in water. It ends with a regression analysis for a predictive model based on the experimental outcomes.

5.2 Repeatability results

The repeatability study results are shown in figure 5.1. These results showed similar peak strengths at the same horizontal displacement (10 mm) with deviations in residual strengths as shown in the figure 5.1.

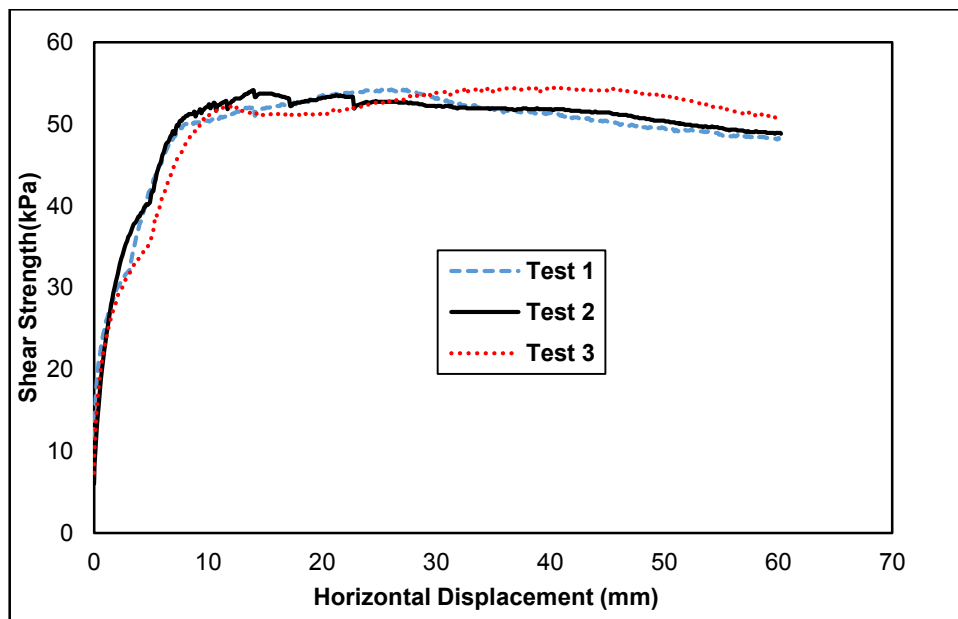


Figure 5.1: Quality test results, showing results at 1.0% fibre, 50 kPa normal pressure

The repeatability results were analysed for deviation from the mean peak shear strength. Deviations of 0.1% and 2% were depicted for the peak and residual strength respectively as presented in table 5.1. However, the deviations were within the acceptable 5% justifying the validity of the test results and the replication of the procedures.

Table 5.1: Repeatability results computations

Test	Peak strength (kPa)	Mean	Deviation	Residual strength (kPa)	Mean	Deviation
1	54.2		0.0%	48.2		-1.8%
2	54.1	54.2	-0.2%	48.8	49.1	-0.6%
3	54.2		0.0%	50.2		2.2%

5.3 Control test results and discussion

To determine the extent of shear strength improvement with varied fibre parameters, control tests were conducted on unreinforced soils, sand/sand and clay/clay interfaces. To obtain the angle of internal friction and apparent cohesion, each test was repeated at 50, 100, and 200 kPa. The results were as given in the sub-sections below.

- **Soil in the dry condition**

The results of the tests done on the unreinforced sand are displayed in figure 5.2. It should be noted that Klipheuwel and Cape Flats sand were compacted to attain 55% of relative density before shearing at a 1.0mm/min rate of shear to a maximum displacement of 60 mm. On the contrary, in Kaolin clay a shearing rate of 0.5mm/min was allowed to a maximum of 30 mm horizontal displacement corresponding to 10% displacement as recommended in ASTM D3080.

Tests on the sandy soils produced smooth curves except Cape Flat sand, which exhibited a slight regain in strength just after failure. This phenomenon was attributed to the roundness of the particles in the Cape Flats sand, which rearranges and dilates in the shear plane causing the regain in strength. Similar results were obtained by Sadek et.al. (2010) attributing this behaviour to the dilation of particles, especially at higher confining stresses.

Tests carried out on Kaolin clay were aimed at gaining insight on how the inclusion of fibres affects the shear strength behaviour of clay. No defined peak shear strengths were observed, although there was a possibility of obtaining higher peak strengths as evidenced in figure 5.2 (b). However, only peak shear strengths mobilised at 30 mm of strain were presented.

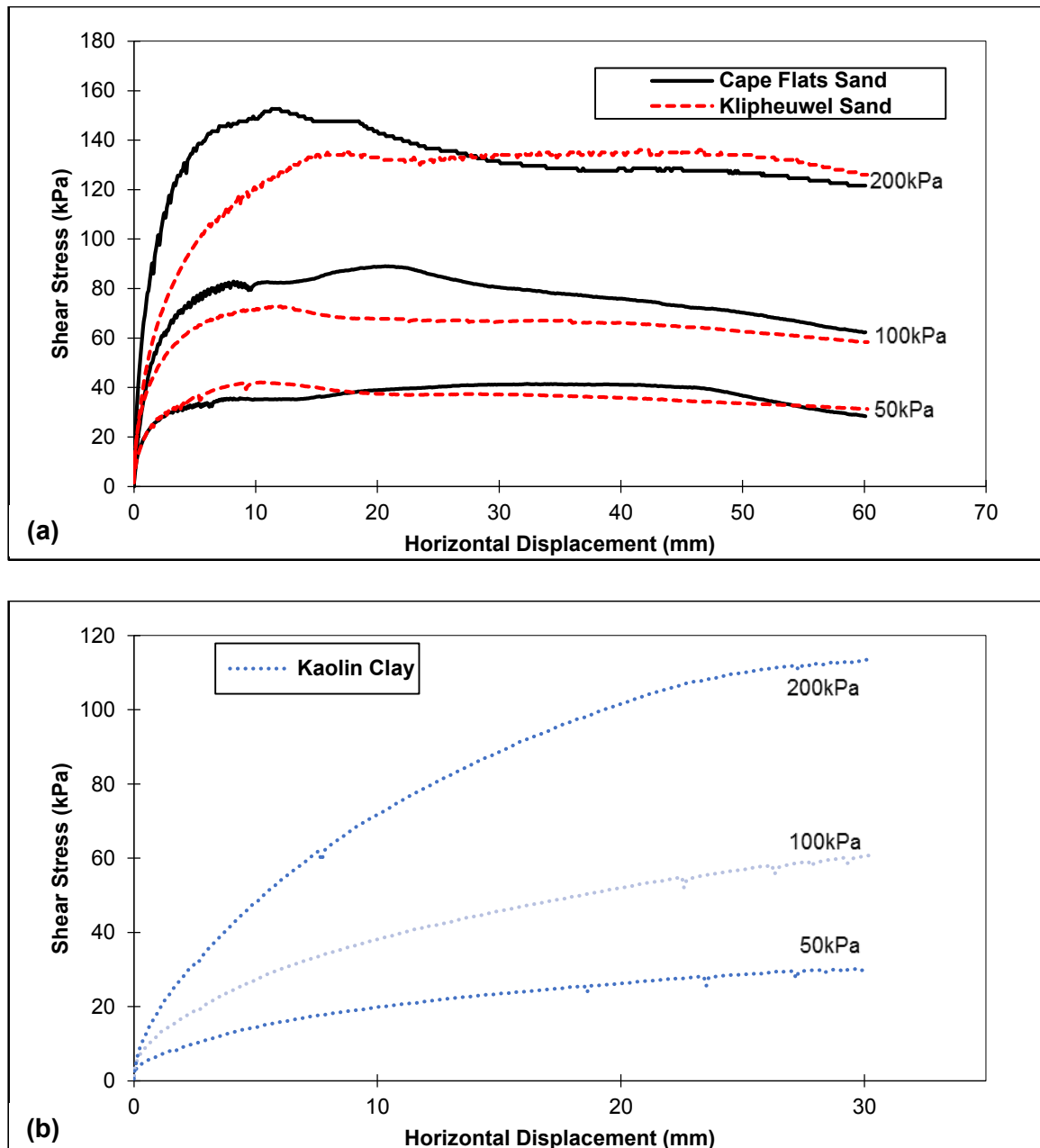


Figure 5.2: Control test results (a) sands (clay) at dry state

▪ **Soil in moist condition**

Figure 5.3 shows the control test results on moist soils compacted at OMC given in table 4.2. The shear strengths appeared to increase continuously and showed no residual strength. This could be explained by the effect of water that lubricated the particles, reducing the inter-particle friction and their resistance to shear. These results contradicted those obtained by Lovisa et.al (2009) which showed that including water in unreinforced soil modifies its relative density and increases strength.

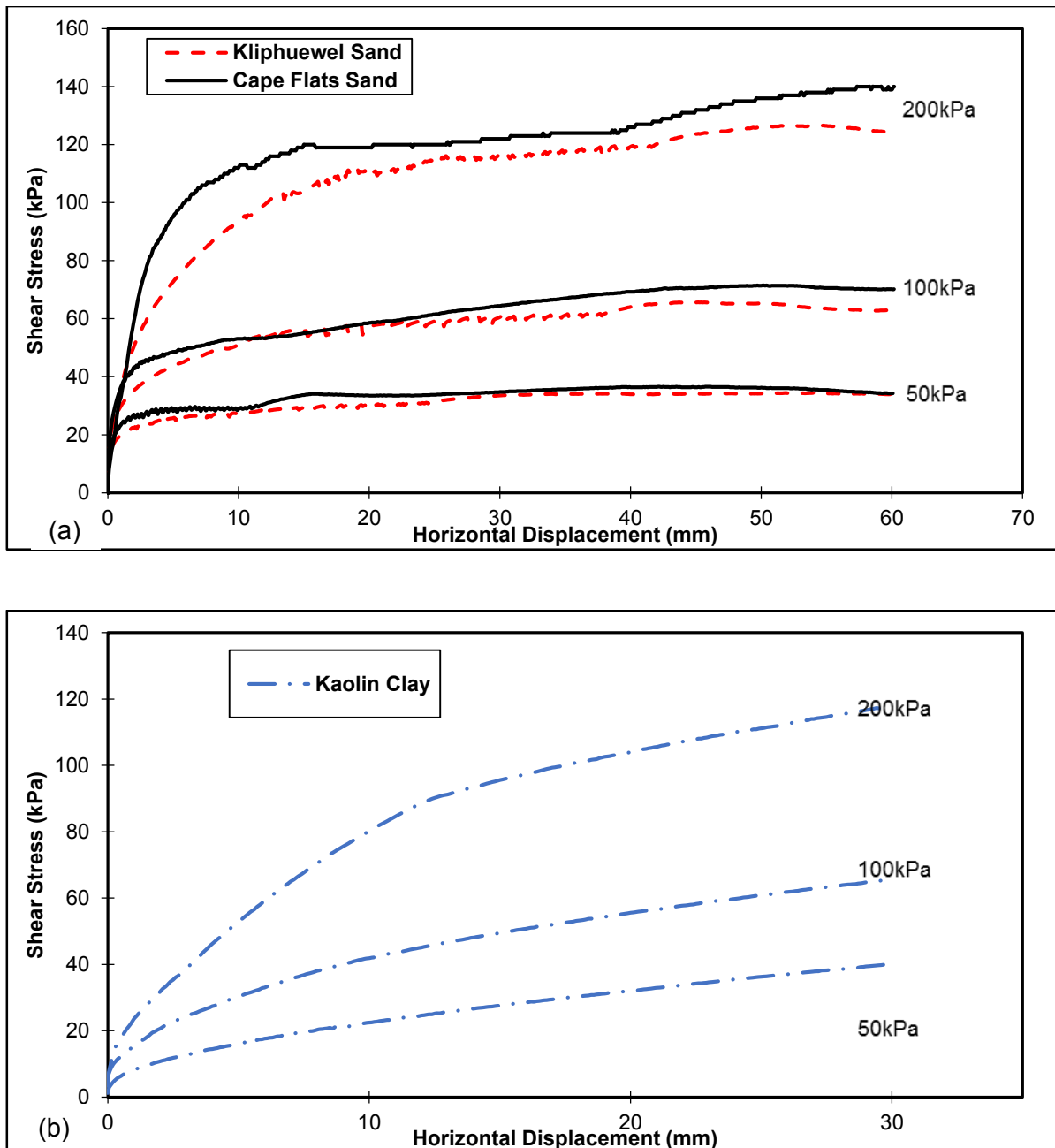


Figure 5.3: Control test results (a) sands (b) clay at moist condition

5.4 Direct shear results on fibre-soil composite

All the direct shear test results on bagasse-reinforced soils are presented in this section. The results are presented and discussed in the form of shear stress deformation and shear envelope for all the soils (dry and moist), and both types of sugarcane bagasse. For each type of soil and bagasse, a different graph is presented at different bagasse contents and three normal pressures. The graphs were plotted on the same chart to show the variation in shear strength with sugarcane bagasse concentrations.

5.4.1 Shear deformation relationships at dry soil conditions

The results obtained from the reinforced soils in their dry states are shown in this sub-section beginning with Klipheuwel sand, Cape Flats sand and then Kaolin clay.

5.4.1.1 Klipheuwel sand

Fibre bagasse

Figure 5.4 shows the shear stress – horizontal displacement results obtained from the direct shear of Klipheuwel sand reinforced with fibre bagasse at concentrations of 0.3% to 1.7% of the dry weight of soil. The stiffness of unreinforced and reinforced Klipheuwel soil remained approximately similar at low strains depending on the magnitude of the normal stress. This showed that the shear-horizontal displacement graph of composites at low strains is not affected by fibre inclusion regardless of the concentration. Similar results were obtained by Anagnostopulos et.al (2013).

As displacement progressed, deviation in the slopes was evident across the applied normal pressures (50, 100, 200 kPa). The peak stresses were obtained at 10 mm to 20 mm of horizontal displacement for all the fibre concentration investigated. This behaviour strongly supported the hypothesis that the shear strength of reinforced soil composite is directly related to the interaction between soil and fibres. At the onset of shear, the soil particles rearrange themselves in the failure plane causing the fibres to stretch and mobilise their shear strengths. As the shear progresses, the spatial network of the randomly distributed fibres interlock with the soil particles resisting the horizontal displacement. This resistance contributed to the inherent deviation in slopes as shown in the figure 5.4.

There was a consistent increase in the peak shear strength as the fibre content increased. The increment was dependent on the applied normal load. This dependence may be attributed to the increased number of fibres in the shear plane causing more interaction of the interlocking matrix between the soil and the fibres, thereby further increasing the shear resistance of the composite.

Inclusion of fibre bagasse also reduced the loss in post peak strength as shown in figure 5.4. This trend increased with the increased fibre content. In addition, the post peak shear stress – horizontal displacement graphs obtained slightly paralleled the unreinforced shear stress – horizontal displacement graph especially at 0.7%. It could be said, therefore, that the inclusion of fibres linearly increased the residual strengths of Klipheuwel sand.

The percentage improvement in the shear strength was observed to decrease at higher normal pressures across all the fibre contents. For instance, at 50 kPa and 0.3% fibre content, about

30% increase was noticed compared to 21% increase at 200 kPa as shown in table 5.2. Anagnostopoulos et.al (2013) explained this behaviour by the arching of sands around the fibres under large normal pressures.

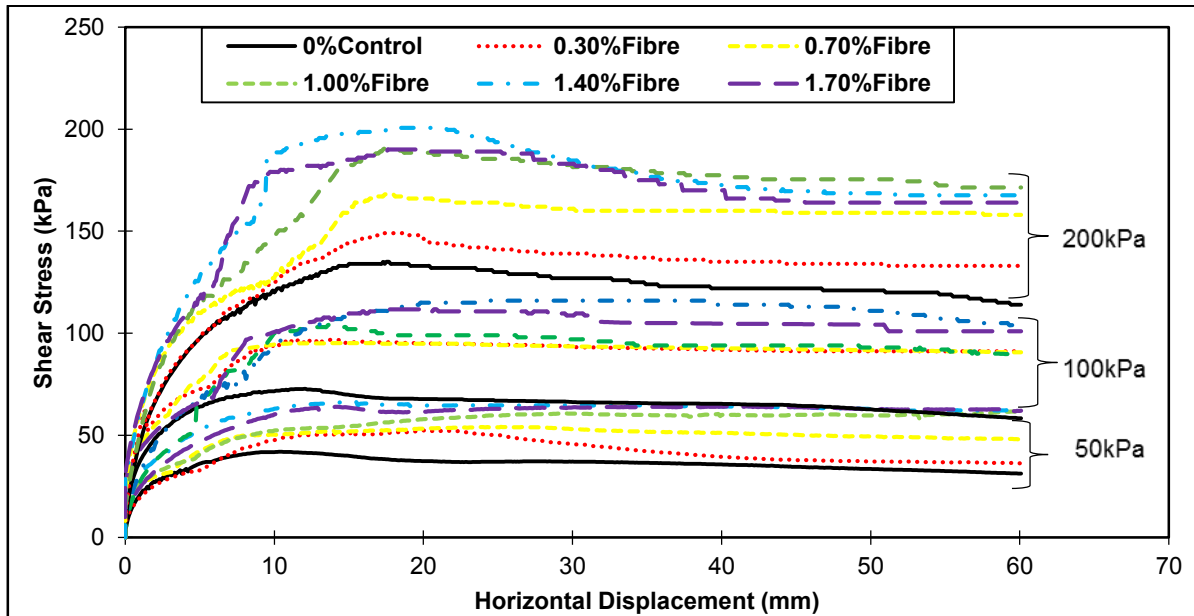


Figure 5.4: Shear deformation of dry Klipheuvel sand with varying fibre content

Furthermore, the increase in peak shear with fibre content was up to a maximum value. An upper concentration existed beyond which, an increase in fibre content decreased the peak shear stress. As fibre content increased, segregation occurred and particle rearrangement was restricted. These restrictions lead to the slippage of the fibres and sand particles, which decreased the peak shear stresses observed. This upper value was noticed at 1.4% fibre concentration. It should be noted however, that achieving the maximum content was not a determining factor in varying the concentrations, but rather fibre segregation. Segregation of fibres occurred at 1.7% fibre content as shown in figure 5.5.



Figure 5.5: Fibre floating at 1.7% fibre content before testing

Table 5.2 gives the summary of the peak shear strengths obtained across the fibre bagasse concentrations with their corresponding percentage increase as compared to unreinforced Klipheuwel sand.

Table 5.2: Summary of peak shear strength for fibre bagasse reinforced Klipheuwel sand

Fibre Content	50 kPa normal stress		100 kPa normal stress		200 kPa normal stress	
	Peak shear (kPa)	% Increase	Peak shear (kPa)	% Increase	Peak shear (kPa)	% Increase
Unreinforced	40.0	-	72.8	-	135.9	-
0.30%	52.5	31.2%	94.1	29.2%	164.4	21.0%
0.70%	54.2	35.6%	95.4	30.9%	168.1	23.7%
1.00%	61.9	54.7%	104.1	42.9%	190.4	40.1%
1.40%	66.3	65.7%	116.4	59.8%	200.6	47.6%
1.70%	64.3	60.7%	111.7	53.4%	189.8	39.6%

Millrun bagasse

Shear stress – horizontal displacement curve of millrun/sand composite results are as shown in figure 5.6. A considerable change in the peak and residual shear strength was evident in reinforced soil compared to the unreinforced one. As the millrun content increased, a corresponding increase in the peak shear strength was observed up to a maximum concentration of 1.4%. This increase was gradual and was to a lesser extent similar to the trend observed when reinforced with fibre bagasse. For instance, at 1.4% content and 100 kPa normal pressure, an increase of about 40% in the peak shear strength was obtained in millrun compared to 60% in fibre. Millrun bagasse contains both fibre and pith bagasse. Pith occupies some space depending on the concentration hindering full interaction between fibres and soil. This behaviour also explains the inconsistencies in the peak strength ratios experienced at 50 kPa as summarised in table 5.3.

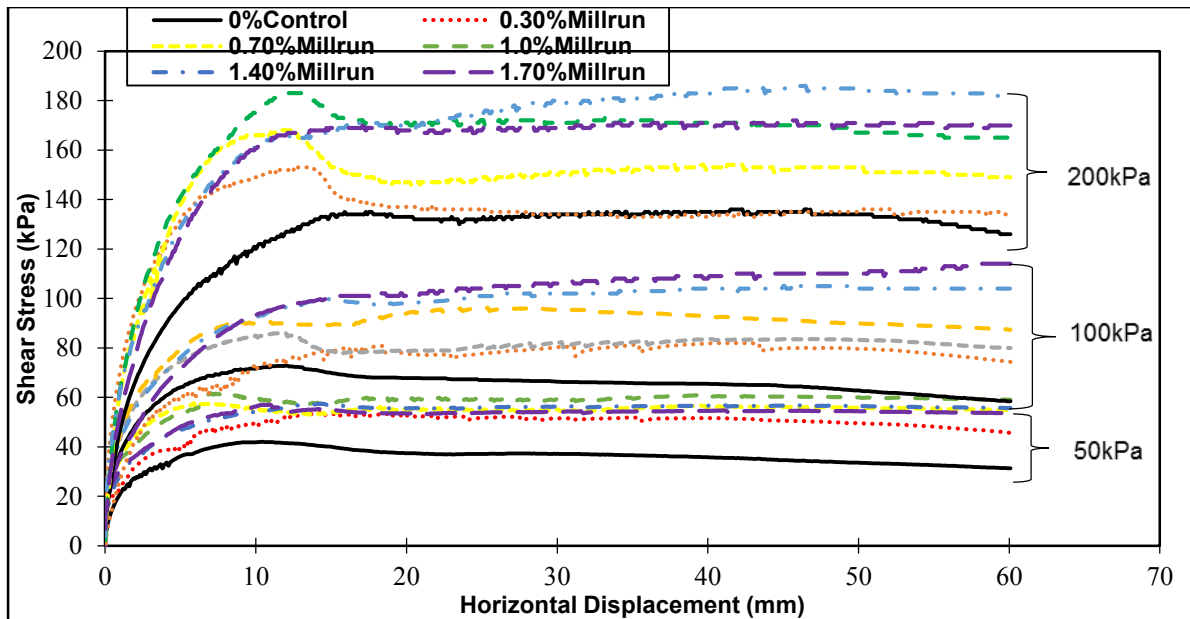


Figure 5.6: Shear deformation of millrun reinforced dry Klipheuwel sand at varied content

No considerable change in the peak shear strength was evident in millrun bagasse at normal pressure 50 kPa. As the normal load increased, the difference in peak stresses got pronounced. It is believed that since millrun bagasse contained pithy materials, there was a possibility of slippage between them and soil particles, hindering the soil/fibre interaction and reducing peak shear strength. At low confining pressure, this slippage was low and increased with the increase in confining pressure due to reduced void ratios.

Considerable increase in post peak strength was also realized. However, the magnitude was low compared to fibre bagasse inclusions at 1.4% concentration.

Table 5.3: Summary of peak shear strengths for millrun bagasse reinforced Klipheuwel sand

Millrun Content	50kPa normal stress		100kPa normal stress		200kPa normal stress	
	Peak shear (kPa)	% Increase	Peak shear (kPa)	% Increase	Peak shear(kPa)	% Increase
Unreinforced	40.0	-	72.8	-	135.9	-
0.30%	53.9	34.8%	82.0	12.6%	153.3	12.8%
0.70%	57.5	43.8%	86.1	18.2%	167.7	23.4%
1.00%	61.6	53.9%	96.1	31.9%	183.4	35.0%
1.40%	57.3	43.3%	104.8	43.8%	185.8	36.7%
1.70%	55.0	42.4%	114.4	57.1%	171.7	26.3%

Pith bagasse

It was hypothesized that the pith bagasse would either reduce the shear stress – horizontal displacement deviation or maintain the deviation due the considerable quantities of residual sugars in the pith bagasse. Nevertheless, as shown in figure 5.7, a slight deviation was

exhibited across the normal pressures. This deviation may be attributed to the ductility of the composite (strength hardening) rather than increased interlocking of the pith and soil. Additionally, it could be attributed to some fine fibres that found their way during depithing. A clear visual inspection of the pith bagasse (figure 4.7) showed some substantial amount of fibres, which could have contributed to the change in the shear stresses.

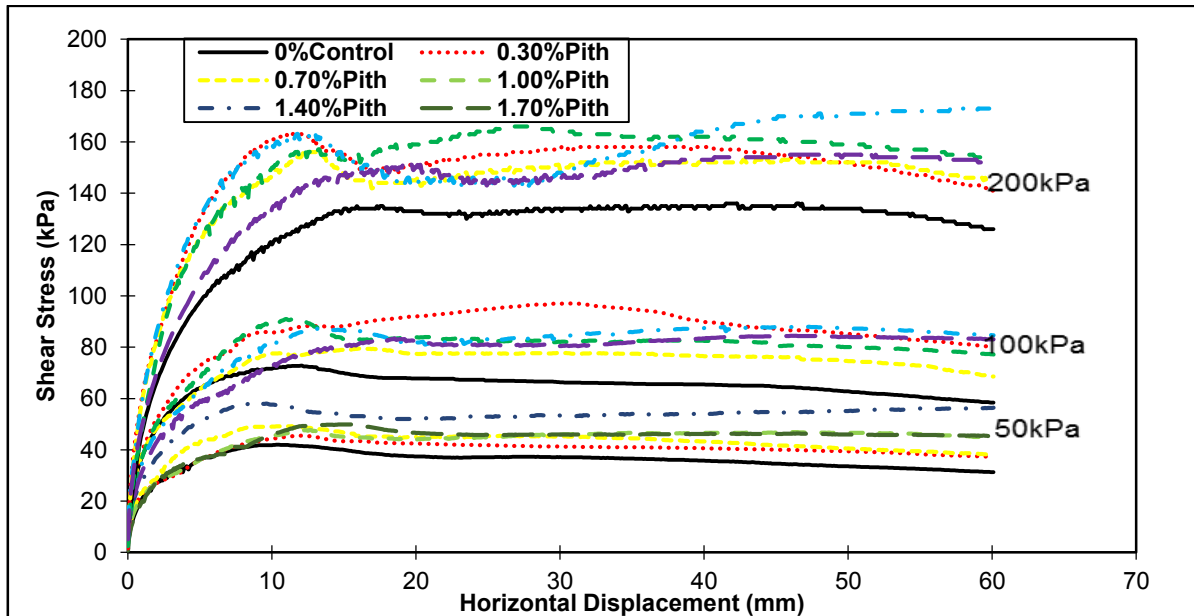


Figure 5.7: Shear deformation of dry Klipheuwel sand at various pith contents

This strength hardening was higher at high normal pressures as summarised in table 5.4. Similar to millrun bagasse, the high deviations at high normal pressures could be attributed to the reduced void ratios as a result increase normal pressures that improved the interaction matrix.

Table 5.4: Summary of peak shear strengths for pith bagasse reinforced Klipheuwel sand

Pith Content	50kPa normal stress		100kPa normal stress		200kPa normal stress	
	Peak shear (kPa)	% Increase	Peak shear (kPa)	% Increase	Peak shear(kPa)	% Increase
Unreinforced	40.0	-	72.8	-	135.9	-
0.30%	46.4	16.1%	97.1	33.3%	163.5	20.3%
0.70%	49.3	23.2%	79.5	9.1%	156.1	14.8%
1.00%	47.7	19.2%	91.1	25.0%	165.8	22.0%
1.40%	58.1	45.4%	87.9	20.6%	172.8	27.2%
1.70%	49.9	24.8%	84.4	15.9%	154.8	13.9%

5.4.1.2 Cape Flats sand

Fibre bagasse

Similar results as those from reinforced Klipheuwel sand were obtained for Cape Flats sand. The Shear stress – horizontal displacement curve of fibre reinforced Cape Flats sand remained unchanged at low strain but deviated considerably as strains increased. The deviation, however, was low compared to Klipheuwel sand. Cape Flat sand is coarser ($D_{50}=0.40$ mm) compared to the Klipheuwel sand ($D_{50}=0.28$ mm) used in this study. Another factor that possibly contributed to this difference is the angularity; Cape Flat sand has sub-round particles while Klipheuwel sand has sub-angular particles. According to Look (2007), the angularity of cohesionless soil affects its strength parameters.

Figure 5.8 shows the shear deformation fibre reinforced Cape Flats sand. From the graphs, it can be seen that at 0 mm to 5 mm of displacement, the unreinforced Cape Flats sand depicted higher strengths compared to reinforced Cape Flats sand. This was because of the fibre-slip discussed in section 2.4.2 and 2.6.2. From 5 mm onwards, the trend was reversed due to particle aggregation and interlocking with the fibres providing greater resistance to shear. The two factors concurrently increased the interaction matrix between the fibres and soil and consequently the peak shear strengths.

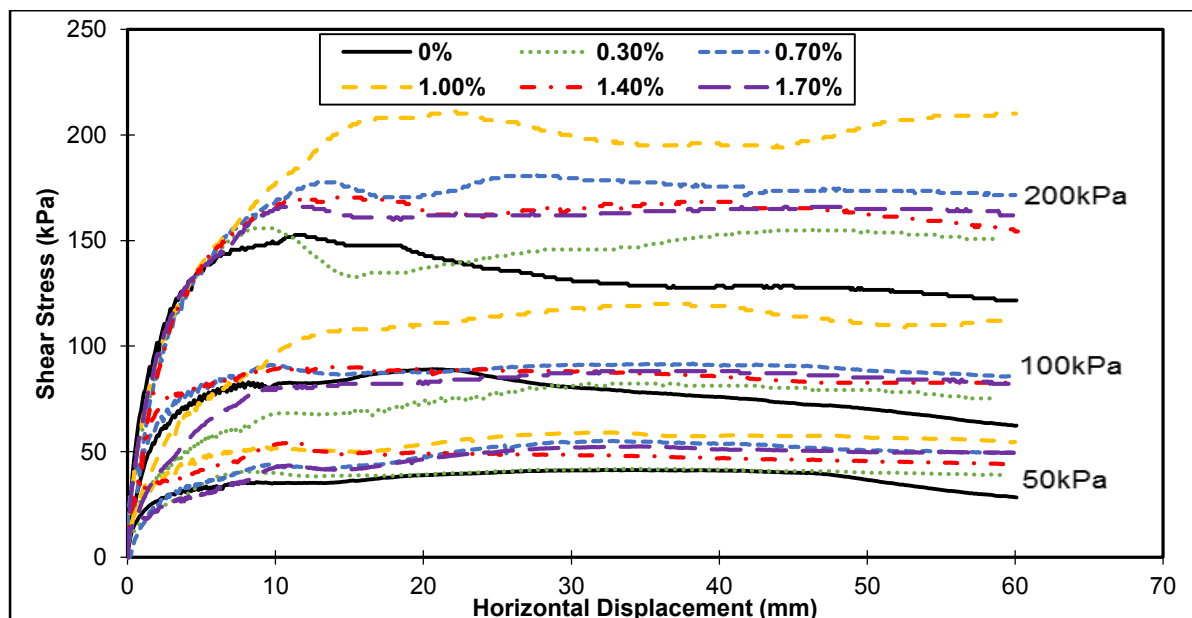


Figure 5.8: Shear deformation of dry Cape Flats sand at various fibre bagasse content

As summarised in table 5.5, there was no significant change in the peak shear strengths at 0.3% fibre bagasse content regardless of the increase in normal load, contrary to the results obtained from Klipheuwel sand. At a higher concentration of fibres, substantial improvement in the peak shear strengths was depicted which reduced with increasing normal pressures.

The angularity and the soil-fibre interaction matrix still played a crucial role in this improvement.

From the literatures (Gray and Ohashi, 1986; Sadek et.al 2010; Anagnostopoulos et, al 2013), the consensus is that coarse sand reinforced with fibres portrays high improvement in peak shear strengths at high normal pressures compared to fine sands. This was not the case in this study as reinforced Cape Flats sand depicted a low increase in peak shear strength except at 100 kPa with 1.0% fibre content. About 50% increase was achieved compared to about 40% for fibre reinforced Klipheuwel sand.

The residual strengths obtained showed a reduction in the post peak loss of strength. This was not as pronounced as in the Klipheuwel sand and showed a lot of scatter with no defined pattern as a result of regained strength just immediately after failure. In addition, the fibre segregation was predominantly experienced with Cape Flat sand during sample preparation.

Table 5.5: Summary of peak shear strengths for Cape flats/ fibre composite

Fibre Content	50kPa normal stress		100kPa normal stress		200kPa normal stress	
	Peak shear (kPa)	% Increase	Peak shear (kPa)	% Increase	Peak shear(kPa)	% Increase
Unreinforced	41.5	-	78.3	-	152.6	-
0.30%	42.0	1.3%	82.3	5.1%	155.7	2.0%
0.70%	55.2	33.2%	95.3	21.7%	181.5	18.9%
1.00%	59.2	42.8%	118.0	50.7%	210.3	37.8%
1.40%	54.2	30.8%	90.3	15.3%	170.3	11.5%
1.70%	52.6	26.9%	88.2	12.6%	166.0	8.7%

Millrun bagasse

In Figure 5.9, the shear stress – horizontal displacement graphs of millrun reinforced Cape Flats sand are presented and summarised in table 5.6. The peak strengths improved with millrun bagasse inclusion. However, the improvement was minimal and not as defined as in the fibre bagasse inclusion. This could be attributed to the difficulty experienced while mixing the samples. Controlling the quantity of fibre and pith combination in the millrun bagasse was not absolute, although care was taken during mixing. In theory, this translates into a variation in strengths obtained.

The above results notwithstanding, well-defined residual strengths were achieved with an increase in millrun bagasse across all the normal pressures. As in Klipheuwel sand, this behaviour was less profound at high normal pressures.

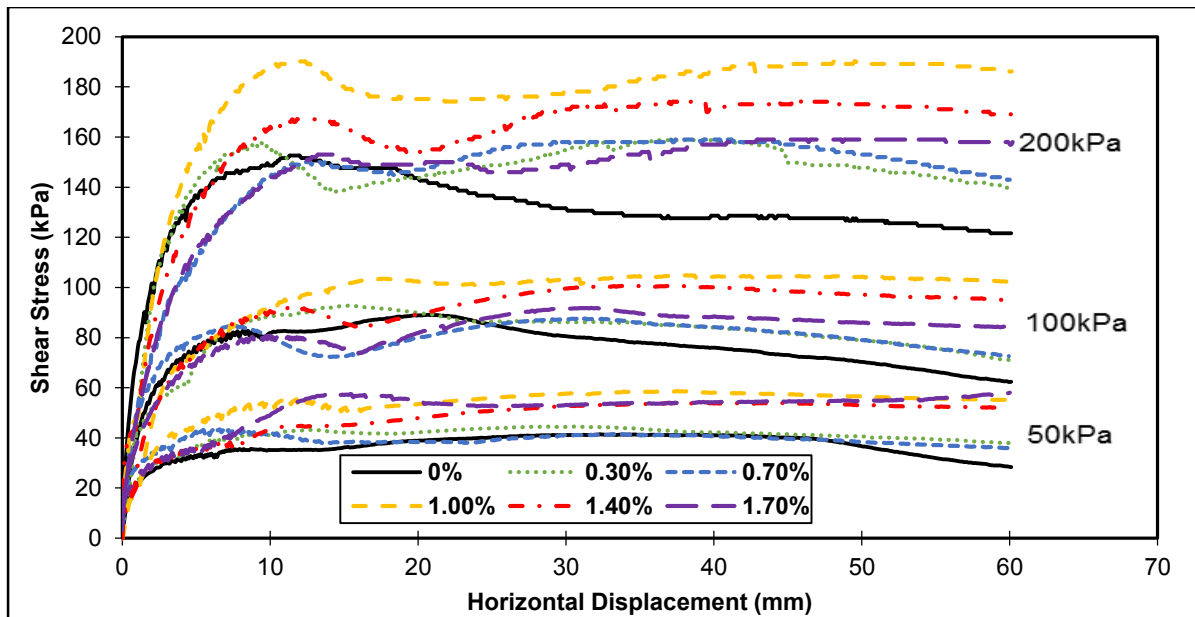


Figure 5.9: Shear deformation of dry Cape Flats sand at various millrun content stress

Maximum peak strength of 0.5 times the unreinforced shear strength was obtained at 1.00% millrun fibre concentration. This peak shear ratio varied at 0.3 and 0.25 between normal pressures of 100 and 200 kPa giving consistent results with those obtained when reinforced with fibre bagasse. Furthermore, comparing these results with those obtained on Klipheuwel sand showed a slight difference of 1.0% in the optimum bagasse content at maximum peak shear strength for all the vertical pressures.

Table 5.6: Summary of peak shear for Cape flats/ millrun composite

Millrun Content	50kPa normal stress		100kPa normal stress		200kPa normal stress	
	Peak shear (kPa)	% Increase	Peak shear (kPa)	% Increase	Peak shear(kPa)	% Increase
Unreinforced	41.5	-	78.3	-	152.6	-
0.30%	44.5	7.5%	92.7	18.4%	158.8	4.0%
0.70%	43.4	4.8%	88.0	12.4%	159.0	4.1%
1.00%	58.7	41.5%	104.8	33.9%	190.2	24.6%
1.40%	53.9	30.1%	100.8	28.7%	174.2	14.1%
1.70%	61.0	47.1%	86.6	10.6%	169.2	10.9%

Pith bagasse

Well-defined shear stress – horizontal displacement curves were obtained in Cape Flats sand reinforced with pith as given in figure 5.10. No distinctive change was realized on the stiffness of the composite between 0 mm to 5 mm of strain. As strain increased, peak strengths

manifested between horizontal displacements of 8 mm to 15 mm corresponding to less than 5% of the relative dimension of the shear box.

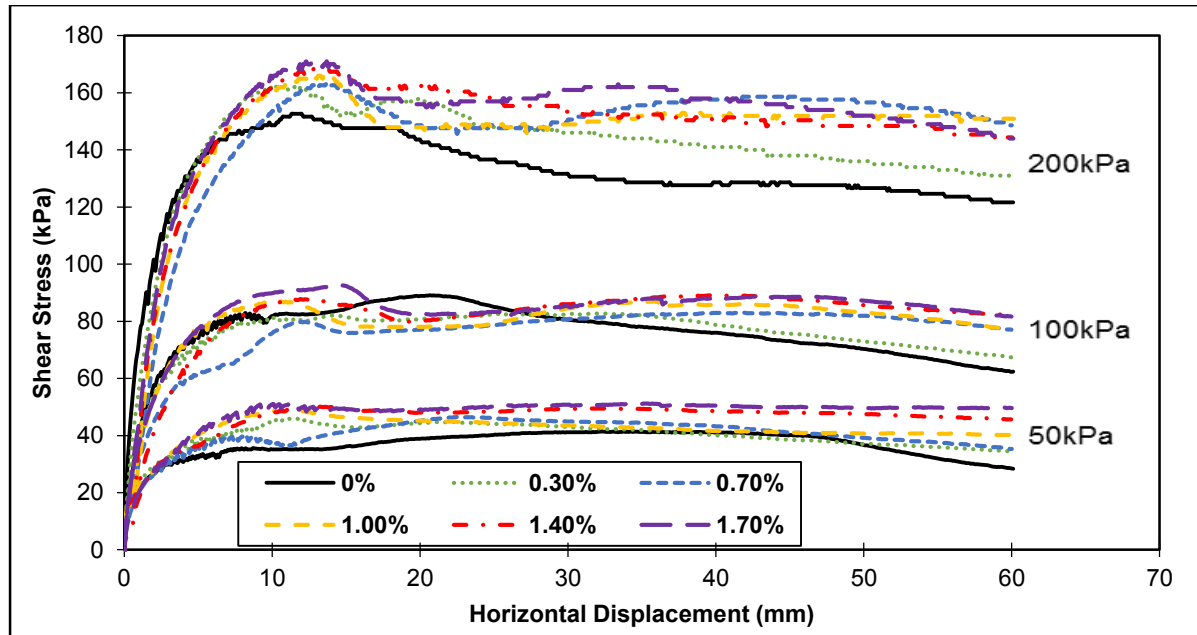


Figure 5.10: Shear deformation of dry Cape Flats sand at various pith contents

There was a gradual increase in the peak shear strengths with increase in pith content. As given in table 5.7, the percentage increase across the vertical pressures was insignificant, especially at higher vertical pressures. It is believed that the large quantity of residual sugars in pith bagasse contributed to this behaviour. In addition, the peak strengths seemed to increase within the pith content of 0.3% to 1.7% investigated. No pith segregation was experienced during sample preparation, confirming that there could be a possibility of obtaining further increase at higher concentrations beyond the range investigated. It can therefore be said that pith bagasse affects the ductility of Cape Flat sand.

Table 5.7: Summary of peak shear strength of Cape flats/ millrun composite

Pith Content	50kPa normal stress		100kPa normal stress		200kPa normal stress	
	Peak shear (kPa)	% Increase	Peak shear (kPa)	% Increase	Peak shear(kPa)	% Increase
Unreinforced	41.5	-	78.3	-	152.6	-
0.30%	45.9	10.8%	82.8	5.7%	162.2	6.3%
0.70%	46.5	12.1%	83.0	6.0%	163.6	7.2%
1.00%	48.6	17.3%	87.0	11.1%	165.9	8.7%
1.40%	50.0	20.7%	89.1	13.8%	168.4	10.3%
1.70%	51.2	23.4%	92.5	18.2%	171.0	12.0%

5.4.1.3 Kaolin clay

Figure 5.11 gives the results of Kaolin clay reinforced with 1.0% fibre, millrun and pith bagasse content.

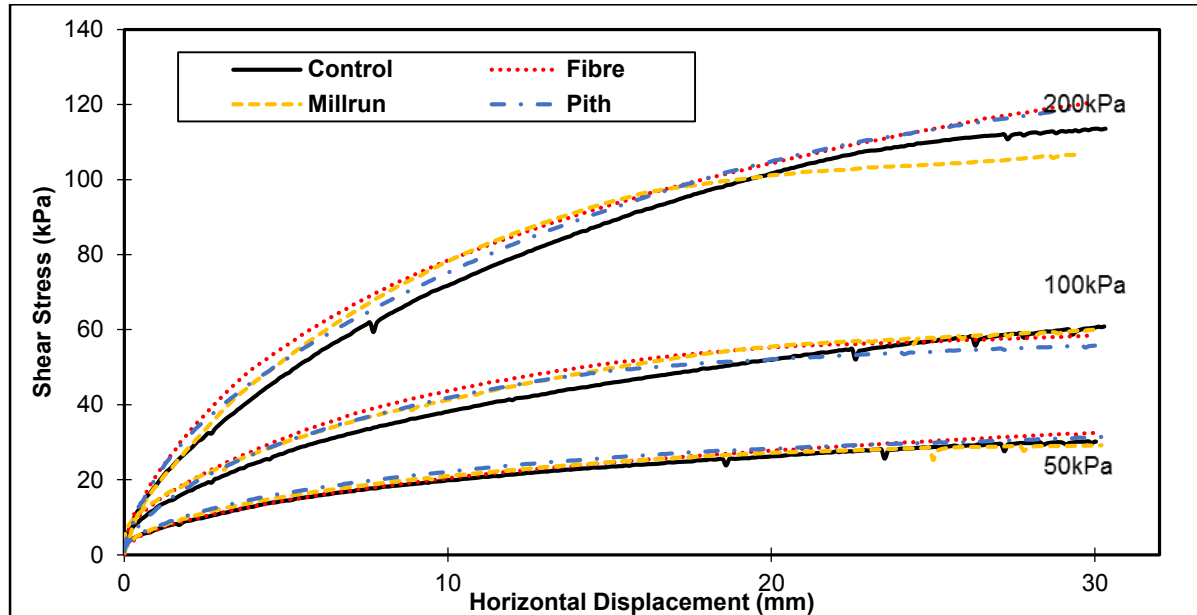


Figure 5.11: Shear deformation of dry Kaolin clay at reinforced with 1.0% fibre/millrun/pith

No distinct peak strengths were observed before the allowed maximum displacement of 30 mm as in the case of loosely placed and sheared soils. At the maximum displacement of 30 mm, a slight change in the shear strength was evident. This change was minimal and not affected by the magnitude of confining pressure or type of bagasse contrary to the results obtained from Klipheuwel and Cape Flat sand. A comparable difference of about 8% was noticed on the Kaolin reinforced with fibre bagasse at 50 kPa with no noticeable trend across the other vertical loads.

Another contrary result to the reinforced sandy soil was the stiffness of the reinforced Kaolin. At 200 kPa, higher stiffness values were noted compared to 50 kPa vertical stress. This was more pronounced in the fibre bagasse and surprisingly high in the pith bagasse, table 5.8.

Table 5.8: Summary of peak shear strengths of Kaolin clay reinforced 1% fibre/millrun/pith bagasse

	50kPa normal stress		100kPa normal stress		200kPa normal stress	
	Peak shear (kPa)	% Increase	Peak shear (kPa)	% Increase	Peak shear(kPa)	% Increase
Unreinforced	30.3	-	58.5	-	113.5	-
Fibre	32.6	7.7%	61.0	4.3%	120.4	6.1%
Millrun	29.2	-3.4%	59.5	1.7%	107.2	-5.6%
Pith	29.0	-4.2%	59.2	1.2%	113.0	-0.4%

5.4.2 Shear deformation relationships at moist conditions

The results obtained from the reinforced soils in their moist conditions are presented in this sub-section.

5.4.2.1 Klipheuwel sand

Fibre bagasse

Several similarities and differences were observed from the results obtained from reinforced Klipheuwel sand at moist conditions i.e. at 10% moisture content. As shown in figure 5.12, a maximum displacement of 60 mm was allowed corresponding to 20% relative displacement.

The shear strength increased with increase in horizontal displacement up to the maximum displacement allowed. The initial slopes of the graphs obtained were not affected by the inclusion of fibre bagasse just like in dry reinforced Klipheuwel sand. These results further confirmed that a considerable amount of shear force, greater than the threshold force, is required to mobilise peak strengths in bagasse-reinforced soils. This force was not affected by the quantity of fibres present in the composite and solely depended on the soil fabric.

As shear progressed, deviation in stress-horizontal displacement curves were evident at displacements of about 15 mm. These deviations continued gradually until 60 mm of displacement contrary to the findings on the dry sand, which displayed peak strengths at 10 mm to 15 mm of displacement. This was due to the addition of water that reduced the friction between the fibres and soil thereby causing the composite to behave like loosely compacted soils.

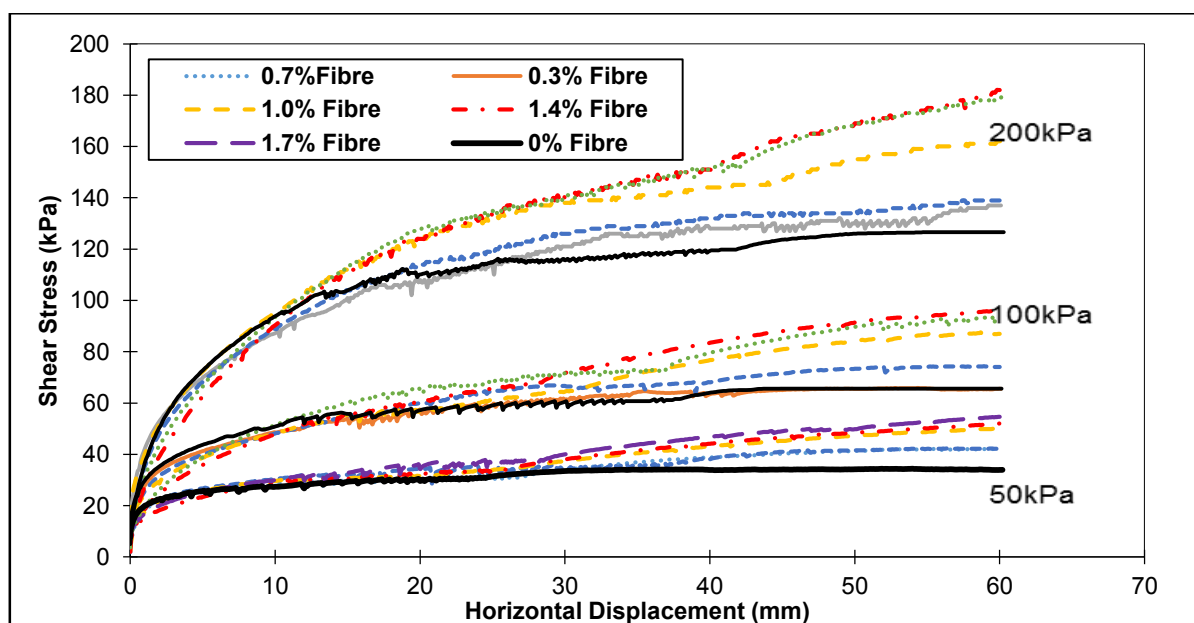


Figure 5.12: Shear deformation of moist Klipheuwel sand at various fibre bagasse content

Table 5.9 shows the peak shear strengths mobilised at 60 mm of horizontal displacement. These peak strengths were slightly lower compared to dry reinforced Cape Flats sand. At 100 kPa and 1.0% concentration, peak shear strengths of 87.5 kPa and 104 kPa were obtained from moist and dry reinforced Klipheuwel soil, respectively. It is important to mention that there was a possibility of mobilising higher peak strengths. However, to enable comparison of results, the peak shear strengths mobilised at 20% as recommended in ASTM D3080 are presented.

The peak shear strengths increased with the addition of fibre content at approximately the same magnitude as those obtained from dry soils. This trend decreased at higher confining pressures. For instance, at 0.7% fibre content, peak ratios of 0.23 and 0.1 were achieved at 50 kPa and 200 kPa, respectively.

Contrary to dry Klipheuwel sand, fibre segregation was significantly reduced with the addition of water. It could be said, therefore, that the low increase in shear strength is not because of fibre segregation, but rather the absorption of water and the subsequent reduction in the friction between soil and fibres.

Table 5.9: Summary of peak shear strengths of fibre bagasse reinforced moist Klipheuwel sand

Fibre Content	50kPa normal stress		100kPa normal stress		200kPa normal stress	
	Peak shear (kPa)	% Increase	Peak shear (kPa)	% Increase	Peak shear(kPa)	% Increase
Unreinforced	34.4	-	65.6	-	126.6	-
0.30%	42.2	22.7%	65.9	0.4%	137.0	8.2%
0.70%	42.3	23.0%	74.4	13.4%	139.0	9.8%
1.00%	50.3	46.2%	87.5	33.4%	162.0	28.0%
1.40%	52.1	51.5%	96.2	46.6%	182.0	43.8%
1.70%	54.7	59.0%	93.6	42.7%	180.0	42.2%

Millrun bagasse

A similar trend to that of fibre reinforced moist Klipheuwel sand was evident when Klipheuwel sand was reinforced with millrun as shown in figure 5.13. In comparison with the unreinforced soil, the reinforced soil showed increased ductility with the addition of millrun content. There was an improvement of about 10% to 40% at concentrations of 0.3% to 1.0%. An increase in the vertical load led to a reduction in ductility.

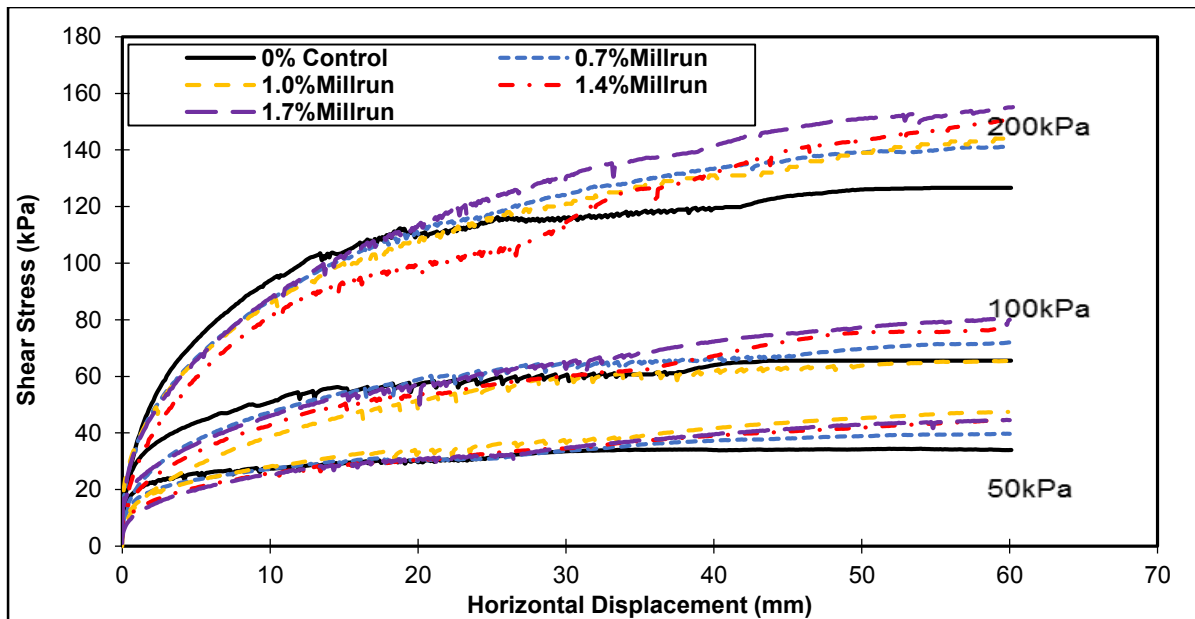


Figure 5.13: Shear deformation of moist Klipheuwel sand at various millrun content

In as much as there was an increase in peak shear strengths, the improvement was minimal compared to its fibre counterpart. Millrun seemed to absorb more water compared to fibre due to the existence of pith in its composition.

Table 5.10: Summary of peak shear strengths for millrun bagasse reinforced moist Klipheuwel sand

Millrun Content	50kPa normal stress		100kPa normal stress		200kPa normal stress	
	Peak shear (kPa)	% Increase	Peak shear (kPa)	% Increase	Peak shear(kPa)	% Increase
Unreinforced	34.4	-	65.61	-	126.6	-
0.30%	38.5	11.9%	68.2	3.9%	135.6	7.1%
0.70%	39.8	15.6%	72.0	9.7%	141.1	11.5%
1.00%	47.5	38.2%	75.6	15.2%	144.0	13.7%
1.40%	44.7	29.8%	76.6	16.7%	150.5	18.9%
1.70%	44.6	29.7%	80.4	22.5%	155.1	22.5%

Pith bagasse

In figure 5.13 and table 5.11 the shear stress – horizontal displacement curves and summary of the peak shear strength ratios of pith reinforced Klipheuwel sand are shown, respectively. It can be seen that at a horizontal displacement of 0 mm to 20 mm, there was a reduction in the stiffness slopes of the graphs obtained with the inclusion of pith bagasse. As horizontal displacement progressed, the shear strength deviated and showed higher values at 60 mm displacement or 20% strain. The trend can be attributed to the high hydrophilic nature of pith bagasse. Pith bagasse absorbed most of the water added to the soil. This coupled with the

lubrication effect subjected to the particles required a higher magnitude of strain to mobilise greater shear strengths. Moreover, pith bagasse contained residual sugars, which dissolve with the addition of water, reducing the resistance of the soil composite to shear regardless of the normal pressure.

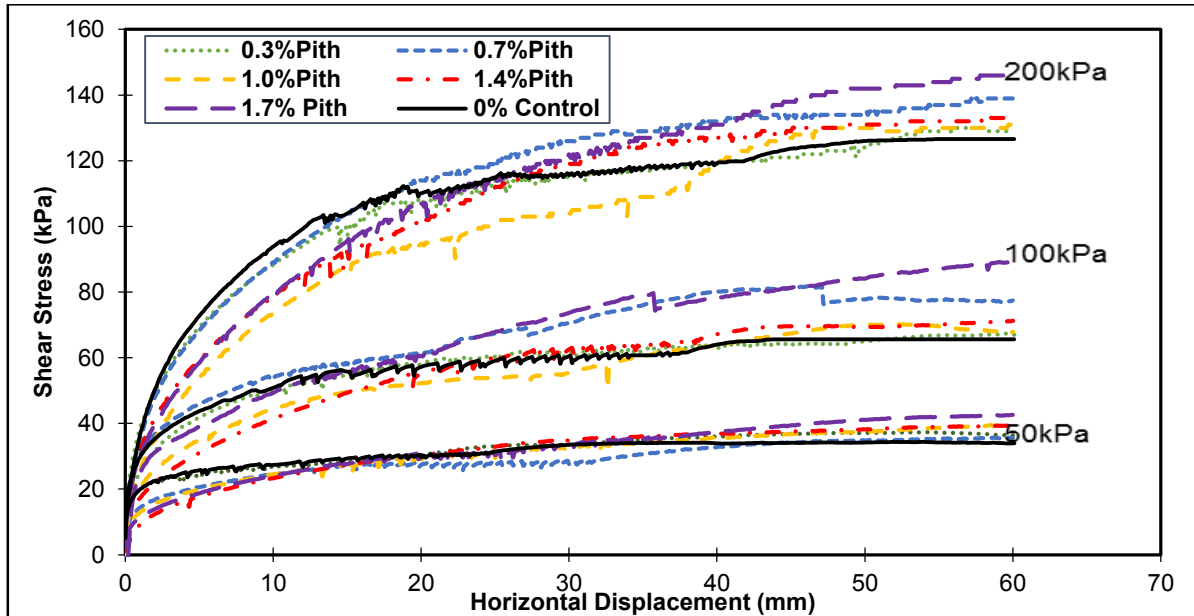


Figure 5.14: Shear deformation of moist Klipheuwel sand at various pith content

The peak strengths at 20% strain showed a slight increase in strength compared to the unreinforced soil. As depicted in table 5.11, the peak ratios seemed to increase with no upper asymptotic value for the concentration range investigated. At 1.7% concentration, considerable improvement was noticed, partly because of the strength hardening caused by piths.

Table 5.11: Summary of peak shear for pith bagasse reinforced Klipheuwel sand at OMC

Pith Content	50kPa normal stress		100kPa normal stress		200kPa normal stress	
	Peak shear (kPa)	% Increase	Peak shear (kPa)	% Increase	Peak shear(kPa)	% Increase
Unreinforced	34.4	-	65.6	-	126.6	-
0.30%	37.3	8.4%	67.4	2.7%	130.0	2.7%
0.70%	38.7	12.5%	70.0	6.7%	132.0	4.3%
1.00%	39.6	15.1%	70.2	7.0%	131.0	3.5%
1.40%	39.5	14.8%	71.3	8.7%	133.0	5.1%
1.70%	42.6	23.8%	90.0	37.2%	147.0	16.1%

5.4.2.2 Cape Flats sand

Having observed the trend in the reinforced moist Klipheuwel sand, the effect of 1.0% of fibre, millrun and pith on Cape Flat sand was investigated and the results shown in figure 5.15. As a general trend, the stiffness of the composite reduced up to 10 mm then improved. At 20 mm of horizontal displacement, there was a scatter in the peak stresses with fibre giving higher improvements. With the exception of millrun at normal stress of 200 kPa, millrun and pith produced the same trend. For millrun at 200 kPa, a slight reduction in strength, less than the control strength, was obtained and could be attributed to the non-uniform distribution of the millrun in the composite.

Higher peak strengths were obtained on Cape Flat sand reinforced with 1.0% fibre compared to Klipheuwel sand. At 200 kPa normal stress, 170 kPa of peak stress was obtained corresponding to a 21% increase compared to 162 kPa in in Klipheuwel sand corresponding to a 28% increase. The high peak values are attributed to the amount of water added and the dry density achieved while compacting the soil, Cape Flats sand being less dense than Klipheuwel sand. The low peak ratios are because of sand-grain effect, which considerably hinders the stress mobilisation as discussed in section 5.4.1. Nevertheless, it is evident that in as much as high stresses were obtained in Cape Flats sand, the percentage increase above the unreinforced soils shear strengths was low compared to Klipheuwel sand

A similar trend was observed in Cape Flats sand reinforced with millrun and pith. A slight deviation was experienced with the inclusion of millrun and pith that reduced across the normal pressures. At 200 kPa for instance, there was an 11.1% reduction in strength for millrun.

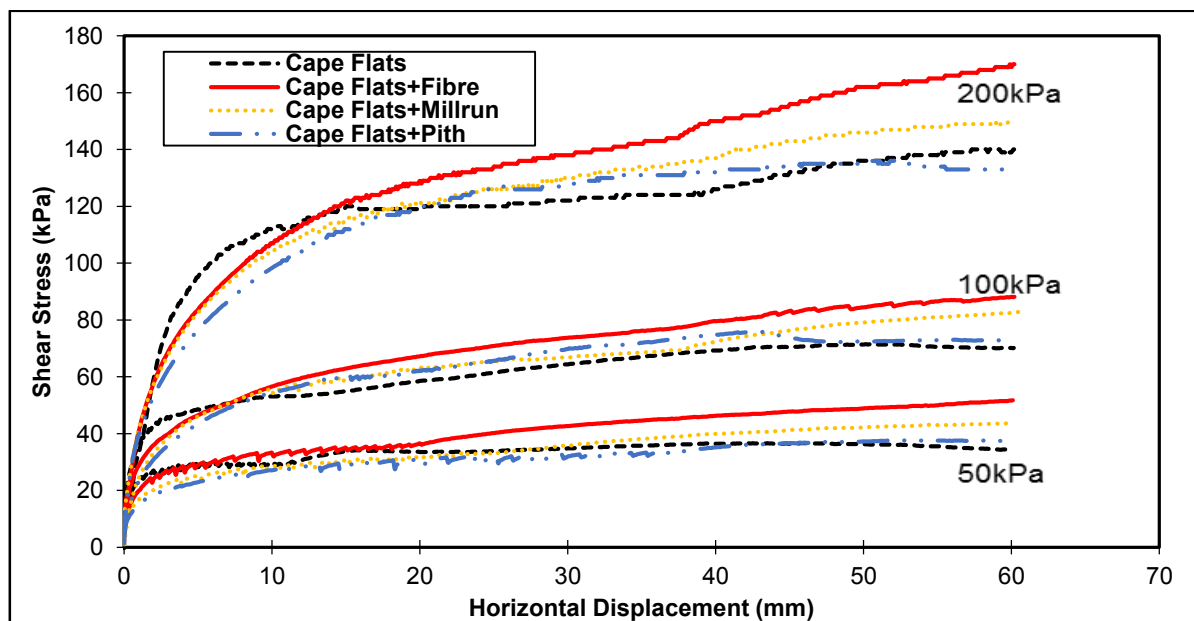


Figure 5.15: Shear deformation of moist Cape Flats sand reinforced with 1.0% fibre/millrun/pith

Table 5.12 gives the strengths obtained from bagasse-reinforced Cape Flat sands. It can be seen that the increase was more pronounced in the fibres as opposed to pith and millrun bagasse. As in the other results, the observed reduction in the peak ratios with the increase in the normal pressures was upheld. At higher normal pressures both sugarcane bagasse types showed a reduction in peak ratios compared to unreinforced soil. An increase of 40% was obtained in fibre at 50 kPa and a 20% increase at 200 kPa.

Table 5.12: Summary of peak shear strengths of moist Cape Flats sand reinforced with 1.0% fibre/millrun/pith bagasse

Pith Content	50kPa normal stress		100kPa normal stress		200kPa normal stress	
	Peak shear (kPa)	% Increase	Peak shear (kPa)	% Increase	Peak shear(kPa)	% Increase
Unreinforced	36.6	-	71.5	-	140.0	-
Fibre	51.8	41.5%	88.1	23.2%	170.0	21.4%
Millrun	43.6	19.1%	83	16.1%	150.0	7.1%
Pith	37.7	3.0%	75.8	6.0%	136.0	-2.9%

5.4.2.3 Kaolin clay

Figure 5.16 shows the shear stress – horizontal displacement curves obtained from bagasse reinforced moist Kaolin soil. Inclusion of bagasse at 1.0% content slightly reduced the stiffness of the Kaolin clay. Thus, it can be said that 1.0% fibre, millrun or pith does not affect the peak shear strength of moist Kaolin Clay. From the work by Estabragh et.al (2013), concentration of 10% to 30% of fibres was used with the optimum effect obtained at a 20% concentration. Comparing the concentrations with those considered in this study explains the absence of deviation in the shear strength. It also shows that for maximum strengths to be attained, higher concentrations of bagasse should be used.

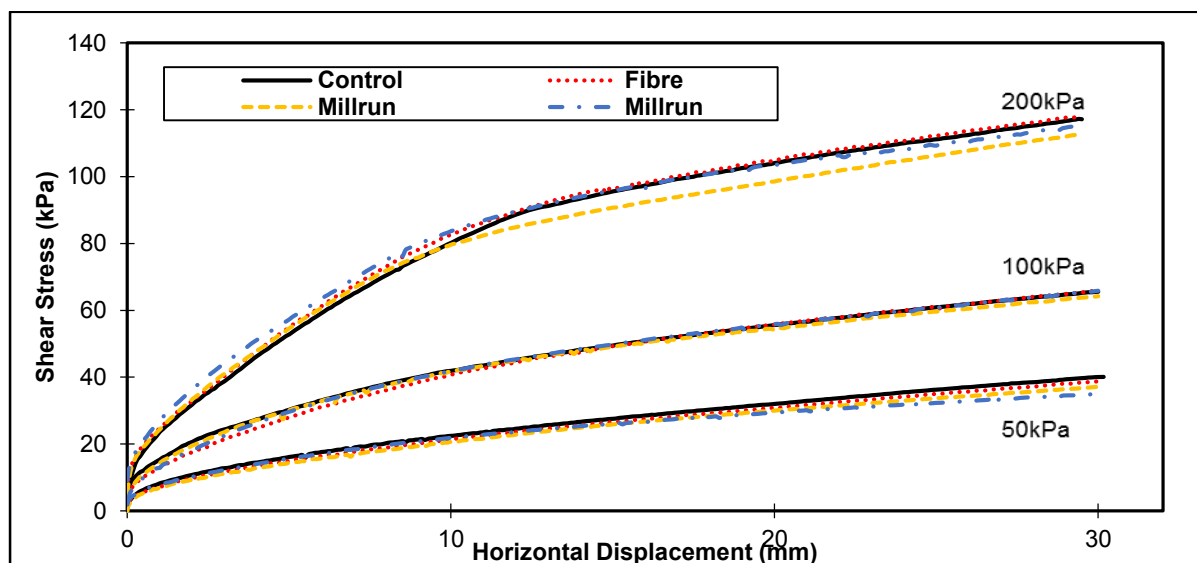


Figure 5.16: Shear deformation of moist Kaolin clay reinforced with 1.0% fibre/millrun/pith.

Moist Kaolin composite was prepared differently compared to dry Kaolin. Moist Kaolin was compacted while dry Kaolin was loosely placed then consolidated. These notwithstanding, moist Kaolin showed slight reductions in peak shear strength, which could be attributed to the effect of water. As shown in table 5.13, the reduction in peak ratio was greater at 50 kPa compared to 200 kPa

Table 5.13: Summary of peak shear strengths for Kaolin reinforced with 1.0% fibre/millrun/pith

Pith Content	50kPa normal stress		100kPa normal stress		200kPa normal stress	
	Peak shear (kPa)	% Increase	Peak shear (kPa)	% Increase	Peak shear(kPa)	% Increase
Unreinforced	40.1	0.0%	65.6	0.0%	117.9	0.0%
Fibre	38.8	-3.2%	66.4	1.3%	119.1	1.0%
Millrun	37.3	-7.1%	65.8	0.3%	118.0	0.1%
Pith	35.3	-11.9%	65.9	0.5%	116.4	-1.3%

5.4.3 Shear stress-normal stress relationships

The shear envelope diagrams generated from the shear stress – horizontal displacement results presented in section 5.4.1 and 5.4.2 are discussed in this section. The envelopes are shown in the form of the relationship between peak shear strength and the normal applied load in the ordinate and abscissa, respectively. The plot was derived by considering three normal loads as in the Mohr-coulomb theory. A regression analysis was then carried out to obtain the slope and the y-intercept. From all the regression analysis conducted, a coefficient of determination (R^2) of 0.9987 to 1 was achieved. The y-intercept of the graphs constituted cohesion while the inverse tangent of the slope constituted the angle of internal friction.

5.4.3.1 Shear envelope for fibre bagasse

Figures 5.17 and 5.18 show the Mohr-Coulomb envelope of Klipheuwel and Cape Flat sand at 0 % to 1.7% fibre bagasse content while figure 5.22 shows the results of Kaolin at 1.0% fibre content. At 0% concentration of fibre bagasse (sand only), Klipheuwel sand ($C_u=1.8$) gave an angle of internal friction of 32.8° compared to 36.6° for Cape Flat sand ($C_u=2.25$). The slight difference in the angle of internal friction is because of inconsistencies in the particle distribution.

At various concentrations of bagasse, the angle of internal friction considerably increased up to a maximum concentration of fibre for both sandy soils, and then reduced. At 0.3% fibre content, the angle of internal friction of Klipheuwel sand and Cape Flat sand was 36.5° and 37° , respectively. This corresponded to a percentage increase of 11% compared to 1% in

Cape Flats sand. This was due to the improved soil-fibre interaction matrix by the inclusion of fibre bagasse, which is more pronounced in soils with fine particles.

On the contrary, different results manifested at higher concentrations of fibre. The improvement in Cape Flat sand became more pronounced at higher fibre contents than Klipheuwel sand. At 1.0% concentration for instance, the Cape Flats sand angle of internal friction increased by 27% compared to 9% for Klipheuwel sand. A good explanation is the sand-grain size effect. Soil with coarse particles interacts more with fibres at high normal pressures. This is because of the reduced void ratios and increased interlocking friction of the particles and the fibres. As the void ratios are reduced, the coarse grains dilate more. There was also a possibility of grain crushing which consequently improved their internal resistance.

Both soils depicted some slight cohesion: 5.2 kPa for Klipheuwel and 4.3 kPa for Cape Flats as shown in figure 5.16 and 5.17. These were apparent cohesion because of the slight cementation and built up of pore water pressure in the soil particles.

Likewise, as in the case of angle of internal friction, the apparent cohesion increased across the fibre bagasse concentration. The increase was more pronounced in Klipheuwel sand than Cape Flats sand. Fibre adhesion and segregation during mixing could have contributed to this difference in cohesion.

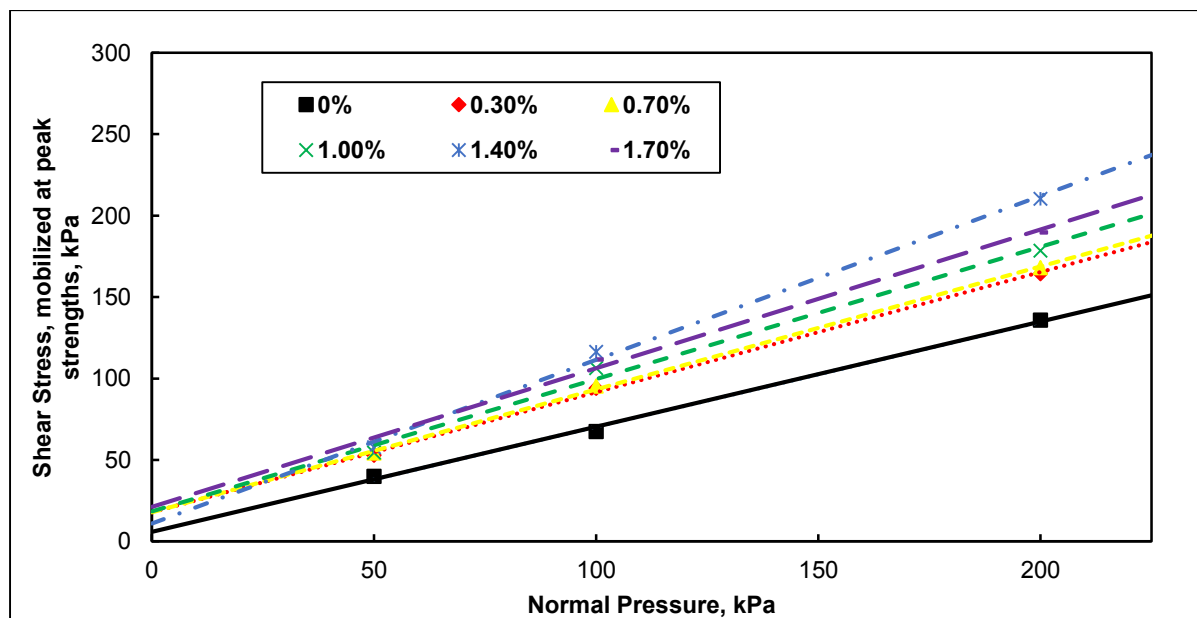


Figure 5.17: Shear strength parameters of dry Klipheuwel sand reinforced with fibre bagasse

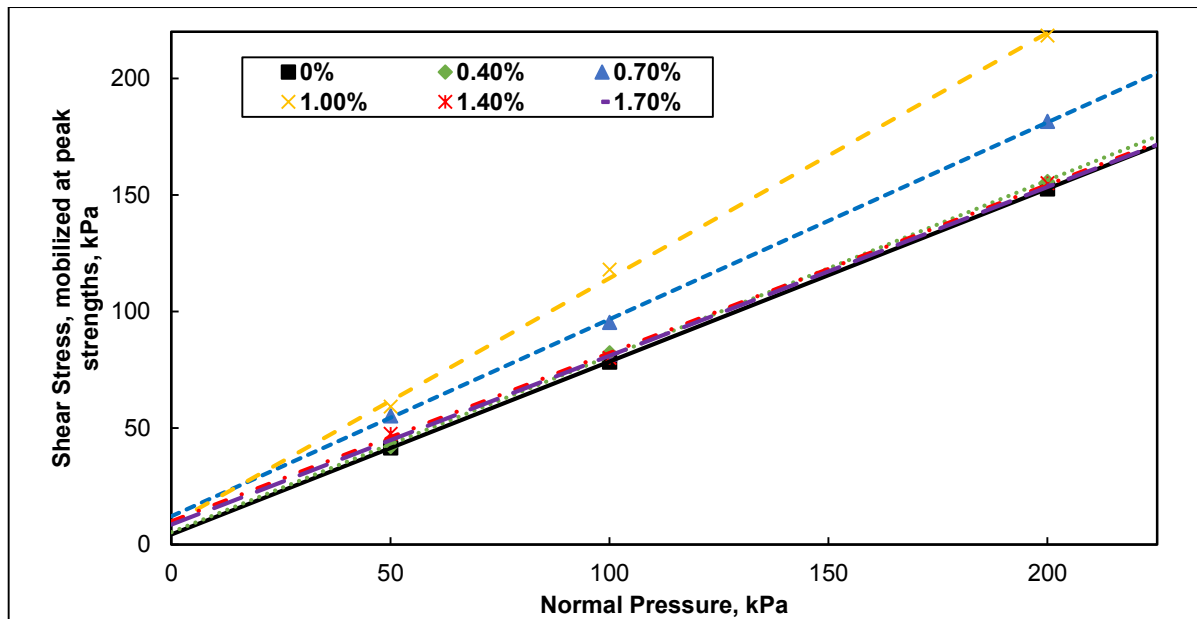


Figure 5.18: Shear strength parameters of dry Cape Flats sand reinforced with fibre

Maximum internal friction angle was obtained at 1.4% fibre content for Klipheuwel sand and at 1.0% concentration for Cape Flats sand. It is believed that the higher fibre segregation leading to non-uniform distribution of fibres in Cape Flat sand caused this difference. Furthermore, it can be said that the increased interlocking mechanism between Klipheuwel sand particles and fibres required more fibres to mobilise the maximum angle of internal friction. Table 5.14 gives the summary of the internal angle of friction mobilised at peak shear strengths.

Table 5.14: Summary of peak strength parameters for fibre reinforced soils

Fibre Concentration	Klipheuwel Sand		Cape Flats Sand		Kaolin Clay	
	ϕ_{peak} (deg)	C_{peak} (kPa)	ϕ_{peak} (deg)	C_{peak} (kPa)	ϕ_{peak} (deg)	C_{peak} (kPa)
Unreinforced	32.8	5.2	36.6	4.3	28.9	2.8
0.3%	36.5	17.3	37.0	5.3		
0.7%	37.0	17.9	40.2	12.1		
1.0%	40.6	18.7	44.8	13.2	30.4	2.9
1.4%	41.6	24.2	37.9	14.0		
1.7%	39.6	25.2	37.2	13.7		

5.4.3.2 Shear envelope for millrun bagasse reinforced soils

In figures 5.19 and 5.20, the shear envelopes of millrun bagasse reinforced soils are presented. The summary of the shear strength parameters (c and ϕ) is given in table 5.15.

Similar to the trend observed with the fibre bagasse reinforcement, there was an improvement in the peak angle of internal frictions and cohesions in both soils. At the lowest concentration of 0.3%, 34.8° and 36.8° was attained for Klipheuwel and Cape Flats, respectively. Unlike fibre bagasse, the percentage increase was minimal. This phenomenon was attributed to the millrun bagasse containing fewer fibres per unit area. Because of millrun bagasse containing residual sugars, the cohesion values obtained were higher compared to its counterparts.

Figure 5.23 shows that no improvement was observed on the angle of internal friction for the clay soil (Kaolin). However, the cohesion increased considerably at 1.0% millrun content.

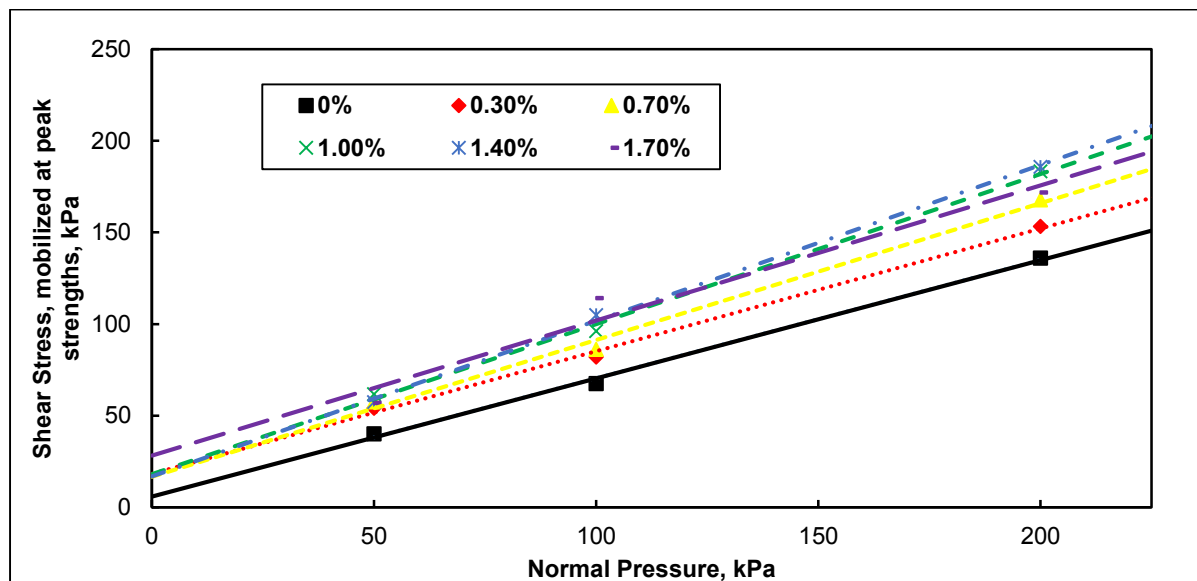


Figure 5.19: Shear strength parameters of Klipheuwel sand reinforced with millrun

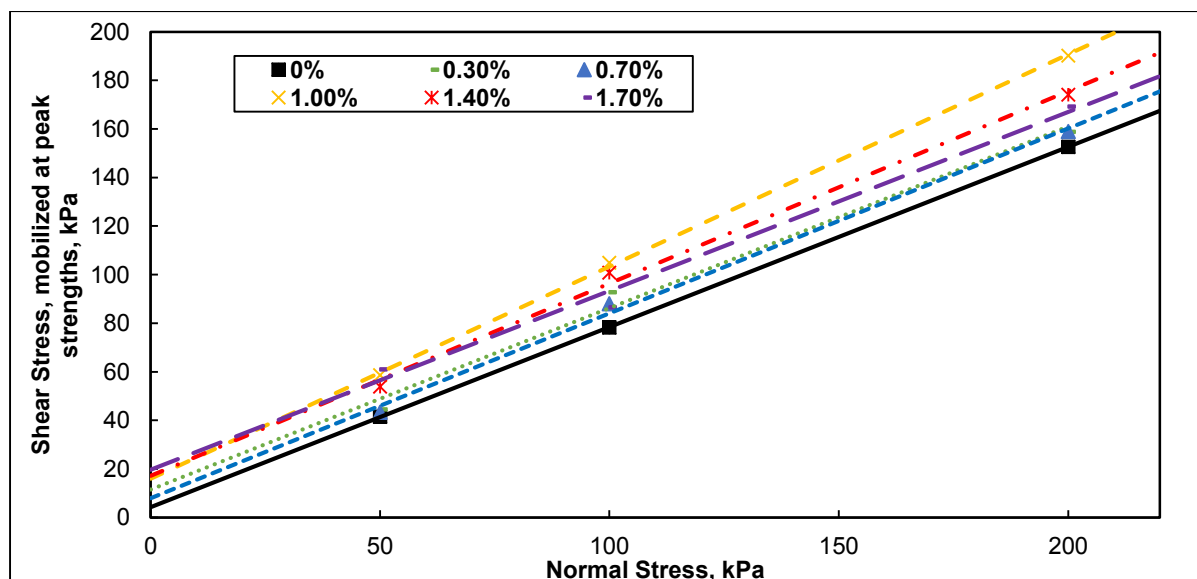


Figure 5.20: Shear strength envelope of Cape Flats sand reinforced with millrun

Table 5.15: Summary of peak strength parameters for millrun reinforced soils

Millrun Concentration	Klipheuwel sand		Cape Flats sand		Kaolin clay	
	ϕ_{peak} (deg)	C_{peak} (kPa)	ϕ_{peak} (deg)	C_{peak} (kPa)	ϕ_{peak} (deg)	C_{peak} (kPa)
Unreinforced	32.8	5.2	36.6	4.3	28.9	2.8
0.3%	34.8	15.5	36.8	11.5		
0.7%	36.0	18.6	37.4	8.0		
1.0%	36.2	27.0	41.1	16.0	27.2	5.4
1.4%	37.2	26.0	38.4	17.2		
1.7%	36.0	29.5	36.4	19.7		

5.4.3.3 Shear envelope for pith bagasse reinforced soils

Figures 5.21 and 5.22, and table 5.16 show the regression analysis results mobilised at peaks shear strength of pith-reinforced soils.

As in the case of the previous types of bagasse, inclusion of pith bagasse improved the angle of internal friction of Klipheuwel and Cape Flats soil. However, this improvement was minimal especially in Cape Flats sand as shown in figure 5.22. These observations were attributed to the residual sugars that were in the pith bagasse and the shorter length of the visible fibres.

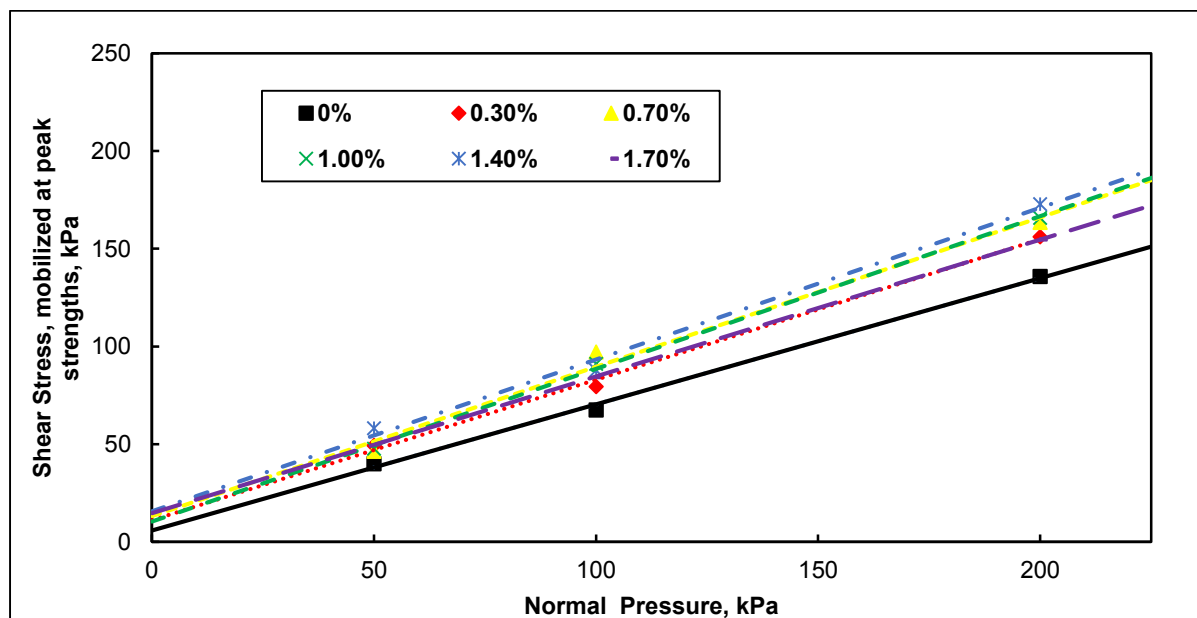


Figure 5.21: Shear strength envelope of Klipheuwel sand reinforced with pith

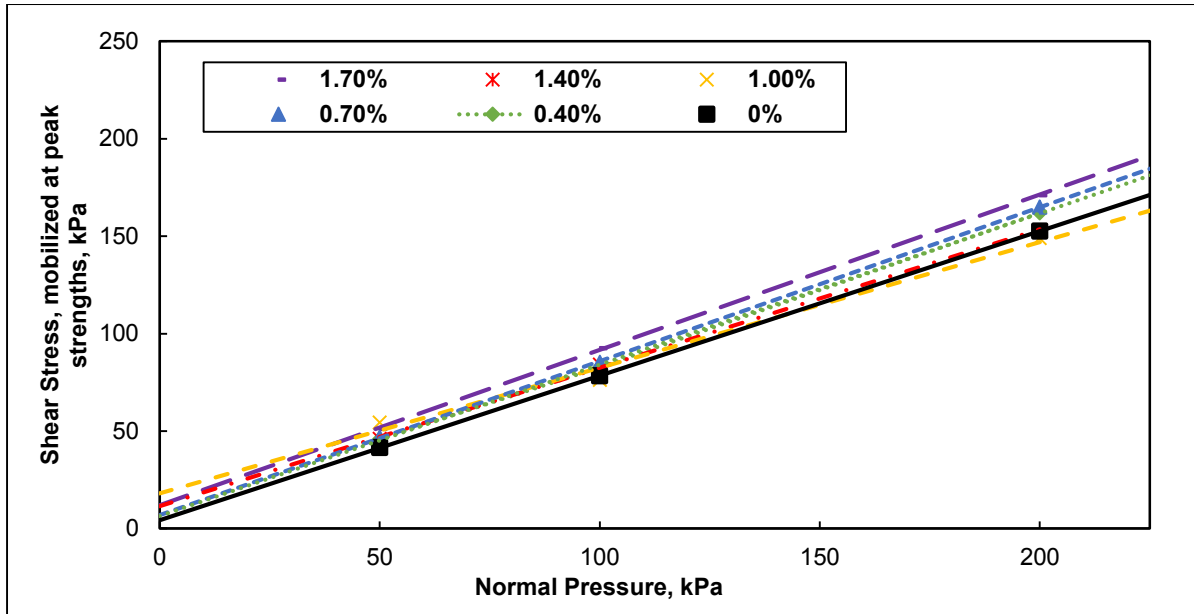


Figure 5.22: Shear strength envelope of Cape Flats sand reinforced with pith

In Kaolin soil, pith bagasse at 1.0% concentration slightly improved the angle of internal friction. Cohesion values were even more increased compared to the sandy soils.

It was interesting to note that no major increase in the cohesion was observed as earlier envisioned. The original hypothesis was that pith bagasse would cause particle cementation and hence increase on the apparent cohesion.

Table 5.16: Summary of peak strength parameters for pithreinforced soils

Pith Concentration	Klipheuwel sand		Cape Flats sand		Kaolin clay	
	ϕ_{peak} (deg)	C_{peak} (kPa)	ϕ_{peak} (deg)	C_{peak} (kPa)	ϕ_{peak} (deg)	C_{peak} (kPa)
Unreinforced	32.8	5.2	36.6	4.3	28.9	2.8
0.3%	34.5	21.1	37.9	5.9		
0.7%	32.9	18.5	38.1	6.2		
1.0%	35.1	18.5	38.1	9.2	29.1	2.1
1.4%	34.4	25.0	38.2	10.4		
1.7%	35.0	14.7	38.5	12.0		

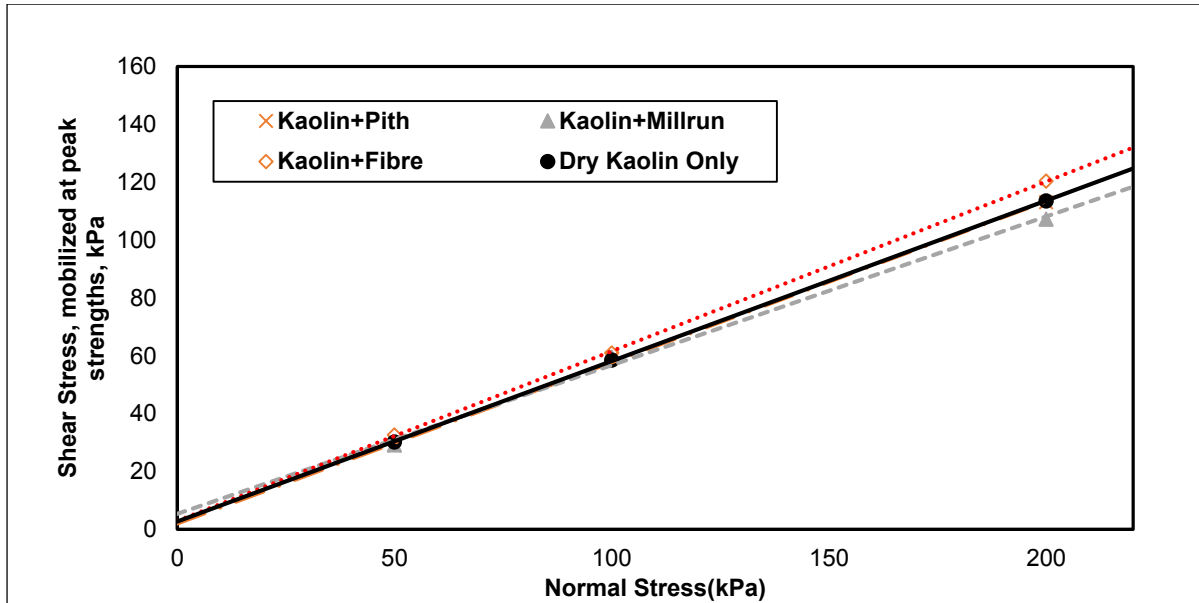


Figure 5.23: Shear strength envelope of Kaolin clay at dry moisture content reinforced with 1.0% fibre/millrun/pith

5.4.4 Shear stress-normal stress relationship for moist soils

As was the case for the dry soil, the Mohr-Coulomb envelopes were generated for tests done on the soils at optimum moisture content as presented in figures 5.24 to 5.28. Results are presented for the Klipheuwel sand at concentrations of 0.3% to 1.7% as well as Cape Flat sand and Kaolin Clay at 1.0% bagasse concentration.

5.4.4.1 Shear envelope for fibre bagasse moist-reinforced soils

In figures 5.23, 5.24 and 5.27, the shear envelope corresponding to peak strengths for various fibre bagasse concentrations are shown.

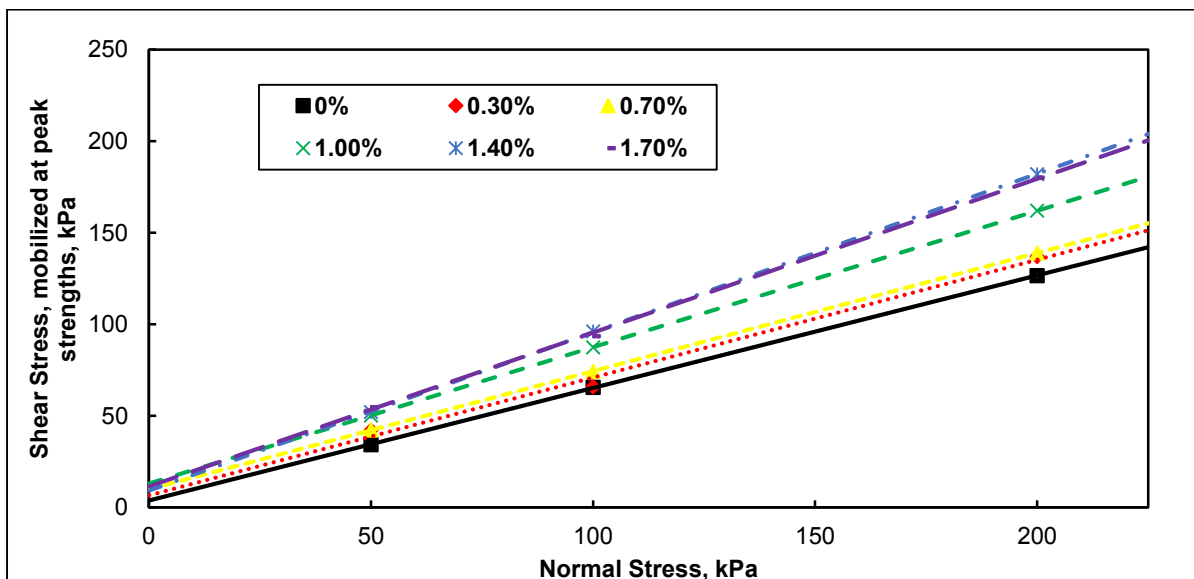


Figure 5.24: Shear strength envelope of moist Klipheuwel sand reinforced with fibre bagasse

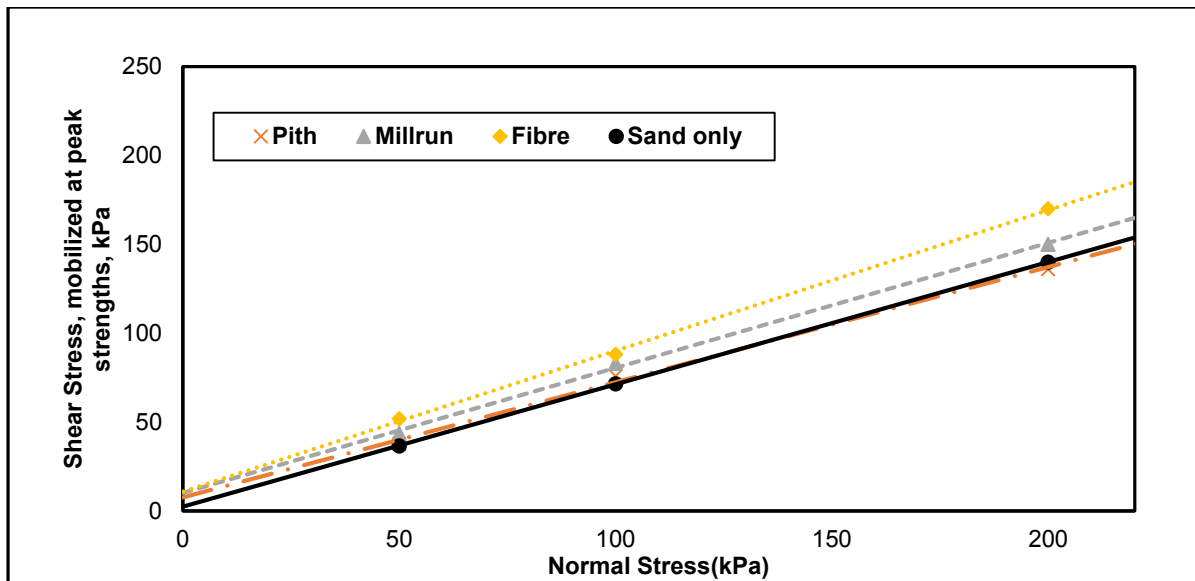


Figure 5.25: Shear strength envelope of moist Cape Flats sand reinforced with 1.0% fibre/millrun/pith bagasse.

Unreinforced Klipheuwel sand and Cape Flats sand showed an angle of internal friction of 31.5° and 36.4° , respectively. This was a reduction compared to the angle of internal friction obtained from dry soils. It is believed that the presence of water caused this difference in results.

Adding fibre to the moist soils gradually increased the angle of internal friction up to a maximum of 40.9° for Klipheuwel sand at 1.4% concentration. Angles of internal friction of 36.7° , 38.4° and 28.1° were attained for Klipheuwel sand, Cape Flat sand and Kaolin respectively, at 1.0% fibre concentration. This corresponded to an increase of 16%, 5% and 3% for the Klipheuwel sand, Cape Flat sand and Kaolin respectively. A summary of the results is given in table 5.17.

Table 5.17: Summary of peak strength parameters for fibre reinforced moist soils

Fibre Concentration	Klipheuwel Sand		Cape Flats Sand		Kaolin Clay	
	ϕ_{peak} (deg)	C_{peak} (kPa)	ϕ_{peak} (deg)	C_{peak} (kPa)	ϕ_{peak} (deg)	C_{peak} (kPa)
Unreinforced	31.5	3.9	36.4	2.4	27.4	13.9
0.3%	32.7	6.7				
0.7%	33.0	9.7				
1.0%	36.7	13.1	38.4	10.6	28.1	12.5
1.4%	40.9	9.2				
1.7%	39.9	11.8				

A slight decrease in apparent cohesion was experienced in the sandy soil investigated. For example, at 1.0% fibre bagasse concentration, cohesions of 13.1 kPa, and 10.6 kPa were obtained compared to 18.7 kPa and 13.2 kPa for dry Klipheuwel sand and Cape Flat sand, respectively. A contrary trend was experienced in the clay soil investigated. Moist Kaolin clay showed an increase in cohesion (3.7 kPa to 12.5 kPa) at 1.0% fibre content.

This behaviour is most likely attributed to the presence of water in sandy soil, which reduced the adhesion between the fibres and the soil particles consequently reducing cohesion. Since fibre bagasse is hydrophilic, the fibres slightly assumed a smooth surface with the introduction of water limiting their interlocking capability.

On the other hand, the behaviour in clay soil is attributed to the clay fabrics, which become deflocculated with the introduction of water and compaction thereby increasing their adhesive force. This as a result, increases the cohesive force as summarised in table 5.17.

5.4.4.2 Shear envelope of millrun moist reinforced soils

The shear envelopes of millrun-reinforced soils in the moist state are as shown in figures 5.25 for Cape Flats sand, 5.26 for Klipheuwel sand, and 5.25 for Kaolin clay.

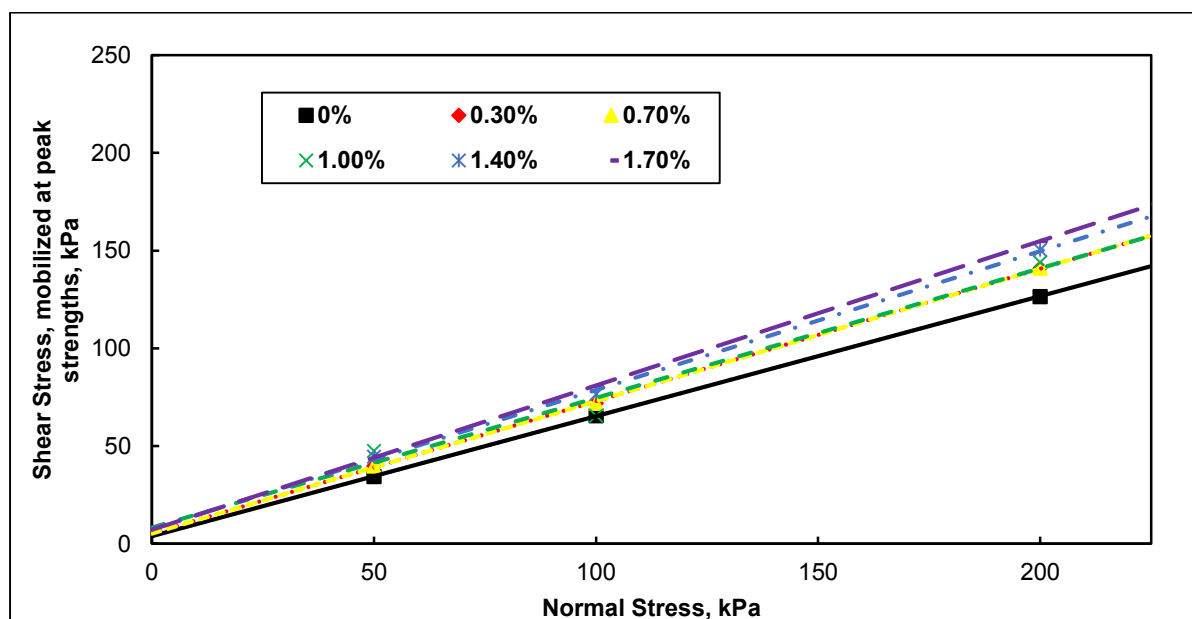


Figure 5.26: Shear strength envelope of moist Klipheuwel sand reinforced with millrun

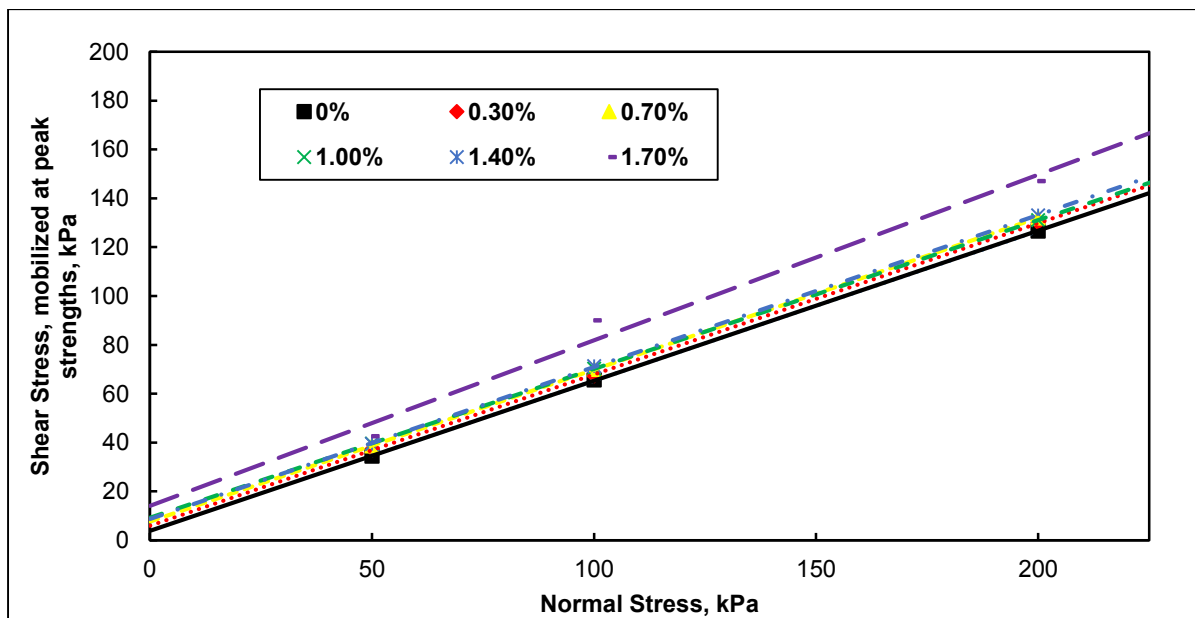
Similar to fibre reinforced moist soils, the angle of internal friction slightly increased except for Cape Flats sand where there seemed to be a decrease, probably because of the non-uniform distribution of millrun bagasse. The summary of the results is as shown in table 5.18.

Table 5.18: Summary of peak strength parameters for millrun reinforced moist soils

Millrun Concentration	Klipheuwel sand		Cape Flats sand		Kaolin clay	
	ϕ_{peak} (deg)	C_{peak} (kPa)	ϕ_{peak} (deg)	C_{peak} (kPa)	ϕ_{peak} (deg)	C_{peak} (kPa)
Unreinforced	31.5	3.9	36.4	2.4	27.4	13.9
0.3%	33.1	4.8				
0.7%	34.1	5.2				
1.0%	33.5	8.4	35.1	10.3	26.9	12.6
1.4%	35.4	7.7				
1.7%	36.4	7.2				

5.4.4.3 Shear envelope of pith bagasse moist reinforced soils

Figures 5.25, 5.27 and 5.28 show the results on pith bagasse reinforced moist soils. It is evident that at concentrations of 0.3% to 1.0% pith content, no change was experienced for the Klipheuwel sand. At a 1.7% concentration, a 34.1° internal friction angle was obtained accounting for an 8% increase in the internal friction angle.

**Figure 5.27: Shear strength envelope of moist Klipheuwel sand reinforced with pith bagasse**

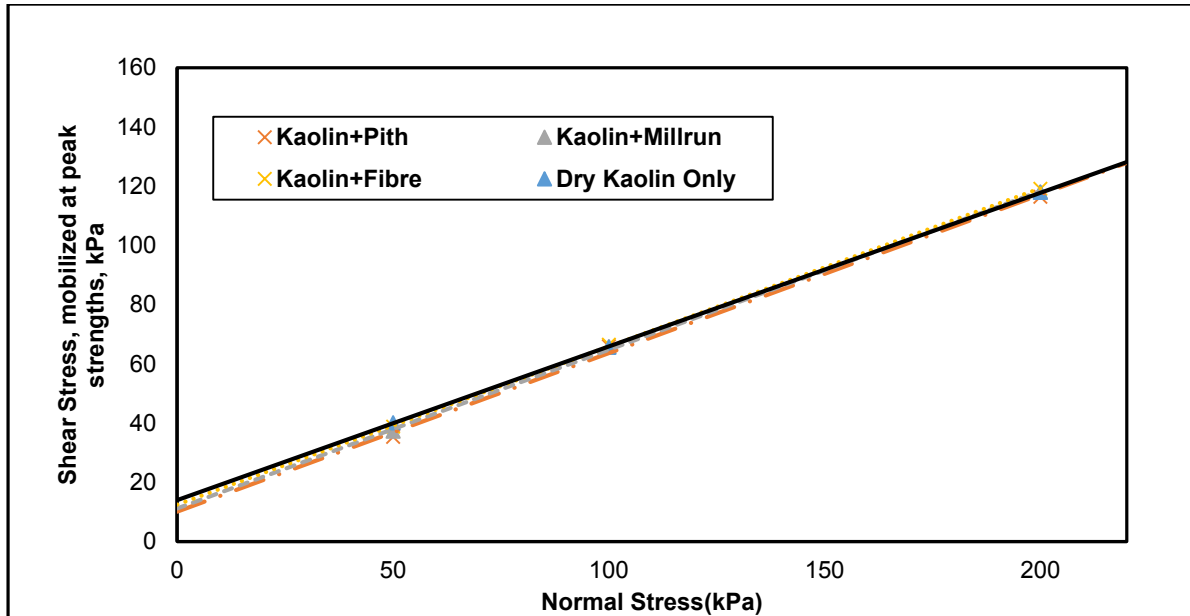


Figure 5.28: Shear strength envelope of moist Kaolin Clay reinforced with 1.0% fibre/millrun/pith bagasse

Similarly, there was a reduction in ϕ from 36.4° to 32.9° in Cape Flats sand possibly due to the absence the soil-fibre matrix.

At 1.0% concentration, differing results were obtained for the Kaolin clay with a ϕ of 28.2° corresponding to an increase of 3% in the internal friction angle.

The cohesive strength obtained seemed reduced compared to the fibre and millrun reinforced moist soils as shown in table 5.19.

Table 5.19: Summary of peak strength parameters for pith reinforced moist soils

Pith Concentration	Klipheuwel sand		Cape Flats sand		Kaolin clay	
	ϕ_{peak} (deg)	C_{peak} (kPa)	ϕ_{peak} (deg)	C_{peak} (kPa)	ϕ_{peak} (deg)	C_{peak} (kPa)
Unreinforced	31.5	3.9	36.4	2.4	27.4	13.9
0.3%	31.8	6.0				
0.7%	31.9	7.7				
1.0%	31.3	9.2	32.9	7.9	28.2	10
1.4%	31.9	8.7				
1.7%	34.1	14.1				

5.5 Effect of bagasse concentration on angle of internal friction (ϕ) and cohesion (c) of dry soils

5.5.1 Fibre bagasse

Figures 5.29 (a) and (b) show the scatter plots of the relationship between internal friction angle of the typical sandy and clay soil investigated and the increase in fibre bagasse content.

It is evident that increasing fibre concentration improved the angle of internal friction of the selected soils by up to a maximum of about 30% over the fibre content range investigated.

An increase in fibre concentration had a greater effect on Klipheuwel sand compared to Cape Flats sand. At 0.3% concentration, an 11% increase in the angle of internal friction was achieved compared to 1.1% in Cape Flats sand. This percentage change in the angle of internal friction became gradual at concentrations of 0.7% to 1.4% in Klipheuwel sand and became more distinct in Cape Flats sand as in figure 5.29(a).

However, a maximum angle of internal friction was achieved at a concentration of 1.0% and 1.4% for Klipheuwel sand and Cape flats sand, respectively. This behaviour is best explained by Pradhan et al. (2012) who attributed it to the reduced interlocking mechanism in soil-fibre matrix beyond optimum fibre content.

By comparing the ϕ values obtained at the maximum concentration for the two sands, it can be said that a greater improvement in ϕ was depicted in finer soils than coarse soils. In Klipheuwel sand ($D_{50}=0.28$ mm), a 30% increase was achieved while a 20% increase was achieved in Cape Flats sand ($D_{50}=0.40$ mm). This behaviour may be attributed to the dilation of the particles, which was shown to be greater in finer soils than coarse-grained soils. Sample results of the vertical-horizontals displacement are included in appendix B.

On the contrary, at 1.0% fibre concentration, a slight increase of 5.2% (28.9° to 30.4°) was observed for the reinforced Kaolin clay. This increase however was minimal and could be attributed to strength hardening rather than fibre-clay fabric interaction. As presented in section 3.6.1, quantifying the load transfer in shear strength tests on Kaolin clay was very difficult.

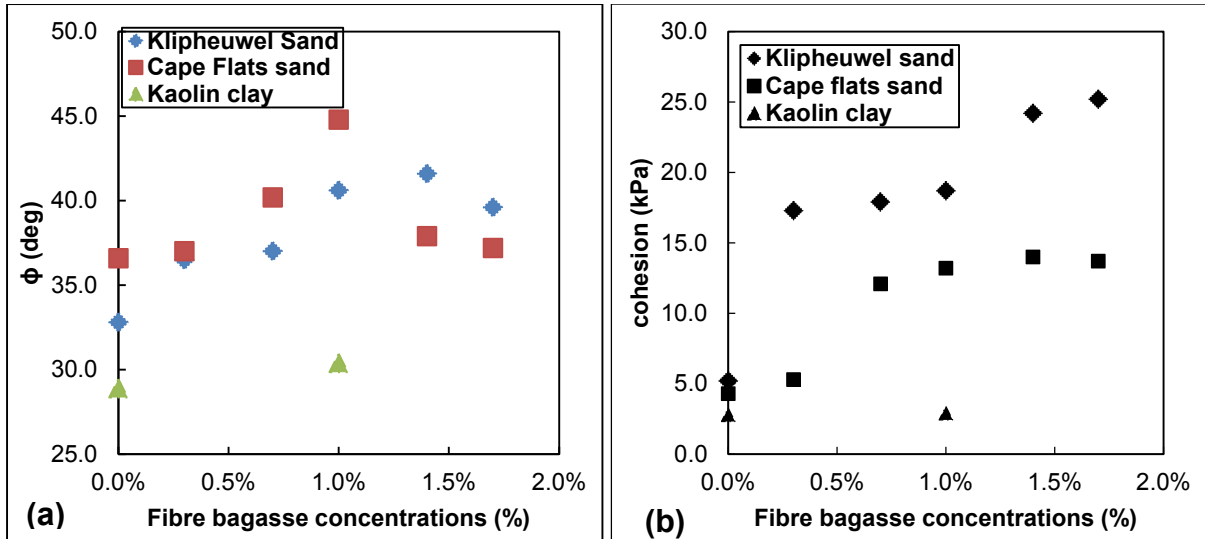


Figure 5.29: Effect of fibre bagasse concentration on (a) angle of internal friction (b) cohesion

5.5.2 Millrun bagasse

The effect of millrun bagasse on the dry selected soil is as shown in the scatter plots shown in figures 5.30(a) and (b). Similar to the results in fibre bagasse, there seemed to be a linear relationship between millrun concentration and the angle of internal friction up to a maximum millrun content. As millrun concentration increased, ϕ gradually improved up to an optimum concentration of 1.4% and 1% for Klipheuwel sand and Cape Flats sand, respectively. More pronounced peak strength was obtained at 1.0% millrun content in Cape Flats sand compared to Klipheuwel sand. However, the increase in ϕ was approximately constant i.e. at optimum millrun content; a 13% and 12% increase was observed.

The relationship between cohesion and millrun bagasse concentration showed a linear relationship with a slight decline at 0.7% millrun content for both soils as shown in figure 5.30 (b).

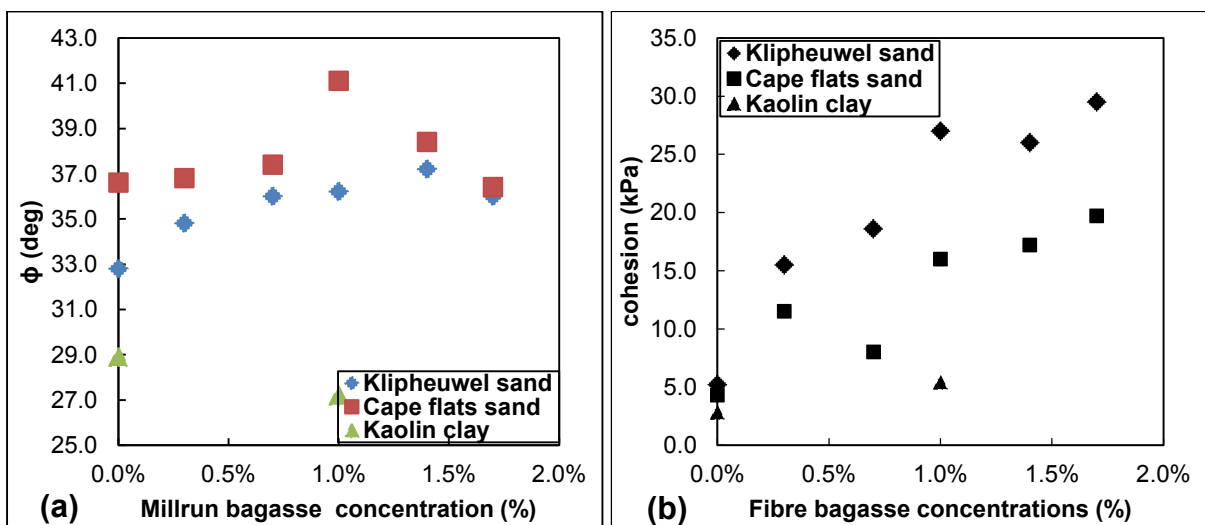


Figure 5.30: Effect of millrun bagasse concentration on (a) angle of internal friction (b) cohesion

5.5.3 Pith bagasse

Figures 5.31 (a) and (b) show the effect of pith bagasse on the internal friction angle and cohesion of dry soils.

A clear linear relationship was evident for the Cape Flats sand whereas for the Klipheuwel sand a slight decrease was noticed at 0.7% concentration followed by an increase. These results from Klipheuwel sand could possibly be because of the non-uniform distribution of pith bagasse rather than the existing residual sugars.

Comparing the three types of bagasse, pith bagasse contributed the least to the improvement of the angle of internal friction. For example in Klipheuwel sand, a clear inspection of the results showed an improvement of 5% compared to 30% for fibre, and 15% in millrun at 1.4% concentration.

In the same way, there was an increase in the apparent cohesion with increasing pith content. In Klipheuwel sand, a sharp increase was observed at 0.3% with a slight decrease thereafter, which was followed by a more constant improvement up to 17%. In Cape Flat sand, the increase was linear whereas in Kaolin Clay no change was depicted at 1.0% concentration.

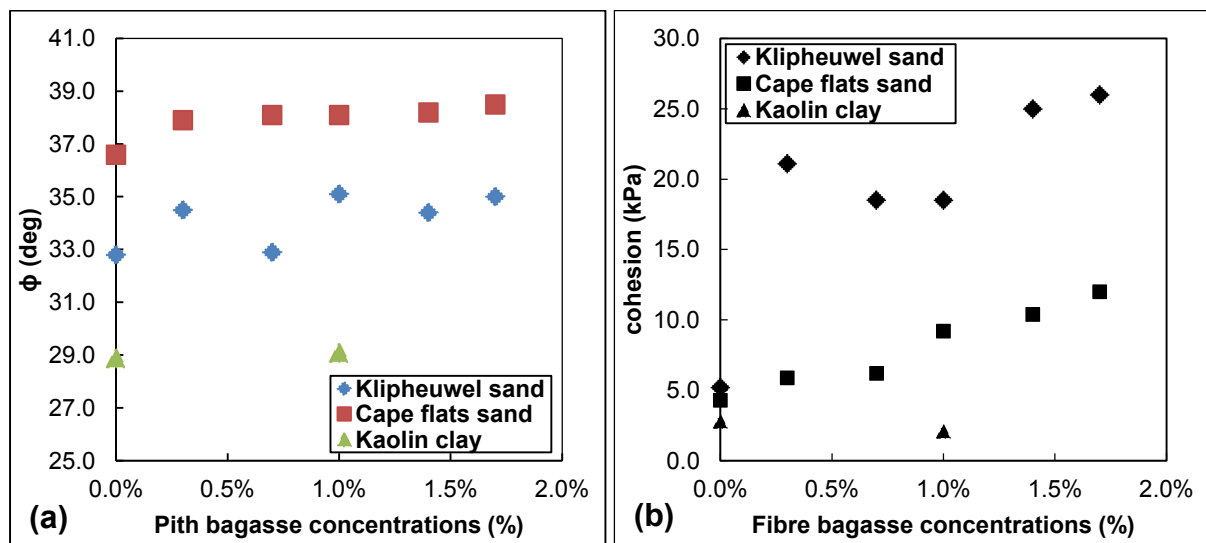


Figure 5.31: Effect of pith bagasse concentration on (a) angle of internal friction (b) cohesion

5.6 Effect of bagasse concentration on angle of internal friction (ϕ) and cohesion (c) of moist soils

In this sub-section, the influence of bagasse on moist soils as per the shear envelope results outlined in section 5.4.4 is discussed. It should be noted that the full extent of the concentration (0.3% to 1.7%) was only considered for Klipheuwel sand. The effect on the other types of soil was investigated at 1.0%. This was due to the observed trends in Klipheuwel sand, which

showed an optimum effect at 1.0 % content of bagasse. Results are thus compared at 1.0% for moist soils and the principal outcome examined for consistency.

Figures 5.32(a) and (b) show the influence of fibre on ϕ and c respectively. A gradual change was evident for Klipheuwel sand up to 0.7% concentration followed by a significant increase to a maximum at 1.4% before reducing. An increase of about 30% was noted at maximum fibre content similar to the improvement obtained in the dry state. This shows that even though the presence of water reduced the angle of internal friction of unreinforced Klipheuwel sand, the improvement in ϕ is independent of water when fibres are included.

In contrast, there was a slight increase in ϕ for Cape Flats sand and Kaolin clay at 1.0% concentration, suggesting that fibre bagasse had no effect on these two soils at the concentrations investigated. Higher concentrations could have further improved ϕ .

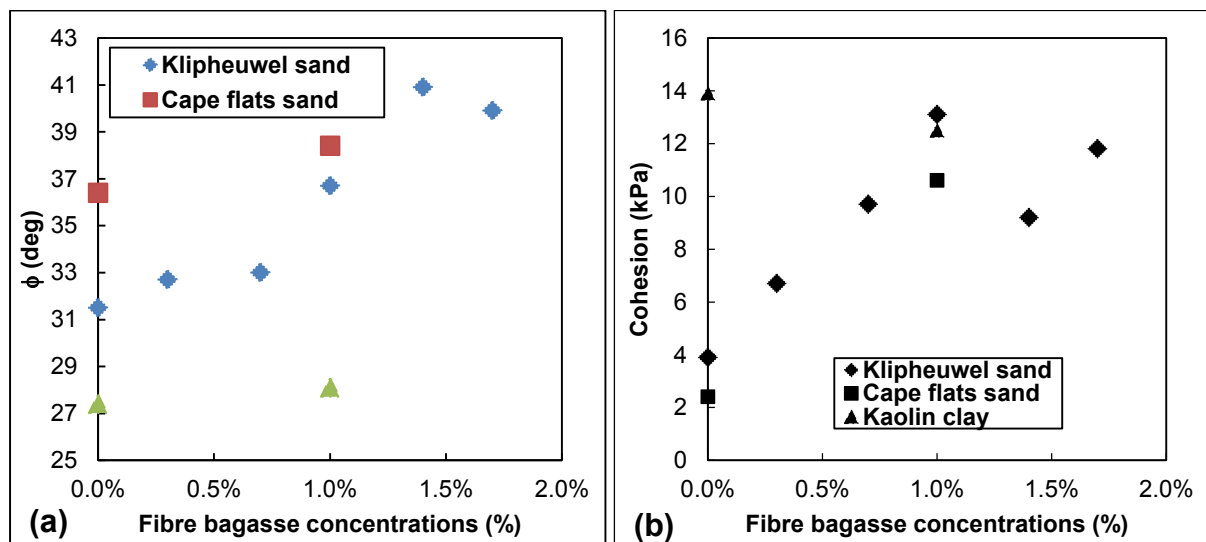


Figure 5.32: Effect of fibre concentration on (a) angle of internal friction (b) cohesion of moist soils

Reinforcing moist Klipheuwel sand with millrun bagasse showed an indefinite improvement over the content investigated as shown in figure 5.33 (a). A maximum improvement of about 15%, half that shown in fibre, was obtained at 1.7% concentration. This showed similarity with the improvement obtained while using Klipheuwel sand in the dry state, but at higher concentration. Note that the maximum ϕ was obtained at 1.4% concentration in millrun reinforced dry Klipheuwel sand.

Millrun bagasse had little effect on the Cape Flats sand and Kaolin clay although there was a slight change in cohesion. This gave the credence to the likelihood that substantial change could be observed at higher concentrations.

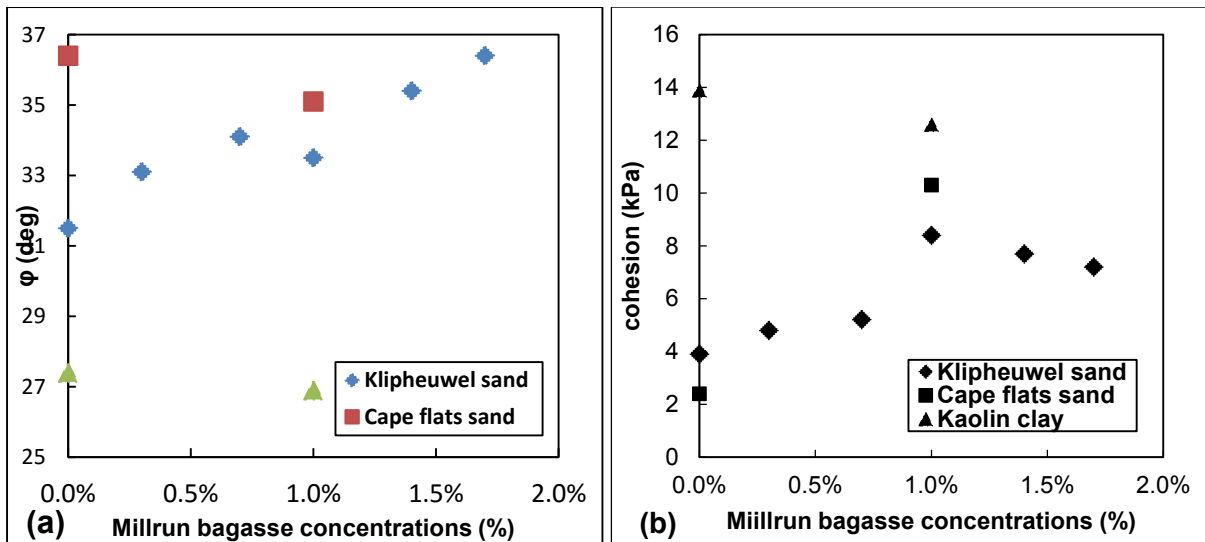


Figure 5.33: Effect of millrun bagasse concentration on (a) angle of internal friction (b) cohesion of moist typical soils

Figures 5.34 (a) and (b) show the relationship between pith bagasse content and the shear strength parameters of moist soils. As in the fibre and millrun discussed above, an improvement in ϕ was achieved at higher concentrations of pith in Klipheuwel sand. The improvement was a half and a quarter that obtained in millrun and fibres, respectively. Furthermore, the improvement was similar to that obtained in dry Klipheuwel sand, about 8%.

A small increase in ϕ of 2.8% was obtained for Kaolin Clay and a decrease of about 5% in Cape Flats sand. This change in Cape Flats sand was significantly since it was hypothesized that there would be no change in the ϕ obtained.

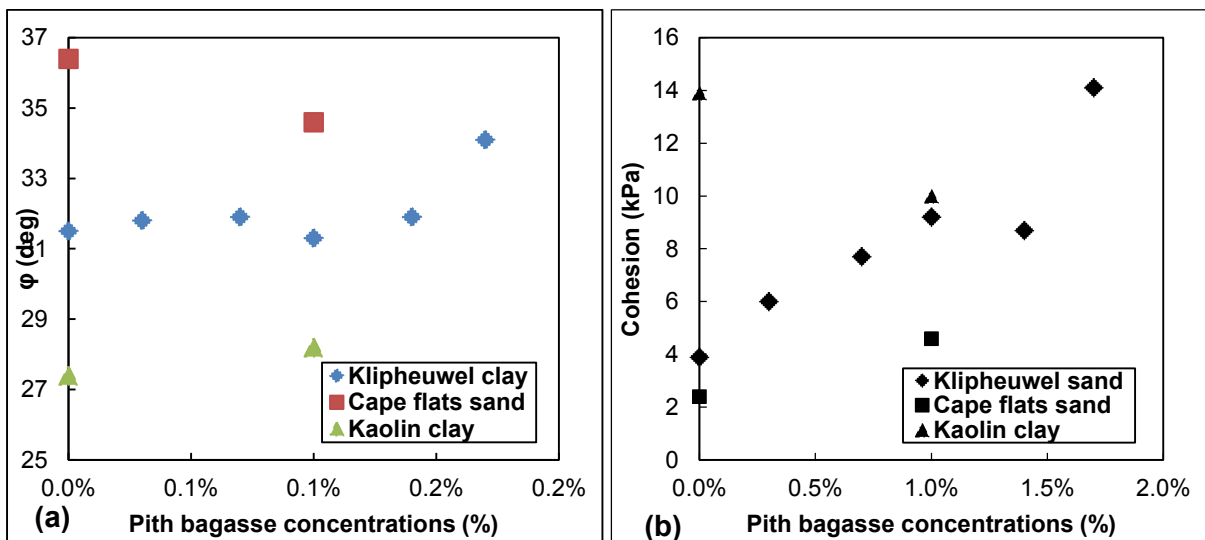


Figure 5.34: Effect of pith bagasse concentration on (a) angle of internal friction (b) cohesion of typical moist soils

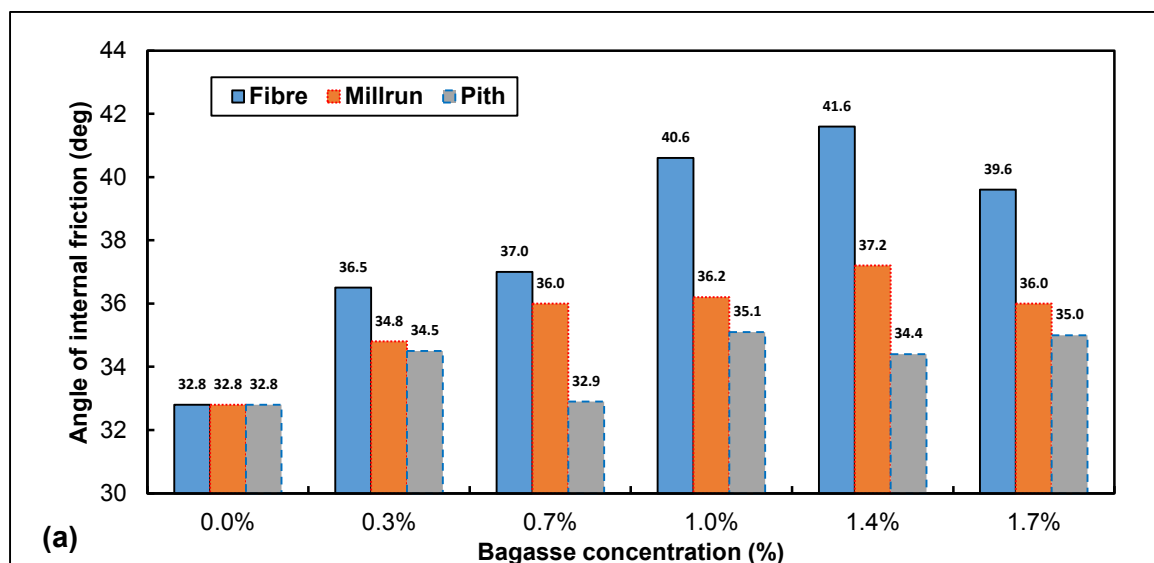
5.7 Comparison of results on the various bagasse type

Figures 5.35 (a) to (c) compare the angle of internal friction results obtained for each type of bagasse (fibre, millrun and pith) mixed with the selected soils in dry conditions. It is evident that fibre bagasse has the greatest effect on the angle of internal friction at peak shear strength across all the bagasse concentrations investigated. This observation is consistent in both dry and moist Klipheuwel sand and Cape Flats sands. Millrun bagasse comes in second, while pith bagasse insignificantly affects the shear strength parameters of Klipheuwel sand.

This effect of sugarcane bagasse on the angle of internal friction linearly increased with addition of bagasse content up to a maximum content of 1.4% for both fibre and millrun, but seemed to remain constant from 0.3% of pith content. The results obtained from millrun is remarkable and it can be concluded that a similar quantity of fibre and millrun is required to mobilise the maximum shear strength of Klipheuwel sand, even though millrun bagasse contains residual sugars. However, higher strengths are mobilised from fibre bagasse.

Similarly, fibre bagasse profoundly improved the angle of internal friction of Cape Flat sand compared to the millrun and pith as shown in figure 5.35 (c). This effect depended on the angularity and distribution of particles in sandy soils, a phenomenon evidenced by the percentage bagasse required for Klipheuwel sand and Cape Flats sand. A maximum shear strength was mobilised at a lower content (1.0%) in Cape Flats sand compared to sandy soil with a wide range of particles as in the case of Klipheuwel sand. This can be explained by the increased segregation (floating) of fibres experienced in coarse soils.

The effect of millrun on the Kaolin clay was minimal compared to fibre and pith as shown in figure 5.35 (c).



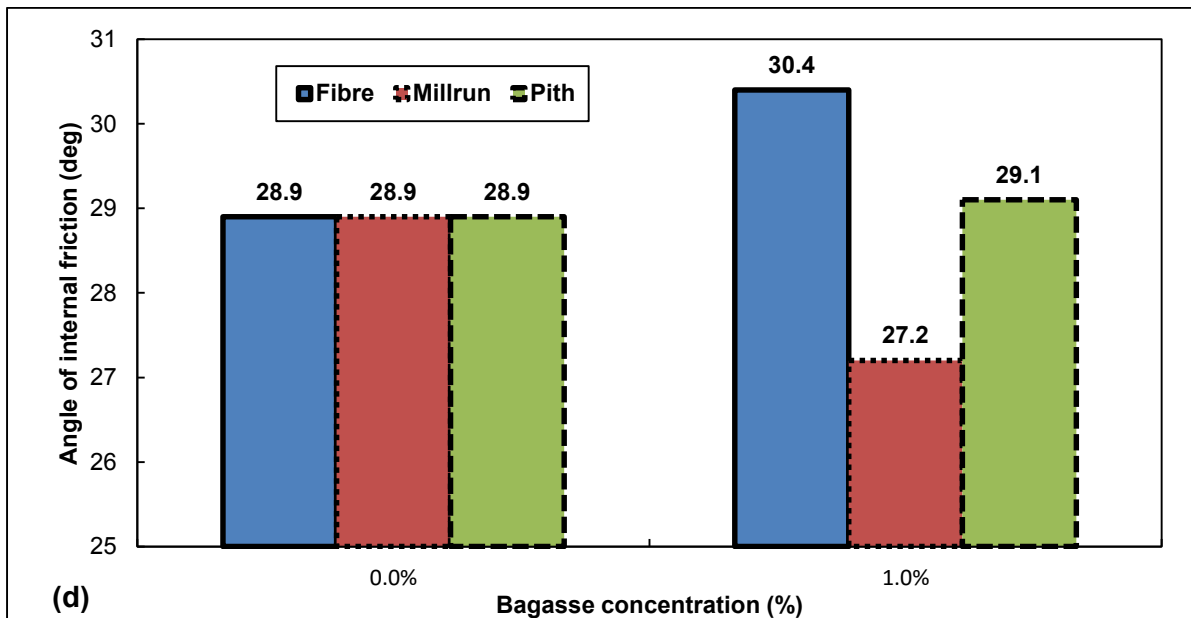
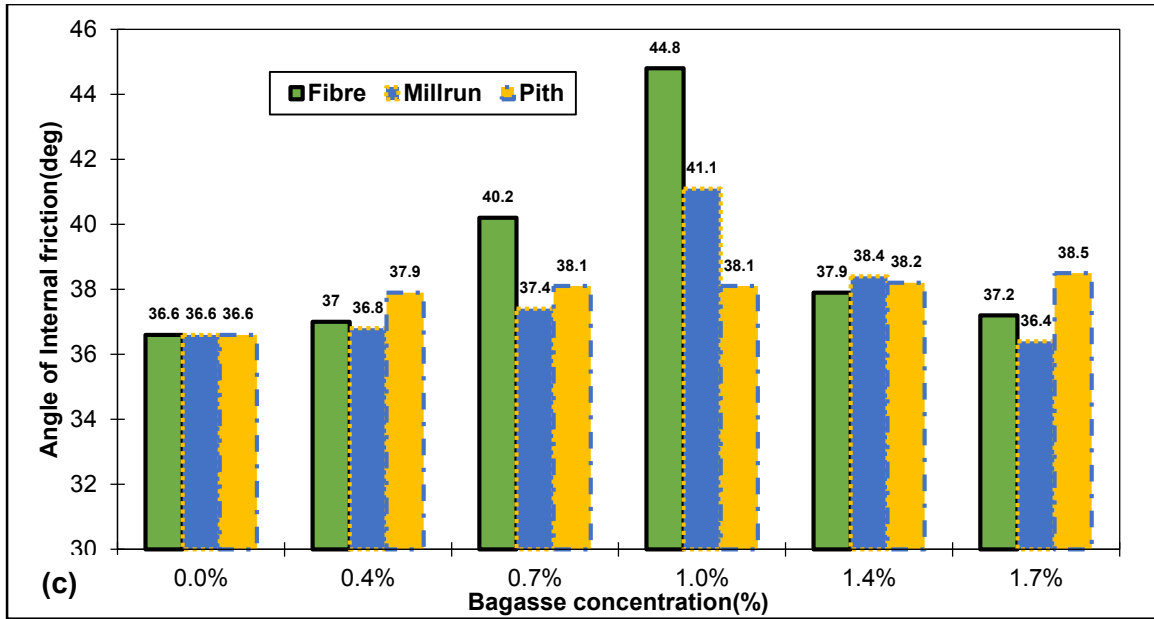


Figure 5.35: Comparison of the effect of the various types of bagasse on dry (a) Klipheuwel sand (b) Cape Flats sand (c) Kaolin clay

5.8 Durability study results and discussions

The durability study was conducted on Klipheuwel sand reinforced with 1.0% fibre content. The other types of soil were not considered to avoid repetition of the results. Fibre was chosen due to its observed resistance to water absorption compared to millrun and pith. The results are presented in sections 5.8.1 to 5.8.2.

5.8.1 12 cycle wetting and drying

The 12 cycles of wetting and drying of Klipheuwel sand reinforced with 1.0% fibre reduced the angle of internal friction from 40.6° to 38.8° , which corresponds to a 4.4% reduction. This is an insignificant change attributed to the smoothening of the fibre surface due to the addition of water.

As water was added to the composite, bagasse absorbed most of it. Upon drying, the fibres resumed their original structure, except for the smoothened surfaces. This regain in structure offered the interaction matrix but at a reduced magnitude compared to the dry fibre-soil composite not subjected to wetting and drying cycles.

A dry single strand of fibre was viewed under X10,000 magnification using an electron microscope. The results are shown in the micrograph figure 5.36, note the smooth surface obtained after wetting and drying.

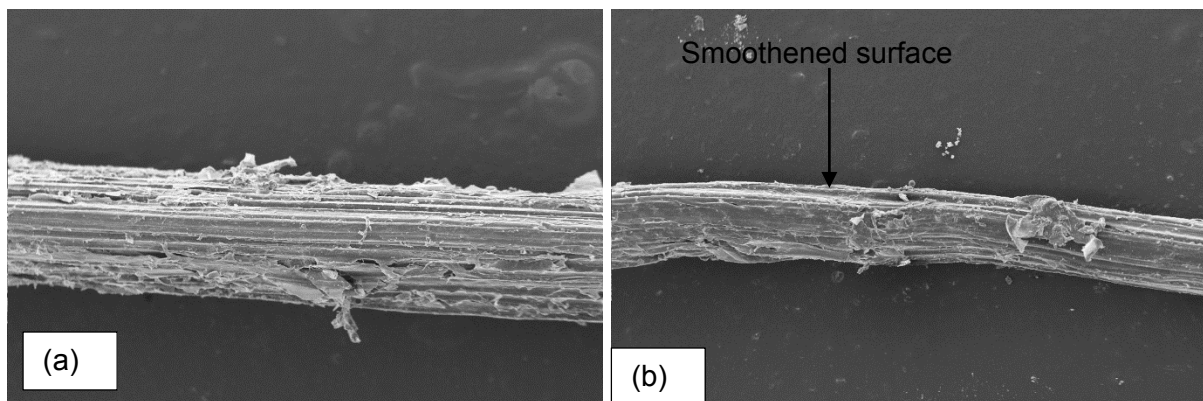


Figure 5.36: Micrograph of an isolated dry fibre strand (a) before and (b) after 12 cycles of wetting and drying

5.8.2 Soaked composite results

The soaking/submerging of the composite between fibre and Klipheuwel sand in water for a minimum of 6 hours and a maximum of 14 days produced the results summarised in table 5.21.

Table 5.20: Peak shear strengths of soaked Klipheuwel sand reinforced with 1% fibre bagasse.

Duration	Peak strengths						
	0 hours	6 hours	12 hours	24 hours	48 hours	7 days	14 days
50 kPa	61.9	58.3	52.8	47.8	42.3	43.5	43.4
100 kPa	104.1	102.4	87.5	83.7	76.6	72.7	72.6
200 kPa	190.4	184.5	166.5	153.4	146.1	145.3	145.5

From the results, it is evident that submerging the fibre-Klipheuwel sand composite in water for 6 hours insignificantly affected the peak shear strength of reinforced Klipheuwel sand. This could be attributed to the restriction of water by allowing it to access the mould in one direction (from the top) reducing the surface area for the composite wetting. In addition, compaction of the composite produced little “pockets” of uncompact regions, which retained water requiring more time to infiltrate the whole composite. This meant that not all the bagasse and soil particle got moist within the 6 hours of soaking, hence the insignificant change in peak strengths.

As hours of soaking progressed to 48 hours, the ingress of water increased causing a significant reduction in the peak shear strengths as shown in table 5.20. Increased water absorption dissolved part of the fibre cellulose and lignin weakening the interaction matrix by making the outer covering (rind) smooth. This combined with the lubrication of the soil particles, limited the resistance within the shear plane. Nevertheless, this limitation was prevented during consolidation and shear as flow of water out of the shear box was evident due to the low water retaining capacity of sands with increase in normal pressure. An overall percentage reduction in the peak shear strength of 31.6%, 30.2 % and 23.7 % was observed after 7 days for 50 kPa, 100 kPa and 200 kPa, respectively.

After 2 days of soaking, the angle of internal friction reduced from 40.6° to 34.7° representing a 15% reduction as shown in figure 5.37. From 7 to 14 days no change was realised on the angle of internal friction. This behaviour may be attributed to the optimum water absorption achieved by the fibres. Fibre was fully saturated after about 2 days limiting further smoothening of the outer covering. This meant that increasing the fibre exposure time in water did not affect the fibre cells. However, some breakage of the fibres was observed as shown in figures 5.39 (a). Furthermore, the design of the durability mould limited full anaerobic condition that could have facilitated decay thereby maintaining the tensile strength of the fibres. This observation was confirmed through the visual inspection of the exhumed fibres shown in figure 5.39(b). Similar results were obtained by Sarbaz et.al (2013) who concluded that submerging fibres in water insignificantly affected the CBR of reinforced sand after 5 days of soaking.

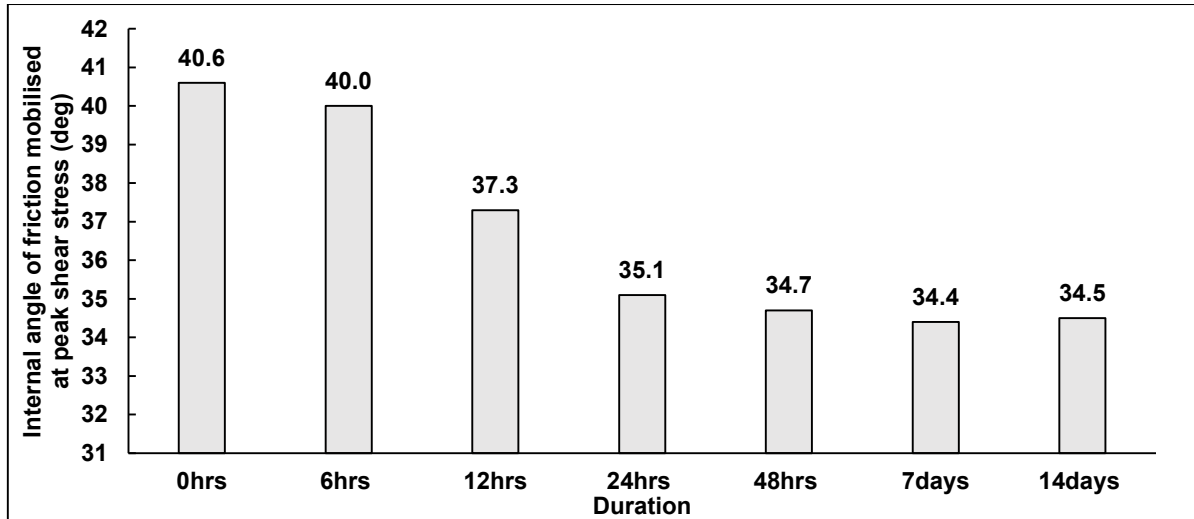


Figure 5.37: Effect of submerging on shear strength parameters on reinforced Klipheuwel sand

Similar reduction in cohesion was observed with increased water exposure time of the reinforced Klipheuwel sand as shown in figure 5.38. This was attributed to the increased lubrication of the soil particles, reduced interaction and the consequent breakages of fibre with water ingress over time. In theory, apparent cohesion of soils increases with the increase moisture up to an optimum value due to cementation of particles and build-up of negative pore pressure during shear. Introducing biodegradable fibres offers an opposing behaviour by absorbing most of the water added to the composite. This coupled with the flow of water out of the shear box during consolidation stage could explain the reduction in cohesive strength observed in the study.

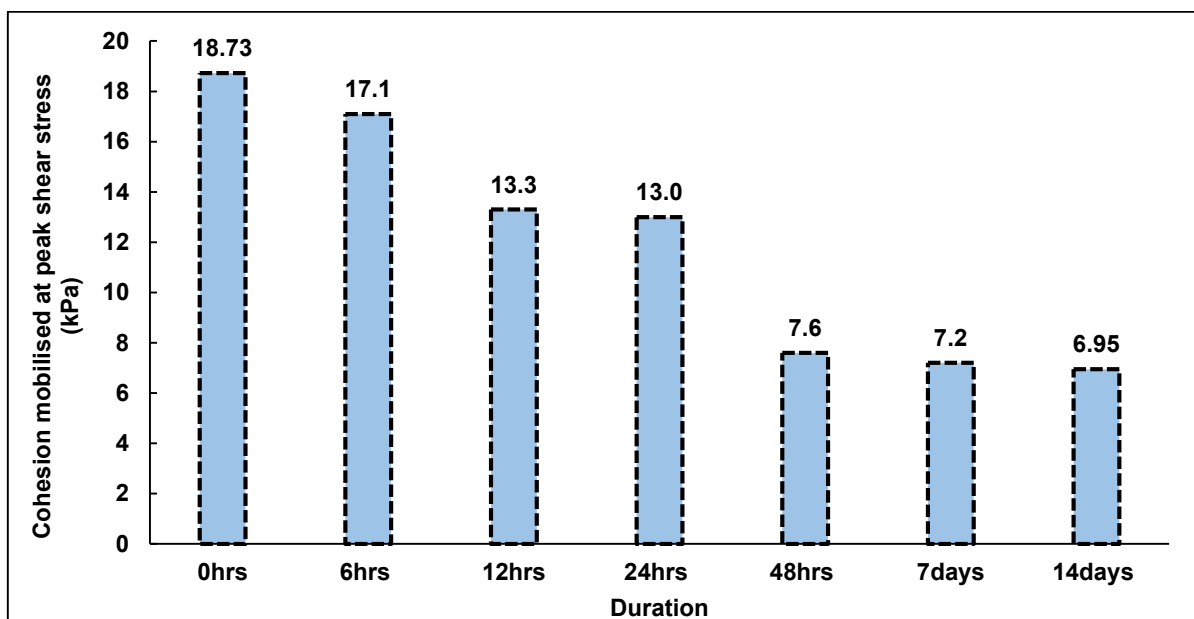


Figure 5.38: Effect of submerging on shear strength parameters on reinforced Klipheuwel sand

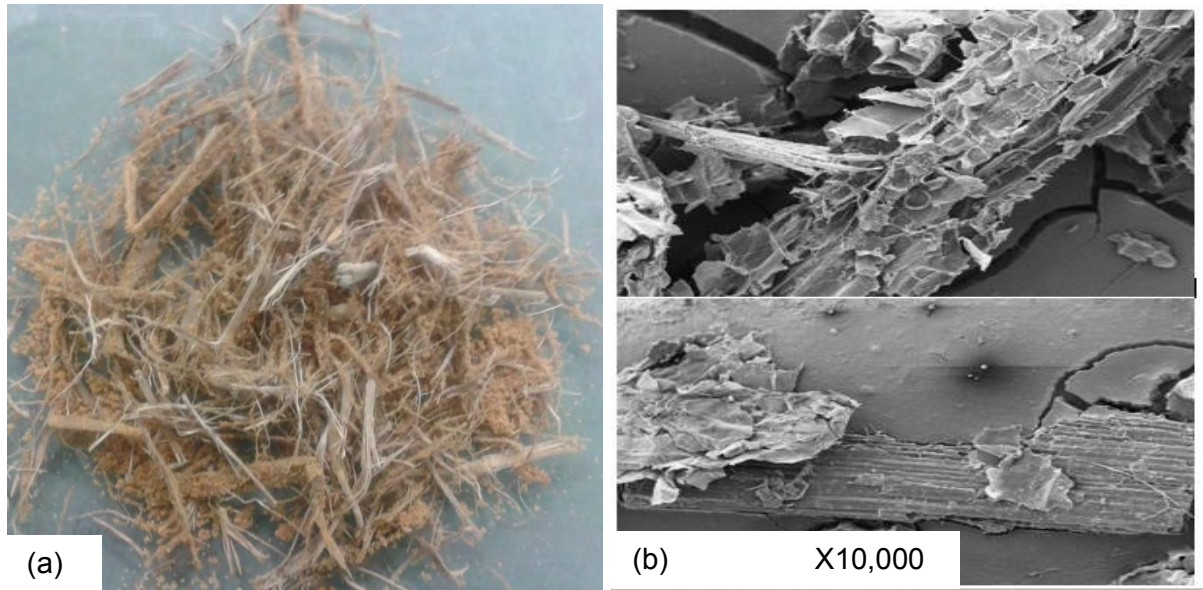


Figure 5.39: Exhumed fibres after soaking (a) visual (b) micrograph

5.9 Regression models for granular soils

A regression analysis was performed on the results obtained from the direct shear tests conducted on sandy soils to predict the peak shear strengths at failure. The clay soil studied was not considered in the model to enable comparison of soils with similar grain properties.

Ninety direct shear experimental data was used in generating the model in SPSS 22, software for statistical analysis. The predicted peak shear strength at failure was presented as a function of the normal load, bagasse content, ratio between fibre diameter and soil particle mean size, and a coefficient that estimated the shear strength parameters (c and ϕ) of unreinforced sand as given in equation 31. In other words, the variables were limited to those considered by the study.

$$\tau_p = f\left(\sigma_n, v, \frac{d_f}{D_{50}}, \mu\right) \quad (31)$$

Where σ_n is the normal load in kPa, v is the bagasse content in %, $\frac{d_f}{D_{50}}$ is the ratio of the

bagasse diameter to the mean diameter of the sand particles, and $\mu = \tan \phi$ is the coefficient of friction. The equation ignores the apparent cohesion in the unreinforced sand. The apparent cohesion obtained from the unreinforced soil parameters was negligible. In addition, the concentration of bagasse was considered due to its noticeable influence on the values of peak strengths achieved.

It should be noted that the fibre diameter was estimated as 6 mm for fibres, 4 mm for millrun and 2 mm for pith bagasse as determined in the fibre characterization study. Fibre length could not be used as a descriptor variable, due to the varied lengths observed on bagasse.

A stepwise multiple regression analysis was executed by trying out different models such as linear, power, quadratic and non-linear analysis with a confidence interval level of 95%. A non-linear relation shown in equation 32 produced the best correlation.

$$\tau_p = a.v^b.\sigma_n^c.\left(\frac{d_f}{D_{50}}\right)^d.\mu^e \quad (32)$$

Where a, b, c, d and e are constants that were obtained from the regression analysis as 2.4, 0.850, 0.063, 0.136 and 0.687, respectively. Therefore, the predictive model is given in equation 33.

$$\tau_p = 2.4 \times \sigma_n^{0.850} \times v^{0.063} \times \left(\frac{d_f}{D_{50}}\right)^{0.136} \times \mu^{0.687} \quad (33)$$

The value of R^2 for the model was 0.97 indicating that 97% variance in the predicted peak shear strengths was explained by the model using the four variables in equation 31. A significance value (P-value) of 0.029, which is less than 0.05, was obtained demonstrating that the model could adequately predict the behaviour of the bagasse reinforced sandy soils.

Furthermore, F-test and student's t-test checks for adequacy of the coefficient of each variable produced significant values of less than 0.05 (95% level of confidence) as summarised in table 5.21. These tests were computed by transforming the non-linear equation 29 into a natural logarithm enabling a linear regression.

Table 5.21: t-test results

Constants	Coefficients		t-value	P-value	Remarks
	Beta	Std. Error			
A	2.357	0.110	8.032	4.8778x10 ⁻¹²	P<0.05
B	0.850	0.016	54.074	1.2864x10 ⁻⁶⁷	P<0.05
C	0.063	0.014	5.253	1.0x10 ⁻⁴	P<0.05
D	0.136	0.035	4.059	1.09x10 ⁻⁴	P<0.05
E	0.687	0.253	2.228	2.8518x10 ⁻²	P<0.05

The residuals were plotted on a P-P plot as shown in figures 5.40 and 5.41.

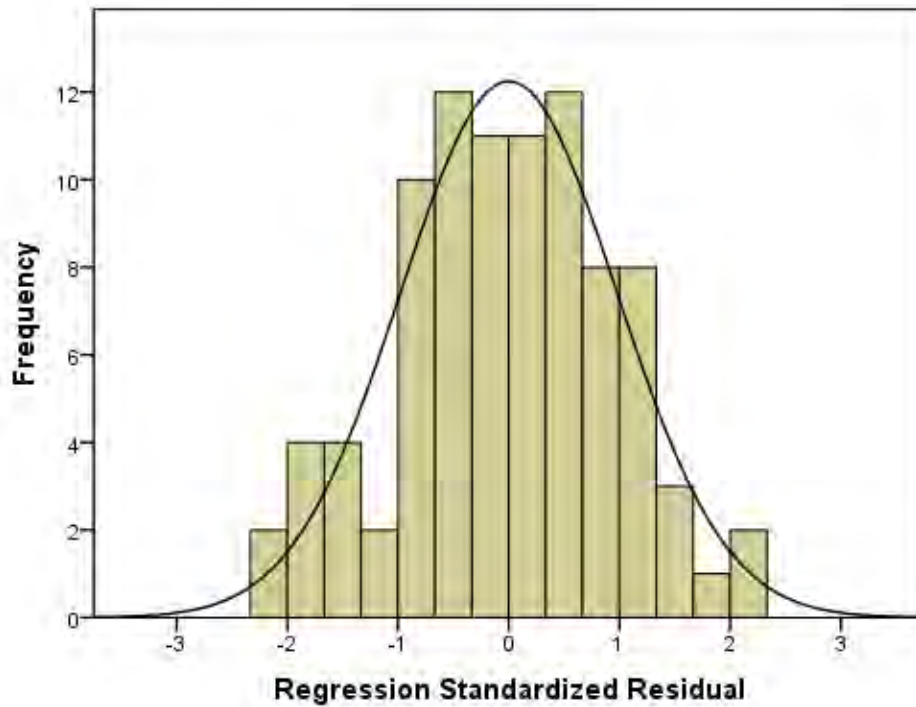


Figure 5.40: Histogram of plots

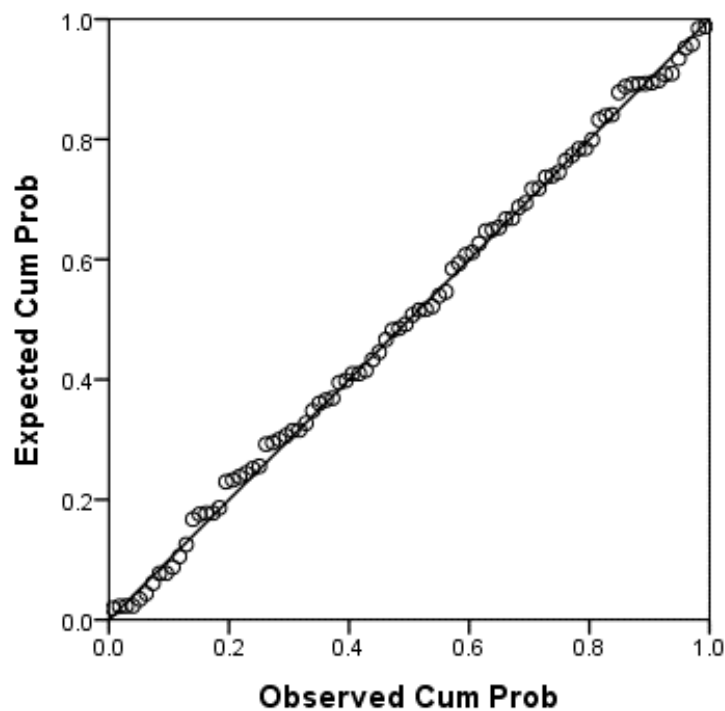


Figure 5.41: Normal P-P Plot of Regression Standardized Residual

The predicted values using the model in equation 33 were plotted against experimental measured values as shown in figure 5.42. This was to investigate how the variance obtained from the model would compare with the experimental results. The plots seem to cluster around the perfect equality line indicating that the model could adequately predict the peak shear strength of bagasse-reinforced sands.

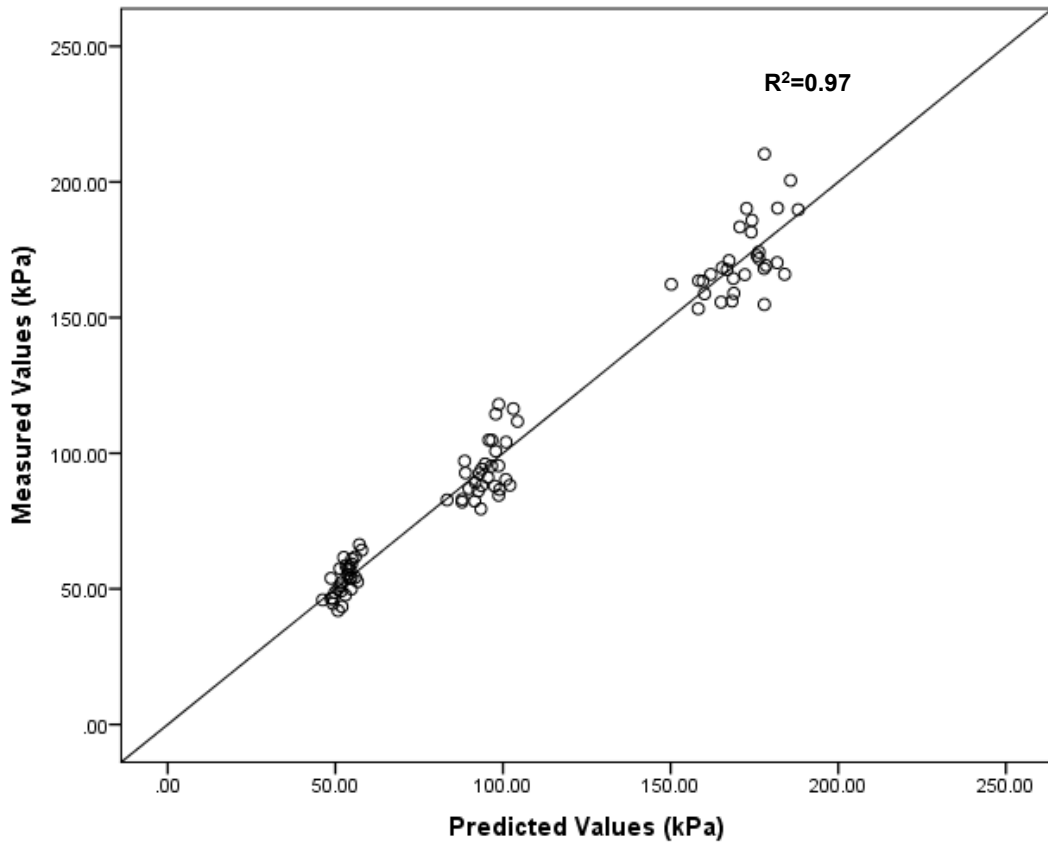


Figure 5.42: Predicted and measured values of peak shear stress for bagasse fibre reinforced sand

The predictive model given in equation 33 was used in calculating the peak shear strengths of a third sandy soil that was not used in the model formulation. This procedure was aimed at further validation of the model.

The sandy soil used was a whitish brown soil obtained from a construction site in Burgundy, Cape Town, South Africa. From the characterization tests, it is a well-graded soil with a $C_u=2.4$, $C_c = 1.25$, $D_{50} = 0.32$ mm and maximum dry density of 1678kg/m^3 at 11% OMC as shown in figure 5.43.

The sand was reinforced with 1.0% fibre bagasse and direct shear tests conducted to obtain its experimental parameters. It should be noted that only fibre bagasse was used to avoid repetition. The same procedure would apply to the other types of bagasse.

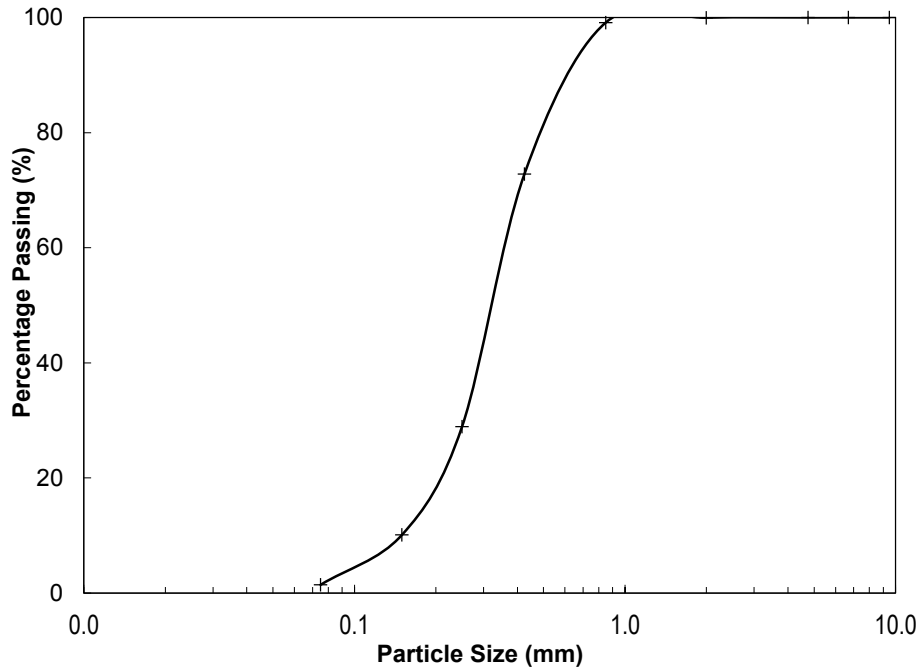


Figure 5.43: Particle distribution of the sandy soil used in the model validation

The predicted values and measured peak shear strength produced a plot as shown in figure 5.44.

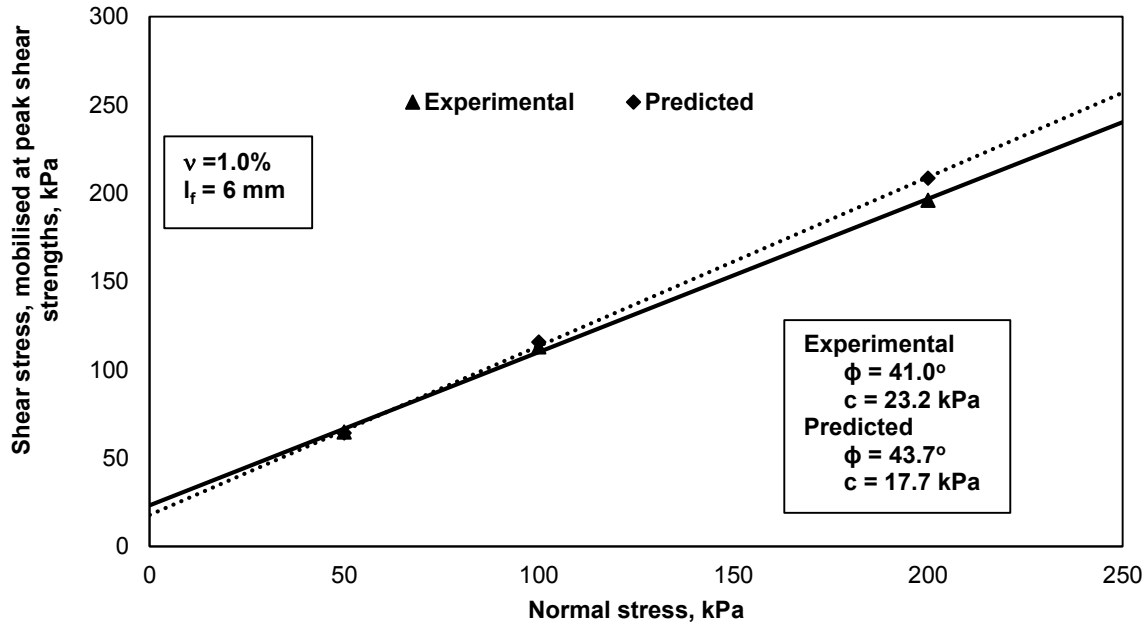


Figure 5.44: Comparison of predicted and experimental values failure envelope using a different sandy soil

The plot generated was similar to that obtained using experimental data. This further proved the possibility of using the model in predicting the peak shear strengths of sandy soil reinforced with sugarcane bagasse.

CHAPTER 6

6 PRACTICAL APPLICATIONS

6.1 Introduction

This chapter discusses simple mix design and guidelines based on the inherent procedures during the laboratory experimentation. It also gives a guideline on how to source for good quality sugarcane bagasse for optimum reinforcement results.

A basic design example is also presented in an embankment fill. Embankment slope stability is analysed using Bishop's Method of slicing and FEM analysis. The design was carried out on Klipheuwel sand to avoid repetition of results. The same procedures apply to all other soils.

6.2 Quality guidelines

Limited case histories on use the of bagasse fibres reinforced soil narrowed the scope of these guidelines. What is presented herein is solely informed by the various laboratory experiments and guidelines on soil stabilization by admixture.

- ***Selection of the best bagasse fibres***

The major source of bagasse fibre is the sugarcane milling companies. The bagasse fibre obtained from the millers should be:

1. Dry or at a moisture content less than 20% which would prevent it from decaying.
2. Free of residual sugars. Any existing residual sugars and pith materials must be screened out.
3. Between 2 mm to 6 mm in diameter. From this research, fibres in this range characterized using a stack of sieves gave an approximate composition as shown in figure 4.4.
4. Approximately, between 20 mm to 100 mm long, this could be difficult to establish for large-scale projects. Visual inspection is thus recommended for longer fibres and their elimination or shredding thereof if existent.

The optimum fibre content that responsible for the maximum shear strength in this study was 1% to 1.4% of the dry weight of soil. In other words, for every 100 tonnes of sand an equivalent 1 tonne of bagasse is required to produce sand-fibre composite with an optimum shear strength. This percentage concentration of bagasse depends on the type of soil, particle size distribution and angularity as presented in this study.

The constitutive relation in equation 33 would give preliminary peak strengths and consequently the required shear strength parameters for design purpose. Designers are only required to determine the unreinforced soil characteristics.

- **During construction**

Any conventional mixer, such as concrete rotary mixer, can be used to obtain a blending mix between the fibres and soil. During mixing, it is preferable to add water to the soil until the targeted moisture content is achieved prior to placing the fibres. This is to avoid fibre segregation and sticking together. According to Tingle et.al (2002), doing this would ensure uniform mixing and greater interaction within the composite. The composite can then be compacted in place using a hand held or any mechanical compactor.

As observed in this study, non-uniform mixing of the fibres resulted in the reduction of the peak shear strengths. As such mixing of the composite should be done for at most 5 minutes because prolonged mixing could result in fibre breakages and a non-uniform mix.

6.3 Design example

A 4 m high embankment with an 8 m long crest is to be constructed over soft clay to accommodate low volume vehicular use. Klipheuwel sand reinforced with fibre bagasse is proposed as an embankment fill with a slope of 2H: 1V. The ground water table is at the ground surface. The underlying foundation and embankment fill soil properties are as summarised in table 6.1. The embankment is to be analysed for the horizontal and vertical displacements using both reinforced and unreinforced fill and its factor of safety against slope failure.

Table 6.1: Plaxis 8.2 input parameters

Material model	Unreinforced Klipheuwel sand	Reinforced Klipheuwel sand	Soft clay*	Units
Type of behaviour	Drained	Drained	Undrained	-
Dry unit weight (γ_d)	17.2	16.8	15	kN/m ³
Saturated unit weight (γ_{sat})	19.88	21.2	18	kN/m ³
Young's modulus(E)**	33,000	33,000	10,000	kPa
Poisson's ratio (η)	0.3	0.3	0.35	-
Cohesion (c)	5.2	24.2	10	kPa
Friction angle (ϕ)	32.8	41.6	25	°
Dilatancy angle (ψ)**	4.875	4.875	0	°

*default values from Plaxis database

**calculated using relation $\psi = -2 + 12.5R_d$ from Brinkgreave et al. (2010)

6.3.1 Model computations

In modelling the problem, Finite Element (FE) method of analysis inherent in Plaxis 8.2 was used. FE methods allow for the equilibrium force calculations in stages of constructions. It is also unrestrained by boundary conditions and can handle very complex geometry and loading. It is from this basis that FE was chosen for the analysis. According to Plaxis (2012) manual, Plaxis is a finite element package that enables modelling, computations and presentation of settlement and slope stability problems without a predetermined stress or failure plane regime.

The problem was modelled as a plain strain using the Mohr-Coulomb model with a 15 node meshing. The Mohr-Coulomb model was chosen because it accurately predicts the drained failures. It also forms the basis for formulating other types of models and it is simple in the number of parameters required. According to the Plaxis (2012) manual, five inputs namely: Young's modulus, Poisson's ration, soil cohesion, angle of internal friction and angle dilatancy are required to fully analyse problems in the Mohr-Coulomb model. As such, the parameters were defined by the values given in table 6.1.

The analysis was divided into stages starting with material model, meshing, defining initial and boundary conditions, application of initial stresses, setting out of the calculation and finally viewing the output. It should be noted that this prototype design problem only simulated the displacements obtained in reinforced fill compared to unreinforced soil mass. Therefore, several inherent assumptions were incorporated for simplicity, such as:

- A surcharge load of 10kN/m^2 was considered to simulate the loading expected on the embankment analysed in the drained conditions.
- Only the improved shear strength parameters of Klipheuwel sand reinforced with 1.4% fibre was considered in the model. This was due to the difficulty of including the individual fibres into the model.
- Deformation at the base of the soft clay founding material was assumed as zero by applying fixities.
- Water was assumed to flow out of the boundaries and excess water pressure dissipated in all directions. However, to allow for symmetry in the embankment, the left boundary was kept closed.
- Initial overburden stresses applied by the embankment was excluded at the onset of the loading.
- The Young's Modulus and Poisson's ratio were approximated from Plaxis reference manual and literatures.

- The dilatancy angle was taken as the same for unreinforced and reinforced soil since compaction was conducted at approximately 55% relative density in both cases.
- The working load overlaying the embankment was modelled as a concrete plate with the following properties obtained from Khan and Abbas (2014) (table 6.2).

Table 6.2: Properties of the embankment concrete platform

Parameter (name)	Value	Unit
Normal stiffness (EA)	1.58×10^{11}	kN/m
Flexural rigidity (EI)	1.179×10^9	kNm ² /m
Equivalent thickness (d)	0.3*	m
Weight (w)	1.8 kN	kN/m/m
Poisson's ratio (ν)	0.15	-

*calculated directly by Plaxis

The embankment was modelled as shown in figure 6.1.

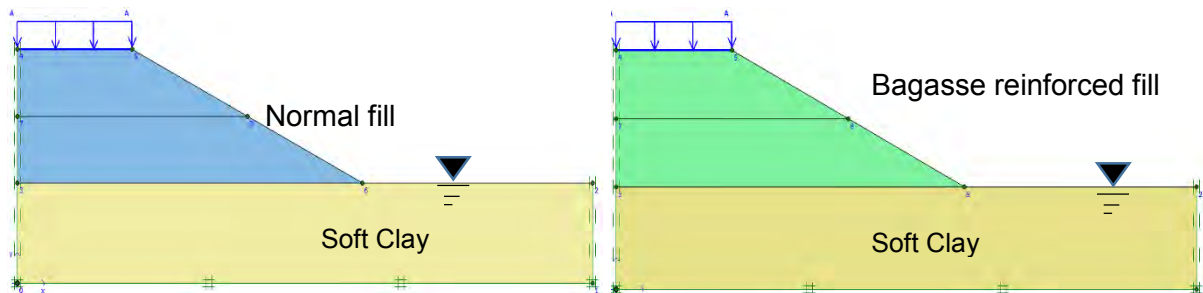


Figure 6.1: Geometry of the normal and reinforced fill

A triangular medium coarse mesh was used to define the boundary conditions. This kept the magnitude of the vertical and horizontal settlements obtained within the recommended limits. The initial conditions consisted of 10 kN/m^3 phreatic level at the ground surface, considering the worst-case scenario. To ensure no free flow of water across the boundary and excess dissipation of excess water the boundary on the left and right was closed. The initial stresses were included by deactivating the embankment fill layer to enable the KO procedure in the calculation of initial stresses as outlined in the Plaxis (2012) manual. KO values were computed from $KO = 1 - \sin \phi$ and represented the at rest earth pressure coefficient. The embankment was however reactivated during the calculation stage of the simulations.

Construction of the embankment was modelled in two lifts of 2 m each with an intermediate consolidation period of 60 days to allow dissipation of excess pore water pressure. In addition, consolidation was allowed during embankment surface construction, surcharge loading, and finally to a minimum pore water pressure of less than 1 kN/m^2 for safe design.

To obtain the global factor of safety, further staged construction was conducted using Phi-c reduction calculations and resetting the initial displacement for every stage of construction and consolidation. The slope failure analysis was carried out because of the 2:1 embankment slope proposed. Other different slope configurations were not considered in this analysis. Figure 6.2 summarises these calculation stages.

Identification	Phase no.	Start from	Calculation	Loading input	Time	Water	F
Initial phase	0	0	N/A	N/A	0,00 ...	0	0
✓ 1st Embankment ...	1	0	Consolidation	Staged Construction	30,0...	1	1
✓ Consolidation	2	1	Consolidation	Staged Construction	60,0...	1	2
✓ 2nd Embankment...	3	2	Consolidation	Staged Construction	30,0...	3	3
✓ Consolidation	4	3	Consolidation	Staged Construction	60,0...	4	4
✓ Pavement constr...	5	4	Consolidation	Staged Construction	30,0...	5	5
✓ Loading	6	5	Consolidation	Staged Construction	60,0...	6	6
✓ Consolidation till 1m	7	6	Consolidation	Minimum pore pressure	227,...	6	7
✓ Phi-c 2m	8	1	Phi/c reduction	Incremental multipliers	0,00 ...	1	8
✓ Phi-c 4m	9	3	Plastic	Staged construction	0,00 ...	3	9
✓ Phi-c pavement c...	10	5	Phi/c reduction	Incremental multipliers	0,00 ...	5	10
✓ Phi-c loading	11	6	Phi/c reduction	Incremental multipliers	0,00 ...	6	11
✓ Phi-c till 1m	12	7	Phi/c reduction	Incremental multipliers	0,00 ...	6	12

Figure 6.2: Model calculation stage inputs

6.3.2 Results and discussion

The FE results analysis are as given in table 6.3.

Table 6.3: Embankment fill displacement and slope analysis results

	Unreinforced embankment	Reinforced embankment
Total displacement (mm)	177.96	143.41
Horizontal displacement (mm)	68.55	50.47
Vertical displacement (mm)	177.96	143.41
Total strain (%)	10.79	7.84
Total stress (kPa)	120.69	114.85
Shear stress (kPa)	91.17	89.82
Factor of safety (FE)	1.42	2.04
Factor of safety (Bishops)	1.48	1.78

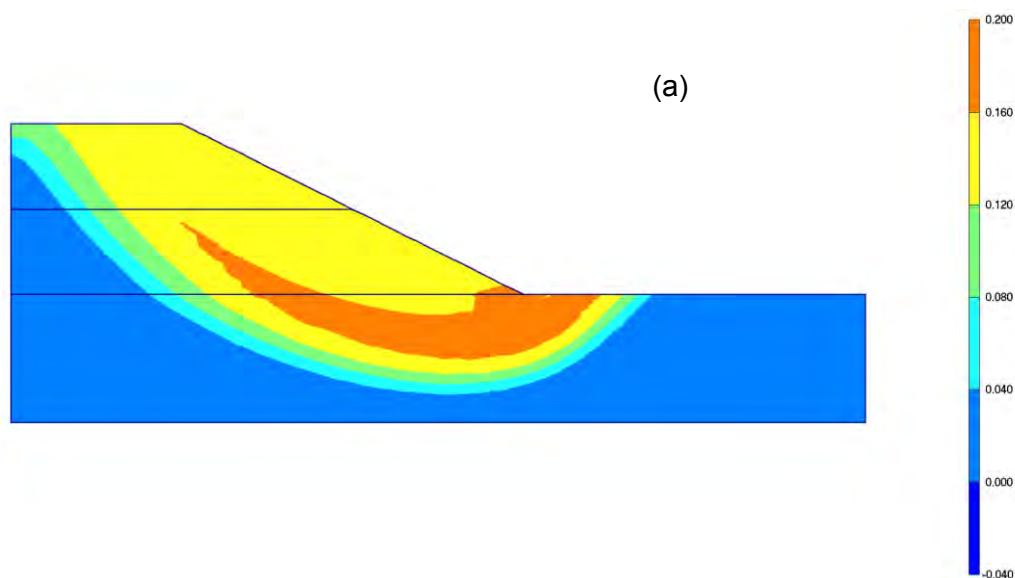
From the results, it is evident that reinforcing the embankment fill reduces the total vertical settlement and horizontal movement by 26% and 19%, respectively. Settlement is defined by Holtz & Kovacs (1981) as the total vertical deformation at the surface of a soil due to loading.

Loadings at soil surfaces induce immediate and consolidation settlements. Immediate settlement refers to the reduction of volume due to the re-arrangement of particles immediately after loading whereas consolidation is a time dependent process involving drainage of water. According to Holtz and Kovacs (1981), consolidation in soil structures depends on their coefficient of permeability and the rigidity of the soil skeleton.

It can therefore be inferred that the addition of fibres in the embankment fill improved the rigidity of the soil mass and marginally created voids within the composite, which in turn reduced the vertical deformations due to the dissipation of the excess pore water pressure. This implied that with the inclusion of fibres, there was a reduction in the settlements due to the consolidation and loading of the embankment.

Furthermore, the Phi-c slope stability analysis using FE yielded results as shown in figures 6.3 (a) and (b). The method predicted a deep-seated failure. The global factor of safety obtained using FE method was compared with the Bishop's method of slicing in Prokon software. The Bishop's method is a limit equilibrium method involving an iterative process to determine the failure plane with the least factor of safety in slope stability analysis. It enabled the verification of the factor of safety obtained with the FE method. The results of the slope stability analysis are given in figures 6.3 (a) to (d).

The global factor of safety improved at the end of the construction stage with the introduction of reinforcements. Figure 6.3 shows the total deformation increment for the phi-c reduction stages.



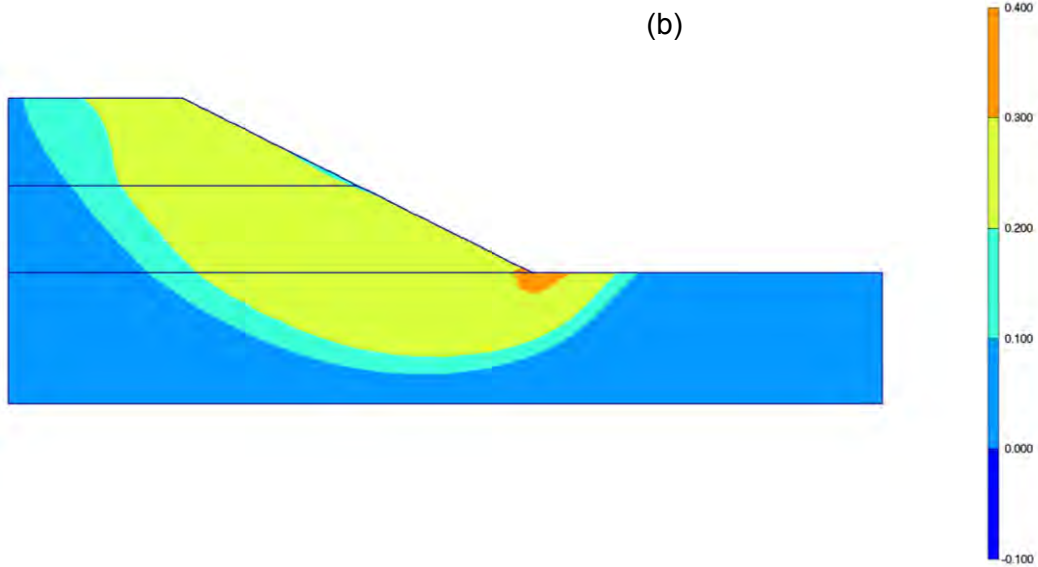


Figure 6.3: Probable failure mechanism (a) unreinforced fill (b) reinforced fill, scale in m

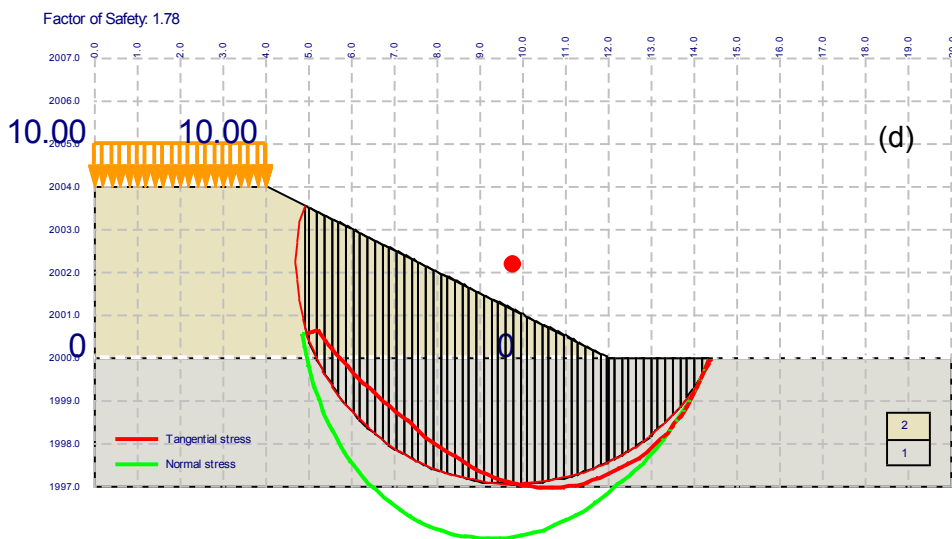
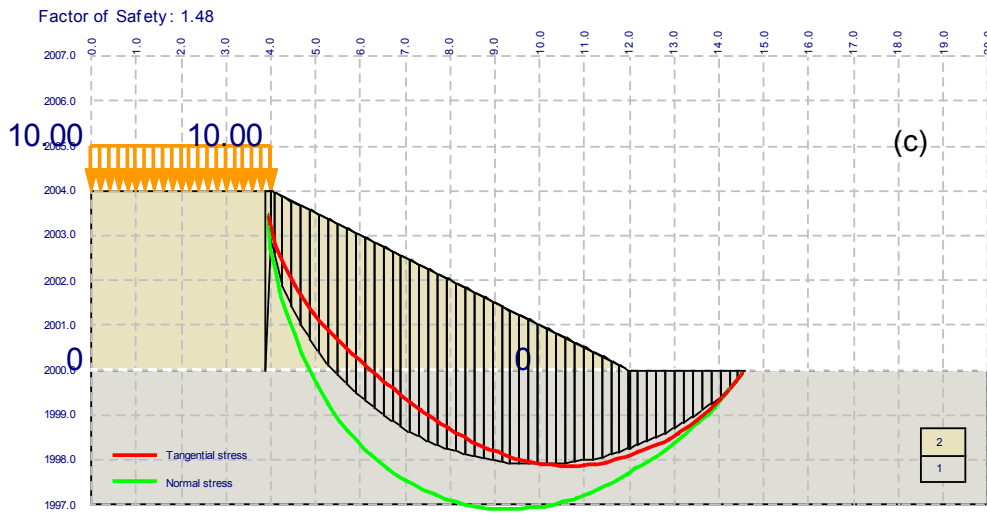


Figure 6.4: Failure plane results from Plaxis (a) unreinforced (b) reinforced embankment, and Prokon (c) unreinforced (d) reinforced embankment

CHAPTER 7

7 CONCLUSIONS AND RECOMMENDATIONS

7.1 Introduction

In this study, the usefulness of sugarcane bagasse as a soil reinforcement material was investigated through direct shear tests conducted on reinforced Klipheuwel sand, Cape Flats sand and Kaolin clay using three types of sugarcane bagasse. Fibre bagasse was mixed together with the selected soils at 0.3% to 1.7% content by dry weight of soil. The same concentrations were applied to millrun and pith. The choice of the concentrations was governed by the segregation of fibres that hindered complete mixing beyond a 1.7% content by dry weight of soil. In addition, the effect on the shear strength due to moisture, wetting and drying as well as soaking on the shear strength behaviour was investigated. The following section presents the conclusions of the findings and the recommendations for further research.

7.2 Conclusions

7.2.1 Specific conclusions

The objectives of this study were fulfilled and the following specific outcomes drawn from the experimental work.

- Sugarcane bagasse can be used as a reinforcement material. It improves the peak shear strength of sandy and clay soils up to maximum bagasse content and reduces the post peak loss in strength by making the soils more ductile. For bagasse reinforcement to be effective, all the residual sugars must be screened out. Residual sugars impede interaction in the composite mass due to the large amount of organic matter present. Thus, fibre bagasse would be preferred to the two types of bagasse as the best reinforcement material.
- Increasing bagasse content increased the shear strength parameters of the soils up to an optimum content of 1.4% responsible for an increase of 26.8% in the angle of internal friction of Klipheuwel sand, and optimum content of 1.0% responsible for an increase of 22.4% in the angle of internal friction of Cape Flat sands. Kaolin clay showed a 5.2% increase in the angle of internal friction at 1.0% fibre content. Comparing the two sandy soils at low confining pressures, the increase was more in the well-graded soil with a wide range of particle sizes.
- The addition of bagasse did not affect the stiffness of the soils at low strains. A strain of 15% to 25% was required to mobilise the peak shear strengths in bagasse - reinforced soils as observed in this study. It can be concluded that a threshold pressure

is required to effect the improvement in the shear strengths of bagasse-reinforced soils.

- Even though the addition of water reduced the shear strength of soils, it did not deter the increase in shear strength of bagasse reinforced sandy soils. Tests conducted on dry and moist soils approximately displayed a 30% increase in the angle of internal friction of Klipheuwel sand in both dry and moist conditions.
- The durability study indicated that 12 cycles of wetting and drying do not affect the dilatancy of Klipheuwel sand. However, wetting and drying slightly “smoothened” the fibre surface lowering the fibre friction. On the other hand, soaking of bagasse-soil composite in water for 14 days decreased the peak shear strengths as well as the angle of internal friction of Klipheuwel sand by about 15% after 2 days. This implies that for the bagasse-soil composite to retain its strength proper drainage systems must be in place.
- Relating the experimental peak shear strength with the descriptor variables studied, produced a non-linear model that could be used in determining the optimal bagasse characteristics based on the prevailing soil properties.
- In addition, modelling fibre-reinforced embankment using FEM presented a reduction in the total vertical settlement and horizontal movements by 26% and 19% respectively, and improved the factor of safety from 1.42 to 2.04 confirming that fibre bagasse could be useful in mitigating the probable slope failure in an embankment fill meant for low volume roads.

7.2.2 General conclusions

The general conclusions, which seek to generalise the finding for use in engineering applications, were as follows:

- All the three types of bagasse improved the peak shear strength of soils with fibre bagasse significantly contributing to improvement of the peak shear strength compared to millrun and pith. It can be inferred that, shear strength behaviour is not a function of tensile strength of the bagasse fibres but a dependent on the interaction mechanism between the fibres and soil, which in turn depends on the length of fibres. This observation was evidenced with pith bagasse which improved the shear strengths of soil regardless of it having a near zero tensile strength.
- The effect on the peak shear strengths of fibre-reinforced soils can be taken as dependent on the type of fibres, normal loads, type of soil (grain size), fibre content and soil moisture content for fibres whose length determination is difficult.

- Mixing fibres as a ratio of dry mass of soil rather than replacement method is more feasible and easier to replicate in-situ.

7.3 Recommendations

1. Obtaining uniform lengths of bagasse fibre from sugar mill sourced bagasse is difficult. Since the length of fibres is a determining factor in fibre-reinforced soils, further study is recommended to characterize bagasse based on lengths.
2. Investigations using a wide variety of soils to further develop the regression model.
3. Durability studies for longer durations should be constituted to investigate the effect of water on the bagasse fibre reinforced soil using a wide range of soils.
4. Because bagasse fibre is biodegradable, coating the fibres and studying the effect of coating on the shear behaviour is recommended. In addition, settlement studies are recommended to investigate the settlement behaviour of bagasse-reinforced soils.
5. Vast studies seem to have been conducted on fibre-reinforced soils and the existing theories are sufficient. Addition studies should be constituted aimed at developing the design standards and in-situ tests in large scale.

References

- Aggarwal, P. Sharma, B., 2011. Application of Jute Fiber in the Improvement of Subgrade Characteristics. *International Journal on Transportation and Urban Development*.1 (1): 56-58.
- Ahmad, F., Bateni, F. & Azmi, M. 2010. Performance evaluation of silty sand reinforced with fibres. *Geotextiles and Geomembranes*. 28(1): 93-99.
- Al-Refeai, T.O. 1991. Behavior of granular soils reinforced with discrete randomly oriented inclusions. *Geotextiles and Geomembranes*. 10(4): 319-333.
- Amu, O., Ogunniyi, S. & Oladeji, O. 2011. Geotechnical Properties of Lateritic soil stabilized with sugar cane straw ash. *American Journal of Scientific and Industrial Research*. : 323-331.
- Anagnostopoulos, C.A., Papaliangas, T.T., Konstantinidis, D., and Patronis, C. 2013. Shear Strength of Sands Reinforced with Polypropylene Fibers. *Geotechnical and Geological Engineering*, 31(2), pp.401–423
- Anyiko, F., Kalumba, D. and Bagampadde, U. 2011. Investigation of the suitability of recycled carpet fibre as a soil reinforcement material. In J.A. Mwakali and H.M. Alinaitwe (eds), *Proceedings of the Second International Conference on Advances in Engineering and Technology*, 31 January - 1 February 2011, Entebbe, Uganda. Uganda: Macmillan. ISBN 978-9970-214-00-7
- ASTM D1557-12. 2012. Standard test methods for laboratory compaction characteristics of soil using modified effort. ASTM International, West Conshohocken, PA, USA.
- ASTM D2216. 2010. Standard test methods for laboratory determination of water (moisture) content of soil and rock by mass. ASTM International, West Conshohocken, PA, USA.
- ASTM D3080. 2011. Standard test method for direct shear test of soils under consolidated drained conditions. ASTM International, West Conshohocken, PA, USA.
- ASTM D422. 2007. Standard test method for particle-size analysis of soils. ASTM International, West Conshohocken, PA, USA.
- ASTM D4318 - 10e1. 2010. Standard test methods for liquid limit, plastic limit, and plasticity index of soils. ASTM International, West Conshohocken, PA, USA.
- ASTM D854. 2010. Standard test methods for specific gravity of soil solids by water pycnometer. ASTM International, West Conshohocken, PA, USA.

-
- Azwa, Z.N., Yousif, B.F., Manalo, A.C. & Karunasena, W. 2013. A review on the degradability of polymeric composites based on natural fibres. *Materials & Design*. 47(0): 424-442.
- Basu, D., Puppala, A.J. & Chittoori, B., 2013. Sustainability in geotechnical engineering – general report. *Proceedings of the 18th ICSMGE, Paris*, pp.3155–3162.
- Bilba, K., Arsene, M. & Ouensanga, A. 2003. Sugar cane bagasse fibre reinforced cement composites. Part I. Influence of the botanical components of bagasse on the setting of bagasse/cement composite. *Cement and Concrete Composites*. 25(1): 91-96.
- Bledzki, A.K. & Gassan, J. 1999. Composites reinforced with cellulose based fibres. *Progress in Polymer Science*. 24(2): 221-274.
- Brinkgreve, R.B.J., Engin, E., & Engin, H.K. 2010. Validation of empirical formulas to derive model parameters for sands. In *Numerical Methods in Geotechnical Engineering*. T, Benz et al., Eds. London, United Kingdom: Taylor & Francis Group. 137-142.
- Cao, Y., Shibata, S. & Fukumoto, I. 2006. Mechanical properties of biodegradable composites reinforced with bagasse fibre before and after alkali treatments. *Composites Part A: Applied Science and Manufacturing*. 37(3): 423-429.
- Chebet, F.C., Kalumba D. & Banzibaganye G., 2013. An Investigation of Waste Tyre Shreds as Reinforcement Material for Typical South African Sandy Soils. *Proceedings of the 20th WasteCon Conference 6-10 October 2014*. Somerset West, Cape Town.
- Consoli, N.C. et al., 2007. Shear Strength Behavior of Fiber-Reinforced Sand Considering Triaxial Tests under Distinct Stress Paths. *Journal of Geotechnical and Geoenvironmental Engineering*, 133(11), pp.1466–1469.
- Das, B. M. 2002. *Principles of geotechnical engineering*. Pacific Grove, CA, Brooks Cole/Thompson Learning.
- De Wet M. 2015: *Soil Behaviour Course*. Stellenbosch University.
- Diambra, A Russell, A R Ibraim, E Wood, D M. 2007. Determination of fibre orientation distribution in reinforced sands. *Géotechnique*. 57(7): 623-628.
- Donaldson, A.L, Kalumba D. 2014. Geotechnical Application for Expanded Polystyrene Waste. Unpublished paper presentation at: 20th Wastecon Conference on Information Quality, October 4-5, 2014, Somerset West, Cape Town.
- Estabragh, A., Bordbar, A. & Javadi, A. 2013. A Study on the Mechanical Behavior of a Fiber-Clay Composite with Natural Fiber. *Geotechnical and Geological Engineering*. 31(2): 501-510.

- Faruk, O., Bledzki, A.K., Fink, H. & Sain, M. 2012. Biocomposites reinforced with natural fibres: 2000–2010. *Progress in Polymer Science*. 37(11): 1552-1596.
- Food Agriculture Organization. 2013: Sugarcane Production in Africa.
- Fuqua, M. a., Huo, S. & Ulven, C. a., 2012. Natural Fiber Reinforced Composites. *Polymer Reviews*, 52(3-4), pp.259–320.
- Gao, Z. & Zhao, J. 2013. Evaluation on Failure of Fiber-Reinforced Sand. *Journal of Geotechnical and Geoenvironmental Engineering*. 139(1): 95-106.
- Gray, D. & Ohashi, H. 1983. Mechanics of Fiber Reinforcement in Sand. *Journal of Geotechnical Engineering*. 109(3): 335-353.
- Head, K. H., 1980, *Manual of Soil Laboratory Testing, Volume 1, Soil Classification and Compaction Tests*, Engineering Laboratory Equipment Limited, Pentech Press, London: Plymouth.
- Hejazi, S.M., Sheikhzadeh, M., Abtahi, S.M. & Zadhoush, A. 2012. A simple review of soil reinforcement by using natural and synthetic fibers. *Construction and Building Materials*. 30100-116.
- Holtz, R.D. & Kovacs, W.D. 1981. *An Introduction to Geotechnical Engineering*. Englewood Cliffs, New Jersey: Prentice-Hall, Inc.
- Hugot, E. 1986. *Handbook of Cane Sugar Engineering*. 3rd edition. Elsevier Science Publishers B.V, Amsterdam.
- Jamellodin, Zalipah and Abu Talib, Zaihasra and Kolop, Roslan and Md Noor, Nurazuwa 2010. The effect of oil palm fibre on strength behaviour of soil. In: *Proceedings of the 3rd International Conference on Southeast Asian Natural Resources and Environmental Management (SANREM) 2010* , 3-5 August 2010, Kota Kinabalu, Sabah.
- John, M. & Thomas, S., 2008. Biofibres and biocomposites. *Carbohydrate Polymers*, 71(3), pp.343–364
- Jones, C.J.F.P., 1996. *Earth reinforcement and soil structures*. London; New York: T. Telford; ASCE Press.
- Kalumba D. and Chebet F. C. 2013. Utilisation of polyethylene (plastic) shopping bags waste for soil improvement in sandy soils. *Proceedings of the 18th ICSMGE*, Paris, pp.3223–3226.
- Khan, S.A. & Abbas, S.M. 2014. Numerical modelling of highway embankment by different ground improvement techniques.

- Koerner, R. M. 2005. *Designing with geosynthetics*. Upper Saddle River, NJ, Prentice Hall
- Ladd, R. S., 1978. Preparing Test Specimens using Undercompaction," *Geotechnical Testing Journal*, GTJODJ, Vol. 1, No. 1, March, pp. 16-23.
- Laurianne, S.A., 2004. *Farmers Lungs*. www.emedicine.com/med/topic771.htm/13.10.2014
- Li, C. & Zornberg, J. 2013. Mobilization of Reinforcement Forces in Fiber-Reinforced Soil. *Journal of Geotechnical and Geoenvironmental Engineering*. 139(1): 107-115.
- Lin, C. 2005. *Mechanical Response of Fibre-Reinforced Soil*. Ph.D Dissertation. University of Texas at Austin.
- Loh, Y.R. et al., 2013. Sugarcane bagasse—The future composite material: A literature review. *Resources, Conservation and Recycling*, 75, pp.14–22.
- Look, B. G. 2007. *Handbook of Geotechnical Investigation and Design Tables*. Taylor & Francis/Balkema, London.
- Lovisa, J., Shukla, S. K. & Sivakugan, N. 2010. Shear strength of randomly distributed moist fibre-reinforced sand. *Geosynthetics International*, 17(2), pp.100–106
- Maher, M. & Gray, D. 1990. Static Response of Sands Reinforced with Randomly Distributed Fibers. *Journal of Geotechnical Engineering*. 116(11): 1661-1677
- Maliakal, T. & Thiyyakkandi, S. 2013. Influence of randomly distributed coir fibers on shear strength of clay. *Geotechnical and Geological Engineering*. 31(2):425-433.
- Marandi M, Bagheripour H, Rahgozar R, Zare H. 2008. Strength and ductility of randomly distributed palm fibers reinforced silty-sand soils. *Am J Appl Sci*; 5:209–20
- McGown, A., Andrawes, K. & Al-Hasani, M. 1978. Effect of inclusion properties on the behaviour of sand. *Geotechnique*. 28(3): 327-346.
- Michalowski, R. & Čermák, J. 2003. Triaxial Compression of Sand Reinforced with Fibers. *Journal of Geotechnical and Geoenvironmental Engineering*. 129(2): 125-136.
- Mirzababaei, M., MirafTAB, M., Mohamed, M. & McMahon, P. 2013. Unconfined Compression Strength of Reinforced Clays with Carpet Waste Fibers. *Journal of Geotechnical and Geoenvironmental Engineering*. 139(3): 483-493.
- Mohanty, A.K., Misra, M. & Hinrichsen, G. 2000. Biofibres, biodegradable polymers and biocomposites: An overview. *Macromolecular Materials and Engineering*. 276-277(1): 1-24.
- Mwasiswebe, D. 2005. *Production of activated carbon from South African sugarcane bagasse*. (M.Sc. Eng.) Chemical Engineering. University of KwaZulu-Natal.

- Nataraj, M. S., Mcmanis, K. L. 1997. Strength and deformation properties of soils reinforced with fibrillated fibers. *Geosynthetics Int.*, Vol. 4, No. 1, pp. 65-79.
- Osinubi, K., Bafyau, V. & Eberemu, A. 2009. Bagasse ash stabilization of lateritic soil. In *Appropriate Technologies for Environmental Protection in the Developing World*. Springer. 271-280.
- Paturau, J.M. 1989. *By-products of the cane sugar industry*. Elsevier, Amsterdam, the Netherlands.
- Pedley MJ, Jewell RA, Milligan GWE. 1990. A large-scale experimental study of soil-reinforced interaction—Part I. *Ground Engineering; July/August*: 45–48.
- PLAXIS. 2012a. PLAXIS 2D 2012 – Material Modules Manual. Available: <http://www.plaxis.nl/files/files/2D2012-3-Material-Models.pdf> [2015, August 5].
- Prabakar, J. & Sridhar, R., 2002. Effect of random inclusion of sisal fibre on strength behaviour of soil. *Construction and Building Materials*, 16(2), pp.123–131.
- Prabakar, J., Dendorkar, N. & Morchhale, R. 2004. Influence of fly ash on strength behavior of typical soils. *Construction and Building Materials*. 18(4): 263-267.
- Puppala, A. J., Musenda, C. 2000. Effects of fiber reinforcement on strength and volume change in expansive soils. *Soil Mechanics 2000*, No. 1736, pp. 134-140,
- Rahman, M.M., Mallik, A.K. & Khan, M.A. 2007. Influences of various surface pretreatments on the mechanical and degradable properties of photografted oil palm fibers. *Journal of Applied Polymer Science*. 105(5): 3077-3086.
- Ranjan G, Vasan RM, Charan HD 1996. Probabilistic analysis of randomly distributed fiber-reinforced soil. *J Geotech Eng* 122(4):419–426
- Rein, P. W. 1972. A study of the cane sugar diffusion process. Doctoral dissertation, University of Natal, Durban.
- Sadek, S., Najjar, S. & Freiha, F. 2010. Shear Strength of Fiber-Reinforced Sands. *Journal of Geotechnical and Geoenvironmental Engineering*. 136(3): 490-499
- Sarbaz, H., Ghiassian, H. & Heshmati, A.A. 2014. CBR strength of reinforced soil with natural fibres and considering environmental conditions. *International Journal of Pavement Engineering*. 15(7):577-583.
- Shao, W. et al., 2014. Experimental Investigation of Mechanical Properties of Sands Reinforced with Discrete Randomly Distributed Fiber. *Geotechnical and Geological Engineering*, 32(4), pp.901–910.

- Sharma, Hari D., Reddy, Krishna R., 2004. Geoenvironmental engineering: site remediation, waste containment, and emerging waste management technologies. Hoboken, N.J.: Wiley.
- Shukla, Sanjay K., Sivakugan, Nagaratnam, Das, Braja M., and Singh, Ashish K. 2009. Fundamental concepts of soil reinforcement - an overview. *International Journal of Geotechnical Engineering*, 3 (3). pp. 329-342
- Sivakumar Babu, G. & Vasudevan, A. 2008. Strength and stiffness response of coir fiber-reinforced tropical soil. *Journal of Materials in Civil Engineering*. 20(9):571-577.
- Smith, I. M. (2006). *Smith's elements of soil mechanics*. Oxford, Blackwell Pub.
- South African Sugar Association (2014). *Industry Directory 2014/2015*. Available <http://www.sasa.org.za/Files/IndustryDirectory2014-2015.pdf>
- Stephens, D. 1994. Natural fibre reinforced concrete blocks. 20th WEDC Conference: Affordable Water Supply and Sanitation. Colombia, Sri Lanka. 1994.
- Swami Saran. 2010. Reinforced soil and its engineering applications. New Delhi: I.K. International Pub. House.
- Tingle, J.S., Santoni, R.L. & Webster, S.L. 2002. Full-scale field tests of discrete fiber-reinforced sand. *Journal of Transportation Engineering*. 128(1):9-16.
- Torres Agredo, J, Mejía de Gutiérrez, R, Escandón Giraldo, C. E, & González Salcedo, L. O. 2014. Characterization of sugar cane bagasse ash as supplementary material for Portland cement. *Ingeniería e Investigación*, 34(1), 5-10
- United Nations Data 2010. Bagasse Production in South Africa. Available: <http://data.un.org/Data.aspx?d=EDATA&f=cmID%3aBS%3btrID%3a01> [June 5, 2014].
- Vaniček M., Jirásko D. and Vaniček I. 2013. Geotechnical engineering and protection of environment and sustainable development. *Proceedings of the 18th ICSMGE, Paris*, pp.3259–3262.
- Walford, S. 2008. Sugarcane bagasse: How easy is it to measure its constituents? *Proceedings of the South African Sugar Technologists Association*, vol. 81, pp. 266-273.
- Yetimoglu, T. & Salbas, O. 2003. A study on shear strength of sands reinforced with randomly distributed discrete fibers. *Geotextiles and Geomembranes*. 21(2): 103-110.
- Ziegler, S., Leshchinsky, D., Ling, H. I., and Perry, E. B. 1998. Effect of short polymeric fibers on crack development in clays. *Soils and Foundations*, Vol. 38, No. 1, pp. 247-253.
- Zornberg, J. G. 2002. Discrete framework for limit equilibrium analysis of fiber-reinforcement. *Journal of Geotechnique* 52 (8), pp. 227–241

Appendices

APPENDIX A. Bagasse

A.1 Sugar production process

A.2 Bagasse tensile strength data

APPENDIX B. Classification tests:

B.1 Determination of OMC and maximum dry density (Proctor method)

B.1.1 Compaction test – Klipheuwel sand

B.1.2 Compaction test – Cape Flats sand

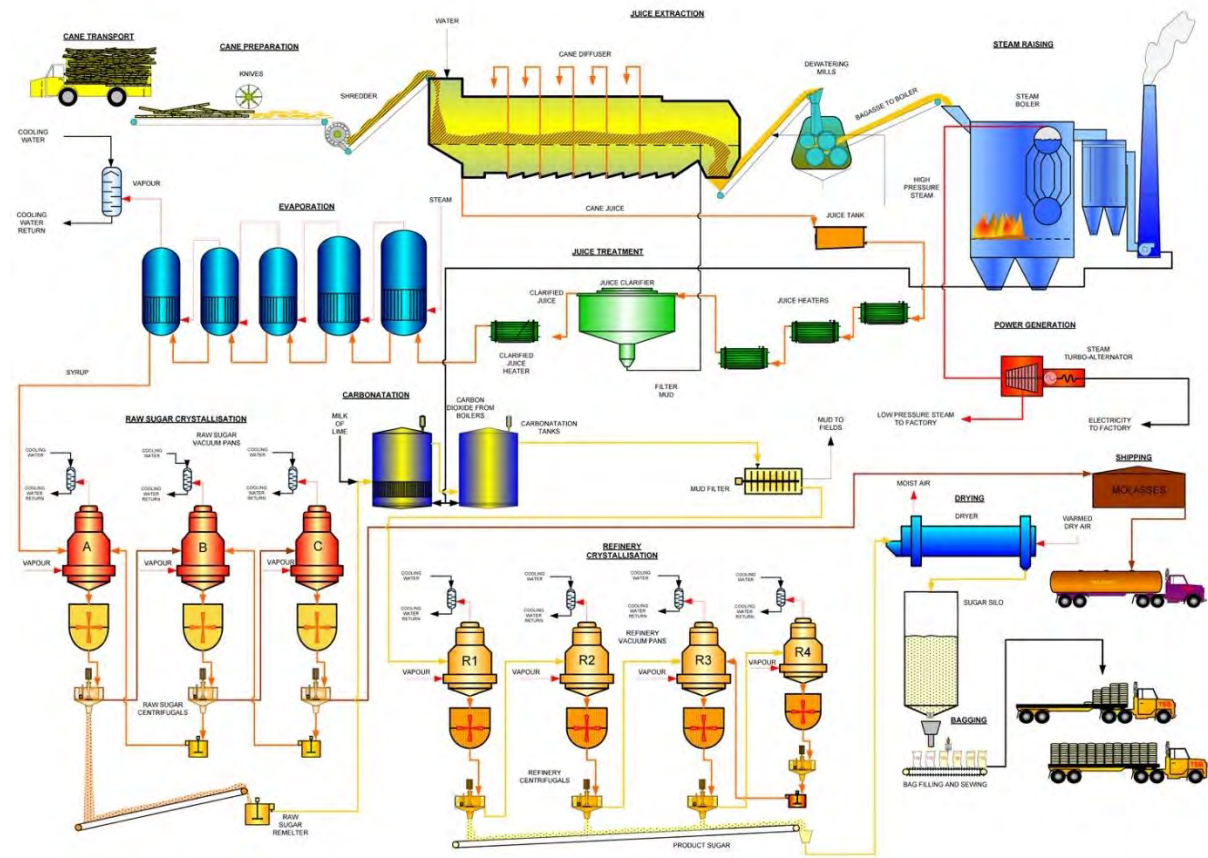
B.1.3 Compaction test – Kaolin

B.2 Determination of the Atterberg limits (Casagrande)

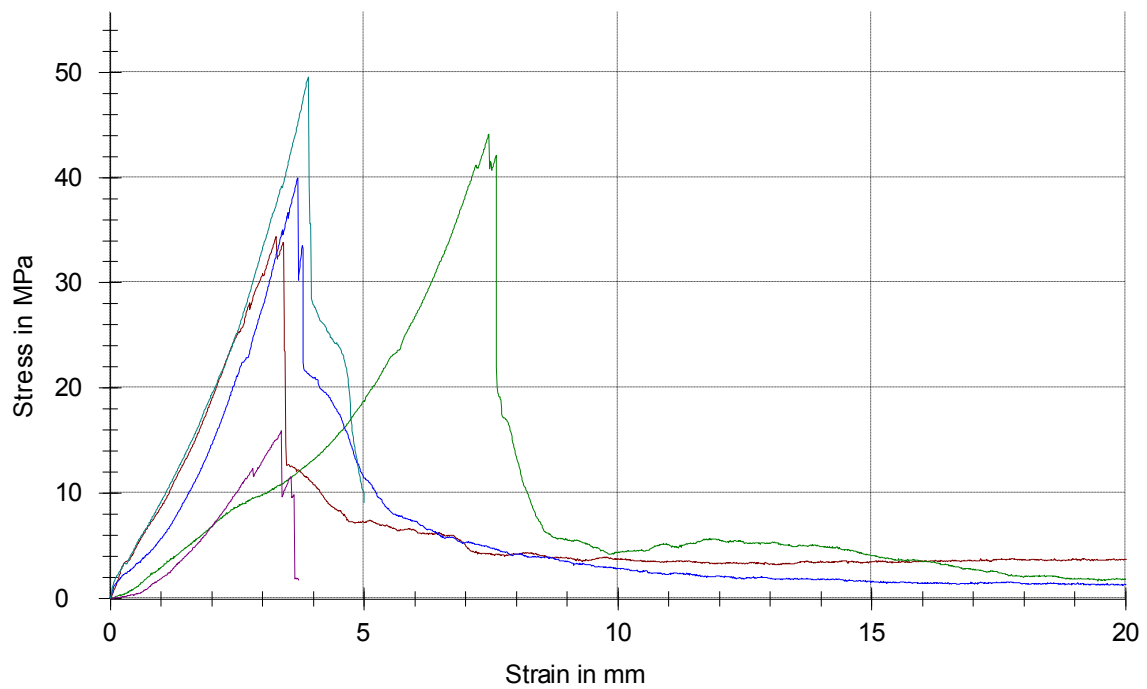
B.2.1 Atterberg limits – Kaolin

B.3 Sample volume change in soil reinforced with 1.0% fibre

A.1 Sugar production process (TSB sugar)

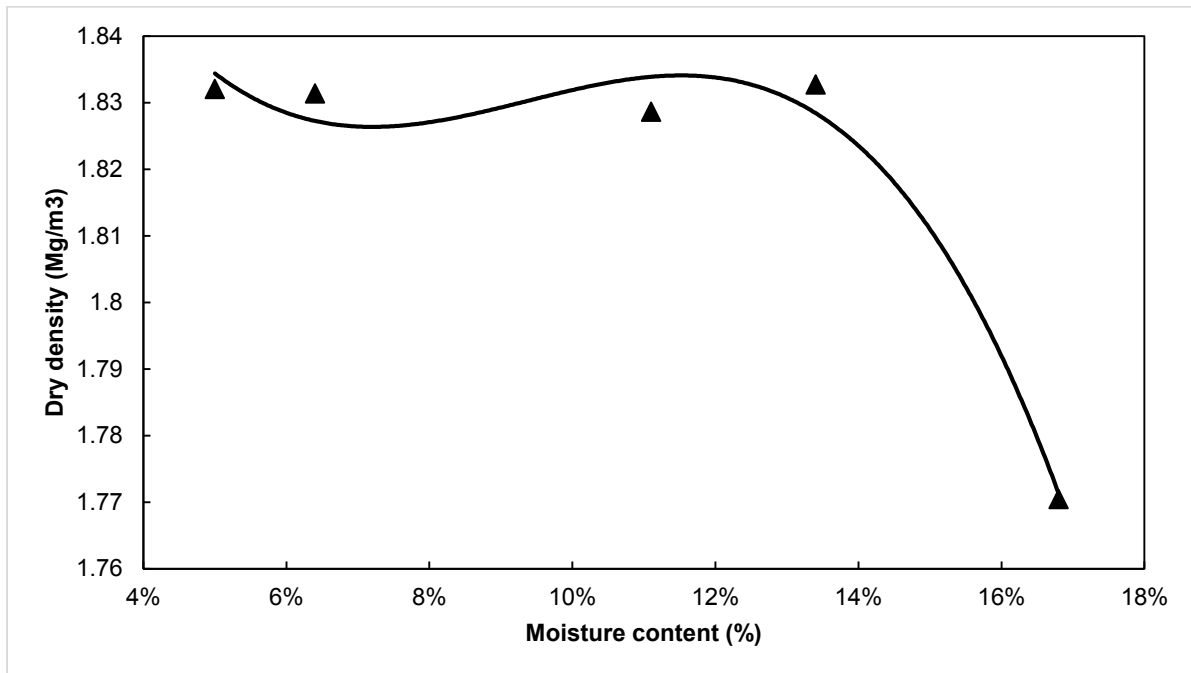


A.2 Bagasse tensile strength data

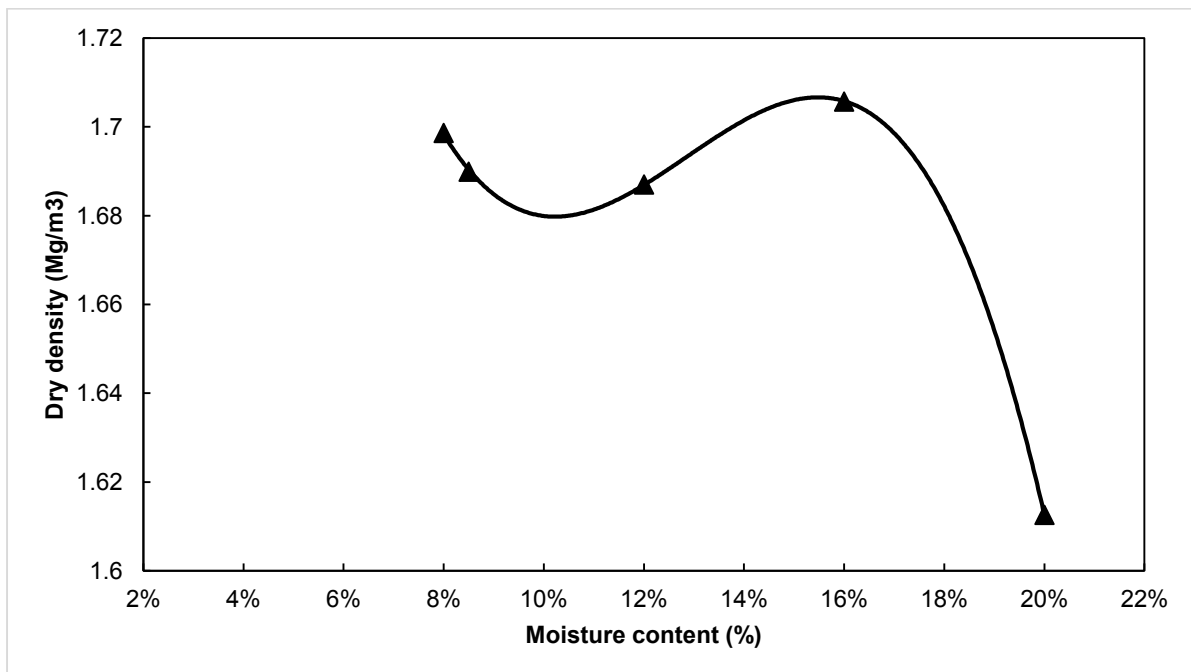


B.2 Determination of OMC and maximum dry density (Proctor method)

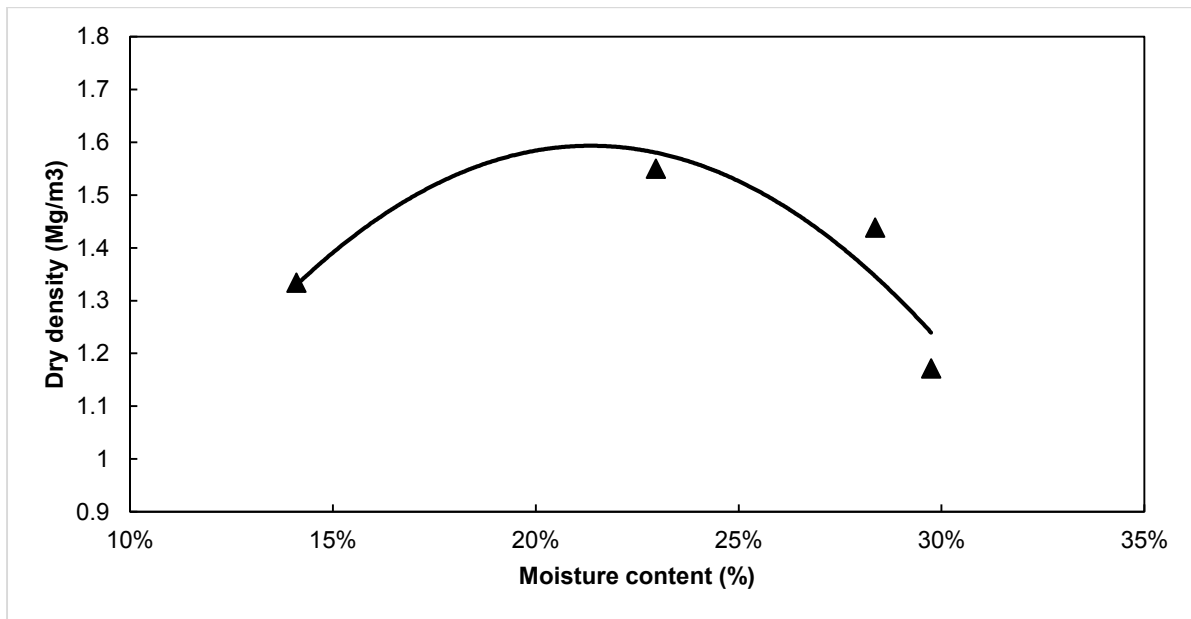
B.2.1 Compaction test – Klipheuwel sand



B.2.2 Compaction test – Cape Flats sand



B.2.3 Compaction test – Kaolin



B.2 Determination of limiting densities

Loosest Density

Height	0.12051	m				
Diameter	0.15233	m				
Volume of Mould	0.0022	m ³				
	Klipheuwel sand			Cape Flats sand		
	1	2	3	1	2	3
Mass of Mould (kg)	16.8	16.8	16.8	16.8	16.8	16.8
Mass of Mould + Soil (kg)	20.32	20.34	20.32	20.22	20.16	20.18
Mass of Soil (kg)	3.52	3.54	3.52	3.42	3.36	3.38
Density (kg/m ³)	1603	1612	1603	1557	1530	1539
Average (kg/m ³)		1606			1542	

Densest Density

Height	0.10122	m		0.10291	m	
Diameter	0.15233	m		0.15233	m	
Volume of Mould	0.00184	m ³		0.00188	m ³	
	Klipheuwel sand			Cape Flats sand		
	1	2	3	1	2	3
Mass of Mould (kg)	16.8	16.8	16.8	16.8	16.8	16.8
Mass of Mould + Soil (kg)	20.32	20.34	20.32	20.22	20.16	20.18
Mass of Soil (kg)	3.52	3.54	3.52	3.42	3.36	3.38
Density (kg/m ³)	1908	1919	1908	1824	1792	1802
Average (kg/m ³)		1912			1806	

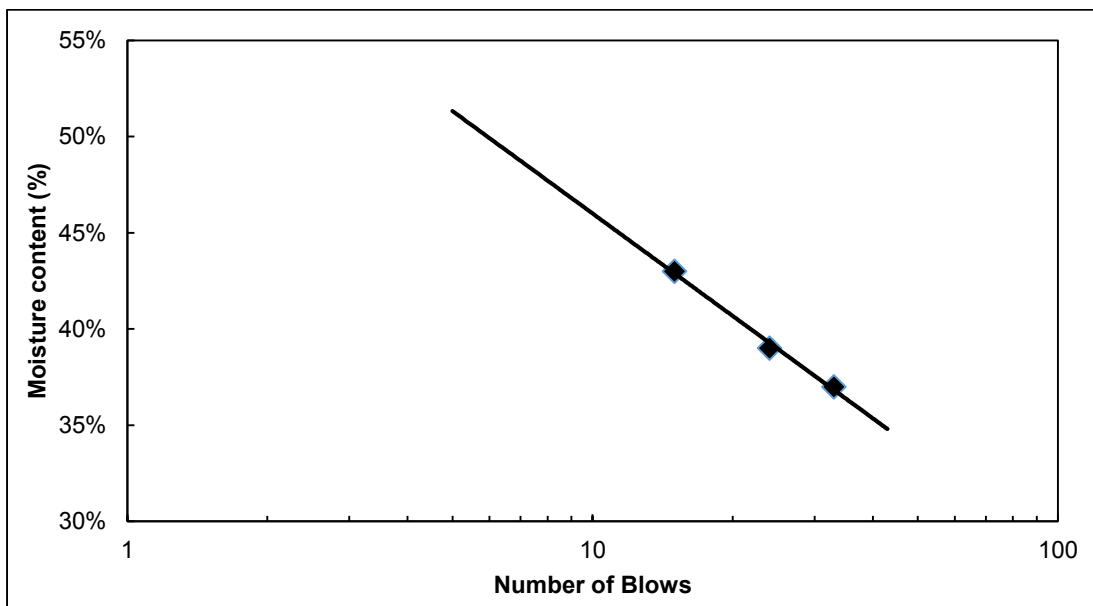
B.2 Determination of the Atterberg limits (Casagrande)

B.3.1 Atterberg limits – Kaolin

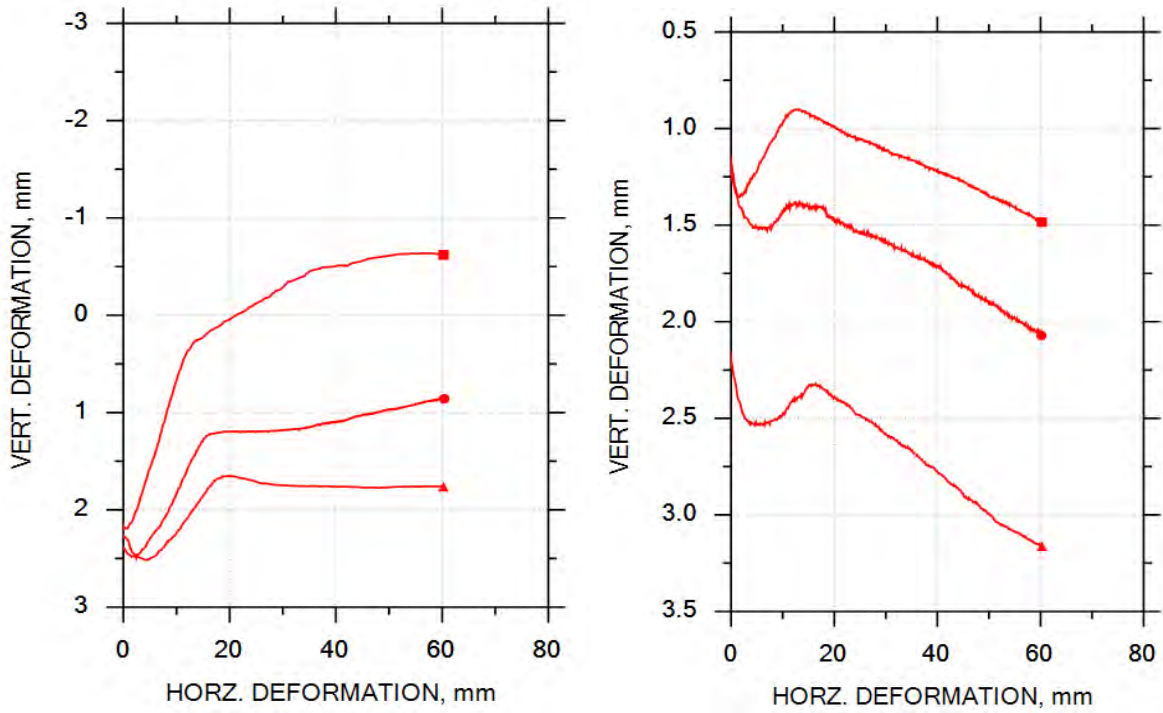
(a) Plastic limit of Kaolin

Sample No	1	2	3
Mass of container(g)	9.6	9.6	9.6
Mass of container + wet soil (g)	32.6	33.8	35
Mass of container + dry soil (g)	27.6	28.5	29.5
Mass of water (g)	5.0	5.3	5.5
Mass of dry soil (g)	18.0	18.9	19.9
Moisture content (%)	27.8%	28.0%	27.6%
Average		27.8%	

(b) Liquid limit



B 3.1 Change in Volume Klipheuvel sand (a) Reinforced at 1.0% fibre (b) Unreinforced



B 3.2 Change in Volume Cape Flats sand (a) Reinforced at 1.0% fibre (b) Unreinforced

